EANDC (E) 76 "U"

PROGRESS REPORT

ON NUCLEAR DATA RESEARCH IN THE EURATOM COMMUNITY

for the period January 1 to December 31, 1966

Submitted by the Joint Euratom Nuclear Data and Reactor Physics Committee

(Secretariat : Central Bureau for Nuclear Measurements, Euratom, Geel, Belgium)

January, 1967

EUROPEAN AMERICAN NUCLEAR DATA COMMITTEE

EANDC(E) 76 "U"

PROGRESS REPORT
ON NUCLEAR DATA RESEARCH IN THE EURATOM COMMUNITY

for the period January 1 to December 31, 1966

Submitted by the Joint Euratom Nuclear Data
and Reactor Physics Committee

(Secretariat : Central Bureau for Nuclear
Measurements, Euratom, Geel, Belgium)

January, 1967

EUROPEAN AMERICAN NUCLEAR DATA COMMITTEE

I N D E X

I. KERNFORSCHUNGSZENTRUM KARLSRUHE (GERMANY) INSTITUT FÜR ANGEWANDTE KERNPHYSIK

1. 3 MeV Van de Graaff

1.1. High Resolution Resonance Spectroscopy

G. Rohr, E. Friedland, K.N. Müller

In the period covered by this report the analysis of the total neutron cross section data of ^{51}V and ^{55}Mn has been completed (1). The measured cross sections as a function of the neutron energy are given in Figs. 1 and 2. The solid line represents the values as calculated with the R-matrix multilevel formula including energy resolution effects of the spectrometer. Table I and II give the resonance parameters found by this fit. (The resonances of table I marked with an asterisk, were determined by Firk et.al. (2)).

Using these resonance parameters the following conclusions can be made:

1) The experimental distribution function of the reduced width is not of the Porter-Thomas type in the case of vanadium.

2) The strength functions of the two elements are:

$$^{51}V \quad S = 8.2^{+2,2}_{-1,9} \times 10^{-4}$$

$$^{55}Mn \quad S = 3.1^{+0,9}_{-0,7} \times 10^{-4}$$

3) For both elements no spin dependence of strength function could be detected, as the difference of the strength function for the two spin systems were in both cases of the same order as the statistical errors.

4) A spin cut-off factor of $\sigma = 2,5^{+0,75}_{-0,35}$ has been computed for the isotope ^{55}Mn.

Using a resolution of 0.39 nsec/m (at 220 keV) the isotope ^{57}Fe has been measured in the energy range of 20 - 220 keV. The experimenta cross section is shown in Fig. 3. The analysis of this measurement is still in progress.

TABLE I Resonance Parameters of ^{51}V

E/keV/	Γ_n/keV/	J	E/keV/	Γ_n/keV/	J
* 4.17	0.508 ± 0.006	4	68.1	4.70 ± 0.10	4
* 6,89	1.28 ± 0.014	3	83.0	1.20 ± 0.05	4
* 11.81	5.5 ± 0.05	3	87.6	3.20 ± 0.08	4
* 16.60	0.35 ± 0.04	4	110.8	0.25 ± 0.03	3
* 17.40	0.35 ± 0.04	4	113.5	0.11 ± 0.01	4
21.65	0.79 ± 0.05	3	114.8	0.08 ± 0.01	3
29.45	0.191 ± 0.02	4	116.6	2.40 ± 0.08	4
39.3	0.57 ± 0.04	3	118.7	20.5 ± 1.0	4
48.15	0.15 ± 0.02	4	118.7	0.13 ± 0.02	3
49.55	0.63 ± 0.04	3	134.7	3.20 ± 0.15	4
51.95	0.115 ± 0.02	4	141.3	3.60 ± 0.15	3
53.0	0.98 ± 0.04	3	145.7	1.50 ± 0.10	3
62.9	3.80 ± 0.10	3	152.9	3.50 ± 0.15	4

TABLE II Resonance Parameters of ^{55}Mn

E/keV/	Γ_n/keV/	J	E/keV/	Γ_n/keV/	J
53.4	0.09 ± 0.01	2	123.5	0.51 ± 0.05	2
57.45	0.81 ± 0.03	3	127.0	2.03 ± 0.20	3
58.0	0.06 ± 0.01	2	128.1	1.51 ± 0.15	2
59.5	0.27 ± 0.02	3	129.5	1.21 ± 0.15	2
59.95	0.10 ± 0.01	2	131.0	0.22 ± 0.03	3
64.1	1.01 ± 0.05	3	142.1	0.55 ± 0.06	3
66.6	0.16 ± 0.02	2	151.3	0.41 ± 0.08	2
69.55	0.14 ± 0.02	3	155.8	1.02 ± 0.10	2
70.07	0.32 ± 0.02	2	158.7	0.92 ± 0.05	3
73.9	0.71 ± 0.04	3	166.9	0.31 ± 0.05	2
81.3	0.44 ± 0.03	2	172.2	1.72 ± 0.15	3
84.35	1.31 ± 0.05	3	176.9	0.32 ± 0.03	3
96.05	0.21 ± 0.02	2	179.9	0.35 ± 0.05	2
98.2	0.45 ± 0.04	3	181.0	0.25 ± 0.05	3
103.7	0.27 ± 0.02	2	184.4	1.00 ± 0.15	2
104.9	1.51 ± 0.06	2	186.2	2.20 ± 0.20	3
107.0	0.41 ± 0.04	2	188.5	0.81 ± 0.10	3
109.4	1.32 ± 0.13	2	193.9	0.30 ± 0.03	3
110.9	1.83 ± 0.15	3	197.6	0.62 ± 0.05	2
116.1	0.47 ± 0.03	3	203.4	2.70 ± 0.30	3
118.4	0.71 ± 0.04	3	207.7	2.80 ± 0.30	2

(1) Rohr, G., Friedland, E. and Nebe, J., Conf. on Nuclear Data, Paris (1966) P. CN-23/9

(2) Firk, F.W.K., Lynn, J.E., and Moxon, M.C., Proc. Phys. Soc. 82 (1963) 477

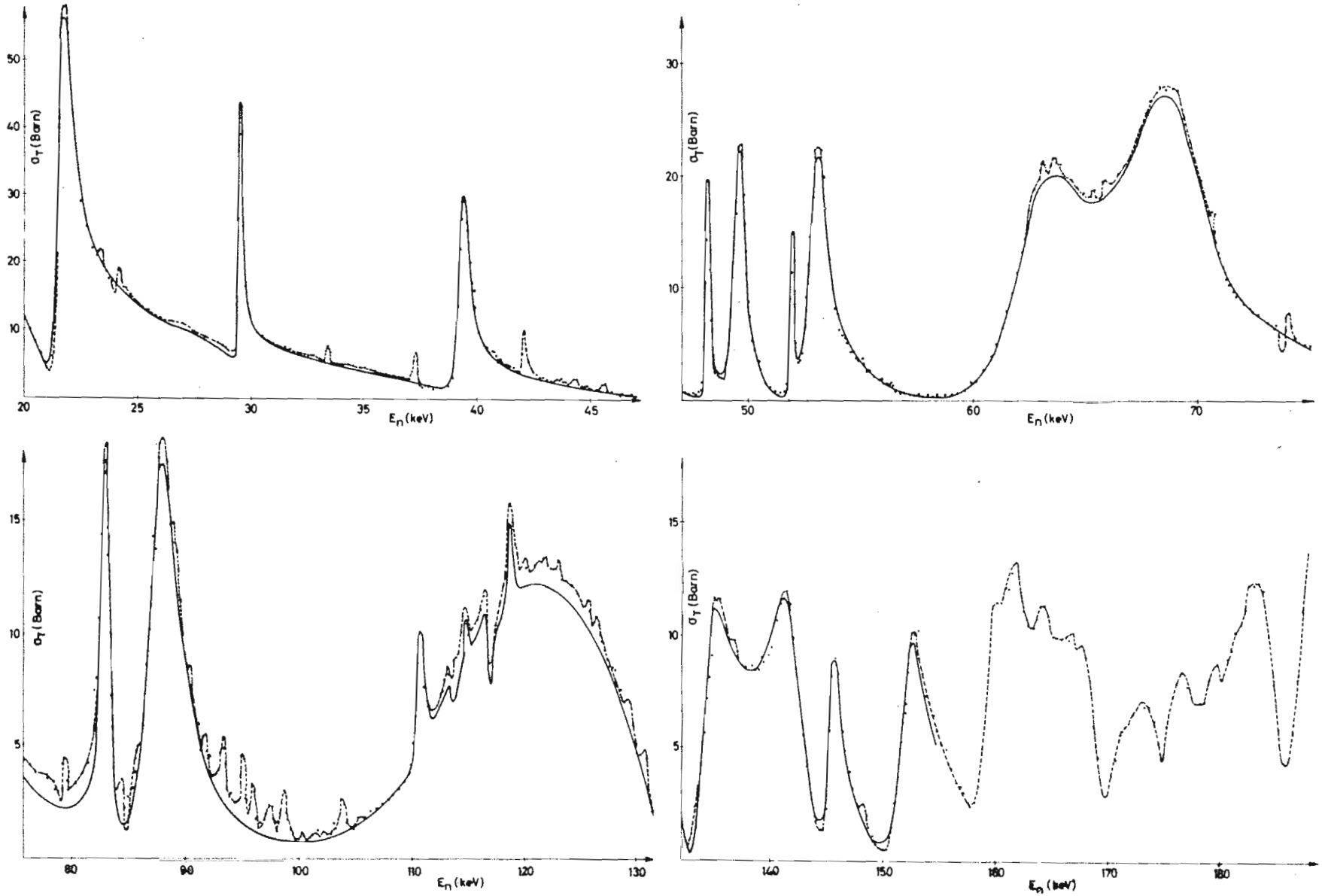

Fig.1 Total neutron cross section curve for ^{51}V. The solid line represents the multilevel fit.

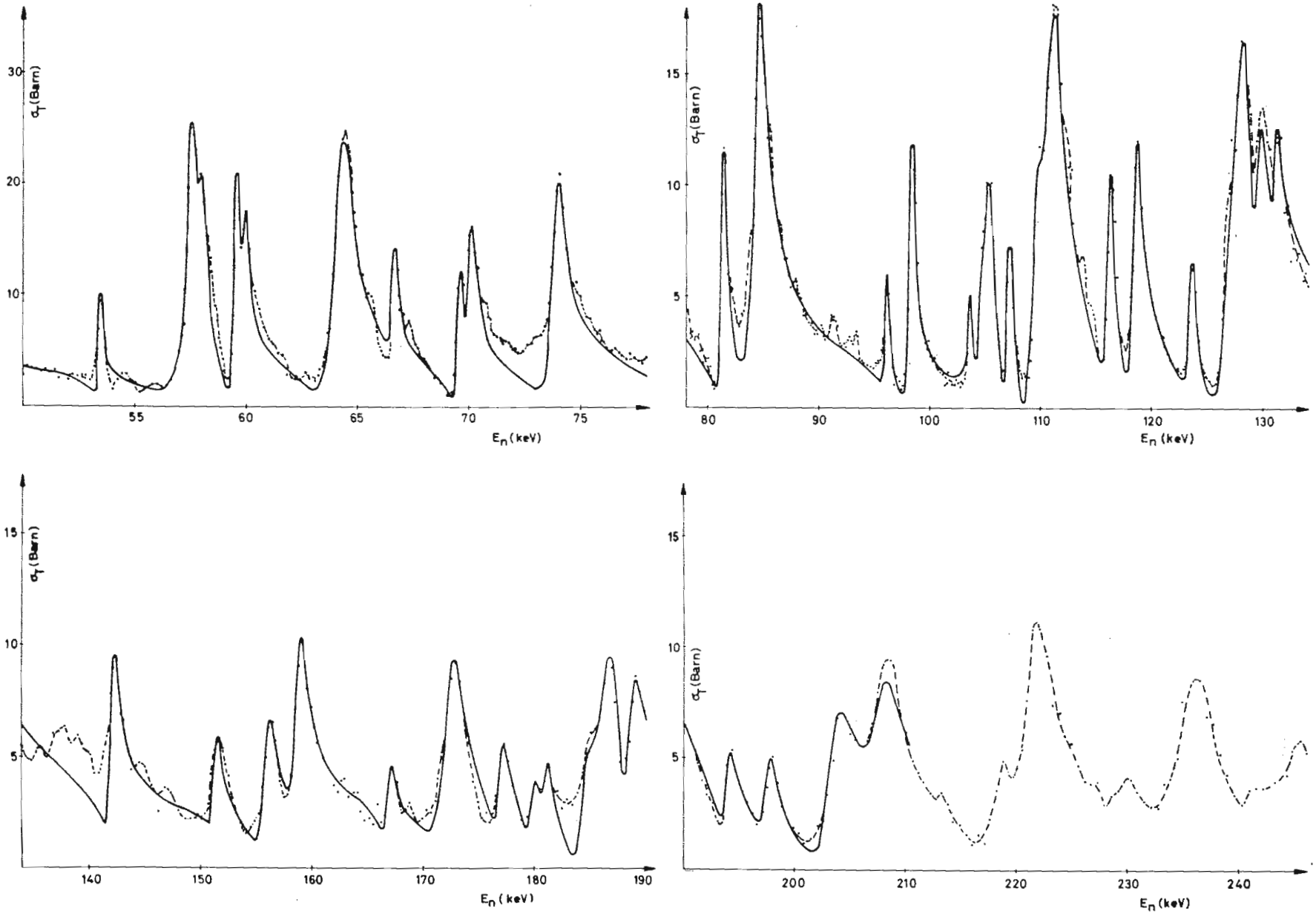

Fig. 2 Total neutron cross section curve for ^{55}Mn. The solid line represents the multilevel fit.

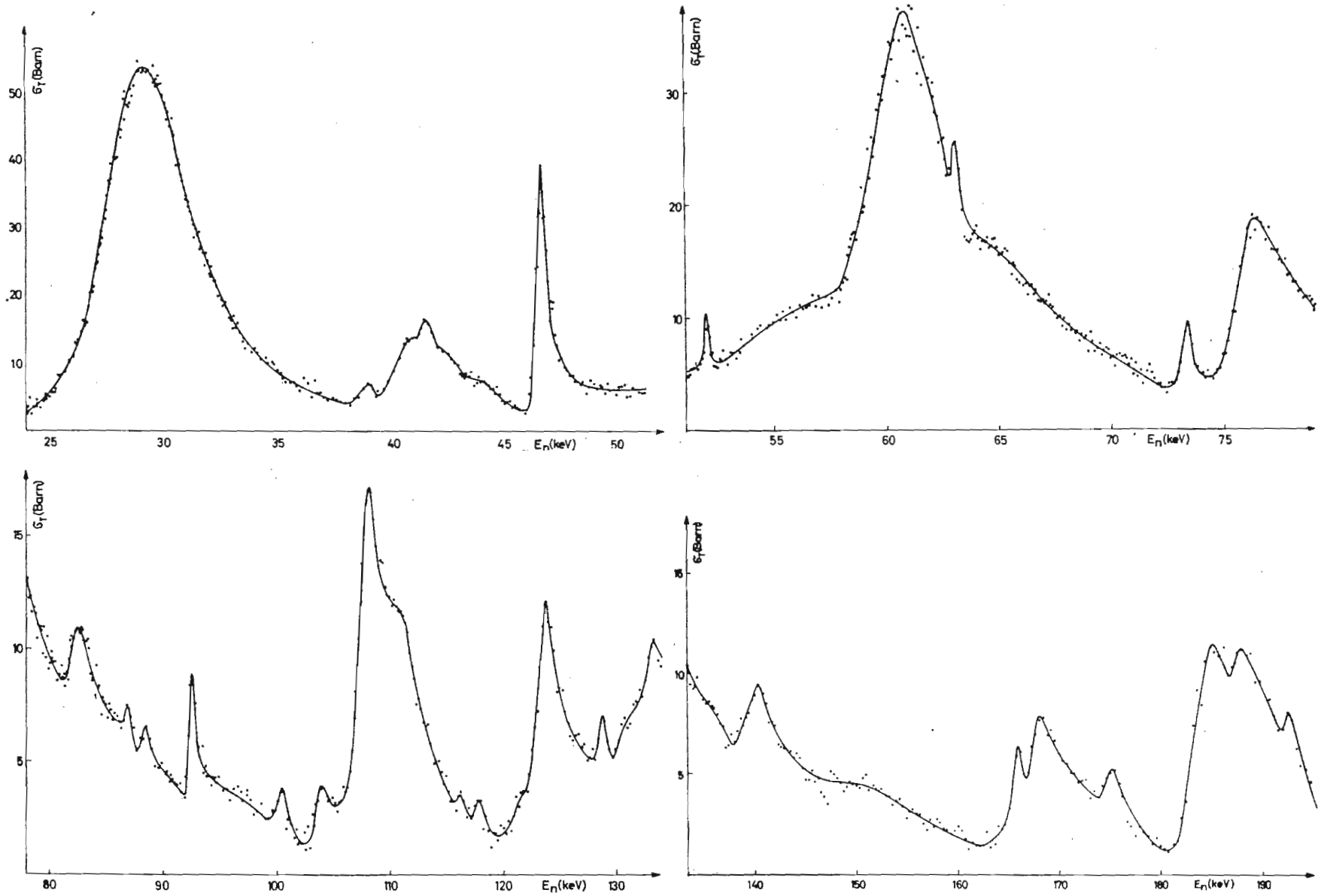

Fig. 3 Total neutron cross section curve for *Fe.

1.2. Measurement of Radiative Capture Cross Sections

D. Kompe

In the energy range from 10 to 150 keV radiative neutron capture cross sections of the elements Nb, Mo, Pd, Ag, Cd, In, Cs, Hf, Ta, W and Re were measured relative to the capture cross section of Au at the 3 MeV pulsed van de Graaff generator. Energies of the neutrons produced in a thick Li-target were determined by time of flight. Capture events in the sample were detected by a large liquid scintillator. The resolution of the experiment was 7 ns/m.

A measurement for determining the shape of the capture cross section of Au, used as a standard, was performed by comparison with the shape of the $Li^6(n,\alpha)$ cross section as given by Schwarz et.al. (1). The Au cross section curve from this measurement was normalized at 30 keV to the value given by Pönitz (2). Because of discrepancies in the shape Pönitz has assumed in his evaluation of several Au cross section measurements a mean curve with a corresponding large error which is represented by the solid line in Fig. 1. The points in this figure show the Au cross section as observed with the resolution of this measurement normalized to the smooth curve of Pönitz. In Fig. 2 to 4 preliminary capture cross section results are shown which are based on the Au capture cross section of Fig. 1. For comparison the renormalized curves of Pönitz and results of other authors if available are shown in the figures. For Hf no other results, and for Cs only measurements up to 50 keV by Popov et al. (3) were known. For the present data an error of 12 % to 15 % is estimated.

We hope that further investigations of the Au cross section that we plan will improve the accuracy of this standard cross section which could cause a renormalization of the present data.

(1) Schwarz, S., Strömberg, L.G., Bergström, A., Nucl. Phys. 63, 593 (1965)

(2) Pönitz, W.P., CN-23/6

(3) Труда ФИАН, ТОМ XXIV (1964)

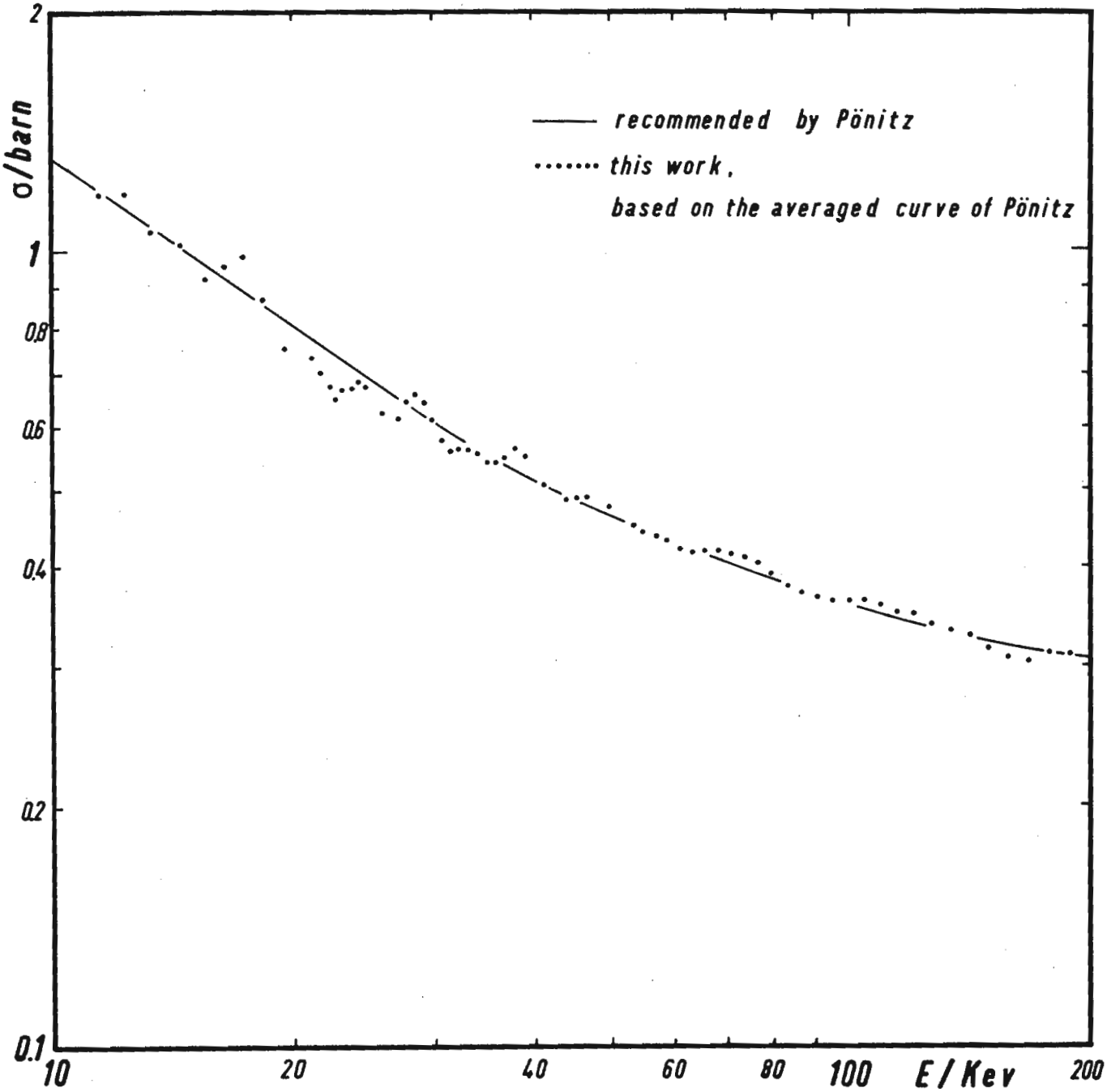

Fig. 1. Capture cross section of Au, normalized at 30 Kev.

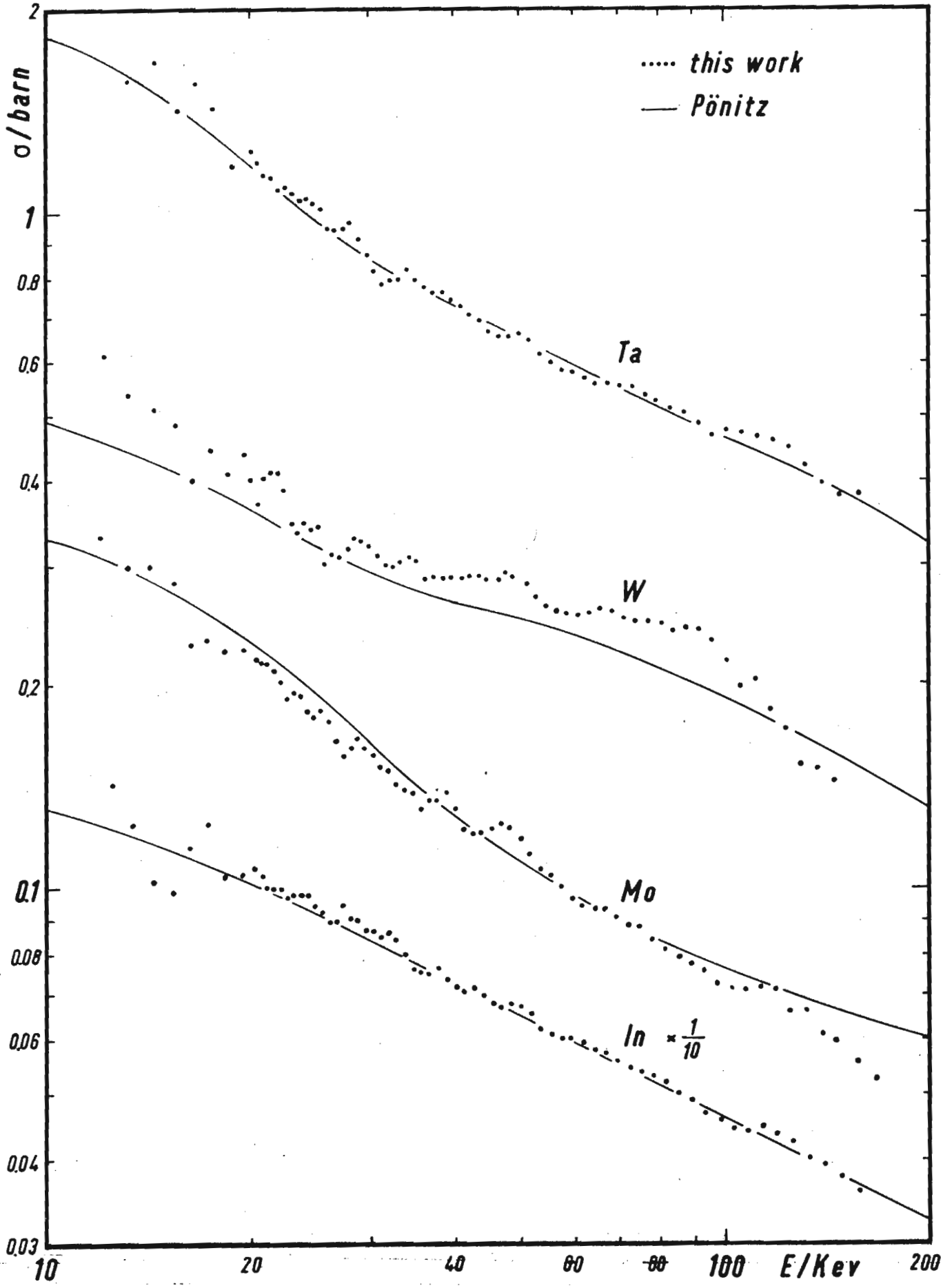

Fig. 2. Capture cross sections of Ta, W, Mo, In.

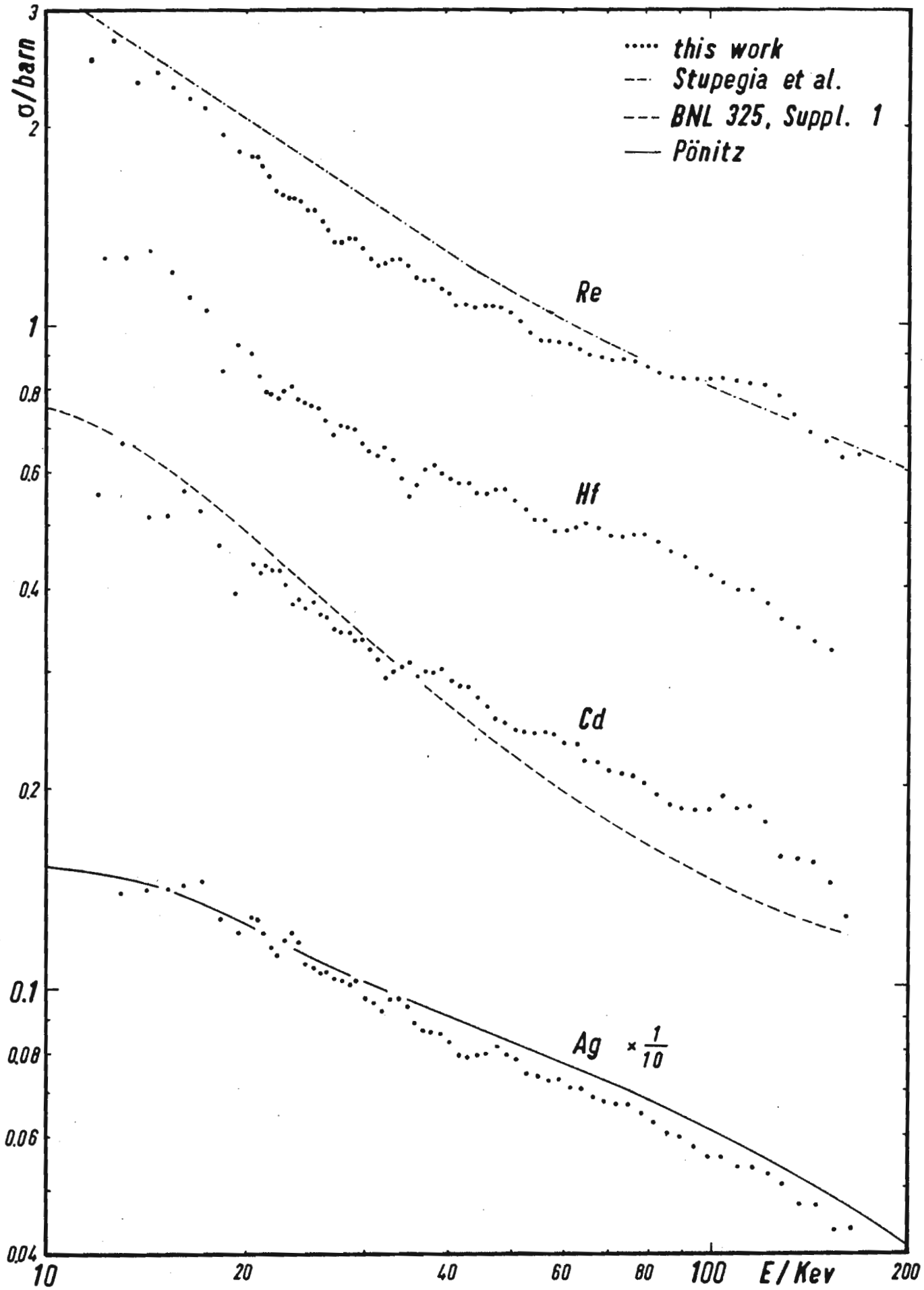

Fig. 3. Capture cross sections of Re, Hf, Cd, Ag.

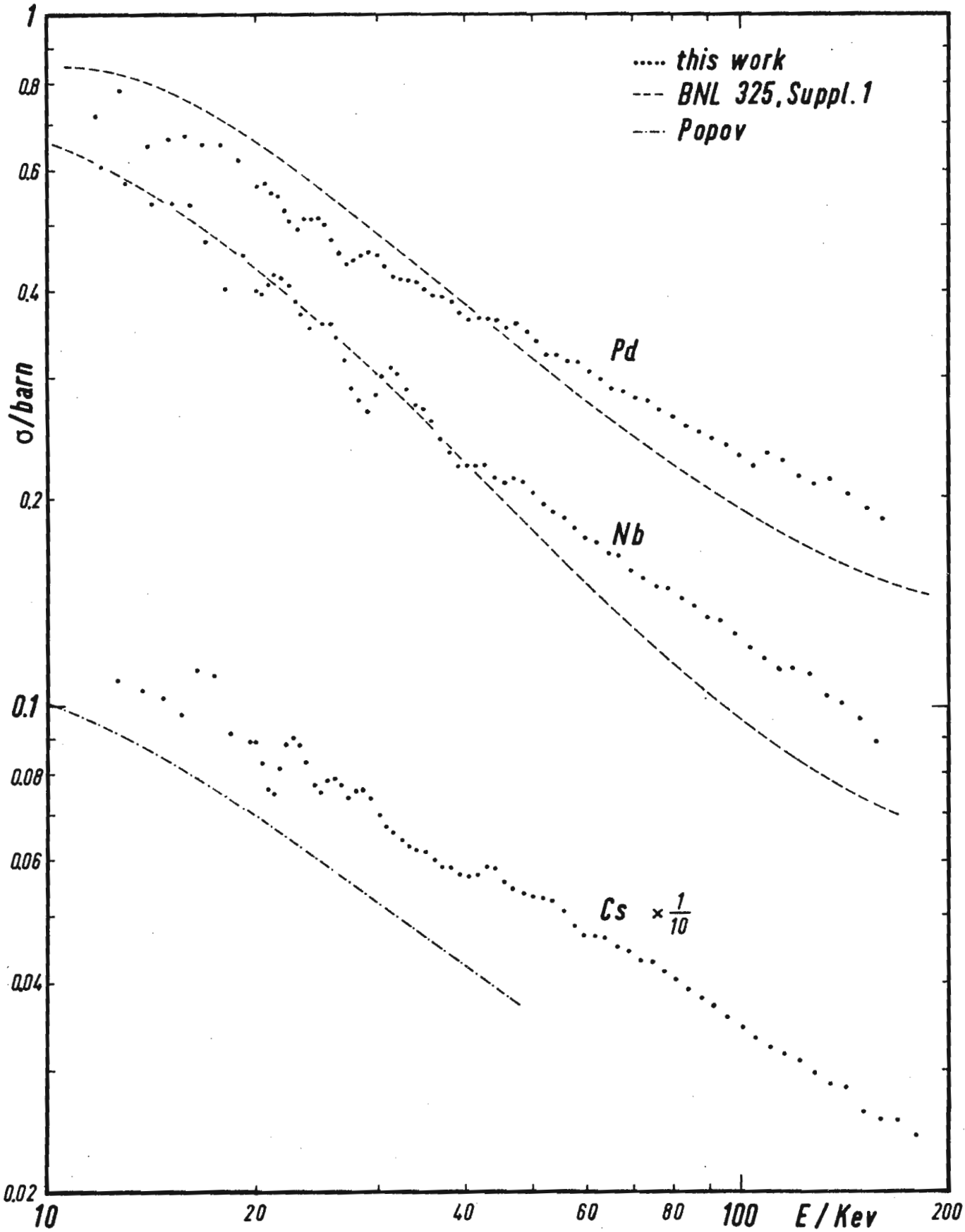

Fig. 4. Capture cross sections of Pd, Nb, Cs.

1.3. Fast Neutron Life Time Measurements

H. Miessner, E. Arai

The fast neutron life time measurements in the keV region for measuring effective (resonance self-shielded) cross sections have been continued. The measurements of capture and transport cross sections of U and Pb at 7,5 keV and 30 keV have been improved and completed. The effective cross sections measured by the present method agree with values computed from calculated self-shielding factors (1) and infinite dilution average values $\langle \sigma \rangle$ (see Ref. (2,3)). The present method can be used to determine f factors, if $\langle \sigma \rangle$ values are obtained by other methods. Details of these measurements are given in (2,3).

Furthermore, fast neutron life time measurements have been carried on in mixtures of a resonance absorber (^{238}U) and a pure potential scatterer (Pb) in order to study the resonance self-shielding as a function of the dilution. The latter measurements are not yet completed.

(1) L.P. Abagjan et al. INDSWE 17 (1964)

(2) E. Arai, H. Miessner, K.H. Beckurts, Nucl. Sc. Eng. 26 (1966) 573

(3) H. Miessner, E. Arai, Nukleonik 8 (1966) 428

1.4. Absolute Capture Cross Sections

W.P. Pönitz

The absolute activation cross section of Au^{197} was measured at the neutron energy of 30 keV. The cross section was measured using two different methods and the results were averaged as described in ref. 1. The description of the experimental method is given in ref. 2. The result for the cross section is

$$\sigma^{Au}_{n,\gamma}\ (30\ \text{keV}) = 0{,}598 \pm 0.012\ \text{barn}.$$

This value and 13 other values of $\sigma^{Au}_{n,\gamma}$ (30 keV) were used to evaluate a most probable value at 30 keV. The resulting cross section is

$$\sigma^{Au}_{n,\gamma}\ (30\ \text{keV}) = 0.603 \pm 0.012\ \text{barn}.$$

All available measurements of the shape of the (n,γ)-cross section of gold were renormalized to the cross section at 30 keV and averaged. The result was recommended as an absolute cross section in the keV-energy region (1 - 1000 keV).

This cross section was used to renormalize the (n,γ)-cross section of Mo, Rh, Ag, In, Sb, I, Ta and W (s. Tab. I), (s. also ref. 2).

An experiment for the determination of the (n,γ)-cross section shape of Au in the energy region from 10 - 300 keV is in preparation.

(1) W.P. Pönitz, J. Nucl. Energy 20 (1966) 825

(2) W.P. Pönitz, KFK 454, CN-23/6, 1966

TABLE I Capture Cross Section Values in the Energy Region 1 - 1000 keV

	σ/barn								
E/keV	Au	Mo	Rh	Ag	In	Sb	I	Ta	W
1	6.77	0.72	2.82	4.27	2.59	2.13	3.38	10.16	2.49
2	4.08	0.63	2.35	2.91	2.18	1.43	2.50	6.33	1.43
3	3.03	0.56	2.09	2.44	1.98	1.16	2.15	4.61	1.06
5	2.11	0.47	1.73	1.94	1.65	0.91	1.68	3.16	0.75
10	1.31	0.33	1.27	1.52	1.29	0.69	1.17	1.83	0.49
20	0.811	0.234	1.00	1.28	1.02	0.574	0.90	1.18	0.364
30	0.603	0.165	0.85	1.02	0.81	0.480	0.72	0.85	0.292
50	0.460	0.110	0.72	0.85	0.65	0.370	0.570	0.65	0.250
70	0.400	0.090	0.64	0.73	0.56	0.285	0.460	0.545	0.220
100	0.355	0.076	0.54	0.61	0.46	0.216	0.375	0.460	0.192
200	0.304	0.062	0.364	0.406	0.321	0.145	0.246	0.321	0.132
300	0.245	0.056	0.258	0.310	0.287	0.130	0.197	0.256	0.113
500	0.159	0.045	0.150	0.198	0.267	0.114	0.142	0.182	0.095
700	0.118	0.036	0.103	0.150	0.267	0.106	0.102	0.145	0.090
1000	0.093	0.027	0.075	0.112	0.269	0.111	0.073	0.119	0.098
	Δσ/σ / %								
1-10	7	30	20	10	15	30	20	10	15
10-40	8	20	20	10	10	20	15	10	15
40-200	12	20	20	15	15	15	15	15	15
200-1000	7	20	15	10	15	20	20	20	15

1.5. Fission Cross Section Measurements (H. Miessner, W. Pönitz, W.B. Gilboy, G.F. Knoll, E. Pfletschinger)

1.5.1. Fission Cross Section Ratios $^{239}Pu/^{235}U$ and $^{240}Pu/^{235}U$

The fission cross sections of ^{239}Pu and ^{240}Pu have been measured relative to the fission cross section of ^{235}U over the neutron energy range 5 - 150 keV. A pulsed continuous ("white") spectrum of neutrons from the $^{7}Li(p,n)^{7}Be$ reaction was produced by bombarding a thick metallic lithium target with a pulsed and bunched proton beam (pulse length 1 ns) of the 3 MeV van de Graaff. The fissile samples [^{239}Pu: (1.100 ± 0.055) mg/cm^2 PuO_2, ^{240}Pu: (0.290 ± 0.015) mg/cm^2 PuO_2, ^{235}U: (1.204 ± 0.0015) mg/cm^2 U_3O_8, chemical purity > 99,9 % in each case] were mounted in Xenon gas scintillation counters (time resolution ~ 1 ns) to detect the induced fissions.

Pairs of these fission counters were mounted symmetrically round the pulsed neutron source. The number of fission events was measured as a function of the neutron energy by means of the time-of-flight method (flight path ~10 cm).

The $^{239}Pu/^{235}U$ cross section ratio is presented in Fig. 1. Method A is an absolute one and requires the thickness of the samples. The Pu masses are given to 5 % and are only provisional pending a more accurate assay by destructive analysis. In method B the cross section ratio was measured relatively to the ratio at 41 meV which is known to about ± 2 % accuracy. This method obviates the need to know the masses to the two fissile samples. Fig. 2 shows the $^{240}Pu/^{235}U$ cross section ratio. The number of induced fissions in the ^{240}Pu sample is measured relatively to the spontaneous fission rate. This obviates the need to know the mass of ^{240}Pu since the spontaneous fission half life is known to about 1 %.

1.5.2. Absolute Fission Cross Section Measurement on ^{235}U

A first step was done to adjust also the absolute values of the fission cross sections in the keV-energy region. The fission cross section of ^{235}U was measured at 30 keV and 64 keV neutron energy using kinematically collimated neutrons at the threshold of the $Li^7(p,n)Be^7$, and the $T(p,n)He^3$ reaction. The number of fission events in a 1.2 mg/cm^2 U_3O_8

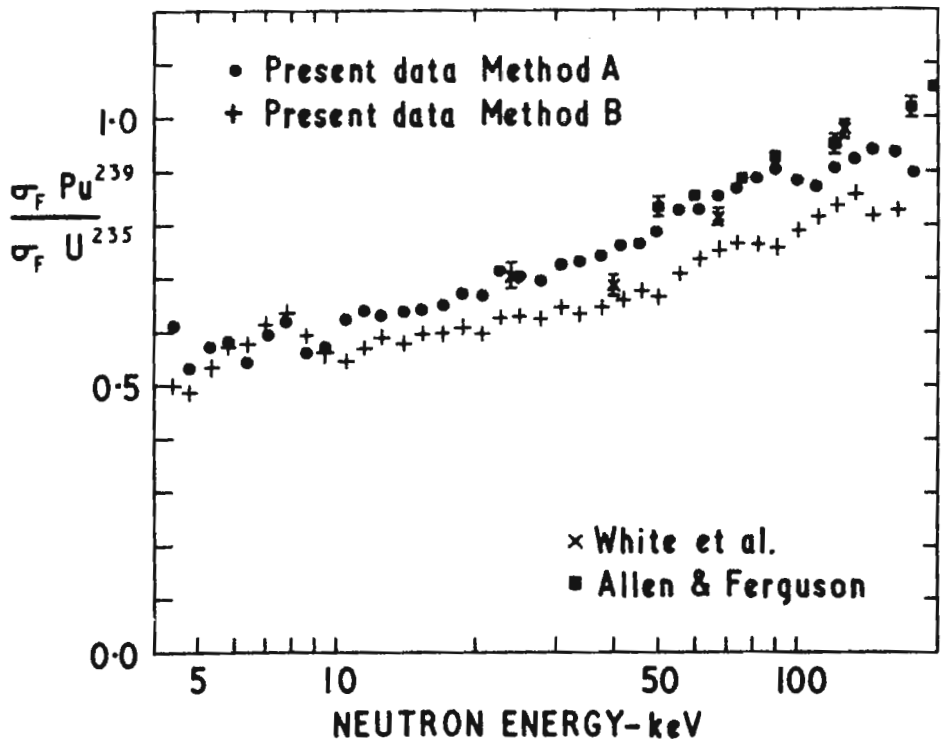

FIGURE 1. $^{239}Pu/^{235}U$ FISSION CROSS-SECTION RATIO at 10 % LETHARGY INTERVALS

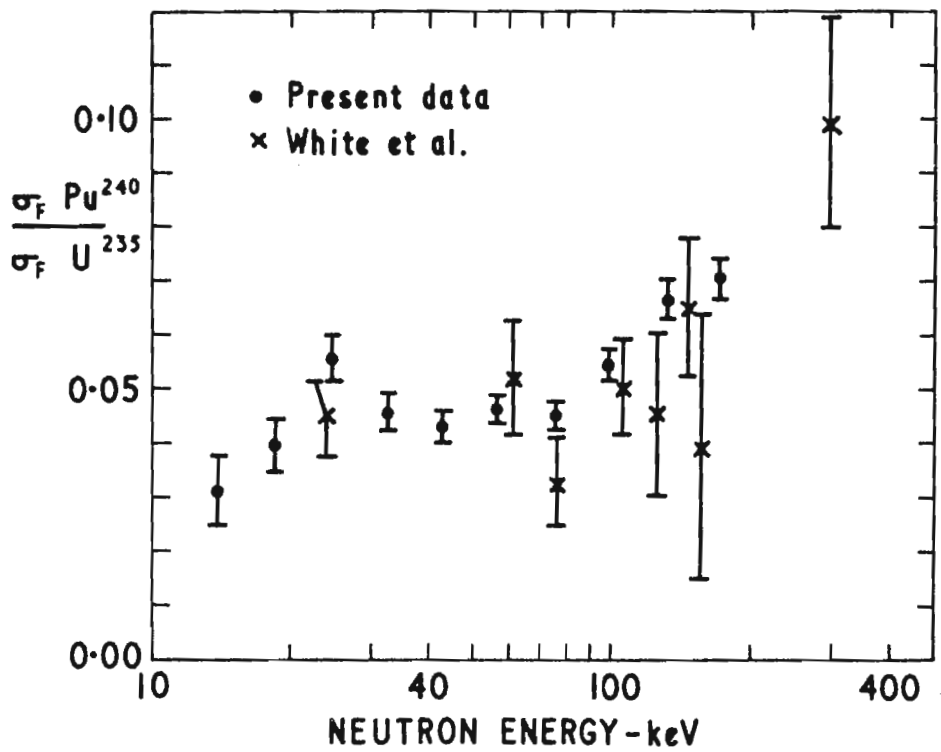

FIGURE 2. $^{240}Pu/^{235}U$ FISSION CROSS-SECTION RATIO AT 30 % LETHARGY INTERVALS

foil was determined by counting the fission fragments in a gas scintillation detector. The neutron flux at 30 keV was measured both by counting of the induced Be^7 activity in the target and through a parallel measurement of the induced Au^{198} activity in a gold foil. For the reaction $Au^{197}(n,\gamma)Au^{198}$ a cross section value of 0.604 ± 0.025 barn was obtained by evaluation of a weighted average from a variety of recent experiments. The flux at 64 keV was normalized by assuming a value

$$\sigma^{Au}_{n,\gamma}\ (30\ \text{keV})/\sigma^{Au}_{n,\gamma}\ (64\ \text{keV}) = 1.633 \pm 0.065.$$

Values obtained for the fission cross section are 2.19 ± 0.06 barns at 30 keV and 1.78 ± 0.13 barns at 64 keV.

1.6. Isobaric Analogue States

E. Arai and H. Miessner

Isobaric analogue states of ^{60}Co in the compound nucleus ^{60}Ni were investigated with the $^{59}Co(p,n)^{59}Ni$ and the $^{59}Co(p,\gamma)^{60}Ni$ reaction. In the (p,n) measurement a thick target (a few hundred keV for 2 MeV protons) was used and the neutron spectrum was measured by the time-of-flight method. In this way the energy resolution is independent of the stability of the beam energy and the target thickness (both limit the energy resolution in the conventional method with monoenergetic protons), and is given by the time-of-flight spectrometer only. In the present work this spectrometer consisted of a pulsed 3 MeV van de Graaf (pulse length 1 ns) and a proton recoil detector with a flight path of 10 m. Fig. 1 a shows as an example a (p,n) cross section measurement in the range from 2.09 to 2.30 MeV. The energy resolution is 800 eV. The cross section shows a fine structure superimposed in a gross structure. For a better identification of the latter the measured curve was folded into a Gaussian with a width ΔE which must be large in comparison with the width of the fine structure and still small enough not to deform the gross structure (the averaged curves have been found to be independent of ΔE within ΔE = 6 to 12 keV). Fig. 1 b shows the (pn) cross section vs. proton energy averaged with ΔE = 8 keV. The position of the peaks 6, 7, 8 agree satisfactorily with those observed as single peaks in an additional (p,γ) cross section measurement. In this experiment a thin Co target ($\sim$8 keV thick for 2 MeV protons) was used and the γ-intensity was measured as a function of the proton energy (conventional method) with a NaI detector. The (p,γ) cross section shows maxima at the proton energies given in Table I column 6. These maxima can be interpreted as analogue states of ^{60}Co in ^{60}Ni by comparing the measured proton energies with the expected energies calculated from the binding energy differences, the Coulomb displacement energy ΔE_c = 9.013 $\pm$ 0.07 MeV (obtained by a semiempirical formula) and the low laying states of ^{60}Co known from the (d,p) reaction (1) and from recent (n,γ) work (2). The Coulomb displacement energy obtained from this (p,γ) experiment is 9.020 $\pm$ 0.025, which is consistent with the calculated value. The measurement of isobaric analogue states of ^{60}Co confirm the statement in (2) that the low lying states in ^{60}Co have

Table I. Isobaric Analogue States in ^{60}Ni obtained from the (p,γ)reaction.

States in ^{60}Co				Analogue states measured in proton energies [MeV] (c.m. system)		Peak No.
(d,p)[1] [MeV]	(n,γ)/8/ [2]	J^{π} [2]	Configuration [2]	Expected	observed	
0	0	5^+	$(f_{7/2})^{-1}(f_{5/2})^2(p_{3/2})^{-1}$	1.587	1.594 ± 0.004	1
0.058	0.0575	2^+	"	1.654	1.650 1.665	2
0.282	0.2760 *) 0.2881	4^+ 3^+	$(p_{3/2})^4(p_{1/2})^1$	1.863 1.875	1.867 1.886	3
0.432	0.343	5^+	$(p_{3/2})^4_n(f_{5/2})^1_n$	2.021	2.037	4
0.501	0.5051	3^+	$(f_{5/2})^2_n(p_{3/2})^{-1}_n$	2.092	2.092	5
0.541	0.5405	2^+	$(p_{3/2})^4_n(f_{5/2})^1_n$	2.128	2.149	6
0.612	0.6131	3^+	-	2.200	2.219	7
0.738	(0.738)	$(1^+,2^+)$	-	2.325	2.273	8

*) This doublet was suggested already in [1]

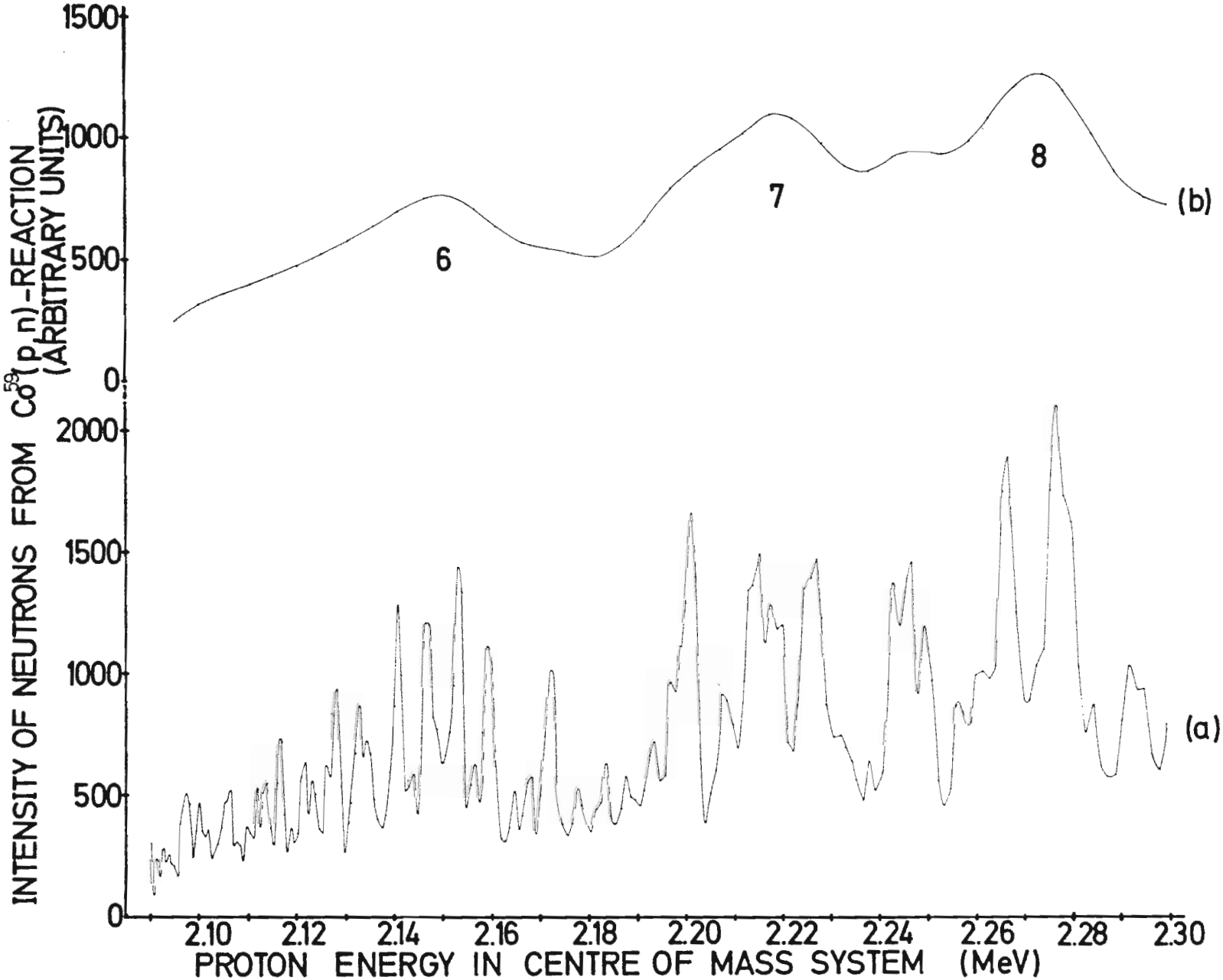
INTENSITY OF NEUTRONS FROM Co^{59}(p,n)-REACTION (ARBITRARY UNITS)
1500
1000
500
0
2000
1500
1000
500
0
6
7
8
(b)
(a)
2.10
2.12
2.14
2.16
2.18
2.20
2.22
2.24
2.26
2.28
2.30
PROTON ENERGY IN CENTRE OF MASS SYSTEM (MeV)

Fig.1

single-particle character. Detailed results of these experiments have been published in ref. (3).

(1) H.A. Enge et at. Phys. Rev. 119 (1960) 735

(2) E. Brooks Shera and D.W. Hafemeister, Phys. Rev. 150 (1966) 894

(3) E. Arai and H. Miessner, submitted to Phys. Letters

1.7. Operation of the Machine

H. Miessner

The pulsed 3 MeV van de Graaff worked without any serious breakdowns during the period covered by this report and only routine repairs were necessary. The totalweekly operation time of the machine was about 120 hrs; 90 % of this time was effectively used as measuring time.

To test a new deflection chamber (both pairs of deflection plates behind the einzel-lens) and to develop ion sources of higher output, a high vacuum station is installed with the whole terminal equipment of the machine (ion source, deflection chamber, pulsing device and power supply).

2. (n,γ)-Spectroscopy

W. Michaelis, U. Fanger, G. Markus, H. Schmidt, C. Weitkamp

During the period covered by this report several modifications of the apparatus were made. The primary detector of the 5-crystal pair spectrometer was replaced by a Ge(Li)-diode. In short runs the resolution is better than 10 keV FWHM at 7.5 MeV. An anti-Compton assembly (1) (2) with a Ge-detector was installed which will be used in the energy range up to 3 MeV. The resolution is 2.15 keV FWHM for the Cs-137 gamma ray. Coincidence measurements are performed with a 34 cm^3 Ge-diode and a 4" Ø x 5" NaI(Tl) crystal. Most of the semiconductor detectors are now operated with cooled FET preamplifiers (3). A pulse shape discriminator was developed which considerably improves the spectrum shapes obtained with germanium counters (4). Angular correlation measurements are performed with 4" Ø x 5" NaI(Tl) detectors using the Karlsruhe Multiple Input Data Acquisition System (MIDAS).

A lot of data have been accumulated during 1966 both for even spherical nuclei [Fe^{58}, Ni^{62}, Ge^{74} (ref. 5 and 6), Sr^{88} (refs. 7 and 8)] and for deformed odd-A nuclei [Dy^{165} (ref. 9 and 10), Er^{167} (ref. 10), Yb^{169} (ref. 10)].

(1) W. Michaelis and H. Schmidt, KFK 429 (1966)

(2) W. Michaelis and H. Küpfer, Nucl. Instr. and Meth. (to be published)

(3) U. Tamm, KFK 509 (1966)

(4) U. Tamm, W. Michaelis and P. Coussieu, Nucl. Instr. and Meth. (in press)

(5) C. Weitkamp, W. Michaelis, H. Schmidt and U. Fanger, Z. Physik 192 (1966) 423

(6) C. Weitkamp, KFK 510 (1967)

(7) H. Schmidt, W. Michaelis, C. Weitkamp and G. Markus, Z. Physik 194 (1966) 373

(8) H. Schmidt, Frühjahrstagung d. Deutschen Physk. Gesellschaft, Bad Pyrmont, 10. - 15. April 1967

(9) G. Markus, W. Michaelis, H. Schmidt and C. Weitkamp Z. Physik (in press)

(10) G. Markus, Frühjahrstagung d. Deutschen Physik. Gesellschaft, Bad Pyrmont, 10. - 15. April 1967

3. Slow Neutron Inelastic Scattering

3.1. Scattering Law Measurements

W. Gläser, F. Carvalho, G. Ehret

3.1.1. Graphite

Double differential scattering cross section measurements for graphite at 260° C have been completed. The energy and wave vector transfer range for which data have been processed is 0-0.18 eV and 1.5-16 $Å^{-1}$ or in dimensionless unites

$$0 < \beta < 4 \quad \text{and} \quad 10^{-2} < \alpha < 7 \quad \left(\beta = \frac{n\omega}{k_B T},\ \alpha = \frac{n^2 \varkappa^2}{2M_C k_B T}\right)$$

Part of the derived scattering law values $S(\alpha,\beta)$ are represented in Figs. 1 and 2. The solid curves are best fits to the experimental data.

Using the incoherent approximation and the extrapolation technique a frequency distribution was derived. This technique has been considerably improved by including a multiple scattering correction for inelastic processes.

Lit.: F. Carvalho, Verhandl. DPG(VI),1,400 (1966)

3.1.2. Metal Hydrides

The multiple scattering correction allowed the evaluation of an improved distribution of acoustical modes for Zirconium Hydride from the differential cross section measurements at 483°K reported earlier.

Powder samples of Cerium Hydride (CeH_2 and CeH_3) have been investigated. Measurements of the total cross section σ_T have been made for energies between 0.01 and 1 eV and for temperatures of 293 and 523°K. σ_T shows minima at about 0.125 and 0.25 eV corresponding to the harmonic oscillator levels of the H-vibration in the crystal lattice.

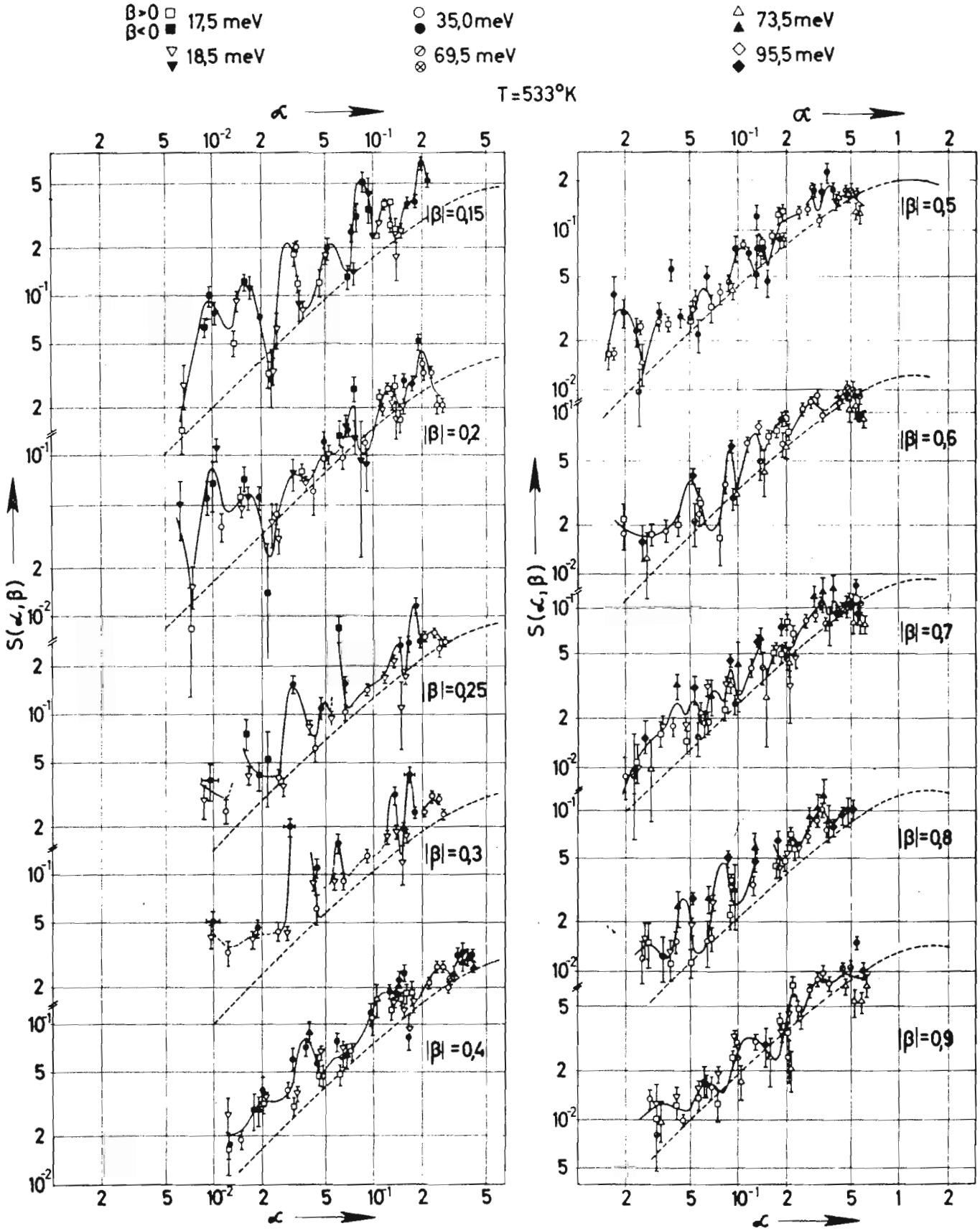

Abb. 1 Experimental results for the scattering law $S(\alpha,\beta)$ of graphite at $T = 533^{\circ}K$; --- calculation with LEAP

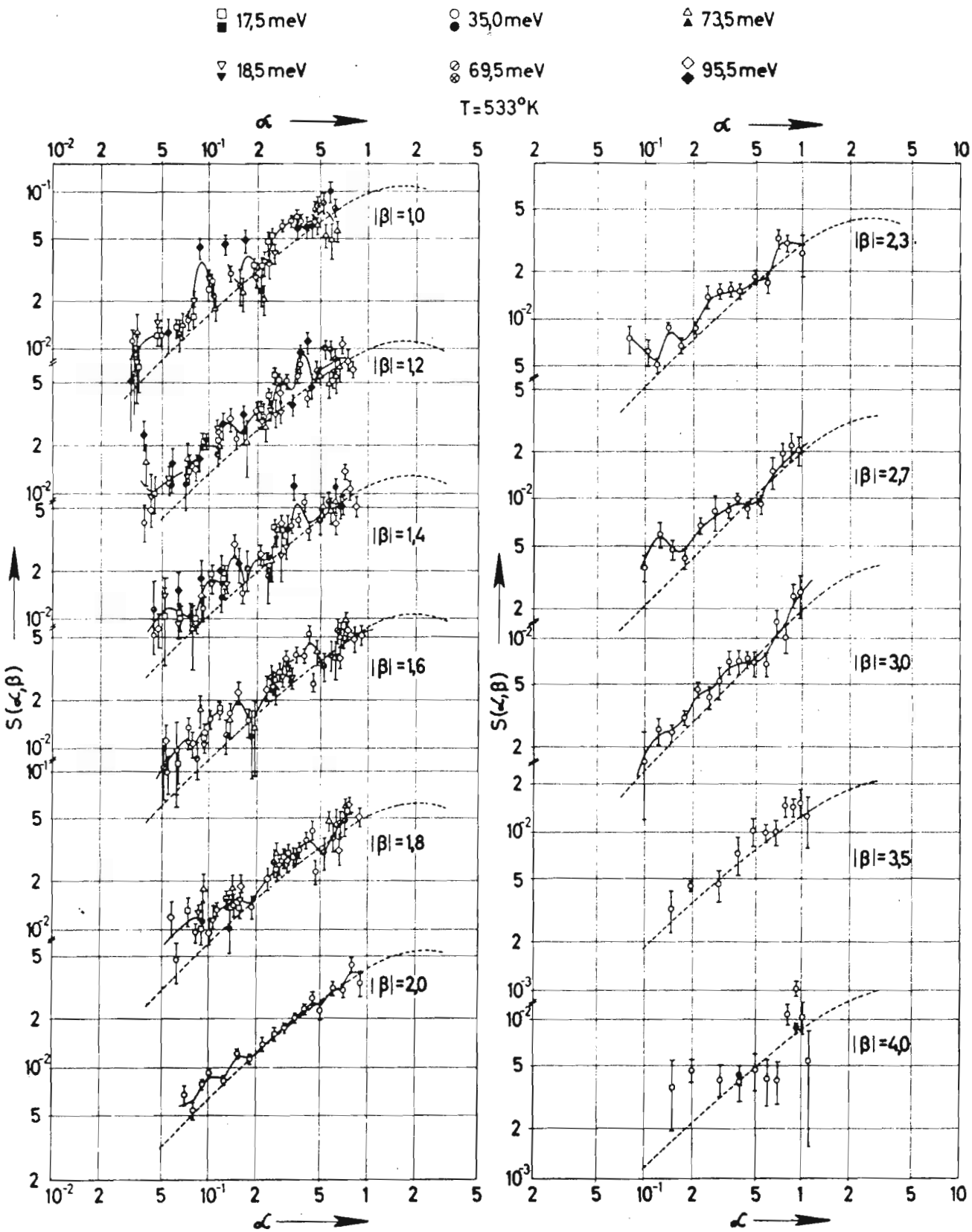

Abb. 2 Experimental results for the scattering law $S(\alpha,\beta)$ of graphite at $T = 533^{\circ}K$; --- calculation with LEAP

3.2. Other Experiments

W. Bührer, W. Gläser, T. Schneider, P. Schweiss

3.2.1. Copper

The phonon dispersion in copper at 293°K has been measured. More than 1200 phonons have been determined in the (100) and (110) planes. A third nearest neighbour Born- von Kármán model was fitted to the points in the 3 symmetry directions [100], [110] and [111]. Using the root sampling techniques a frequency distribution has been calculated from these data.

Lit.: W. Bührer, T. Schneider, W. Gläser, Solid State Communications Vol. 4, pp. 443-446 (1966)

3.2.2. Iron

The phonon dispersion in iron at 293°K has been measured. Sor far about 300 phonons have been collected in the (110) plane.

Lit.: W. Gläser, Verhandl. DPG (VI), 1, 398 (1966)

4. Isochronous Cyclotron

S. Cierjacks et al.

4.1. Development of the T.O.F. Spectrometer

The time-of-flight spectrometer was in operation for several periods during the last year. The facility proved its reliability by several total cross section measurements (see 4.2). The neutrons produced by a thick uranium target were detected with a liquid proton-recoil detector at the end of an evacuated flight path, 56.599 m in length. A typical neutron spectrum obtained from the uranium target is shown in Fig. 1 a.

For the time-of-flight measurements the spectrometer is now provided with a digital time sorter with a maximum of 262.000 channels and a minimum channel width of 0.5 nsec. The data output signals are transfered to an on-line computer, a CDC 3100 with a core storage of 8 K - 22 bit words.

The measurement of the energy resolution showed the expected value of 0.025 nsec/m. This resolution had beendetermined both by the time distribution of γ-rays within the peak of the prompt γ-rays from the target and by measuring the two pairs of closely spaced resonances of Fe^{56}. These pairs are at 512 keV (shown in Fig. 1 b) and 530 keV, respectively. From a comparison of the measured half widths of these resonances with the calculated ones, assuming the 513 and 527 keV resonances to be S-wave resonances, an energy resolution of 200 $\pm$ 50 eV was deduced.

The following possible improvements for the spectrometer are in progress: It is planned to increase the repetition rate from 20 kc/sec to about 160 kc/sec. This leads to a gain in neutron intensity by a factor of about 8. Studies on a suitable H.V. fast pulse generator are in progress. Repetition rates up to 200 kc/sec are acceptable with the present length of the flight path. The increase of the H.V. pulse frequency makes possible time-of-flight measurements with a flight path of 150 m which is under discussion. Also attempts are being made to increase the beam current during the pulses. Test runs with intense ion sources and with the inclusion of source pulsing are in progress.

4.2. Total Cross Section Measurements

In the period covered by this report transmission measurements have been performed with the time-of-flight spectrometer using the following samples: carbon, oxygen, aluminium, calcium and iron. The shape of the total cross sections was determined as a function of energy for these nuclei. Some of the results are given in Figs. 2 - 4.

The appearance of intermediate structure in the shape of the total cross sections of aluminium, calcium and iron have been investigated by means of an autocorrelation analysis. This analysis showed that for the above mentioned elements a significant structure with intermediate widths is present. The averaged distances for aluminium, calcium and iron are the following ones:

element	energy range (MeV)	averaged distance (keV)
Al^{27}	1 - 2	400 ± 50
	2 - 4	300 ± 40
	4 - 6	350 ± 50
	6 - 8	(400)±* 50
Ca^{40}	1 - 2	180 ± 20
	2 - 4	160 ± 15
	4 - 6	(200)±* 30
Fe^{56}	0.5 - 2	240 ± 20
	2 - 4	250 ± 20
	4 - 6	(80)±* 30

* The values in parenthesis do not fill strictly the condition of significance.

4.3. Partial Cross Section Measurements

The use of the liquid scintillators NE 213, o-Fluortoluene, and the method of pulse-shape discrimination of Owen made possible the measurements of the (n,α) cross sections of C^{12} and F^{19} with 14.08 MeV neutrons. In this case the liquid scintillators simultaneously served as target and detector. The energies of the α-particles were > 5.3 MeV. The cross section for the $C^{12}(n,\alpha)Be^{9}$ reaction was found to be (72.7 ± 6.8) millibarns, and for the $F^{19}(n,\alpha)N^{16}$ reaction the cross

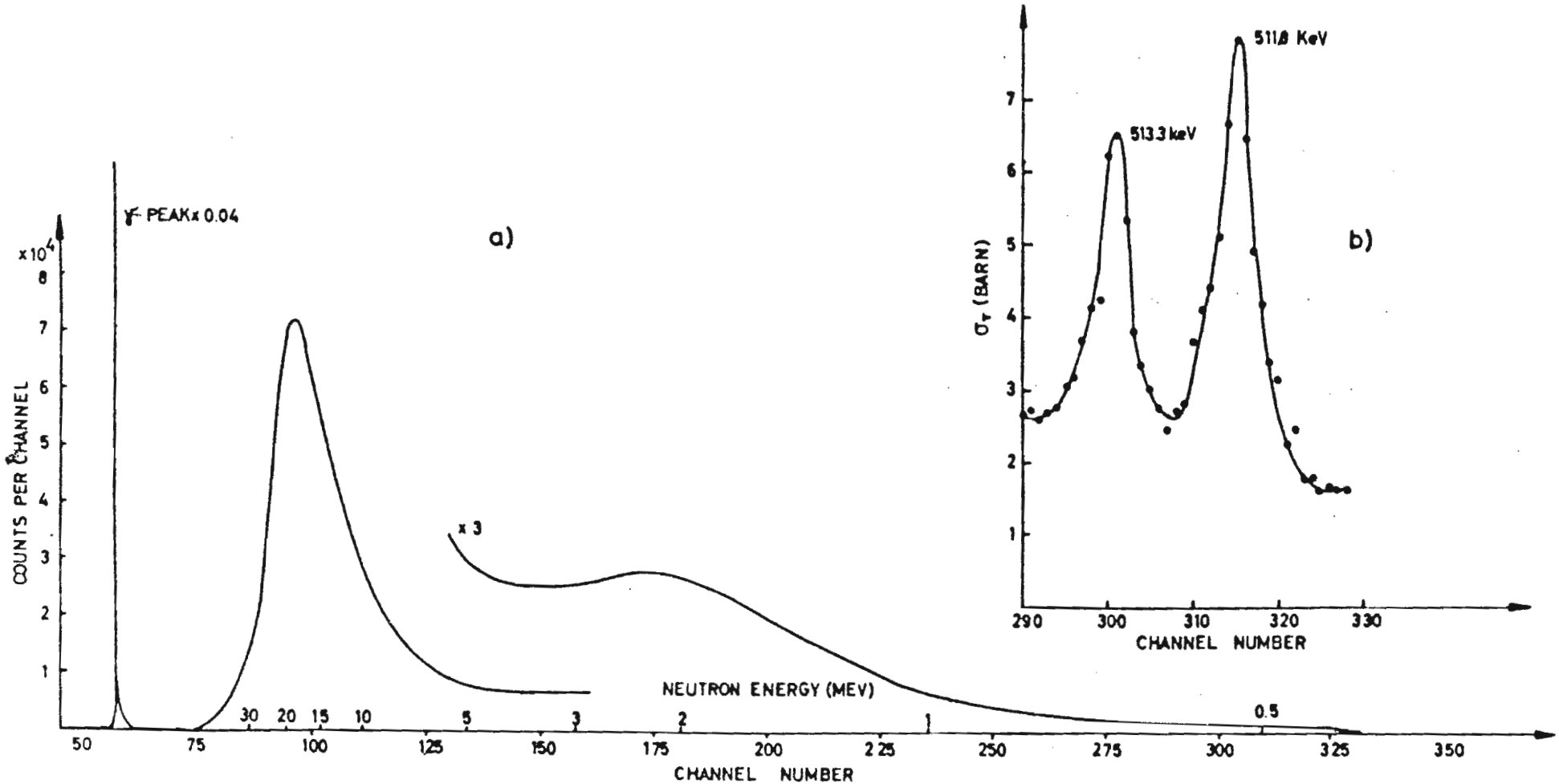

Fig.1 a) Typical neutron time-of-flight spectrum
b) σ_T for natural iron in the 510 keV region.

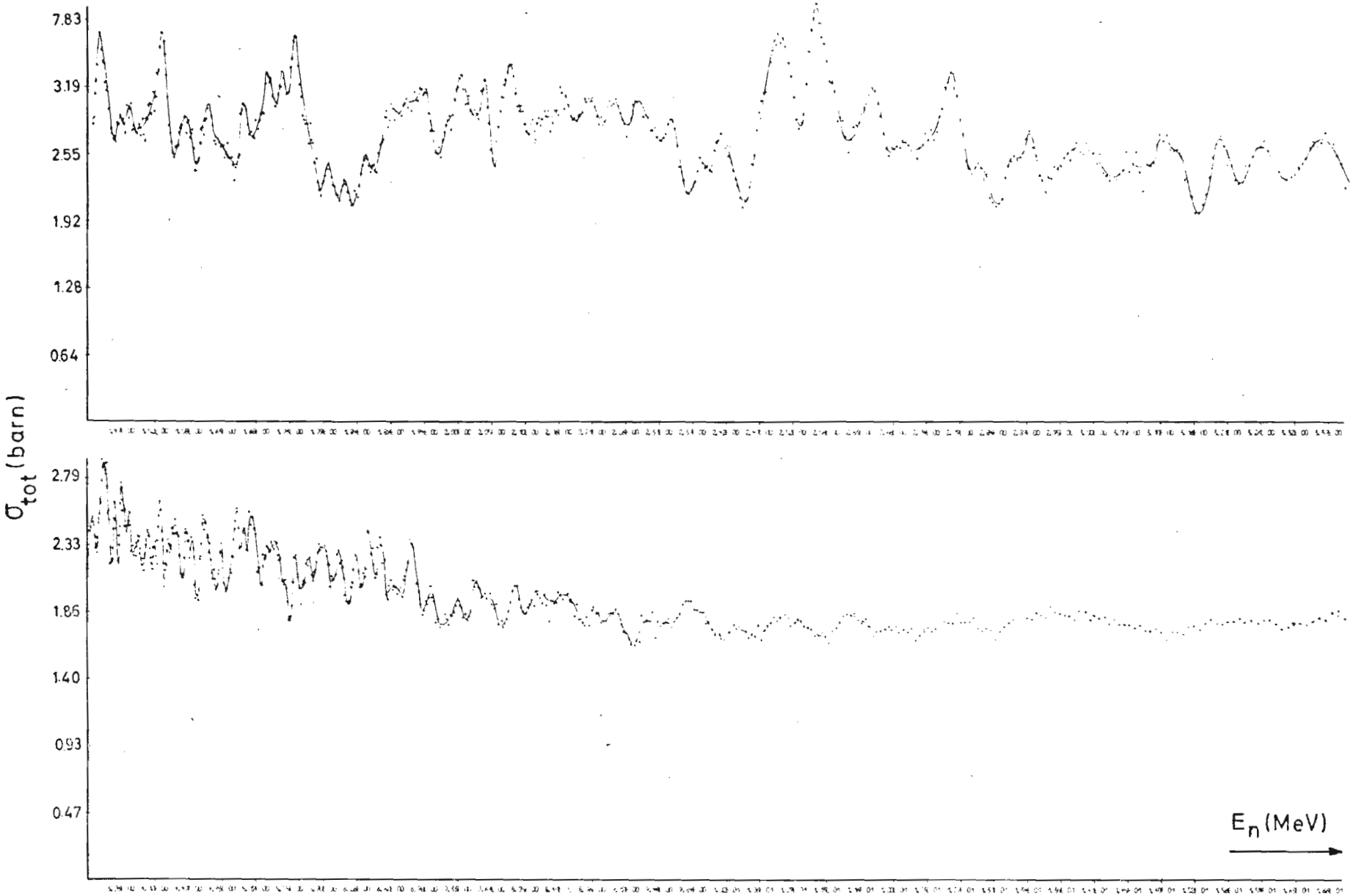

Fig. 2 Total neutron cross section of aluminium in the region from 1.4 to 16.6 MeV

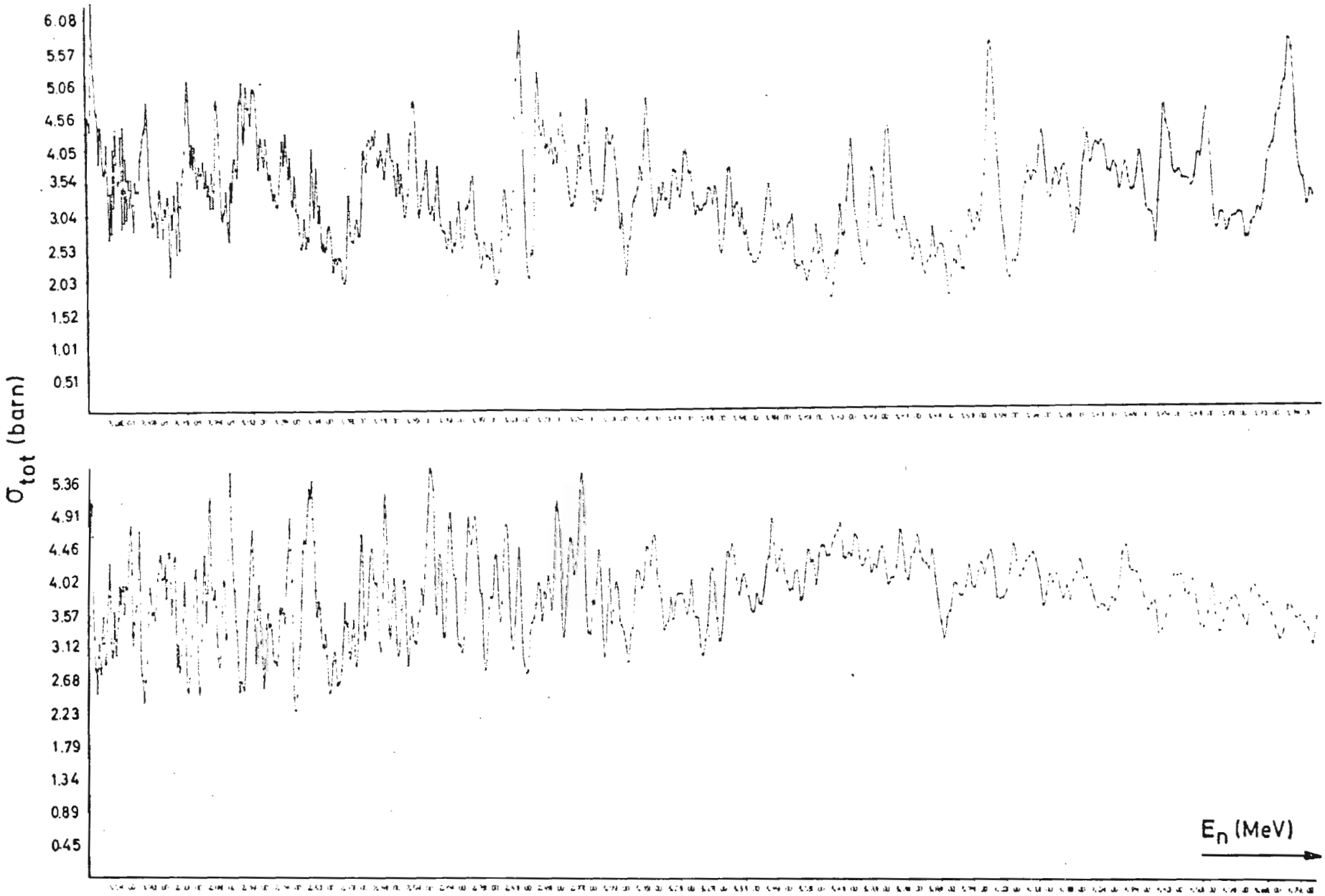

Fig. 3 Total neutron cross section of natural calcium in the region from 0.9 to 4.8 MeV .

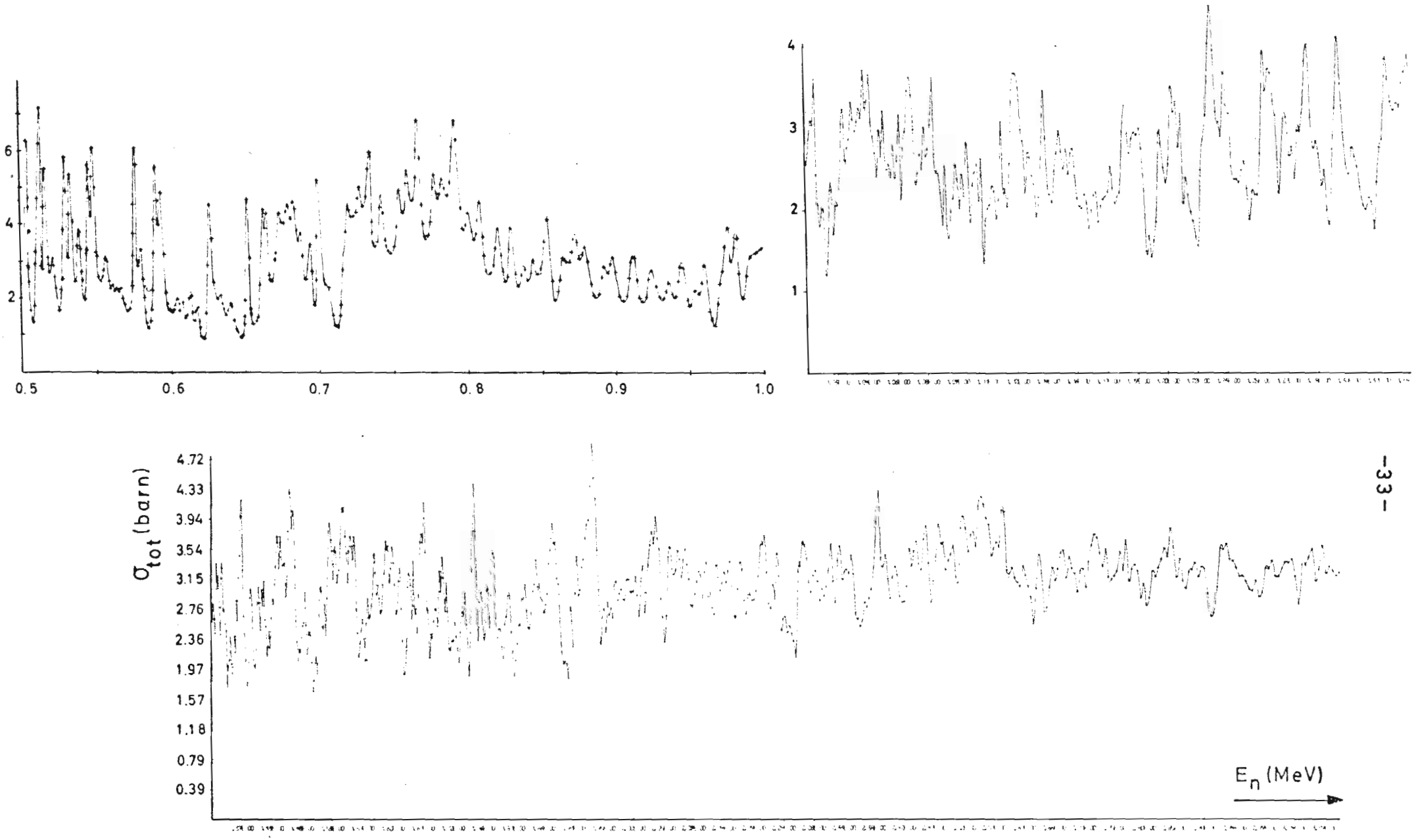

Fig. 4 Total neutron cross section of natural iron in the region from 0.5 to 3.1 MeV

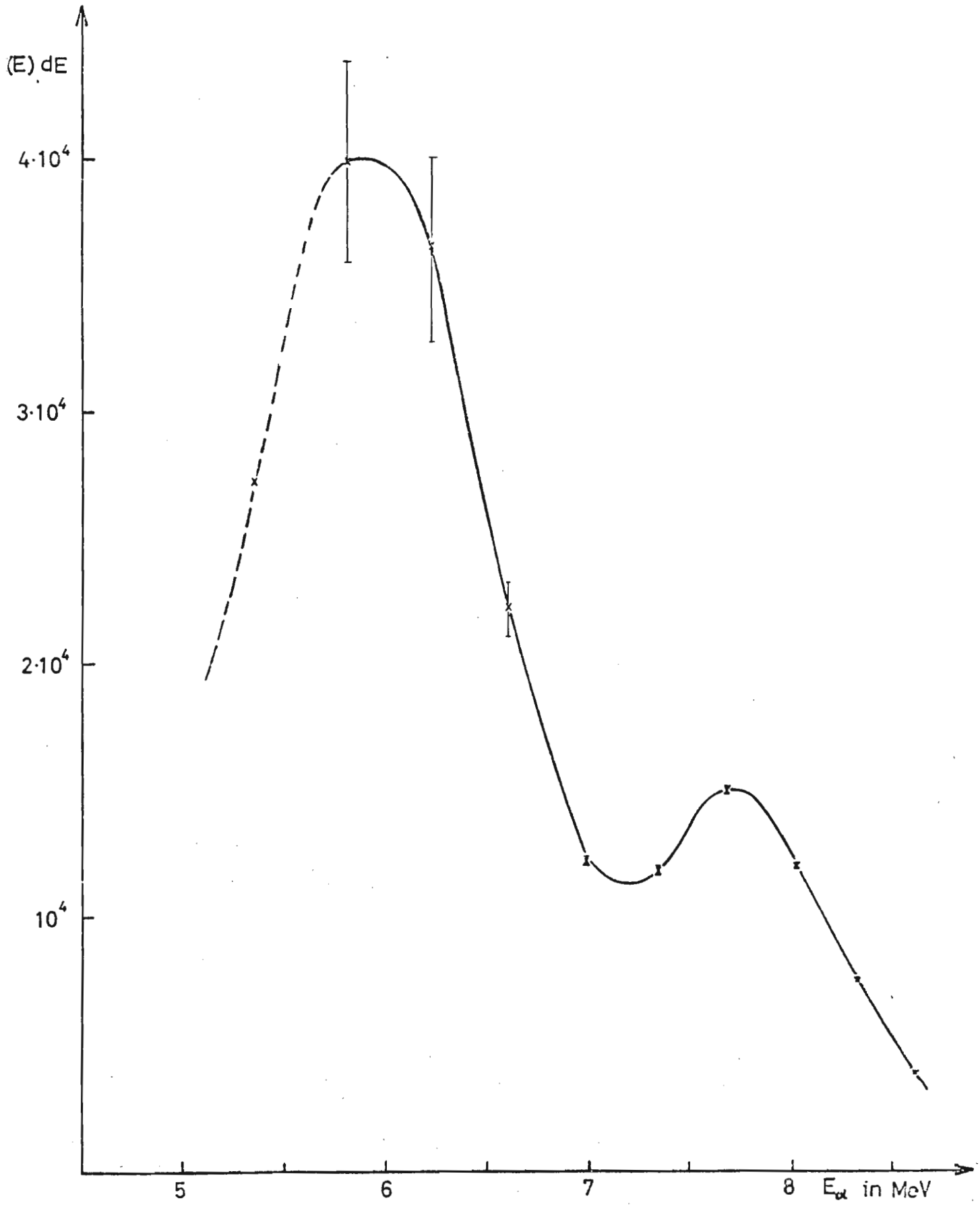

Fig. 5 Energy distribution of the emitted α-particles

section was (36.6 ± 9.2) millibarns.

The study of the energy distribution of the α-particles emitted in these reactions (see Fig. 5 for $C^{12}(n,\alpha)Be^{9}$) showed evidence for an assumption of direct processes.

At the same time, measurements with solid state detectors are going on. For this purpose a chamber, provided with semiconductor telescopes, was put into operation. The operation of the apparatus was checked by preliminary measurements on Si^{28}. With this set-up it seems possible to measure partial cross sections and angular distributions on medium weight nuclei for several energy regions at the same time (in the range from 5 to 30 MeV).

5. New Developments in Instrumentation

5.1. On-line Computers

G. Krüger

5.1.1. Small On-line Computers Coupled with Experiments

The small on-line computer equipment of the IAK was further extended during the last year.

An additional 8 K 18 bit memory and a correlated display unit have been added to the CAE 510 computer at the van de Graaff accelerator. A new program was written which allows a direct evaluation of time-of-flight cross section measurements on-line.

The institute developed a newly designed input interface for the CDC 3100 of the cyclotron-laboratory. For the time-of-flight cross section measurements of the Isochron-Cyclotron group (IV) a sophisticated program was written, which allows e.g. automatic correction of instrumental drifts during the measurements.

The data-input-system of MIDAS was extended, so that now 10 experiments can be connected to the computer. Some of the remote buffer and control stations have also been increased to 48 bit input capacity. Most parts of the extended MIDAS 66 are now in operation (1). The duration of the programming effort for the new operating system MESPRO 66 was much longer than originally planned. There is a lack of higher organized real-time programming language; all of the programming work must therefore be done on the assembler language level.

Some features of the new operating system are now proved. The newly designed accumulation program for multichannel experiments based on a special list-processing technique is running very successfully. With this procedure, the computer - disc combination (a CDC 8090 and an IBM 1311) can operate as a 256 K multichannel analyser. From the user's point of view there is no serious difference between this machine and a ordinary magnetic core analyser.

To increase the safety of the system a checkpoint technique was built into the operating system. The contents of the different storage units are dumped in regular intervals into magnetic tape. In the same

way all important changes in the system status are logged into the tape. After a breakdown of the system, the tape is rewound to the last checkpoint. An automatic recovery routine updated step-by-step the different status changes and restarts the measuring process exactly in the same status as existed at the time the breakdown occured.

5.1.2. Data Transmission

A data transmission system, using normal twisted pair cables, was proved very useful. We can now exchange data with a rate of more than 100 KHz between the institute, the reactor and the cyclotron building.

Using a CRT-display station and a command panel the experimenter can now control the progress of his experiment in the reactor hall from his office.

5.1.3. Large Time-sharing System

The development of the small computers has nearly reached its final stage. The next steps for closer integration of experiments and data processing equipment require new features which the small machine cannot offer.

Performance of more sophisticated experiments with closer man-machine interaction in the nuclear physics field demands:

- more computation power
- selforganizing direct-access storage with higher capacity
- easier programming and manipulating of the whole system by the experimenter.

Studies of the feasibility and the structure of such an integrated system were made. We have chosen as our solution of the problem a large multiprocessor, time-sharing system with a hierarchy of direct-access storage, preferable operating in a kind of "fail-soft" mode. The KFK will install such a system and both the existing on-line computers and a number of different experimental systems should be directly integrated.

The IAK participates in this project. Its major objective will be the development of a new experiment-oriented real-time language, which facilitates the interaction between experiment hardware, experimenter, and the "logic power" of the computer system.

Another essential point is the implementation of a generalized interface system to connect the experiment via data transmission to the I/O channels of the computer. The functional structure of such a modularized interface system has been designed, so that the industry can begin to construct the hardware.

(1) G. Krüger, G. Dimmler, G. Zipf, H. Hanak, R. Merkel
Ein Doppelcomputersystem zur integrierten Datenverarbeitung am Reaktor FR 2, KFK-Bericht No. 458 (1966)

5.2. Neutron Flash Tube

A. Schmidt

During the last yearthe neutron flash tube device has been used successfully as a pulsed neutron source for time-of-flight measurements at the fast subcritical reactor assembly SUAK. The tube was operated at a pulse recurrence frequency of 200 c/sec with an intensity of about 5×10^8 n/pulse and a pulse duration of 1 μsec. Several improvements have been made during 1966. By solving some material problems which arise under conditions of high pulse recurrence frequencies and high average power the reliability was improved considerably. Still higher target lifetimes of several 100 hours are now achieved by operating the tube at ultra high vacuum conditions. New targets have been developed with a material thickness of about 2 mg/cm^2 average titanium sheet thickness. A special feature of these targets is a preselected 2 : 1 variation in thickness from the center of the 5 cm Ø, 20 cm^2 target to the edge to account for the higher sputtering rate at the center due to the ion current distribution.

The new tubes will be used under long-run conditions for further measurements at the SUAK facility. A second device will be tested under shortpulse conditions. We expect to obtain the same neutron output of 5×10^8 n/pulse for pulses of about 0,1 μsec duration. This will increase the time resolution for fast neutron spectra measurements.

5.3. Semiconductor-Detector Development

O. Meyer

Fully depleted surface-barrier-detectors are now fabricated with depletion layers (=crystal-thickness) up to four mm. Fully depleted windowless counters can be used

1. as dE/dx counters
2. as high resolution counters used in a stack to stop energetic charged particles
3. as counters with short pulse risetime
4. as counters for the detection of uncharged particles (γ or neutrons) without "edge-effects".

Germanium-lithium-drifted γ-spectrometers are now fabricated with sensitive volumes up to 45 cm^3. These diodes are coaxially drifted with the p-core open at both ends. The special geometry (a circular cross section instead of a trapezoidal cross section and the two open ends) gives a considerable improvement in the rise-time distribution and, as a consequence, a considerable reduction of resolving time in coincidence experiments.

II. PHYSIK-DEPARTMENT, TECHNISCHE HOCHSCHULE MÜNCHEN (GERMANY)

1. Cross-Section Measurements for Subthermal Neutrons

K. Knorr

The total neutron cross sections of the rare earth elements Tb, Dy, Ho, Er, Tm, and Lu were measured for neutron energies between 0.14 and 3 MeV. For the transmission experiment a mechanical velocity selector with an energy resolution of 15% was used. The specific energies of the neutrons were found by the time of flight method and by comparison with equivalent Au foils and $1/_v$ extrapolation from 97.8 b for 25.3 MeV. The purity of the metal foil samples (specified with 99.9% by the manufacturer) was checked by activation analysis (for Dy and Eu) and with neutron capture gammas on a crystal spectrometer (for Gd and Sm). The values of the total cross section with an estimated error of 1.5% are given in figure 1. Presently the paramagnetic cross sections of the rare earth elements will be measured to obtain a definite value for the absorption cross section.

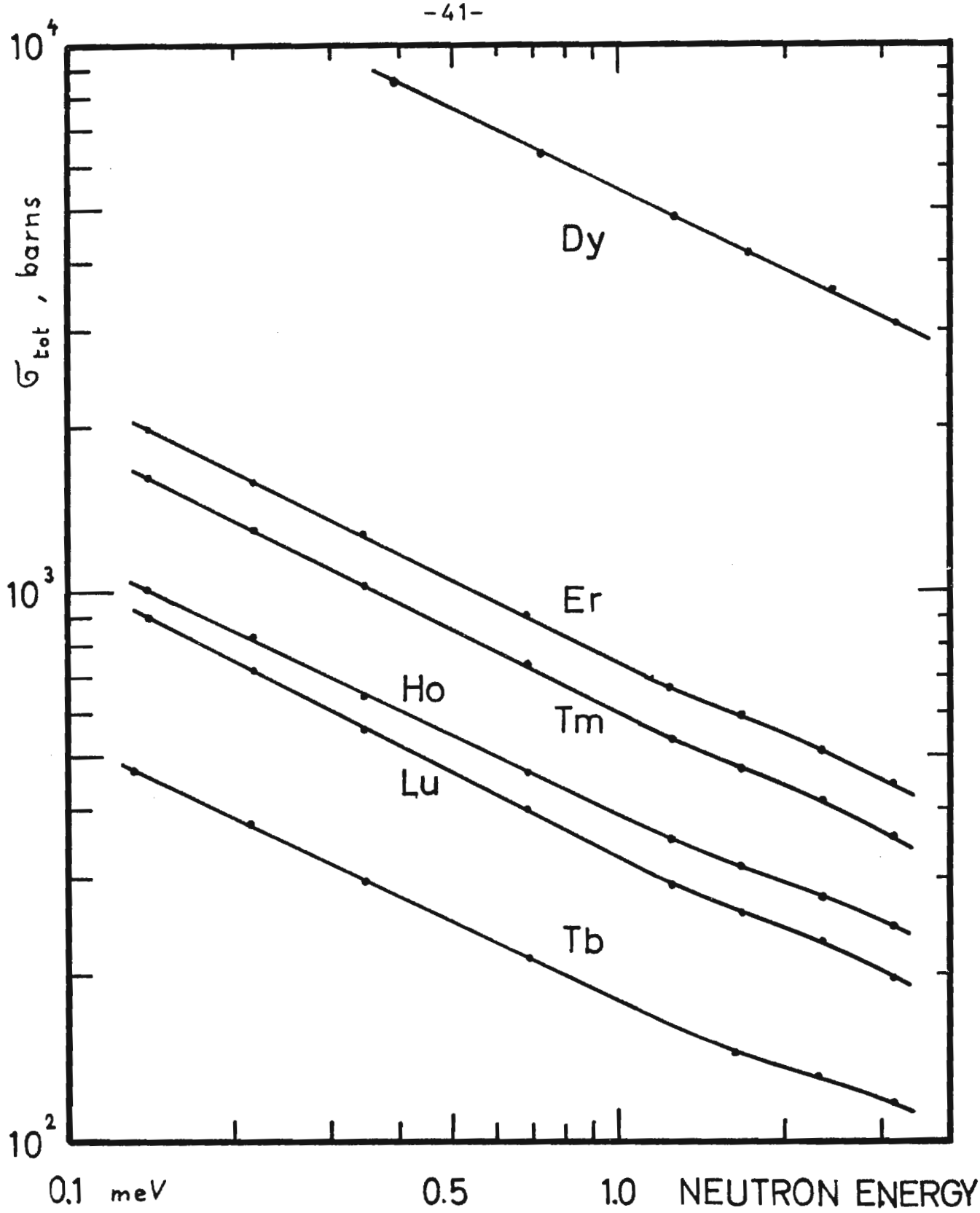

TOTAL CROSS SECTION σ_{tot} FOR SUBTHERMAL NEUTRONS

K. Knorr

T.v.Egidy, H.Mahlein, W.Kaiser, B.Dutta, A.Suarez

2. Measurement of conversion electrons following neutron capture with a betaspectrometer at the reactor FRM.

Results in 1966:

Dy^{165}, about 250 lines between 0 keV and 7 MeV, multipolarities determined, level scheme with spins and parities derived.

Re^{186}, about 130 lines between 0 keV and 500 keV, multipolarities determined, level scheme with spins and parities derived.

Re^{188}, about 70 lines between 0 keV and 500 keV, multipolarities determined, level scheme with spins and parities derived.

Sm^{153}, about 50 lines between 0 keV and 500 keV, multipolarities determined.

Cd^{114}, about 140 lines between 1350 keV and 9200 keV, multipolarities determined, level scheme with spins and parities derived.

Ag^{110}, about 30 lines between 0 keV and 500 keV.

As^{76}, about 3 lines, too small.

3. Measurements of (n, 2n) cross-sections for 14 MeV neutrons

3.1. Measurements with the Fermi-water-tank method

J.Feicht and H.Vonach

The (n, 2n) cross-section of Bi was determined to 2 . 25 ± 0,25 bn using this new method. Further measurements for a number of other elements are planned in the near future.

3.2. Measurements of (n, 2n) cross-sections in the heavy element region (A = 100 - 200) by means of the activation method.

W.Dilg and H.Vonach

Determinations of (n, 2n) cross-sections for about 20 nuclides are in progress by means of absolute measurement of the K-Xradiation emitted in the decay of the nuclides formed in the reactions.

4. Measurements of thermal neutron capture cross-section and isomeric cross-sections ratios by the activation method.

W.Mannhart and H.Vonach.

Thermal neutron capture cross-sections and isomeric cross-section ratios were determined for a number of even nuclei in the region of the neutron numbers 38 - 48 in course of the systematic study of the behaviour of the $2p_{1/2}$ - $1g_{1/2}$ neutron shell model states. Preliminary results are:

a) cross-sections

Reaction	cross-section (bn)
Zn^{69} (n,γ) Zn^{69m}	0,072 ± 0.004
Zn^{70} (") Zn^{71m}	0,0081 ± 0,0012
Zn^{70} (") Zn^{71g}	0,083 ± 0,007
Ge^{70} (") Ge^{71g+m}	3,15 ± 0,16
Ge^{79} (") Ge^{75m}	0,143 ± 0,014
Ge^{76} (") Ge^{77m}	0,092 ± 0.010
Se^{76} (") Se^{77m}	17,8 ± 1,8
Se^{78} (") Se^{75m}	0,25 ± 0,015
Se^{82} (") Se^{83m}	0,039 ± 0,005
Se^{82} (") Se^{83g}	0,0058 ± 0,0007
Sr^{84} (") Sr^{85m}	0,506 ± 0,040
Sr^{86} (") Sr^{87m}	0,810 ± 0,060

b) cross-section ratios

Reaction	$\frac{\sigma_H}{\sigma_H + \sigma_L}$ Ratio
Zn^{68} (n,γ) Zn^{69}	0,082 ± 0,006
Zn^{70} (") Zn^{71}	0,093 ± 0,016
Ge^{74} (") Ge^{75}	0,319 ± 0,018
Ge^{76} (") Ge^{77}	0,335 ± 0,020
Se^{78} (") Se^{79}	0,37 ± 0,004
Se^{80} (") Se^{81}	0,114 ± 0,010
Se^{82} (") Se^{83}	0,129 ± 0,022
Sr^{84} (") Sr^{85}	0,374 ± 0,030

σ_H = cross-section for formation of the high spin state,
σ_L = cross-section for formation of the low spin state.

In most cases the meta -stable state is identical with the high-spin state, in some cases, however the level order may be reversed.

5. Measurements of total mass-absorption coefficients for X- and γ-rays

R.Knerr and H.Vonach

Using the crystal diffraction spectrometer of the FRM as a source of monochromatic X- and γ-rays, total mass-absorption coefficient for about 20 Elements were measured for photon energies in the range 30 - 200 KeV with an accuracy of about 2%.

L.Koester, N.Nücker, W.Nistler

6. "Neutron Gravitation-Refraktometer"

With the neutron gravitation refractometer, at the FRM, the coherent scattering lengths for bound atoms were measured for the elements

hydrogen: $a_{coh} = -(3{,}719 \pm 0{,}002)F$
carbon: $a_{coh} = +(6{,}648 \pm 0{,}004)F$
chlorine: $a_{coh} = +(9{,}633 \pm 0{,}006)F$.

By an intercomparison of the value for carbon with data already known, the gravitational acceleration on free neutrons could be determined. Compared to the local value g, it is $(0{,}9992 \pm 0{,}0021)g$ and $(0{,}9973 \pm 0{,}0030)g$. Besides, it is shown, that the difference in gravitational acceleration between the two orientations of neutron spins ($\pm 1/2$) to the direction of gravity cannot exceed $5 \cdot 10^{-3}$ g. /1/

Current experiments deal with the measurement of scattering lengths for Bi, Pb, S, Sn and Zn (N.Nücker). The coherent scattering lengths for deuterium, oxygen, nitrogen and halogenics will be measured in near future (W.Nistler).

/1/ L.Koester, Z.Physik 198 (1967)187

W.Köhler

7. "Measurements of Average n,n'-Reaction Cross-Sections" +)

For several n,n'-reactions, leading to a metastable residual nucleus, the cross-sections averaged over the neutron spectrum of the light-water moderated reactor FRM were determined by the activation method. The measurement of the induced activity was done either by γ-spectrometry with a calibrated 3x3 inch NaI(Tl)-crystal or in the case of highly converted isomeric states by X-ray measuring of the K_α-line with a 1 mm thick NaI(Tl)-crystal, covered by a 0,2 mm beryllium window. The flux density in the irradiation position was datermined by the reaction $Ni^{58}(n,p)Co^{58}$, using an average cross section of 100 mbn. The preliminary results of the measurements are compiled in the following table.

+) Summary of the FRM-Bericht Nr.81(1966), W.Köhler:"n,n'-Reactions for Flux Density Measurements"

Average n,n'-Reaction Cross Sections

Reaction	Isomeric State Energy [keV]	Halflife	Kind and Energy [keV] of detected radiation		Average n,n'-Cross-Section [mbn]
$Rh^{103}(n,n')Rh^{103m}$	40	58 min	X	20,2	403 ± 40
$Se^{77}(n,n')Se^{77m}$	160	17,4 s	γ	160	652 ± 30
$In^{115}(n,n')In^{115m}$	335	4,5 h	γ	335	181 ± 10
$Sr^{87}(n,n')Sr^{87m}$	390	2,8 h	γ	390	91 ± 5
$Cd^{111}(n,n')Cd^{111m}$	397	48,6 m	γ	247	289 ± 15
$Au^{197}(n,n')Au^{197m}$	410	7,2 s	γ	280	450 ± 70
$Ba^{137}(n,n')Ba^{137m}$	661	2,6 m	γ	661	189 ± 10
$Y^{89}(n,n')Y^{89m}$	909	16 s	γ	909	113 ± 10
$Os^{190}(n,n')Os^{190m}$	1700	9,9 m	γ	500 361	3,9 ± 0,2
$Pb^{204}(n,n')Pb^{204m}$	2190	67 m	γ	912 898	15,3 ± 0,7

Measurement of the Resonance-Activation Integral of Mo^{98}

E. Schneider

8. The methods for measuring the resonance-activation-integral (R I) of Mo^{98} used in this experiment were the cadmium-ratio (CR) and the quasi-absolute method based on the following formulae: /1/

$$(RI)^x = \frac{(Act)^x}{(Act)_{ref}} (RI)^{ref} \qquad \text{(quasi absolute method)} \qquad (1)$$

$$(RI)^x = \frac{(CR - 1)^{ref} \quad x \; (RI)^{ref}}{(CR - 1)^x \; . \quad ref} \qquad \text{(CR - method)} \qquad (2)$$

As reference material gold was chosen with the thermal cross-section $\sigma_o = 98,8$ bn and (RI) = 1490 ± 30 bn /2/: σ_o for Mo^{98} must also be known, when the CR-method is used. The same result by either method was obtained, when in (2) a value of σ_o Mo^{98} = 0,18 barn /3/ was inserted.

The absolute and relative activities of both gold and molybdenum were measured by counting the 411 keV photopeak of Au^{198} and the 780 + 740 keV peaks of Mo^{99} with a 3 x 3 NaJ(Tl) crystal. Absolute intensities for the γ-abundance of Mo^{99} could be found in /4/. For the gold wires the self-shielding-factors of ref./5/ were taken. Those for the Mo samples were calculated by the method given in ref./6/.

For the resonance-activation-integral of Mo^{98} a preliminary value of 6,6 ± 0,6 bn is given ($I_{1/v}$ subtracted, cutoff energy 0,56 eV /7/), which is in good agreement with 6,3 bn calculated by Kapchigashev and Jn.P.Popov from the resonance parameters 181. They take into account the 12 eV resonance in their work which before was not identified.

The determination of the resonance activation integrals for Rh^{103} and Jr^{191} is not yet finished.

References:

/1/ Studies of the (RI) of Re and Tm
IITRI 578 P 24-2 (1961)
/2/ Jirlov and Johansson, J.of Nucl.En. 11 (1860) 101-
/3/ Baumann, M.P., DP 817 (1963)
/4/ Crowther and J.S. Eldridge, Trans.-Amer.Nucl.Soc. 7 (1964) 87
/5/ E.D. Mc.Garry, Trans.-Amer.Nucl.Soc. 7 (1964) 86
/6/ J.Gilat and Y.Gurfinkel, Nucleonics 21, No.8 (Aug.63) 143
/7/ R.Takeoa and K.Inove, J.Nucl.Sci.Tech. 1 (1964) 172
/8/ Kapchigashev and. Jn.P.Popov, Soviet Atomic Energy 15 (1964) 808

III. INSTITUT FUER KERNPHYSIK, UNIVERSITY OF FRANKFURT/MAIN (Germany)

Fast Neutron Excitation Functions

(R. Bass, P. Haug, K. Krüger, J. Müller, G. Presser, F. Saleh-Bass, B. Staginnus, W. Strassheim, R. Wechsung)

The reactions listed in table I have been investigated during the last three years. Experimental details and graphs showing some of the results have been given in previous EANDC progress reports. Final data evaluation has now been completed and tables with numerical results have been prepared, which are available on request.

Work started previously on the reactions $^{7}Li(n,n'\gamma)^{7}Li(0.48)$ and $^{6}Li(n,n'\gamma)^{6}Li(3.56)$ has been interrupted to await improvements of the experimental arrangement. The reactions $^{88}Sr(n,p)^{88}Rb$ (E_n = 8-9 and 14 MeV) and $^{208}Pb(n,p)^{208}Tl$ (E_n14 and 17-18 MeV) are currently under investigation.

Table I: Summary of excitation function measurements

Reaction	Neutron Energy Range E_n(MeV)	Neutron Energy Spread ΔE_n(keV)	Typical Uncertainty abs. %	Typical Uncertainty rel. %	Exp. Technique +)	Final States Invest. ++)
$^{19}F(n,p)^{19}O$	5.0-9.0	25	15	7	a	
$^{19}F(n,\alpha)^{16}N$	5.0-9.0	25	12	5	a	
$^{23}Na(n,p)^{23}Ne$	5.8-9.0	25	15	7	a	
	5.3-8.0	25	15	10	b	0
$^{23}Na(n,\alpha)^{20}F$	6.8-9.0	25	15	7	a	
$^{27}Al(n,p)^{27}Mg$	6.0-9.0	25	15	5	a	
$^{28}Si(n,p)^{28}Al$	6.0-9.0	25	15	5	a	
$^{31}P(n,\alpha)^{28}Al$	6.1-9.0	25	15	5	a	
$^{31}P(n,n'\gamma)^{31}P$	1.3-4.3	40	25	10	d	1.27, 2.23 3.13, 3.29
$^{40}Ca(n,p)^{40}K$	2.0-6.0	100-200	10-20	5-15	b,c	0, 0.03, 0.80, 0.89
$^{40}Ca(n,\alpha)^{37}A$	2.0-5.0	100-200	10-20	10	b	
$^{40}Ca(n,n'\gamma)^{40}Ca$	3.4-6.0	100-200	25	10	b,c,d,	0, 3.35, 3.73, 3.90

+) a: activation; b: direct 4π measurement of charged particles in scintillators; c: charged particle - γ-coincidence measurement; d: γ-measurement with ring scatterer

++) Excitation energies of final states are given, where such states have been separated

IV. PHYSIKALISCHES STAATSINSTITUT, I. INSTITUT FÜR EXPERIMENTAL PHYSIK, HAMBURG (Germany)

Excitation Functions of some Fast Neutron Reactions

(M. Bormann, C. Abels, W. Carstens and I. Riehle)

Continuing earlier investigations on cross sections of fast neutron reactions using the activation technique new results have been obtained for some (n,p), (n,α), (n,2n) and (n,n') reactions in a neutron energy region of several MeV above 13 MeV. Neutrons were produced by the reaction $H^3(d,n)He^4$ in thin titanium-tritium targets with the 1 and 3 MeV deuteron beams of two available Van de Graaff generators. For varying the neutron energy on the samples use was made of the angular dependence of the neutron energy in the laboratory system for the source reaction. Gamma activities were detected by means of a NaI well-crystal and counting all pulses above the threshold corresponding to 50 keV gamma energy. For this discrimination setting the counting efficiency for the well crystal was calculated. A pneumatic sample transport system was used in those cases where the activities had short half-lives. The neutron flux on the samples was measured with a stilbene recoil proton spectrometer.

The results are summarised in Table I and II. In most cases also the half-lives of the activities produced have been remeasured. These results are stated in the Tables with error indications. The excitation functions for total cross sections have been compared with the predictions of the statistical theory. Good agreement was found for the (n,2n) reactions.

Table I (n,2n) Cross Sections

$Cl^{35}(n,2n)Cl^{34g}$		$Cr^{52}(n,2n)Cr^{51}$		$Ge^{76}(n,2n)Ge^{75m}$		$Se^{80}(n,2n)Se^{79m}$	
E_n(MeV)	σ (mb)	E_n(MeV)	σ (mb)	E_n(MeV)	σ (mb)	E_n(MeV)	σ (mb)
14.89 ± 0.25	5.1 ± 0.4	12.94 ± 0.20	64 ± 5	13.00 ± 0.12	827 ± 57	13.00 ± 0.14	544 ± 273
15.40 ± 0.26	5.6 ± 0.7	$13.51 {}^{+0.25}_{-0.20}$	147 ± 12	13.25 ± 0.17	868 ± 74	13.25 ± 0.15	466 ± 207
15.91 ± 0.27	11.3 ± 1.8			13.50 ± 0.19	771 ± 53	13.50 ± 0.16	893 ± 453
		$14.10 {}^{+0.28}_{-0.26}$	276 ± 19	13.75 ± 0.19	908 ± 71	13.75 ± 0.18	591 ± 282
$T_{1/2} = 1.77 \pm 0.08$ s				14.00 ± 0.20	952 ± 80	14.00 ± 0.19	782 ± 394
		$14.88 {}^{+0.30}_{-0.31}$	412 ± 29	$14.25 {}^{+0.20}_{-0.22}$	956 ± 77	$14.50 {}^{+0.19}_{-0.20}$	1337 ± 524
		$15.62 {}^{+0.31}_{-0.35}$	476 ± 33	$14.50 {}^{+0.18}_{-0.21}$	1008 ± 78	$14.75 {}^{+0.19}_{-0.23}$	1286 ± 646
		$16.31 {}^{+0.30}_{-0.38}$	506 ± 35	$14.75 {}^{+0.19}_{-0.21}$	1056 ± 83	$15.00 {}^{+0.20}_{-0.25}$	1515 ± 607
		$17.23 {}^{+0.26}_{-0.42}$	491 ± 34	$15.00 {}^{+0.19}_{-0.21}$	1064 ± 87	$15.25 {}^{+0.19}_{-0.24}$	1304 ± 531
		$18.02 {}^{+0.24}_{-0.37}$	515 ± 36	$15.50 {}^{+0.19}_{-0.23}$	1013 ± 76	$16.00 {}^{+0.16}_{-0.25}$	1264 ± 607
		$18.89 {}^{+0.15}_{-0.22}$	493 ± 35	$15.75 {}^{+0.18}_{-0.26}$	1074 ± 85	$16.25 {}^{+0.13}_{-0.27}$	1102 ± 283
		19.56 ± 0.14	462 ± 32	$16.00 {}^{+0.15}_{-0.25}$	977 ± 73	$16.50 {}^{+0.11}_{-0.26}$	1221 ± 417
		$T_{1/2} = 27.8 \pm 0.1$ d		$16.25 {}^{+0.11}_{-0.21}$	968 ± 76	$16.75 {}^{+0.12}_{-0.20}$	1011 ± 317
				$16.50 {}^{+0.10}_{-0.23}$	939 ± 74	$T_{1/2} = 3.9$ m	
		$T_{1/2} = 48.2 \pm 0.1$ s →		$16.75 {}^{+0.10}_{-0.19}$	913 ± 76		

Table I (continued)

$Br^{79}(n,2n)Br^{78}$		$Rb^{85}(n,2n)Rb^{84m}$		$Rb^{85}(n,2n)Rb^{84}$		$In^{115}(n,2n)In^{114m_1}$	
E_n(MeV)	σ (mb)	E_n(MeV)	σ (mb)	E_n(MeV)	σ (mb)	E_n(MeV)	σ (mb)
13.18 ± 0.13	791 ± 85	$12.94^{+0.38}_{-0.34}$	231 ± 17	$12.94^{+0.38}_{-0.34}$	738 ± 59	13.50 ± 0.18	47.3 ± 9.7
13.46 ± 0.12	837 ± 89	$13.51^{+0.38}_{-0.39}$	277 ± 19	$13.51^{+0.38}_{-0.39}$	887 ± 71	13.75 ± 0.19	48.4 ± 17.6
13.71 ± 0.13	870 ± 93	14.10 ± 0.47	341 ± 21	14.10 ± 0.47	964 ± 58	$14.25^{+0.21}_{-0.23}$	34.7 ± 13.0
13.98 ± 0.14	912 ± 98	14.88 ± 0.53	374 ± 28	14.88 ± 0.53	1174 ± 94	$14.50^{+0.20}_{-0.23}$	28.5 ± 6.4
14.24 ± 0.16	969 ± 104	$15.62^{+0.55}_{-0.58}$	393 ± 29	$15.62^{+0.55}_{-0.58}$	1170 ± 93	$14.75^{+0.21}_{-0.25}$	25.3 ± 3.8
14.51 ± 0.18	997 ± 107	$16.31^{+0.54}_{-0.61}$	418 ± 31	$16.31^{+0.54}_{-0.61}$	1160 ± 93	$15.00^{+0.22}_{-0.26}$	22.2 ± 6.1
14.76 ± 0.20	968 ± 103	$17.23^{+0.48}_{-0.67}$	423 ± 32	$17.23^{+0.48}_{-0.67}$	1196 ± 96	$15.25^{+0.22}_{-0.28}$	25.5 ± 11.3
15.53 ± 0.29	993 ± 106	$18.02^{+0.43}_{-0.60}$	438 ± 33	$18.02^{+0.43}_{-0.60}$	1166 ± 93	$15.50^{+0.19}_{-0.29}$	16.6 ± 3.4
16.25 ± 0.33	921 ± 98	$18.89^{+0.29}_{-0.50}$	466 ± 35	$18.89^{+0.29}_{-0.50}$	1114 ± 89	$15.75^{+0.18}_{-0.28}$	17.5 ± 5.6
		$19.58-0.17$	468 ± 35	$19.58-0.17$	1127 ± 90	$16.00^{+0.15}_{-0.27}$	12.1 ± 4.0
						$16.25^{+0.12}_{-0.26}$	15.2 ± 5.5
						$16.75^{+0.12}_{-0.20}$	10.2 ± 4.9
$T_{1/2}=6.67 \pm 0.02$ m		$T_{1/2}$ = 20 m		$T_{1/2}$ = 33 d		$T_{1/2}$= 2.6 $\pm$ 0.4 s	

Table I (continued)

$In^{115}(n,2n)In^{114g}$		$Ce^{140}(n,2n)Ce^{139}$		$Ce^{142}(n,2n)Ce^{141}$		$Pb^{204}(n,2n)Pb^{203m}$	
E_n(MeV)	σ (mb)	E_n(MeV)	σ (mb)	E_n(MeV)	σ (mb)	E_n(MeV)	σ (mb)
13.50 ± 0.18	59.2 ± 4.6	12.88 ± 0.27	1230 ± 118	12.54 ± 0.17	1792 ± 168	$13.00^{+0.12}_{-0.14}$	1014 ± 183
13.75 ± 0.19	56.0 ± 4.5	13.18 ± 0.25	1390 ± 133	$13.31^{+0.24}_{-0.22}$	1778 ± 164	13.25 ± 0.19	1068 ± 195
$14.25^{+0.21}_{-0.23}$	52.4 ± 4.2	13.48 ± 0.26	1440 ± 138	$14.10^{+0.28}_{-0.26}$	1695 ± 102	13.50 ± 0.19	1188 ± 157
$14.50^{+0.20}_{-0.23}$	50.7 ± 4.0	13.98 ± 0.27	1230 ± 118	$14.88^{+0.30}_{-0.31}$	1802 ± 160	$13.75^{+0.18}_{-0.20}$	1235 ± 204
$15.00^{+0.22}_{-0.26}$	42.1 ± 3.4	14.25 ± 0.14	1370 ± 131	$15.62^{+0.31}_{-0.35}$	1581 ± 142	$14.00^{+0.19}_{-0.22}$	1262 ± 271
$15.25^{+0.22}_{-0.28}$	34.1 ± 2.8	14.33 ± 0.30	1190 ± 114	$16.31^{+0.30}_{-0.38}$	1570 ± 141	$14.50^{+0.19}_{-0.23}$	1331 ± 217
$15.50^{+0.19}_{-0.29}$	32.1 ± 2.6	14.53 ± 0.14	1250 ± 120	$17.23^{+0.26}_{-0.42}$	1326 ± 118	$14.75^{+0.23}_{-0.28}$	1289 ± 130
$15.75^{+0.18}_{-0.28}$	32.7 ± 2.7	14.68 ± 0.30	1160 ± 111	$18.02^{+0.24}_{-0.37}$	1199 ± 103	$15.00^{+0.26}_{-0.30}$	1402 ± 123
$16.00^{+0.15}_{-0.27}$	26.7 ± 2.2	14.62 ± 0.16	1150 ± 110	$18.89^{+0.15}_{-0.22}$	876 ± 74	$15.25^{+0.22}_{-0.27}$	1342 ± 168
$16.25^{+0.12}_{-0.26}$	25.7 ± 2.2	15.08 ± 0.17	1140 ± 109	19.56 ± 0.14	794 ± 64	$15.50^{+0.22}_{-0.30}$	1135 ± 135
$16.75^{+0.12}_{-0.20}$	20.2 ± 1.7	15.17 ± 0.30	1130 ± 108			$15.75^{+0.22}_{-0.32}$	1243 ± 129
		15.30 ± 0.18	1180 ± 113			$16.00^{+0.24}_{-0.31}$	1112 ± 107
		15.42 ± 0.30	1070 ± 103			$16.25^{+0.17}_{-0.33}$	1098 ± 108
		15.54 ± 0.19	1080 ± 104				
		15.76 ± 0.19	1100 ± 106				
		15.93 ± 0.21	1025 ± 98.3				
		16.17 ± 0.28	986 ± 94.7				
		16.65 ± 0.20	1015 ± 97.4				
		16.90 ± 0.25	938 ± 90.0				
$T_{1/2} = 72.3 \pm 0.3$ s		$T_{1/2} = 58$ s		$T_{1/2} \equiv 33$ d		$T_{1/2} = 5.9 \pm 0.1$ s	

Table II Cross Sections for (n,p), (n,α) and (n,n') Reactions

$As^{75}(n,p)Ge^{75m}$		$Cl^{37}(n,\alpha)P^{34}$		$Br^{79}(n,n')Br^{79m}$		$Au^{197}(n,n')Au^{197}$	
E_n(MeV)	σ (mb)	E_n(MeV)	σ (mb)	E_n(MeV)	σ (mb)	E_n(MeV)	σ (mb)
12.75 ± 0.13	13.7 ± 1.0	13.18 ± 0.12	160 ± 17	13.18 ± 0.13	284 ± 30	13.18 ± 0.13	453 ± 47
13.00 ± 0.13	14.9 ± 1.1	13.46 ± 0.12	145 ± 15	13.46 ± 0.13	232 ± 25	13.46 ± 0.13	405 ± 42
13.25 ± 0.13	15.2 ± 1.4	13.98 ± 0.12	120 ± 13	13.71 ± 0.14	204 ± 22	13.71 ± 0.14	373 ± 37
13.50 ± 0.14	16.1 ± 1.3	14.24 ± 0.14	125 ± 13	13.98 ± 0.14	191 ± 20	13.98 ± 0.14	324 ± 34
13.75 ± 0.14	17.9 ± 1.6	14.51 ± 0.18	112 ± 12	14.24 ± 0.16	173 ± 18	14.24 ± 0.16	333 ± 35
14.00 ± 0.15	18.3 ± 2.2	14.76 ± 0.19	89.4 ± 9.3	14.51 ± 0.18	151 ± 16	14.51 ± 0.18	298 ± 31
14.25 ± 0.16	17.1 ± 1.5	15.01 ± 0.22	81.6 ± 9.6	14.76 ± 0.20	146 ± 16	14.76 ± 0.20	316 ± 33
$14.50^{+0.16}_{-0.20}$	14.2 ± 1.3	15.28 ± 0.25	86.0 ± 8.5	15.01 ± 0.23	147 ± 16	15.01 ± 0.23	307 ± 32
		15.79 ± 0.32	69.2 ± 7.2	15.53 ± 0.28	125 ± 13	15.27 ± 0.26	314 ± 33
$14.75^{+0.16}_{-0.20}$	14.5 ± 1.3	16.05 ± 0.35	62.0 ± 4.8	16.24 ± 0.32	106 ± 11	15.53 ± 0.29	290 ± 30
$15.00^{+0.16}_{-0.20}$	14.1 ± 1.2					15.79 ± 0.31	294 ± 31
						16.05 ± 0.32	312 ± 32
$15.50^{+0.15}_{-0.21}$	12.3 ± 1.3						
$15.75^{+0.14}_{-0.22}$	12.2 ± 0.9						
$16.00^{+0.11}_{-0.20}$	11.4 ± 0.9						
$16.25^{+0.11}_{-0.20}$	11.7 ± 0.8						
$16.75^{+0.12}_{-0.20}$	10.7 ± 0.8						
$T_{1/2} = 48.0 \pm 0.3$ s		$T_{1/2} = 12.06 \pm 0.24$ s		$T_{1/2} = 4.82 \pm 0.03$ s		$T_{1/2} = 7.61 \pm 0.06$ s	

V. REACTOR CENTRUM NEDERLAND, PETTEN (NETHERLANDS), F.O.M. GROUPS.

1. Nuclear orientation experiments with reactor neutrons.

H. Postma, E.R. Reddingius and J.F.M. Potters.

The anisotropy of the directional distribution of capture gamma rays from aligned ^{143}Nd, ^{145}Nd and ^{165}Ho have been studied during the past year. The neodymium isotopes were aligned at 0.014^{o}K in single crystals of neodymium ethylsulphate. This temperature was reached by adiabatic demagnetization of the sample itself. The holmium nuclei were tried to align in a single crystal of holmium metal ethylsulphate single crystal. The high-energy capture gamma rays were detected with a three-crystal pair spectrometer composed of NaI(Tl)-detectors. In a later stage a 2 cc Ge(Li) detector was used. Very large anisotropies are demonstrated in the case of ^{143}Nd. On the basis of such measurements spins could be assigned to several levels of ^{144}Nd. In order to clarify the electric or magnetic nature linear polarizations of several low-energy gamma rays were measured. With this information the parity of one level and an E2/M1 mixing ratio could be obtained. Capture gamma rays of enriched Nd-isotopes were studied with a Ge(Li)-detector in order to identify the transitions. So far significant effects have not been found in the case of ^{165}Ho. These experiments will be repeated.

Reference

H. Postma and E.R. Reddingius
R.C.N.-F.O.M. report (submitted to Physica).

2. Gamma-gamma angular correlation measurements in (n,γ) reaction

G. van Middelkoop*, P. Spilling, H. Gruppelaar and A.M.F. Op den Kamp.

A short description of the γ-γ coincidence and angular correlation spectrometer at the Dutch High Flux Reactor in Petten has been given in the previous Progress Report.

* Present address: AECL, Chalk River, Canada.

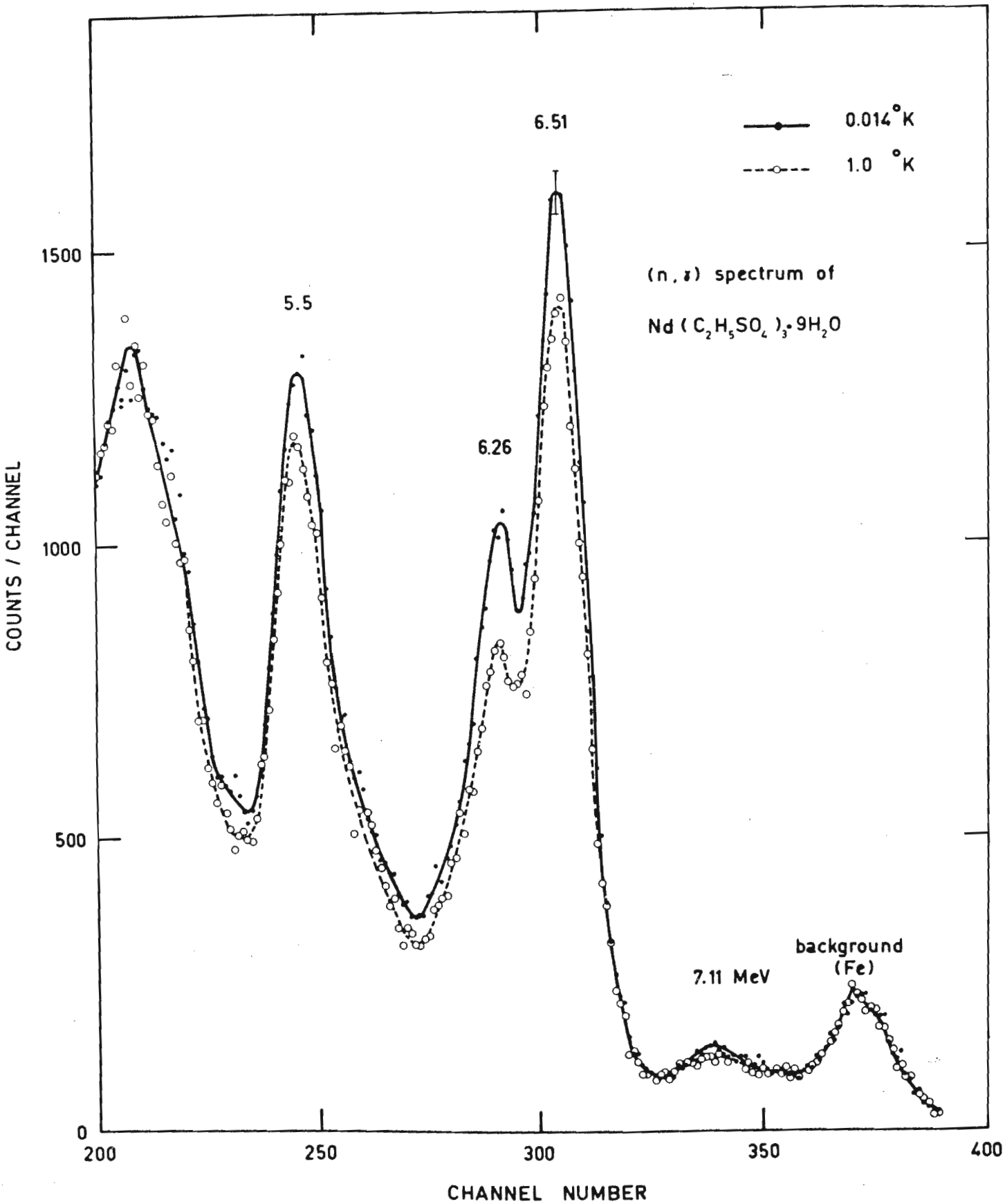
6.51
0.014 °K
1.0 °K
1500
(n, γ) spectrum of
Nd (C2H5SO4)3·9H2O
5.5
6.26
1000
COUNTS / CHANNEL
500
background
(Fe)
7.11 MeV
0
200
250
300
350
400
CHANNEL NUMBER

This set up was used for the study of the $^{25}Mg(n,\gamma)^{26}Mg$ and $^{40}Ca(n,\gamma)^{41}Ca$ reactions. In addition a 5 cm^3 Ge(Li)-detector was installed. Single spectra from the above mentioned reactions and the $^{31}P(n,\gamma)^{32}P$ reaction were measured with this detector. These measurements gave accurate energy levels and intensities of γ-rays, being of great importance for the angular correlation work.

The investigations are a part of the programme of the Dutch Foundation for Fundamental Research ("Stichting voor Fundamenteel Onderzoek der Materie", F.O.M.).

References

(1) G. van Middelkoop and P. Spilling, Nuclear Physics 77 (1966)267.

(2) G. van Middelkoop and H. Gruppelaar, Nuclear Physics 80 (1966)321.

(3) G. van Middelkoop, Ph.D. thesis, Utrecht University, 1966.

VI. INSTITUUT VOOR KERNFYSISCH ONDERZOEK, AMSTERDAM

1. Calibration of a Radium (α,n) Beryllium neutron source

P.W.F. Louwrier.

The absolute yield of the I.K.O. radium (α,n) beryllium source has been measured by means of the manganese bath method.
Corrections have been determined and applied for

1. resonance absorption in manganese
2. escape of neutrons from the tank
3. absorption of neutrons in the source
4. fast neutron reactions with oxygen and sulphur in the solutions

Reference

P.W.F. Louwrier, Thesis Univ. of Amsterdam 1966.

2. Some nuclear reactions induced by D+T neutrons

W. Nagel.

From all values existing in the literature the most likely cross section values for the reactions
$^{6}Li(n,\alpha)T$, $^{56}Fe(n,p)^{56}Mn$, $^{63}Cu(n,2n)^{62}Cu$, $^{65}Cu(n,2n)^{64}Cu$ and $^{27}Al(n,\alpha)^{24}Na$ have been calculated for neutron energies between approximately 12 and 20 MeV.
With two of these reactions as standard the neutron flux density of two different neutron sources was determined.
Thereafter, a set of cross sections has been determined by using the activation method as given in table I.

Reference

W. Nagel, Thesis Univ. of Amsterdam 1966.

Table I

RESULTS (in mb) OF THE CROSS SECTION DETERMINATIONS.
(the numbers between parentheses indicate the number of experiments)

neutron energy and standard reaction	(14.2±0.2)MeV		(14.6±0.2)MeV	
reaction	$^{65}Cu(n,2n)^{64}Cu$ (945±40)mb	$^{56}Fe(n,p)^{56}Mn$ (109±5)mb	$^{65}Cu(n,2n)^{64}Cu$ (980±40)mb	$^{56}Fe(n,p)^{56}Mn$ (103±4)mb
$^{19}F(n,2n)^{18}F$	46.5±5.9 (1)	40.1±5.3 (2)		
$^{35}Cl(n,\alpha)^{32}P$			121±20 (1)	117±20 (1)
$^{35}Cl(n,p)^{35}S$			117±25 (1)	131±20 (1)
$^{42}Ca(n,p)^{42}K$			194±23 (2)	(1)
$^{43}Ca(n.p)^{43}K$			137±30 (2)	
$^{103}Rh(n,n')^{103}Rh^{m}$	507±37 (4)	445±33 (4)		
$^{115}In(n,n')^{115}In^{m}$				50±7.8 (2)
$^{115}In(n,\alpha)^{112}Ag$				3±1.2 (2)
$^{115}In(n,2n)^{114}In^{g}$		350±100 (5)		
$^{133}Cs(n,2n)^{132}Cs$	1682±140 (1)	1577±105 (5)	1612±140 (1)	1540±140 (1)
$^{188}Os(n,p)^{188}Re$				8±1 (2)
$^{190}Os(n,\alpha)^{187}W$				0.43±0.04 (2)

VII. LABORATORIO DI FISICA NUCLEARE APPLICATA, CENTRO DI STUDI NUCLEARI DEL C.N.E.N., CASACCIA (ROMA) (ITALY)

1. Introduction

In the last year the Nuclear Physics Group of the "Centro Studi Nucleari della Casaccia" was engaged in the following activities:

1) Design and execution of a new tangential beam hole going through the TRIGA Mark II reactor.
2) Design of experiments for such a beam hole and set up of the pertaining experimental assemblies.
3) Study of techniques for the experimental data elaboration with computers.
4) Directional (n,n'γ) correlation measurements.
5) Theoretical studies on the nuclear wave functions.

Later on the progresses we obtained in this year will be briefly described.

2.1. Design and execution of a new tangential beam hole going through the TRIGA Mark II reactor

The running of the TRIGA Mark II reactor of the "Centro Studi Nucleari della Casaccia" (Applied Nuclear Physics Laboratory) was stopped in September 1965 for a power increasing from 100 kW to 1 MW. The reactor will work again regularly at the beginning of 1967.

In this occurrence a new facility was planned and executed, consisting in a beam hole tangential to the reactor core and going through the whole biological shield.

Such new facility will allow a great reduction of gamma and neutron's background. Moreover it will be possible to arrange a target at one of its end letting the experimental assembly fixed at the other one. For such a purpose the beam hole was made with a single tube so as to avoid water infiltrations and to enable the sample to slide freely. Temperature measurements and sample

cooling will continually be possible. The active sample extraction will be done by means of a rotatory assembly able to work also during the reactor running.

2.2. Nuclear resonant scattering by radiative capture gamma rays

The aim of this study is to measure the radiative widths of nuclear levels with energy near to the binding energy for particles emission.
Such a study is included in a sistematic research done by this laboratory on the radiative widths for E1 electromagnetic transitions [3,4] . A monochromatic collimated gamma ray beam, produced by thermal neutron's capture, will be used. The resonant scattering cross sections and their change with the scatterer temperature will be studied with an "absorption-scattering method" previously developed. The gamma spectra will be analysed with Ge(Li) detectors. A goniometer was also designed for directional correlation analysis between scattered and incident gamma rays and for cascade gamma ray angular correlations.
For such measurements a Ge(Li) detector pair spectrometer, or an anti-Compton spectrometer both already executed, will be used.

2.3. Thermal neutron's radiative capture

On the basis of the increased reactor neutron flux and of the recent solid state detectors techniques for gamma ray measurements, the group provided a large program in the radiative capture field. The high resolution capture spectra will be studied with the new tangential beam hole, while the old one will be utilized for the cascade gamma ray angular correlations. For this purpose this last beam hole was modified in order to increase the thermal neutron flux at its end, to collimate the outgoing gamma beam and to reduce the fission gamma ray background. To facilitate the experimental data elaboration a 512 channel analyser (LABEN) was modified in order to measure bidimensional spectra.

In the meanwhile a theoretical calculation program on deformed odd-odd nuclei was started (§ 1.3.1) and the next radiative capture experiments will be devoted to the study of such nuclei.

2.4. Data elaboration techniques with electronic computers

An elaboration technique for the complete analysis of resonant scattering experiments was accomplished. For this purpose a computer program (written in Fortran language) for use on the IBM 7094 computer of the "Centro di Calcolo del C.N.E.N." di Bologna, has been compiled.

A Montecarlo program for the detector efficiency calculation of high energy gamma rays in NaI(Tl) scintillators has also been studied.

Such a program was also modified for its application to germanium solid state detectors.

At last a computer program to analyse complex gamma ray spectra is being studied.

2.5. Directional (n,n'γ) correlation measurements

The last year was essentially devoted to set up the experimental apparatus for measuring directional correlations between incoming neutron beam and produced γ-rays.

The neutron beam was obtained by the d(d,n) ^{3}He reaction; further the deuterons were supplied by a 400 KeV Van de Graaff accelerator.

The detection apparatus consisted of two scintillation counters (NaI and liquid NE 213, respectively for γ-rays and neutrons) and a fast coincidence system.

In order to reduce the ratio between physical events and neutron background, we needed to employ a discrimination device based on the "zero cross-over time shift" method. The background counts where so reduced to less than 10% of the true events.

The collection of experimental information on natural Mg targets is now in progress. The next year the measurements will be conti-

nued with Si targets.

In order to analyse the experimental data, a "Montecarlo program" for the determination of the detection system efficiency is being studied.

3.1. Excited levels of odd-odd deformed nuclei

The aim of this program which started in 1965, is to study the residual neutron-proton interactions in deformed nuclei [6].
In a first time we have developed an approximation grounded on the Nilsson model; this approximation has been employed in order to analyse the level scheme of Ta^{182} [7]. In a second time we have improved our physical model by describing the nucleous as an aggregate of quasi-particles in a rotating deformed field; quasi--neutrons and quasi-protons interact by means of both central and tensor forces.
Calculations on the levels of Ho^{166}, Tm^{170}, Ta^{182} are now in progress.
The results of the preceeding calculations will be employed in order to program in detail our future radiative capture experiments.

3.2. Formal treatment of the residual interactions in heavy nuclei

Particular care has been devoted to the problems connected to the neutron-proton interaction. We have employed a technique (suggested by M. Jean) which allowed us to reduce the calculations of the nuclear wave functions to the resolution of a system of infinite non-linear equations [8,9,10]. By the introduction of suitable approximations, the resolution of the preceeding equation system has been reduced to the diagonalization of a finite dimension matrix. After these approximations, we have obtained equations similar to the well-known Hartree-Bogoliuboff equations.
However let us now observe that the Hartree-Bogoliuboff equations do not allow us to conserve the nuclear number, whereas the non-

-linear equations of our method provide a formally exact solution of the nuclear problem.

3.3. Study of intrinsic motion wave functions in shell-model calculations

The nuclear hamiltonian has been substituted with one equivalent with regard to the intrinsic motion of the nucleons, that is the motion of the nucleons in their center of mass. The new hamiltonian can be handled by employing shell model wave functions without giving rise to spurious effects deriving from the motion of the center of mass [11] . The method provides an approach to the study of very light nuclei alternative to the usual variational method.

An application of the method to Pb^{208} spectroscopy is now in progress.

VIII. CENTRO DI INFORMAZIONI STUDI ESPERIENZE (CISE), SEGRATE (MILANO) (ITALY)

1. Measurements of (d,p) and (d,α) reactions

The analysis of the Mg^{25}(d,p) Mg^{26} reaction has been completed. The very detailed and complete experimental data (excitation function in step of 15 KeV and with an overall energy resolution of 10 KeV at 8 angles) have permitted to extract wide information about the properties of Ericson fluctuations, which are in a very good agreement with the theoretical previsions. Particularly the interference effect between compound nucleus formation and direct interaction is confirmed and the percentage of the two mechanism, the number of independent channels contributing to the reaction and the average compound nucleus levels width Γ have been deduced [1].

We have extended the measurements on (d,p) (d,α) reactions to Cl^{35}, Cl^{37}, K^{41}, T^{47} target nuclei only in order to obtain the average compound nucleus levels widths Γ. In these measurements the overall energy resolution is of the same order or bigger than the average level width Γ and a new method for extracting the Γ value from the experimental excitation functions has been suggested [2].

This method applied to our measurements and to other existing data allows to obtain the Γ value for a number of nuclei in the mass range A 40 - 60.

A general agreement between the trend of the experimental Γ values and the calculated ones on the basis of the statistical theory has been found. More detailed calculations are in progress.

2. Low energy fission

The fission mechanisms in the reactions Bi^{209} + 42 MeV α particles, Ra^{226} + 9,8 MeV deuterons and Cf^{252} spontaneous fission are analysed by means of the Newton-Ericson statistical model [3].

With the introduction of a suitable potential barrier acting between the fragments it is possible to estimate: the total kinetic energy and the mass distribution of the final fragments for the different reactions and to compare them with the experimental data.

In the case of Cf^{252} spontaneous fission the number of neutrons emitted by single fragments is also estimated.

The most striking aspects of fission can be reproduced well.

References

[1] V. Bobyr, M. Corti, G.M. Marcazzan, L. Milazzo Colli, M. Milazzo - Energia Nucleare 8 (1966) 13.

[2] M. Corti, M.G. Marcazzan, L. Milazzo Colli, M. Milazzo - - Energia Nucleare 6 (1966) 13.

[3] E. Erba, U. Facchini, E. Saetta-Menichella - Nucl. Phys. 84 (1966) 595.

IX. GRUPPO DI RICERCA DEL CONTRATTO EURATOM-CNEN-INFN - ISTITUTO DI FISICA DELL'UNIVERSITA', PADOVA (ITALY)

1. Elastic and inelastic scattering of neutrons from Holmium in the energy interval 3.0 8.0 MeV(*)

A measurement is in progress of the angular distribution of the elastic and inelastic scattering of neutrons from Holmium, in the energy interval 3.0÷8.0 MeV.

2. Total cross section of neutrons on Ca and Th(*)

The total cross section of neutrons on Ca and Th has been measured in the energy interval 1.5÷8.5 MeV, with steps of 25 KeV for Ca and 50 KeV for Th, and energy resolution of about 30 and about 100 KeV, respectively. The statistical error is 1-2%. Systematics errors are believed to be no larger than the statistical errors.

The Ca cross section fluctuates strongly, particularly at lower energies. The Th cross section varies smoothly with a large maximum near 4.0 MeV.

3. Total cross section of neutrons on Na, Al, Si, P, S in the energy interval 5.0÷8.5 MeV(**)

The total cross section of neutrons on Na, Al, Si, P, S has been measured [1] in the energy interval 5.0÷8.5 MeV, with steps of 25 KeV, energy resolution of 40 KeV and statistical errors of 1-2%.

All cross sections show fluctuations of some tens percent, with apparent widths around hundred KeV. An analysis of the fluctuations with the Ericson theory is in progress.

[1] U. Fasoli, D. Toniolo, G. Zago, F. Fabiani - Nuovo Cimento 44 B (1966) 455.

(*) Work performed under Contract Università di Padova/CNEN

(**) Work performed under Contract EURATOM/CNEN-INFN

X. SOTTOSEZIONE DI FIRENZE DELL'ISTITUTO NAZIONALE DI FISICA NUCLEARE - ISTITUTO DI FISICA DELL'UNIVERSITA', FIRENZE (ITALY)

1.1. ß and γ spectroscopy

The Group for γ and ß spectroscopy has been studying the decays of some nuclei with solid state detectors.

1.2. Decay of ^{114m}In

In particular, in the decay of ^{114m}In a transition has been studied, the existence and intensity of which was based only on indirect evidences. If the reported intensity would have been correct, the corresponding branching of electron capture, with log ft = 3.3, would have represented the only example of non--superallowed transition with log ft 3.8. We could point out that the log ft is at least higher than 4.3 [1] .

1.3. Decay of ^{174}Lu

In the decay of the ^{174}Lu [2] , in collaboration with the Group of Naples, we could confirm the assignment of the 7-spin at the 1510 KeV level in the ^{174}Yb (in contrast with 6+ assignment of other Authors). Such a level is therefore interpreted as second member of the dublet due to the coupling of two neutrons, according to Gallagher's rule.

1.4. Decay of ^{133}Ba

At last a complete study of the scheme of decay of the ^{133}Ba was accomplished, which allowed us to give rather precise values for all the γ intensities and to obtain new values of the log ft of the transition of E.C. more in agreement with the spins of the levels which were already known from measurements of angular correlations. (The various probabilities of transition seem not to be easily understandable with the existent theoretical descriptions, which, on the other hand, are not very abundant in this mass zone).

1.5. Instrumentation

As to the technical field, the possibility of inserting sources

in the chamber of analysis without breaking the vacuum has been described in a letter to Nuclear Instruments and Methods [4]. The study of the backscattering of electrons on silicium detectors was published as I.N.F.N. report [5].

1.6. (p,nγ) reactions

Moreover, we have also carried out measurements on nuclei of the f7/2 shell with the Van de Graaff in Padua in order to determine, with (p,nγ) reactions, the levels of the residual nucleus, and, if possible, analogous states as resonances of compound nucleus. We have completed the measurement of isomeric production ratios for (n,2n) reactions, including also the case $^{144}Sm(n,2n)^{143m,g}Sm$. For this case we obtained $\frac{\sigma \text{ isomeric state}}{\sigma \text{ ground state}} = 1.07 \pm 0.10$. This result, with the other ones previously obtained, has been analysed according to the computation rules suggested by Huinzega and Van den Bosch to obtain information about the "spin cut-off" parameter of the spin distribution of the levels of the compound nucleus. The calculation, performed with the IBM 1620 computer of our University, was also applied to the analysis of other experimental data on (n,2n) reactions. The obtained values of the spin cut-off parameters are in agreements with the values obtained by other Authors, within experimental errors.

1.7. Ericson fluctuations

In the frame of the study of Ericson fluctuations an I.N.F.N. report has been published in which we discuss in details the effect of the isospin selection rule on the correlation width. Furthermore some calculation have been made in order to determine, in a rapid and sure way, the correlation width from the number of maxima and minima in an experimental excitation function. We have taken in account the finite distance between the experimental points and the fact that statistical fluctuations, due to poor statistics may introduce spurious extremes.

2.1. $^{20}Ne(n,2\alpha)^{13}C$ reactions (in collaboration with Bologna group)

About 8000 three prong events produced by 14 MeV neutrons in a Wilson chamber filled up with neon, were observed and measured. At least 95% of these events are due to the $^{20}Ne(n,2\alpha)^{13}C$ reaction as recognized by suitable cinematic fits.
The range-energy relation has been obtained for ^{13}C in Neon.
The angular distribution of the particles, relative to the direction of the incident neutron, being strongly peaked backwards, suggests also for this reaction a strong heavy-stripping contribution. Another interesting characteristic of these events is the angular distribution of the α particles relative to the direction of motion of the ^{13}C, which appears clearly peaked at 90°. Perhaps a statistical increase might allow an interpretation of such a characteristic.

References

[1] P. Blasi, P.R. Maurenzig and N. Taccetti - Il Nuovo Cimento X, 44 (1966) 222.

[2] A. Barone, G. Greco, R. Speranza, R.A. Ricci, P. Blasi, P.R. Maurenzig, P. Sona - LII S.I.F. Meeting Trieste 1966, to be published in "Il Nuovo Cimento".

[3] P. Blasi, M. Bocciolini, P.R. Maurenzig, P. Sona, N. Taccetti - - LII S.I.F. Meeting Trieste 1966.

[4] P. Blasi, P.R. Maurenzig and P. Sona - Nucl. Instr. and Meth. 42 (1966) 305.

[5] A. Benvenuti, P. Blasi, P.R. Maurenzig and P. Sona - INFN report, BE - 66/4 (1966).

[6] P.G. Bizzeti and P.R. Maurenzig - INFN report, BE - 65/6 (1965).

[7] P.G. Bizzeti and P.R. Maurenzig - LII S.I.F. Meeting Trieste 1966, to be published in "Il Nuovo Cimento".

XI. CENTRO SICILIANO DI FISICA NUCLEARE, ISTITUTO NAZIONALE DI FISICA NUCLEARE, SEZIONE SICILIANA - ISTITUTO DI FISICA DELLA UNIVERSITA', CATANIA (ITALY)

1.1. Nuclear Fission

The angular distributions of fragments of neutron induced fission of Thorium have been measured with nuclear emulsions loaded with thorium nitrate and exposed to monoenergetic neutron beams in the energy range $1.7 < E_n < 5.3$ MeV obtained by means of the D(d,n) reaction. Taking into account the accuracy of the data the angular distributions are well represented by polinomials $N(\emptyset) = \sum_m A_m \cos^{2m}\emptyset$ with terms up to $\cos^2\emptyset$ for $E_n > 3$ MeV, while for $E_n < 3$ MeV terms up to $\cos^6\emptyset$ are not negligible. The anisotropy ratios show a maximum of 1.51 ± 0.2 at $E_n = 2.4$ MeV.
From the measured angular distributions we deduced the values of the parameter K_o^2, whose dependence on the excitation energy we compare with that of other even-A target nuclei: we found that the behaviour of $K_o^2(E_n-E_o)$ for the Plutonium seems significantly different from that relative to Uranium and Thorium.
Experiments on the angular distribution for E_n near the $^{232}Th(n,f)$ treshold are in progress [1].

1.2. $^{19}F(d,p\gamma)^{20}F$ reaction

Further measurements have been done on the $^{19}F(d,p\gamma)^{20}F$ reaction for determining the $(d,p_1\gamma)$ correlation function. The experimental data were collected on the orizontal plane for a proton emission angle coincident with the deuteron beam direction and on two azimuthal planes for proton emission angle of 45°.
A preliminary analysis of the data has been done and the complexity of the correlation function curve has been determined by a best fit method [2].

1.3. Resonant absorption of monoenergetic gamma-rays

Using monoenergetic gamma-rays produced by means of $^{23}Na(p,\gamma)^{24}Mg$ reaction at $E_p = 1.34$ MeV, the cross section for absorption of

these gamma-rays in ^{24}Mg has been measured. The gamma-ray energy was defined within 1-2 KeV and was varied by Doppler effect, varying their angle of emission with respect to the incident protons.

The preliminary results show peaks in the cross sections due to the resonant levels of ^{24}Mg in the region $E_x \approx 13$ MeV [3] . From these results one can extract the partial and total widths of the levels and then can obtain the spectroscopic parameters of the levels.

1.4. α-emission from heavy nuclei induced by neutrons of $E_n \approx 12-23$ MeV

The α-emission from neutron induced reactions in heavy nuclei was experimentally investigated by means of several small reaction chambers. The irradiated elements were $^{107}Ag_{47}$, $^{181}Ta_{73}$, Ir_{77}, $^{197}Au_{79}$ and $^{209}Bi_{83}$. Energy spectra, angular distributions and cross sections were analysed in the neutron energy region $E_n = (12-23)$ MeV.

The present results are discussed in a picture including all the known data on this subject and in terms of the contributions due to the direct interaction and to the evaporation. The α-evaporation from neutron induced reactions is found to be in satisfactory agreement with the statistical predictions [4] .

1.5. Neutrons from (α,n) sources

The neutron energy spectrum of a Pu-Be source has been measured using a special fast-neutron spectrometer. Good energy resolution was achieved and the detailed structure of the spectrum was evidenced. Results are discussed and compared with other measurements obtained with Pu-Be, Po-Be and Am-Be sources [5] .

2.1. Theoretical research work on nuclear structure and reactions

It has been shown [6,7] that the typical diffraction-like pattern of angular distributions of some nuclear reactions can be derived from the exact S-matrix theory assuming an appropriate selection

of transferred angular momenta and that the phases of the S-matrix elements in the representation of the transferred angular momenta are all equal. If also a selection of orbital angular momenta is present, (this is the case of surface reactions), this can simulate effects which are usually interpreted as contributions from the heavy particle stripping amplitude or from more values of the transferred angular momenta.
Further investigations are in progress, concerning the relationship between the assumption on the phases of the S-matrix and unitarity.
The discrete levels of some "magic nuclei" have been calculated [8] in an approximation (ETD) which is an extension of the TD one, obtained by completing the set of single particle states so as to include scattering wave functions. These effects have also been evaluated in a schematic model [9] which allowed us to predict also changes in the electromagnetic transition probabilities due to coupling states of the discrete to states of the continuous spectrum.
Calculations are in progress to check the schematic model predictions on the electromagnetic transition probabilities and to evaluate the elastic and inelastic scattering amplitudes in the ETD approximation.

References

[1] S. Lo Nigro and C. Milone - Comm. at the SIF Annual Meeting, Trieste 1966 - Boll. SIF n. 50 (1966) 81.
[2] G. Calvi, S. Cavallaro, A.S. Figuera, F. Porto and M. Sandoli - Comm. at the SIF Annual Meeting, Trieste 1966 - Boll. SIF n. 50 (1966) 78.
[3] G. Calvi, S. Cavallaro, R. Potenza and S. Sciuti - Comm. at the SIF Annual Meeting, Trieste 1966.
[4] A. Rubbino and D. Zubke - Nucl. Phys. 85 (1966) 606.
[5] A. Rubbino, D. Zubke and C. Meixner - N. Cim. 44 (1966) 179.
[6] G. Schiffrer - Proc. of Intern. Summer Meeting on Problems

of Nuclear Structure, held at Herceg Novi 1966 - to be published.

[7] A. Agodi and G. Schiffrer - Comm. at the SIF Annual Meeting, Trieste 1966 - Boll. SIF n. 50 (1966) 33.

[8] A. Agodi, F. Catara and M. Di Toro - Ann. Phys. (N.Y.) 40 (1966) 1.

[9] A. Agodi, F. Catara, M. Di Toro and O. Stazi - N. Cim. in press.

XII. ISTITUTO DI FISICA DELL'UNIVERSITA', TRIESTE (ITALY)

Elastic and inelastic scattering of 14 MeV neutrons from Si

Measurements of elastic and inelastic scattering of 14 MeV neutrons from Si-nat have been undertaken.
The neutrons have been obtained with the 600 KeV Cockroft-Walton of the Istitute di Fisica di Trieste and the reaction d(T,He)n. The energy of the scattered neutrons has been measured with the time of flight Technique and the associated particle method. The resolution of the apparatus turned out to be 1.6 nsec.
Experimental results concerning the differential elastic cross--section and the differential inelastic cross-section related to the first exited level of Si^{28} are reported in Tables I and II.

Table I : Differential cross-section for elastic scattering of neutrons from Si^{28}. $E_n = 14.1 \pm 0.05$ MeV.

$\vartheta_{c.m.}$	$\sigma_{el.}(\vartheta)$ (barn)
20°	$7.64 \pm 0.21 \times 10^{-25}$
30°	$1.35 \pm 0.59 \times 10^{-25}$
40°	$1.58 \pm 0.13 \times 10^{-26}$
50°	$2.88 \pm 0.21 \times 10^{-26}$
58°	$6.04 \pm 0.33 \times 10^{-26}$
65°	$7.85 \pm 0.29 \times 10^{-26}$
70°	$4.75 \pm 0.31 \times 10^{-26}$
90°	$1.23 \pm 0.16 \times 10^{-26}$
110°	$8.90 \pm 0.11 \times 10^{-27}$
120°	$1.57 \pm 0.17 \times 10^{-26}$

Table II : Differential cross-section for inelastic scattering of neutrons from the first level of Si^{28} ($Q = -1.78$ MeV). $E_n = 14.1 \pm 0.05$ MeV.

$\vartheta_{c.m.}$	$\sigma_{inel.}(\vartheta)$ (barn)
20°	$2.41 \pm 0.49 \times 10^{-26}$
30°	$7.02 \pm 0.15 \times 10^{-27}$
40°	$1.59 \pm 0.13 \times 10^{-26}$
50°	$2.42 \pm 0.19 \times 10^{-26}$
58°	$1.38 \pm 0.17 \times 10^{-26}$
65°	$1.43 \pm 0.12 \times 10^{-26}$
70°	$6.97 \pm 0.13 \times 10^{-26}$
90°	$8.38 \pm 0.10 \times 10^{-27}$
110°	$4.17 \pm 0.81 \times 10^{-27}$
120°	$7.32 \pm 1.51 \times 10^{-27}$

XIII. ISTITUTO NAZIONALE DI FISICA NUCLEARE, GRUPPO ACCELERATORE DELLA SEZIONE DI TORINO, TORINO (ITALY)

Scattering of 14.2 MeV neutrons on Cl

Angular distribution of 14.2 MeV neutron elastically and anelastically scattered from Cl have been measured [1]
Angular distributions, for neutrons elastically scattered and for eight groups of neutrons inelastically scattered which can be recognized in all the measured spectra, are deduced. Measured cross sections have been normalized to the known cross sections on H and are given in Tables I and II.

References

[1] G.C. Bonazzola, E. Chiavassa, T. Bressani - Nuovo Cimento 45 (1966) 60.

Table I : Angular distributions for Cl inelastically scattered neutrons.

$\vartheta_{c.m.}$	$d\sigma/d\Omega$ (mb/sr) Q=-1.2 MeV	$d\sigma/d\Omega$ (mb/sr) Q=-1.8 MeV	$d\sigma/d\Omega$ (mb/sr) Q=-2.7 MeV	$d\sigma/d\Omega$ (mb/sr) Q=-3.2 MeV	$d\sigma/d\Omega$ (mb/sr) Q=-4.1 MeV
33°	2,4±0,8	3 ±0,6	2,8±0,9	2,7±0,4	6,4±2,4
39°	2,9±1,3	3,6±0,6	3,3±0,8	1,8±1,2	6,1±2,8
50°30'	2,4±0,8	2,6±0,8	2,1±0,5	3,0±1	6,4±1,7
61°30'	2,1±0,5	2,2±0,6	2,7±0,4	3,0±0,6	7,9±0,8
72°		2,0±0,4	1,5±0,3	2,2±0,4	9,8±0,9
81°30'	2,4±0,5	1,6±0,6	1,3±0,5	1,2±0,4	7,6±2,3
90°30'	1,3±0,8		3,7±1,5	1,4±1	7,0±1,9

$\vartheta_{c.m.}$	$d\sigma/d\Omega$ (mb/sr) Q=-5.9 MeV	$d\sigma/d\Omega$ (mb/sr) Q=-6.5 MeV	$d\sigma/d\Omega$ (mb/sr) Q=-6.9 MeV		
33°	4,6±0,9	7,1±0,9	7,2±2,7		
39°30'	6,5±0,9	7,4±2	8,7±2,3		
51°	4,4±1,4	2,2±1,2	4,0±1,1		
62°	4,1±0,7	2,6±1,3	7,0±2,2		
72°	4,5±0,5	3 ±1,4			
82°	2,7±1	4 ±1	2,2±1		
91°	3,2±1,6	3,4±1,9	7 ±1,4		

Table II : Angular distribution for Cl elastically scattered neutrons.

$\vartheta_{c.m.}$	$d\sigma/d\Omega$ (mb/sr) Q=0
55°	40±2
39°	31±1
43°30'	21±8
50°30'	61±6
61°	65±2
72°	28±2
81°30'	16±1
90°30'	20±3
101°30'	25±4
111°	17±2
121°30'	9±1
130°30'	15±1

XIV. GRUPPO DI ISPRA PER LE MISURE DI SEZIONI D'URTO DEL C.N.E.N. ISPRA (VARESE) (ITALY)

Spin assignment to neutron resonances

Owing to a chopper accident, the activity at the Euratom-Ispra reactor has been discontinued.

A new set of measurements, concerning the spin assignment to neutron resonances, has been planned for the linear accelerator of the BCMN Euratom, Geel. All the equipment has been moved to Geel and set up there.

Preliminary measurements have been taken, showing that the method, based on the detection of neutron capture gamma rays, can be applied to ^{177}Hf(I=7/2) and ^{179}Hf(I=9/2).

XV. LABORATORIO DATI NUCLEARI, CENTRO DI CALCOLO DEL C.N.E.N., BOLOGNA (ITALY)

1.1. Neutron fission product cross section for radiative capture in the 1 KeV-10 MeV energy range

The statistical model has been used for $\sigma_{n\gamma}$ theoretical estimates of fission products nuclei in the energy range 1 KeV-10 MeV. The parameters required by the model have been estimated both from the analysis of experimental $\sigma_{n\gamma}$ or from the values of neighbouring nuclei. About 60 nuclides have been considered. For details, see ref.[1] .

1.2. Particle-hole excitations in the photoreactions of closed shell nuclei

The particle-hole model taking into account excited states in the continuum has been used to calculate the photoreaction cross--sections of C^{12},O^{16},Ca^{40}.
For the particle-hole interaction a δ-function with Soper mixture has been assumed.
The analysis of the giant resonance structure has been done in terms of particle-hole components.
Preliminary results on Ca^{40} have been presented at the Heidelberg Conference on "Recent Progress in Nuclear Physics with Tandems" (July 1966).
Results on C^{12} and Ca^{40} have been submitted to Physics Letters.
Calculations on Si^{28} and S^{32} are in progress.

1.3. Analysis of the intermediate structure in the low energy nucleon scattering from light nuclei by means of a coupled channel method

The coupled channel method used in ref.[2] has been improved in order to reproduce the low energy resonances in the n-C^{12} scattering. In this way an easy identification of the resonant structure is allowed.
A preliminary research of the possible bound and resonant states is made in a Woods-Saxon well, so that the identification of the

resonances obtained in the coupled channel calculation is straightforward.

Calculations on proton scattering from C^{12} are in progress.

1.4. Inelastic scattering based on microscopic description of nuclei

The inelastic scattering of nucleons from nuclei is treated assuming a two-body interaction between the incident particle and the target nucleons. For the target states are assumed to be described by shell-model wave functions calculated in the RPA approximation.

The development of the model is underway.

1.5. Scattering by non spherical nuclei

Two kinds of elastic and inelastic cross sections calculation methods have been considered for non spherical nuclei with even or odd mass number A, described by phenomenological coordinates:

1. A perturbation method
2. A coupled-channel method

In both cases the validity of the adiabatic approximation has been assumed.

1. The perturbation method, to the second order in the perturbation, has been applied to the analyses of elastic and inelastic neutron scattering cross sections by Si^{28}, S^{32}, Cr, Ni, Zn, Sn [3] and P^{31} (to be published). The method is valid, in the case of even A, both for vibrational and rotational nuclei whereas, in the case of odd A, rotational nuclei only can be considered.

2. A model based on the coupled-channel method, in the adiabatic approximation, has been developed. This method is valid for well deformed nuclei, whose excitation spectrum is closely that of an ideal rotational band, with even or odd mass number A.

This model allows the coupling of the elastic channel with all the channels of the rotational band.

References

[1] V. Benzi and M.V. Bortolani - IAEA Conf.on Nuclear Data - - CN-23/115 Paris (1966).

[2] G. Pisent and A.M. Saruis - Nucl. Phys. (in press).

[3] L. Zuffi - IAEA Conf.on Nuclear Data - CN-23/114 Paris (1966).

XVI. GRUPPO DI RICERCA DEL CONTRATTO EURATOM-CNEN-INFN - ISTITUTO DI FISICA DELL'UNIVERSITA', ROMA (ITALY)

Works on photofission

The Group of Rome of the Euratom-CNEN-INFN contract, is working on photofission of ^{238}U and ^{232}Th near threshold, using monochromatic γ-rays. Up to now results have been published on ^{238}U cross-section measurements [1,2,3] , while results on angular distribution are being handled.

The γ-ray sources consist of a series of target-elements placed inside a nuclear reactor [4,5] . By means of the (n,γ) reactions, γ-ray beams are obtained, whose spectra are made up of series of lines, a few of which are above the fission threshold.

The γ-rays impinge on nuclear emulsions, loaded with the fissioning uranium and which are afterwards processed so as to render visible fission fragment tracks only [1,6] .

The fissions found in a given plate are due to γ-ray lines of different energies. One of these - or, for some elements, a set of two or three lines - is more intense than the rest and (we assume) is responsible for most of the fission events, so that the contribution of the secondary lines may be treated as a correction.

For each element one may write

$$\sum \sigma_k \Phi_k = \frac{N_f}{\Phi_m U} \qquad (1)$$

where σ_k is the cross-section at the energy of the kth line, Φ_k the γ-ray flux of that line measured relatively to the main line, N_f the number of counted fissions per cm^2, Φ_m the flux of the main line (in photons/cm^2), and U the number of uranium nuclei loaded into the emulsion per cm^2.

The cross-sections appearing in these equations are firstly approximated with the cross-section of the closest lying main line corresponding to some other measured element. The equations may

thus be solved exactly.

Table I summarizes the experimental data: column 1 lists the reactor targets; column 2, the energy of the main line (or, eventually, of the mean of the main group of lines); column 3, the corresponding flux, Φ_m ; column 4, the experimental results (averaged), costituting the constant terms in the system of equations.

The constant terms of column 4 have been corrected for the contribution of the neutrons contaminating the γ-ray beam [5,2] . Once the solution of the system of equations is obtained, further approximations may be performed by linearly interpolating between the first set of solutions. The procedure may be repeated till the variations introduced are smaller than, say, 1%. The overall approximation introduced was, in all cases, (with the exception of the S-spectrum), less than 3%.

The method seems to be reliable, given the entity of the total correction to which the experimental results are subjected (cfr. columns 4 and 5 of table 1); and it finds further support in the over-all agreement between our results and those of other authors [7] . The cross-sections are shown in column 5 of the table, and plotted in Figure 1.

The errors on the cross-sections listed in the last column of table 1 take into account: statistical fluctuations due to the number of tracks counted; uncertainties in the loading of the emulsions; propagated errors in the correction for secondary lines; a 3% statistical fluctuation in the γ-ray intensity. None of the indicated errors, in the table or the figure, includes a systematic contribution due to uncertainties on the calibration of the flux-measuring crystal, estimated of the order of 10%.

Thus, although the absolute value of the cross-section curve may be in excess or defect by 10%, its form will not be changed.

In spite of the reduced number of energies at which reliable experimental data at present exist, our experimental errors give

sufficient guarantee that the two minima whose possible existence was suggested by the measurements of Katz et al. [7] , do exist in the uranium cross-section between threshold and the giant resonance. The discrepancy both in value and in position between the minima indicated by our experimental points and those suggested by Katz is not very significant if one takes into account the uncertainties inherent to the photon-difference method with which one computes cross-sections when working, as Katz did, with bremsstrahlung beams. The origins of these minima are not clear; an insight should be [8] closely connected with the form of the angular distribution of the fission fragments at the various energies.

The angular distribution of fission fragments has been measured for the same γ energies at which results on cross-section has been already published. The same kind of corrections has to be introduced due to neutron background and γ-rays lines of lower intensity.

We suppose that the angular distribution of fission tracks can be represented by the function

$$W(\Theta) = a+b \operatorname{sen}^2\Theta + c \operatorname{sen}^2\Theta \cos^2\Theta$$

Table I : ^{238}U photofission experimental data.

1	2	3	4	5
Reactor target	Main-line energy (MeV)	Main-line dose ($10^{10}\gamma\ cm^{-2}$)	$\frac{N_f}{\Phi_m U}$ (mb)	σ (mb)
S	5.43	3.32 5.56	1.40 ±0.11	0.08 ±0.20
Dy	5.58	2.62	3.96 ± .34	3.73 ±0.70
Y	6.07	6.80 2.18	6.54 ±0.37	5.99 ±1.05
Ca	6.42	4.51 2.16	7.20 ±0.54	5.68 ±1.02
Ti	6.75	7.99 1.49 1.16	18.5 ±0.9	12.5 ±1.1
Be	6.80	1.01 0.96	1.92 ±0.35	1.92 ±0.35
Mn	7.16	2.39	9.46 ±1.50	7.17 ±1.50
Pb	7.38	0.65 0.67	13.5 ±0.9	12.6 ±1.6
Fe	7.64	21.5 1.40	18.7 ±1.3	12.1 ±3.1
Al	7.72	5.11 3.14	9.28 ±0.55	7.15 ±0.56
Cu	7.91	7.05	31.3 ±6.4	18.9 ±6.7
Ni	8.86	24.6 1.00 1.29	35.2 ±1.8	29.0 ±1.8

normalized so that $\int_0^{\pi/2} W(\Theta)\,\mathrm{sen}\,\Theta\, d\Theta = 1$.

The preliminary measured values of the parameters a,b,c, as a function of the γ-rays energies are shown in fig. 2,3,4.

A qualitative analysis of the results indicates a general agreement with the Bohr hypothesis that at excitation energy slightly in excess to the fission barrier, fission goes, for the even-even nuclei, through a K=0 level, showing an almost pure dipole angular distribution $W(\Theta)=b\,\mathrm{sen}^2\Theta$.

A level with K=1 can be placed about 1 MeV higher than the K=0 level. A small contribution of quadrupole absorption seems to be present at all the measured energies, but the errors on the c term are too high to analyse the results.

There seems to be only a slight indication for a variation of the behaviour of the parameters at the energies where the cross-section shows minima. Further measurements seems to be necessary to decide about such a behaviour.

References

[1] H.G.de Carvalho, A. Manfredini, M. Muchnik, M. Severi, H. Bösch, J. Lang, R. Müller, W. Wölfli - Nuovo Cimento 25 (1962) 534.

[2] A. Manfredini, M. Muchnik, L. Fiore, C. Ramorino, H.G.de Carvalho, J. Land and R. Müller - Nucl.Phys. 74 (1965) 377.

[3] A. Manfredini, M. Muchnik, L. Fiore, C. Ramorino, H.G.de Carvalho, R. Bösch and W. Wölfli - Nuovo Cimento 44B (1966) 218.

[4] L. Jarczyk, J. Lang, R. Müller and W. Wölfli - Helv.Phys. Acta 34 (1961) 488.

[5] L. Jarczyk, H. Knoepfel, J. Lang, R. Müller and W. Wölfli - - Nucl. Instr. and Methods 13 (1961) 287.

[6] H.G.de Carvalho - Prog.Nucl.Tech. and Instrumentation, vol. I (North-Holland-Amsterdam, 1965), p. 247.

[7] L. Katz, A.P. Baerg and F. Brown - Second U.N. International Conference on the Peaceful Uses of Atomic Energy, 45 (1958) 188.

[8] E.K. Hyde - The nuclear properties of the heavy elements, vol. III (Prentice-Hall, New Jersey, 1964) 13, 501.

– Fig. 1 –

238 U PHOTOFISSION CROSS SECTION.

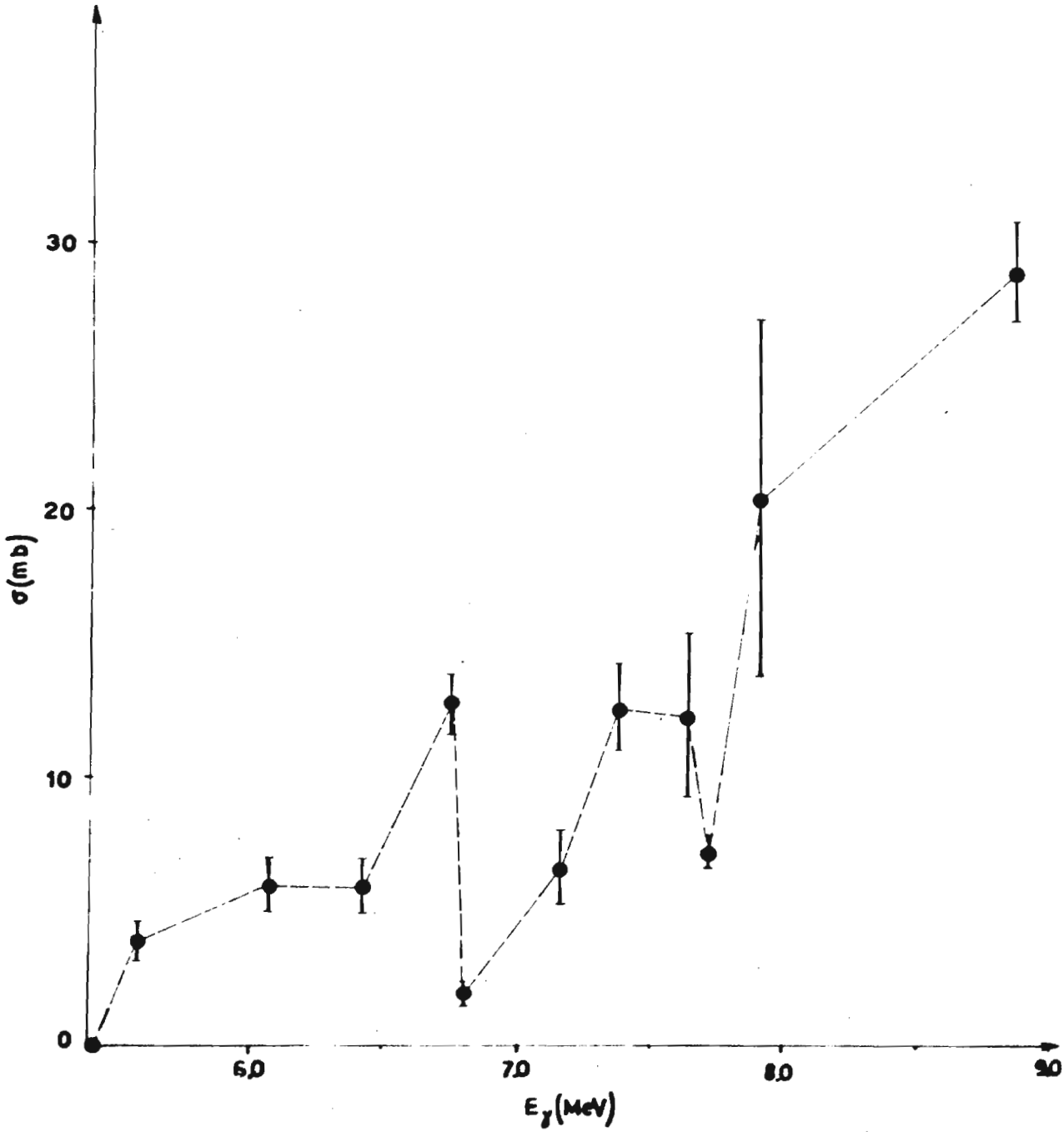

— Fig. 2 —

(a) AS A FUNCTION OF ENERGY.

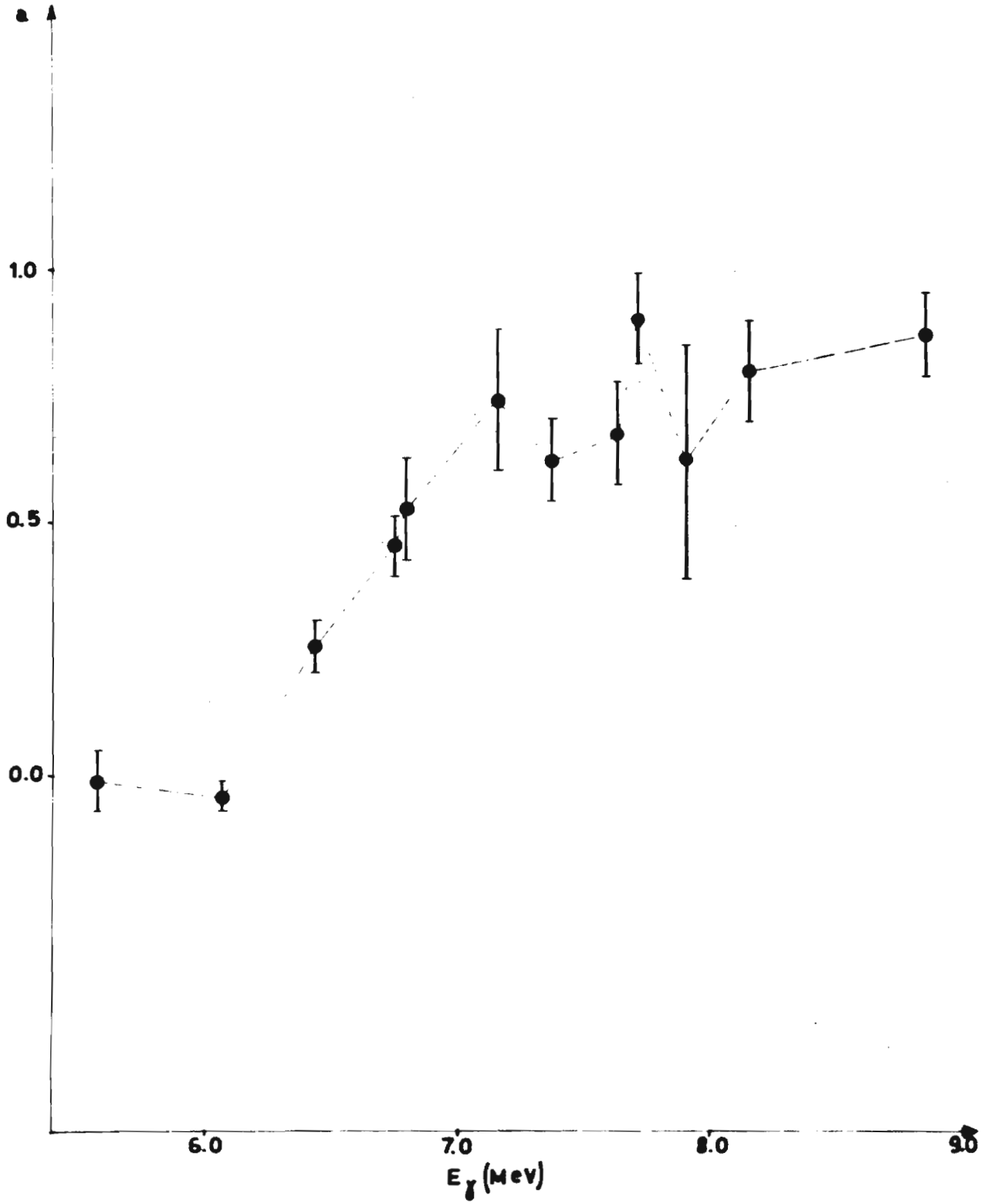

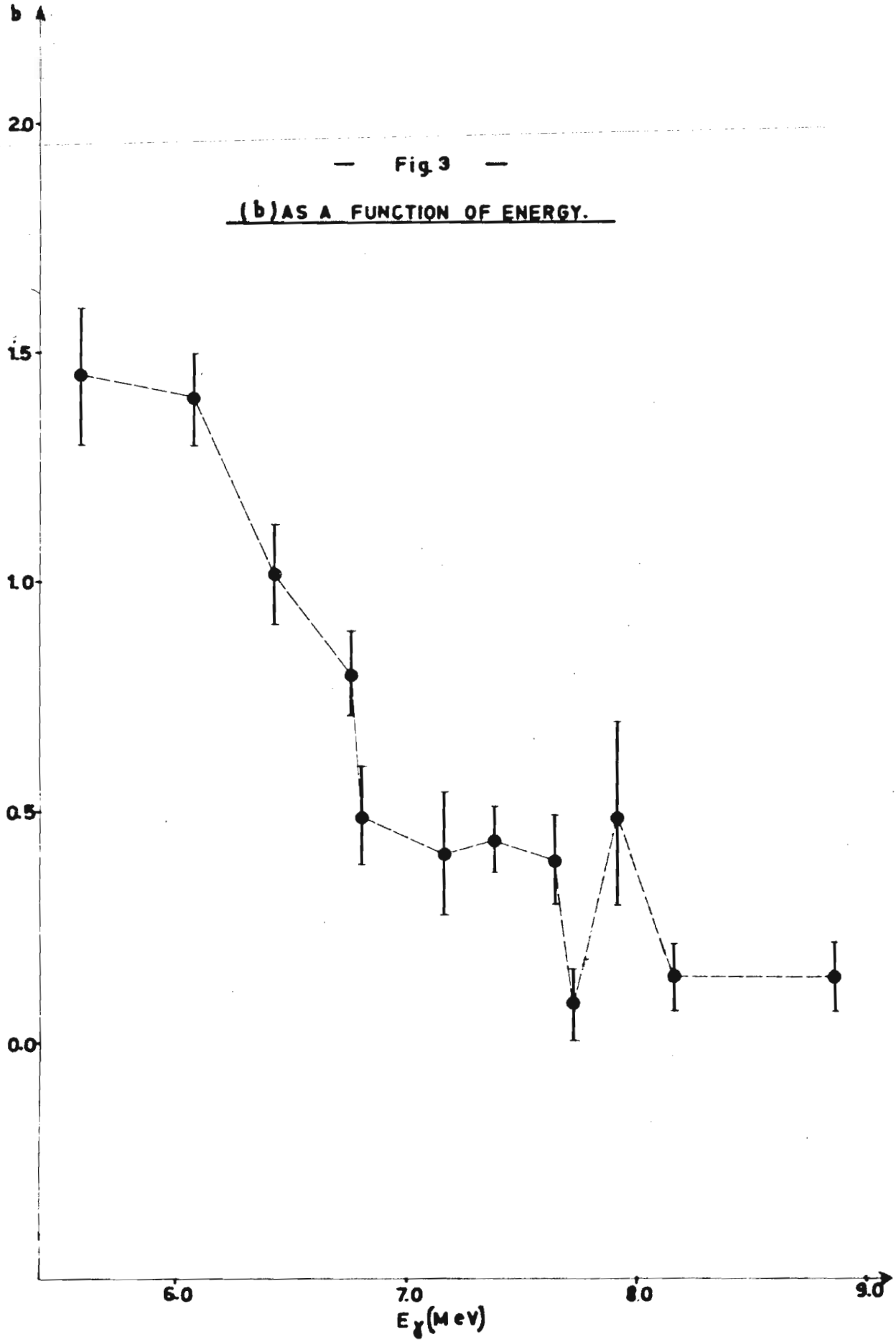

— Fig. 3 —

(b) AS A FUNCTION OF ENERGY.

— Fig. 4 —

(c) AS A FUNCTION OF ENERGY.

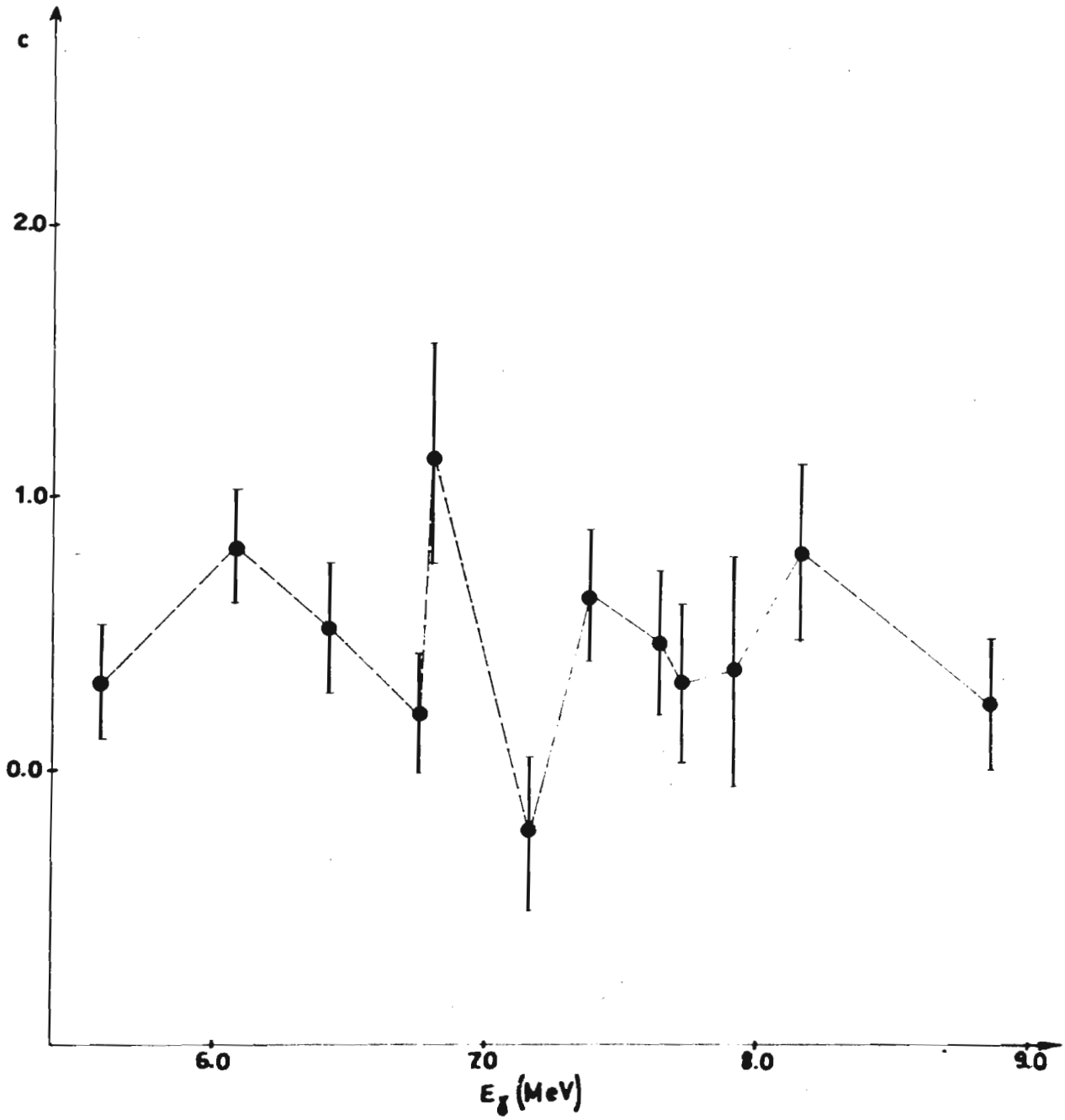

XVII. CENTRE DE PHYSIQUE NUCLEAIRE, UNIVERSITE DE LOUVAIN (Belgium)

1. Intermediate Structure in Calcium 41

(G. DECONNINCK and M. HUSAIN, boursier O.C.D.)

This study has been published [1] ; the abstract follows:

"Total cross sections and elastic scattering measurements of neutrons on Ca^{40} (natural samples) are presented between 1 and 2.5 MeV. When averaged on 115 keV the σ_{tot} results show a strong resonance at 1,5 MeV. This resonance is interpreted as a doorway state ($J = 1/2^+$; Γ = 300 KeV) and compared with recently discovered states in K^{41}. Further measurements are discussed."

2. Neutron Total Cross Section of Calcium

(G. DECONNINCK and M. HUSAIN)

Our previous measurements of the neutron total cross section of Calcium have shown the existence of a resonance at 1.5 MeV [1] and of one or more resonances at 2.3 MeV [2]

The former has been interpreted as a "doorway-state" in Ca^{41} [1] situated at 10.7 MeV, having a spin of $\frac{1}{2}^+$.

In order to confirm this hypothesis, we have undertaken a detailed series of measurements of total cross section between 1 and 3 MeV, with a resolution better than 7 KeV.

The neutrons from the T (p,n) He^3 reaction are detected by the time-of-flight method : the resolution of 4 nanoseconds allows an easy discrimination between neutrons and gamma rays.

The energy scale is accurately determined by different reactions :

a. Threshold $T(pn,)He^3$
b. Threshold $Li^7(p,n)Be^7$
c. $Mg^{24}(p,p')Mg^{*24}$ (level of Mg^{25} corresponding to proton energy of 2.41 MeV), and
d. $T(H_2^+,n)He^3$

The accuracy of the absolute values of neutron energies is estimated to be of the order of 10 KeV.

The total cross sections are measured by the transmission method with a sample of natural Calcium [Fig. 1 (a) to (d)]. The maximum statistical error is of the order of 4%; they are not shown on the figure.

Since we are more interested in the separation between resonances, we have not applied scattering corrections. This correction varies widely from point to point and is difficult to calculate. We estimate that it amounts to a maximum of 2%.

In order to identify a resonance, we have to find out the interference between potential and resonance scattering. A study of the figure in the neighbourhood of 1.5 MeV shows that the resonances overlap each other making their identification impossible. The determination of the spin of the states is also possible by angular distribution measurements. Unfortunately, those distributions are very sensitive to the overlapping of the resonances. These reasons make the determination of the doorway-state components very imprecise. We believe that a resolution of 500 eV is necessary for a precise determination.

3. Optical Model Analysis of Neutron Scattering by C^{12} between 16 and 20 MeV.
(G. DECONNINCK and J.P. MEULDERS)

This study has been published [3] ; the abstract follows:

"Results of optical model and Monte Carlo calculations are presented and discussed. The aim of this work is the study of resonances occuring in $Be^9(\alpha,n)C^{12}$ and $C^{12}(n,n)C^{12}$ reactions corresponding to states in C^{13}. Preliminary results are compared with calculation. It is also shown that discrepancies between Optical Model calculations and measurements of elastic scattering of 14 MeV neutrons cannot be explained by the presence of those resonances".

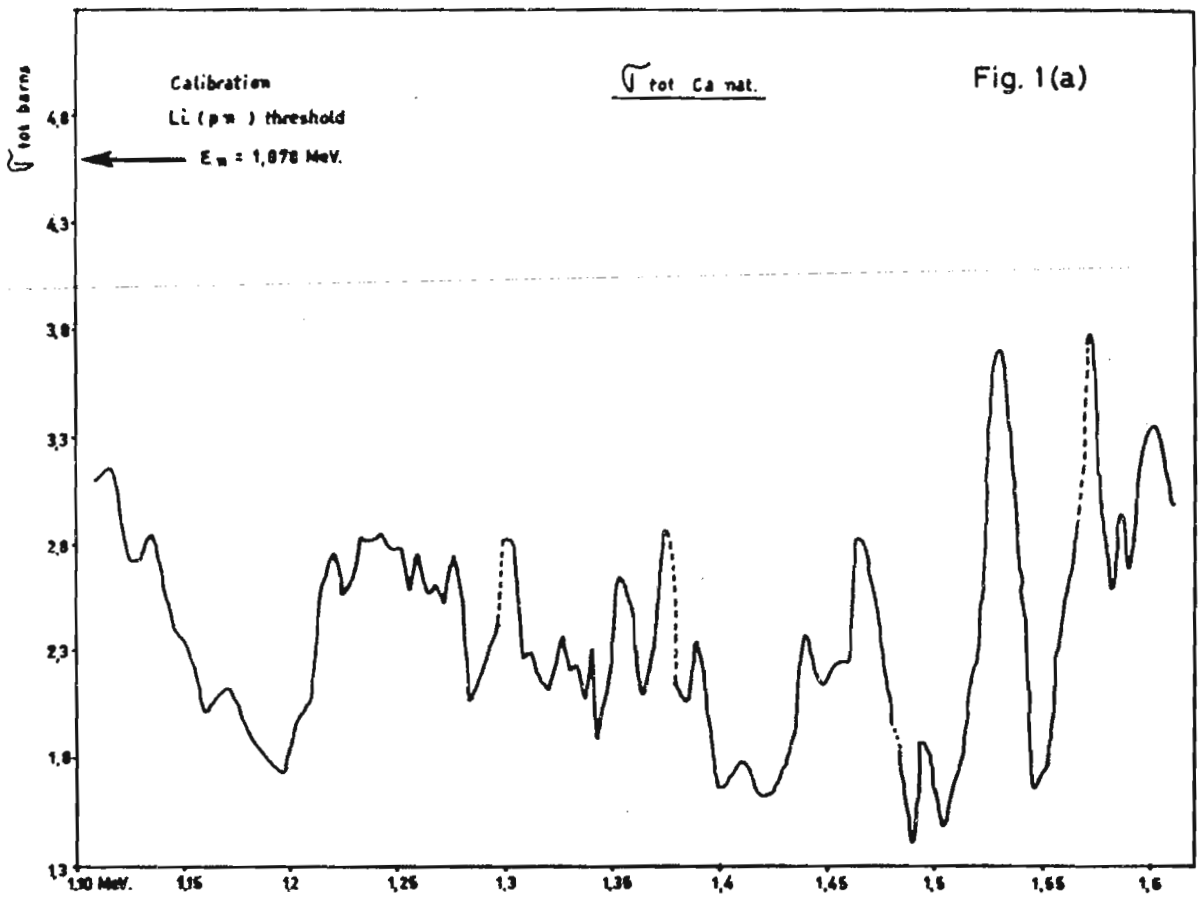
Calibration
Li (p n) threshold
E_n = 1,878 MeV.
σ_{tot} Ca nat.
Fig. 1(a)
σ_{tot} barns
4,8
4,3
3,8
3,3
2,8
2,3
1,8
1,3
1,30 MeV.
1,15
1,2
1,25
1,3
1,35
1,4
1,45
1,5
1,55
1,6

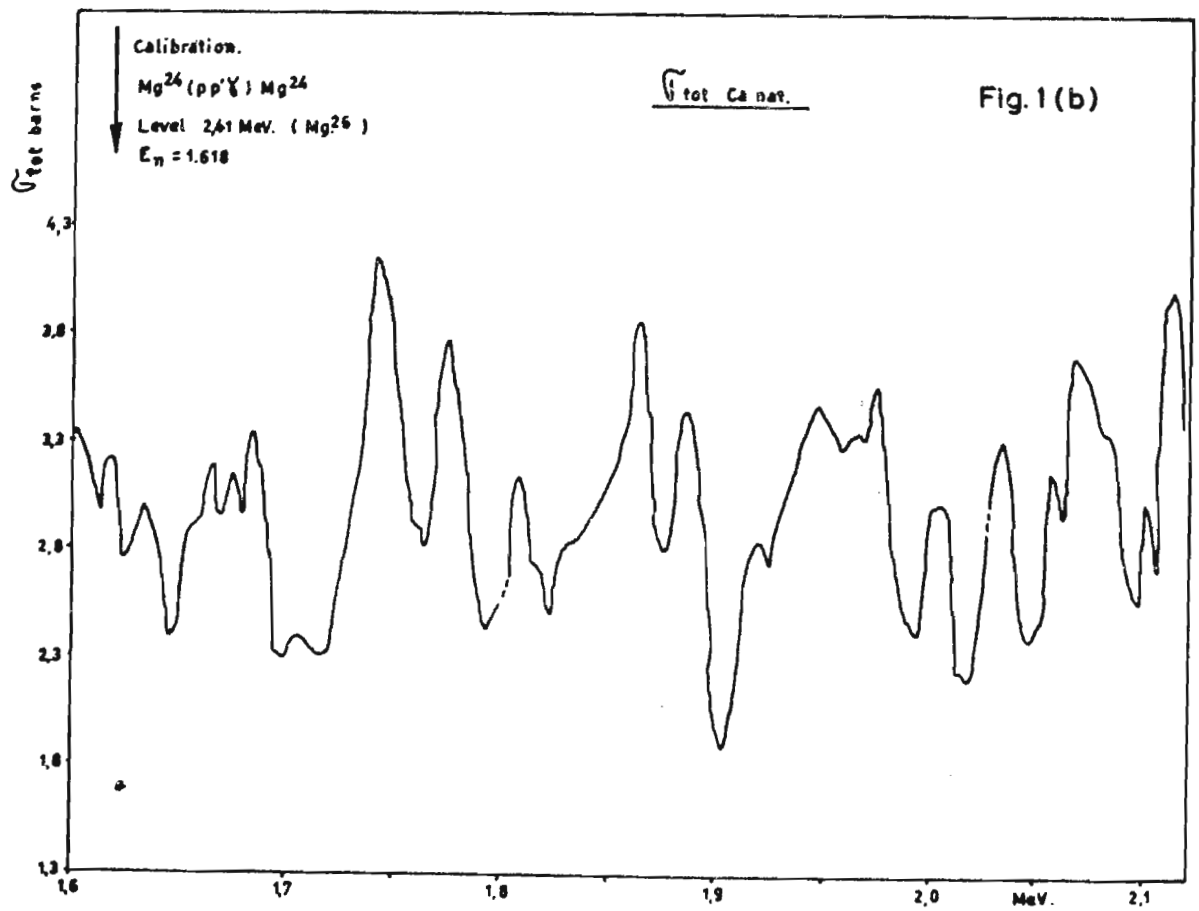
Calibration.
Mg^{24} (p p'γ) Mg^{24}
Level 2,61 MeV. (Mg^{26})
E_n = 1.618
σ_{tot} Ca nat.
Fig. 1(b)
σ_{tot} barns
4,3
3,8
3,3
2,8
2,3
1,8
1,3
1,6
1,7
1,8
1,9
2,0
MeV.
2,1

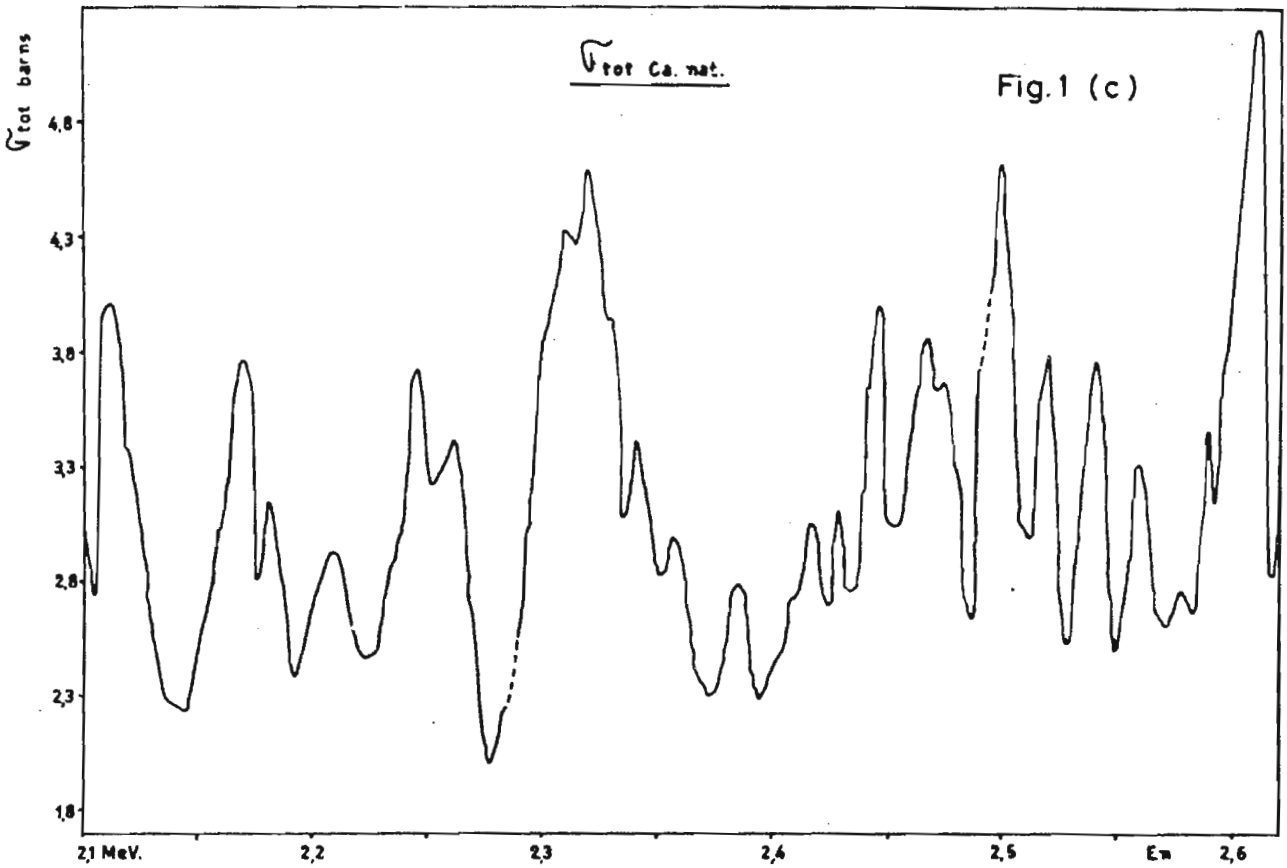
σtot barns
σtot Ca. nat.
Fig. 1 (c)
4,8
4,3
3,8
3,3
2,8
2,3
1,8
2,1 MeV.
2,2
2,3
2,4
2,5
En
2,6

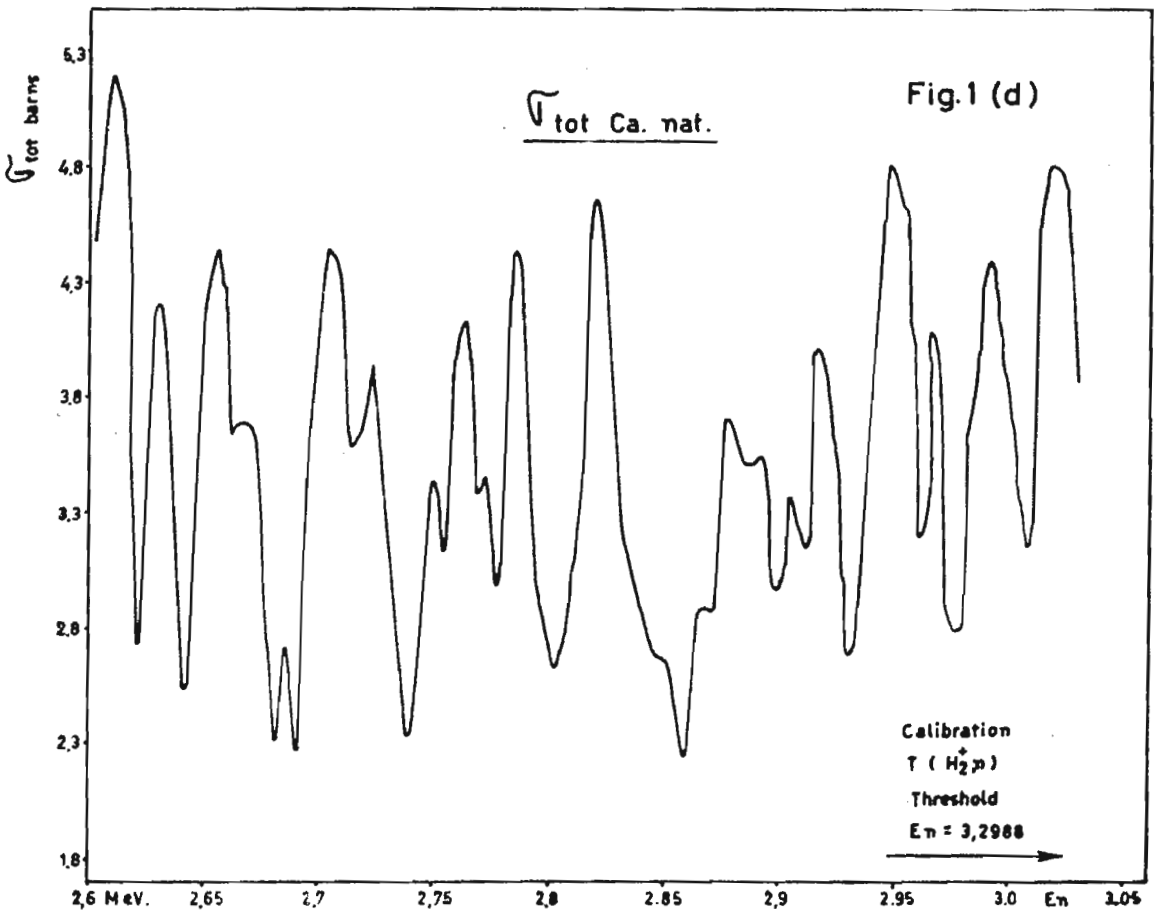
σtot barns
σtot Ca. nat.
Fig. 1 (d)
5,3
4,8
4,3
3,8
3,3
2,8
2,3
1,8
Calibration
T (H2+ p)
Threshold
En = 3,2988
2,6 MeV.
2,65
2,7
2,75
2,8
2,85
2,9
2,95
3,0
En
3,05

4. Elastic Scattering of Neutrons on C^{12}
(G. DECONNINCK and J.P. MEULDERS)

Elastic scattering of 17,5 MeV neutrons is measured on C^{12} by time of flight. The neutrons are produced by the $T(d,n)He^4$ reaction (gas target). Measurements are still underway.

5. (He^3n) and (pn) reactions on light nuclei
(F. BODART and G. DECONNINCK)

The pulsed beam of the 4 MeV Van de Graaff has the following characteristics:

Repetition rate : 5 Mc
Pulse width : 4 nsec (protons and deuterons)
7 nsec (He^3)

A new RF deflector has been installed on the analysed beam; with a frequency of 20 MHz, a peak to peak voltage of 1400 Volt is sufficient to obtain a pulse width of about 1 nsec protons and deuterons and 2 nsec He^3.

Our purpose is to study the following reactions by time of flight: Be^9 (ppn); $Be^2(2\alpha)$; $Be^9(pn)B^{11}$; $Be^9(He^3n)C^{11}$. Measurements are underway.

References (C.P.N. Louvain)

[1] G. Deconninck, M. Husain, Ann. Soc. Sc. Brux. 80, II (1966) 185.
[2] G. Deconninck, M. Husain, Bull. Acad. Roy. Sc. Belg., 5e Série, 14 (1958) 10.
[3] G. Deconninck, J.P. Meulders, Ann. Soc. Sc. Brux. 80, II (1966) 193.

XVIII. LABORATOIRE VAN DE GRAAFF, UNIVERSITE DE LIEGE

(Prof. L. WINAND)

1. Le travail sous contrat Euratom pour la mesure des distributions angulaires de $^{6}Li(n,t)$ a été achevé et les résultats sont publiés [1]

2. L'étude des long-compteurs faisant l'objet d'une thèse de doctorat en sciences (G. ROBAYE) est publiée dans [2] . Ces résultats sont résumés comme suit:
"Une étude de la réponse d'un détecteur à neutrons rapides du type long-compteur" par la méthode de simulation de Monte Carlo a été réalisée. Les résultats de cette étude sont controlés expérimentalement en utilisant des flux de neutrons calibrés au moyen de la détection de la particule associée".

3. Etude au moyen d'un détecteur à semiconducteur avec convertisseur au bore de la distribution de neutrons thermalisés dans le canal central d'un modérateur hydrogéné.
On mesure la distribution des neutrons thermalisés dans le canal d'un long-compteur au moyen d'un détecteur à semi-conducteur avec convertisseur au bore. On mesure également l'effet d'une bague de cadmium sur la réponse d'un long-compteur pour des neutrons de différentes énergies et des positions et dimensions de bagues différentes. On en tire des conclusions sur les possibilités de corriger les courbes de réponse des long-compteurs.

References

[1] L. Winand et al. Communication Euratom 1195 LC/8/66.
[2] G. Robaye , Bull. Soc. Sc. Lg. n° 9-10 (1966).

XIX. CENTRE D'ETUDE DE L'ENERGIE NUCLEAIRE (C.E.N.-S.C.K.) Mol, Belgium

1. Slow Neutron Resonances

(F. POORTMANS)

1.1. Spin measurements of the 8.8 eV and the 12.4 eV resonances of U^{235}

Scattering measurements have been performed in the 8.8 eV and the 12.4 eV resonances of U^{235} [1, 2] using the BR2 crystal spectrometer as a monochromatic neutron source. In order to discriminate against the fission-neutron background, a He^3 proportional counter has been used as scattering detector. The method is essentially the same as for the experiments with non-fissile isotopes [3] except for some small modifications to the analysis of the data due to the higher efficiency of the He^3 counter.

Because of the very low scattering counting rates the detector has been heavily shielded, reducing the total background to approximately 40 counts per hour, which is 300 times less than the scattering signal which would be obtained at 10 eV if all the neutrons were scattered by the target.
The following results have been obtained :

8.8 eV : $\Gamma_n/\Gamma = (1 \pm 0.13)\ 10^{-2}$; $J = 3$

12.4 eV : $\Gamma_n/\Gamma = (1.46 \pm 0.25)\ 10^{-2}$; $J = 4$

1.2. Spin measurement of the 2.4 eV resonance of Hf^{177}

Because of the disagreement between some spin determinations [4, 5] and the recently reported data about the resonant capture γ-spectrum in this resonance [6] we have repeated the scattering experiments. The experimental conditions were much better than in the previous experiments:
resolution (FWHM) : 64 meV
signal to background ratio : 10 : 1
minimum transmission : 0.83
The following results have been obtained :

$\Gamma_n/\Gamma = (12.8 \pm 0.5)\ 10^{-2}$

$g = 0.53 \pm 0.02$ so that $J = 4$ in agreement with our previous results [4]

.2. Fission Physics and Chemistry

.2.1. Study with Nuclear Track Detectors of the Thermal-Neutron Induced Reaction Am^{241} (n,γ) Am^{242m} (fission)

(C. WAGEMANS, Stag. Univ. Gent, and A. DERUYTTER)

The possibilities of natural and synthetic muscovite mica for the detection of heavy charged particles have been examined. These experiments showed that mica is a very useful detector for fission fragments in the presence of a high α-activity because of its excellent discrimination between these radiations. A particular example was the study of the formation of a spontaneously fissioning isomer Am^{242m} (T 1/2 = 13 ms) An Am^{241} source on a rotating disk passed through a high intensity neutron beam extracted from the BR2 reactor and subsequently in front of two mica detectors, placed under 180° with respect to each other. The speed of revolution was such that the time interval between the passage of the source in front of both detectors was equal to 13 msec, i.e. the halflife of the isomer.

From our measurements we were able to put an upper-limit for the thermal cross-section of this reaction [7] :
$\sigma_{th} < 0.13$ mbarn.

.2.2. Binary to Ternary Fission Ratio for U^{235} in the Neutron Resonance Region.

(A. DERUYTTER, BCMN, and C. WAGEMANS, burs. FNRS)

This study is a joint enterprise of CEN and BCMN. The aim is a detailed study of the B/T fission ratio in the resonance region (up to 100 eV max.), where the published results do not seem to be conclusive. Special attention will be given to the correct registration of the ternary fission events.

Two sets of 4 surface-barrier detectors connected in parallel have been developped together with the associated electronic equipment and have been tested at a reactor beam extracted from BR1. A collimator, shutter and detector chamber have been constructed and installed at the CBNM-LINAC at Geel. Preliminary measurements on U^{235} are being started.

2.3. New Arsenic Fission Isotopes
(P. del MARMOL)

The yield of the 2.15 ± 0.15 s delayed neutron emitter, mentioned in the previous EANDC(E)-66-U report, was corrected and contributes to 4 per cent of the total yield of delayed neutrons formed in the thermal neutron fission of U^{235}. It is assigned to As^{85} as delayed neutron precursor, with a neutron emission probability of 11 ± 3 per cent, on the grounds of the fine structure of the fission mass-yield curve in this mass region.

An upper limit to any contribution of a Sb delayed neutron precursor to this activity is 25 per cent.

These results are in print [8] .

Work is in progress to determine the half-lives and fission yields of As^{83} and As^{84} using the same apparatus. A preset timer permits to vary the interval between the end of irradiation and the As separation. The Br^{83} and Br^{84} granddaughters are then separated and their decay followed by means of a Geiger-Müller counter ; their initial activities are directly related to those of As^{83} and As^{84}.
Partial results show that their half-lives are respectively of the order of 10 s and 1 s.

3. Inelastic Scattering of Slow Neutrons
(S. HAUTECLER and W. VAN DINGENEN †)

3.1. Improvements in the BR2 time-of-flight spectrometer

We have added a second flight tube, making a fixed angle with the first one, and a basis, placed in the incident monochromatic beam, which is provided with two monitors used for the calibration.

A program unit was set up which controls the shutter status (open or closed), the selected number of counts in the monitor scaler, the sample orientation,

---

† Deceased

and the count mode of the analyzer memory (add or substract); the orders are given by means of a punched tape program.

A new shielded room, provided with eight evacuated flight tubes, is under construction.

3.2. Lattice dynamics of Ni

Calculation of dispersion curves based on various models was continued and compared with our previous measurements. A final report was written [9, 10]

3.3. Lattice dynamics of α-Fe

In the course of the study on Fe, much effort was devoted to the improvement of the time-of-flight technique when used to determine the phonon dispersion relations. Our results, taken at room temperature, are given in Fig. 2 ; they complete and partially agree with previous results [11]. As in the case of Ni agreement with calculations based on the Krebs force model [12] is obtained; a good fit is also found in non-symmetry directions for the branches of the scattering surface relative to a scattering angle of 100°.

The spin wave dispersion relation has also be measured at 250°C up to a value of 2.25 $\mathring{A}^{-1}$ for the modulus q of the wave vector. For small q-values, the results could be fitted by the quadratic approximation, with a value of (270 ± 40) meV $\mathring{A}^{2}$ for the exchange stiffness parameter.

An article upon this subject is in print [13] .

3.4. Lattice dynamics of Zn

The motivation for a further measurement on Zn lays in the discrepancies for the shape of the $[01\bar{1}0]$ AT_2 branch of the dispersion relations, found between two previous works.

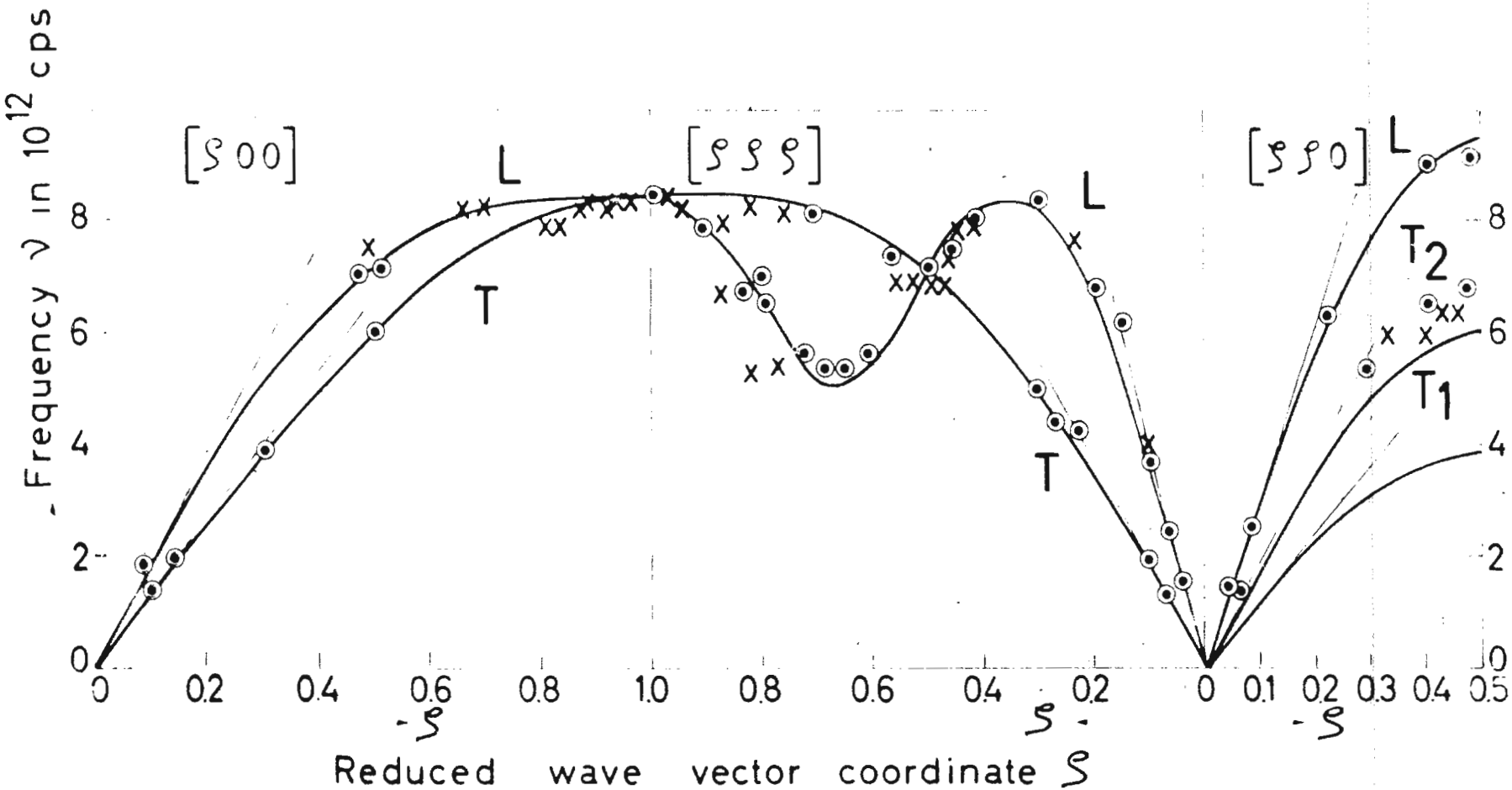

Fig 2 - Phonon dispersion curves for α-Fe.

⊙ our measurements ; x exper data of G.G.E.Low ; — calcul. (Krebs model).

Up to now, we have measured one complete scattering surface, relative to a scattering angle of 100° and an incident wavelength of 4.154 Å; the hexad axis was kept perpendicular to the scattering plane and the angular separation between successive orientations of the sample was equal to 2°.

4. Integral cross section measurements

The 2200 m/sec activation cross sections σ_o for capture reactions of interest in reactor dosimetry are deduced from measurements in the pure maxwellian neutron spectrum of BR1 thermal column [14]. Resonance integrals-denoted I_r, after substraction of 1/v part-are determined in the 1/E spectrum existing in the centre of BR1 lattice cell ($0.5 < E < 500$ eV). Gold is used as a standard characterized by $\sigma_o = (98.7 \pm 0.2)$b. [15] and $I_r = (1490 \pm 40)$b. [16] A few available results are reported hereafter and work continues on the interesting reactions in lutetium, europium and iridium.

4.1. Thermal activation cross section for the reaction $Fe^{58}(n,\gamma)Fe^{59}$ in natural iron

(A. FABRY, J.P. DEWORM)

Our preliminary result reported in EANDC (E) 57 "U" has been reviewed and definitively assessed as :

$$\sigma_o = (1.18 \pm 0.03)\text{b.}$$

assuming 0.33 % abundance, 45.0 d. half life and g = 1.
This is to be compared with a recent measurement by CARTER [17], $\sigma_o = (1.13 \pm 0.05)$b., corrected to be consistent with the cobalt cross section reported below. The recommanded value (1.2 ± 0.1)b. of BNL-325 (second edition, vol. II A, 1966) seems a little bit too high, mainly because of the weight of our previous result $(1.23 \pm 0.035$ barn).

4.2. Thermal activation cross section for the reaction $Co^{59}(n,\gamma)Co^{60m} + Co^{60g}$

(J.P. DEWORM)

The 2200 m/sec activation cross section of cobalt has been found

to be (37.7 ± 0.4)b., in agreement with the recommanded value of (37.2 ± 0.6)b. given in BNL-325 (second edition, vol. II A 1966). The activation rate of cobalt-60 was deduced from comparisons with a CBNM standard source. In the course of that work, the accuracy of the RITCHIE-ELDRIDGE relation (including edge effects) [18] for correction of flux perturbations has been verified up to cobalt thicknesses of 90 mg /cm^2.

4.3. Thermal activation cross section for the reaction $Cu^{63}(n,\gamma)$ Cu^{64}

(B. PINONCELLI, A. FABRY)

Our result σ_o = (4.03 ± 0.17)b. is lower than the renormalized measurements of POMERANCE [19] (σ_o = 4.5 ± 0.35; pile oscillation), MEISTER [20] (σ_o = 4.44 ± 0.26; activation; $4\pi\beta$ counting) and KEATING [21] (σ_o = 4.51 ± 0.10; measurement of σ_t and σ_s). The discrepancy could be related to the assumed value of 0.19 [22] for the β^+ branching ratio in copper-64; it must be noted that, while determining absolute activation rates by means of our calibrated NaI(Tl) 3" x 3" crystal (see also EANDC (E) 57 "U" p. 70), special care was taken to annihilate all β^+ rays at source.

4.4. Study of the reaction $W^{186}(n,\gamma)$ W^{187}

(P.P. DAMLE, burs OCD; A. FABRY; R. JACQUEMIN)

The reaction is characterized by a main resonance at (18.835 ± 0.02)eV; as no bound level effect is apparent and if small corrections (< 6 %) are applied to withdraw the contribution of other known [23] or unresolved positive energy resonances, experimental determination of the ratio I_r/σ_o allows to deduce Γ for the main resonance; Γ_γ is then computed from the measurement of σ_o.
A 3" x 3" NaI(Tl) crystal has been calibrated to better than ± 2 % by means of W^{187} deposits whose activation rates were determined by $4\pi\beta$ measurements; the deadtime of the absolute counter was chosen greater than 5 μsec to eliminate errors due to the metas table level of 0.54 μs in W^{187}. This tungsten foils irradiated with gold in BR1

thermal column were then counted with the calibrated crystal. The WESTCOTT g factor was computed to be 1.001. The half life of W^{187} was measured as (23.74 ± 0.17) hrs.

Tungsten-aluminium alloys (5 and 10 % W in Al) supplied by Mr. VAN-AUDENHOVE (CBNM) were used for the measurement of I_r; the content of tungsten in the alloys was accurately checked by irradiation in thermal column.
The correction for cadmium shielding effect on tungsten was taken from BAUMANN [24], but is presently being redetermined.
Our results, together with the corresponding resonance parameters, are compared to literature in table I.

TABLE 1. Thermal cross section, resonance integral and resonance parameters of 18.8 eV level for W^{186} (n,γ) W^{187} reaction.

σ_o (b)		I_r (b)	
Authors	Result	Authors	Result
POMERANCE (a)	34.1	MACKLIN, POMERANCE(d)	355
SEREN (b)	34.2	FAST, SCOVILLE(e)	490±100
BNL-325 (July 1958)	34±7	JACKS (f)	506± 50
FRIESENHAHN(c)	37.8±1.2	BAUMANN (g)	562± 50
this work	35.4±0.8	this work	534± 50

Resonance parameters (E_r=18.835 eV; g = 1)					
Authors	Γ_n (meV)	Γ_γ (meV)	Γ (meV)	σ_o(b) computed	I_r(b) computed
BNL-325(1958)	266±16	45±6	311±30	32.5	472
JOANOU(h)(1964)	317	52	369	45.0	552
HARVEY(i)(1966)	319± 3	53±8	372± 6	45.3	552
FRIESENHAHN(c)(1966)	272	52	324	37.8	532
this work	251	53±6	304±30	35.4	534

(a) H. POMERANCE - Phys. Rev. 88, 412 (1952).
(b) L. SEREN et al. - Phys. Rev. 72, 888 (1947).
(c) S.J. FRIESENHAHN et al. - see [1] p. 182.
(d) R.L. MACKLIN, H.S. POMERANCE-Geneva Conf.vol.5,96 (1955).
(e) E. FAST, J.J. SCOVILLE - IDO report 16781 (1962).
(f) N.P. BAUMANN - Report DP 817 (1963).
(g) M.K. DRAKE-Nucleonics vol.24 n° 8, 108 (1966)
(h) G.D. JOANOU, C.A. STEVENS - Report GA 5885 (1964).
(i) J.A. HARVEY - see reference [1] p. 31.

References (CEN-SCK, Mol)

[1] F. Poortmans, H. Ceulemans, M. Nève de Mévergnies, Conference on Neutron Cross Section Technology, Washington 22-24 March 1966 AEC Report TID - 4500 p. 755

[2] F. Poortmans, H. Ceulemans, M. Nève de Mévergnies, IAEA Conference on Nuclear Data. Microscopic cross sections and other Data Basic for Reactors, Paris, 17-21 October 1966, paper CN-23/79

[3] H. Ceulemans, M. Nève de Méverngies and F. Poortmans, Nucl. Inst. & Meth. 17 (1962) 342

[4] H. Ceulemans, F. Poortmans, Nucl. Phys. 62 (1965) 641

[5] L.M. Bollinger, R.E. Coté, H.E. Jackson, J.P. Marion and G.E. Thomas, ANL-6879 (1964)

[6] R.R. Spencer, K.T. Faler, Slow Neutron Capture Gamma Ray Conference, Argonne Nat. Lab., November 2-4, 1966

[7] C. Wagemans, Lic. Thesis, Rijksuniversiteit Gent (1966)

[8] P. del Marmol, M. Nève de Mévergnies, J. Inorg. Nucl. Chem. (in print)

[9] S. Hautecler, Doct. Thesis, Université de Liége (1966)

[10] S. Hautecler, W. Van Dingenen, to appear in Physica

[11] G.G.E. Low, Proc. Roy. Soc. (London) 79 (1962) 479

[12] K. Krebs, Phys. Rev. 138 (1965) A143

[13] S. Hautecler, W. Van Dingenen, to appear in Phys. Status Solidi.

[14] A. Deruytter - React. Sci. Techn. 15, 165 (1961).

[15] C.H. Westcott et. al. - Atomic Energy Review Vol. 3 n° 2 (1965).

[16] K. Jirlow, E. Johansson - J. Nucl. Energy A/B 11, 101 (1960).

[17] P. Carter - Conference on Radiation Measurements in Nuclear Power. Berkeley (Glouc.) 12th - 16th September (1966). Paper n° 54.

[18] G.C. Hanna - Nucl. Sci. Eng. 15, 325 (1963).

[19] H. Pomerance - Phys. Rev. 88, 412 (1952).

[20] H. Meister - Z. Naturforschung 13A, 820 (1958).

[21] D.T. Keating et.al. - Phys. Rev. 111, 261 (1958).

[22] K. Way et.al. - Nuclear Data Sheets.

[23] R.C. Block et.al. - ORNL-3924 (1966).

[24] N.P. Baumann - Report D.P. 817 (1963).

XX. Central Bureau for Nuclear Measurements, EURATOM, Geel (Belgium)

1. 3 MeV Van de Graaff Accelerator

1.1. Activation cross sections

H. Liskien, A. Paulsen

1.1.1. Cross sections for neutron induced threshold reactions

Cross sections for the reactions $^{60}Ni(n,p)^{60}Co$ and $^{63}Cu(n,\alpha)^{60}Co$ were determined using the activation technique in the neutron energy range from 8.5 to 11.5 MeV. The $^{14}C(d,n)^{15}N^{g}$ and $^{15}N(d,n)^{16}O^{g}$ reactions were used as neutron sources at the 3 MeV Van de Graaff accelerator. The results are enclosed in fig. 1 and 2. The experimental uncertainties are of the order of $\pm$ 8 to $\pm$ 12%. The energy of the excited state neutrons was not always below the reactions threshold. This gave rise to corrections which were in some cases large, due to the relatively small yield of ground state neutrons in these neutron producing reactions. The uncertainties of these corrections are responsible for the scattering of the results between 10 and 12 MeV. Relative angular distributions for all neutron groups were measured by Knitter and Coppola (CBNM) with time-of-flight techniques for the same targets and deuteron bombarding energies as used for the activations. Absolute neutron fluxes were determined in all cases by means of a telescope counter.

$^{60}Ni(n,p)^{60}Co$ and $^{63}Cu(n,\alpha)^{60}Co$ cross sections were measured also at 6 MeV with the D(d,n) neutron source and at 12.1 MeV and between 16.5 and 19.5 MeV with the T(d,n) neutron source. The complete excitation functions containing these results together with the earlier ones are shown in fig. 1 and 2. A paper is prepared for publication.

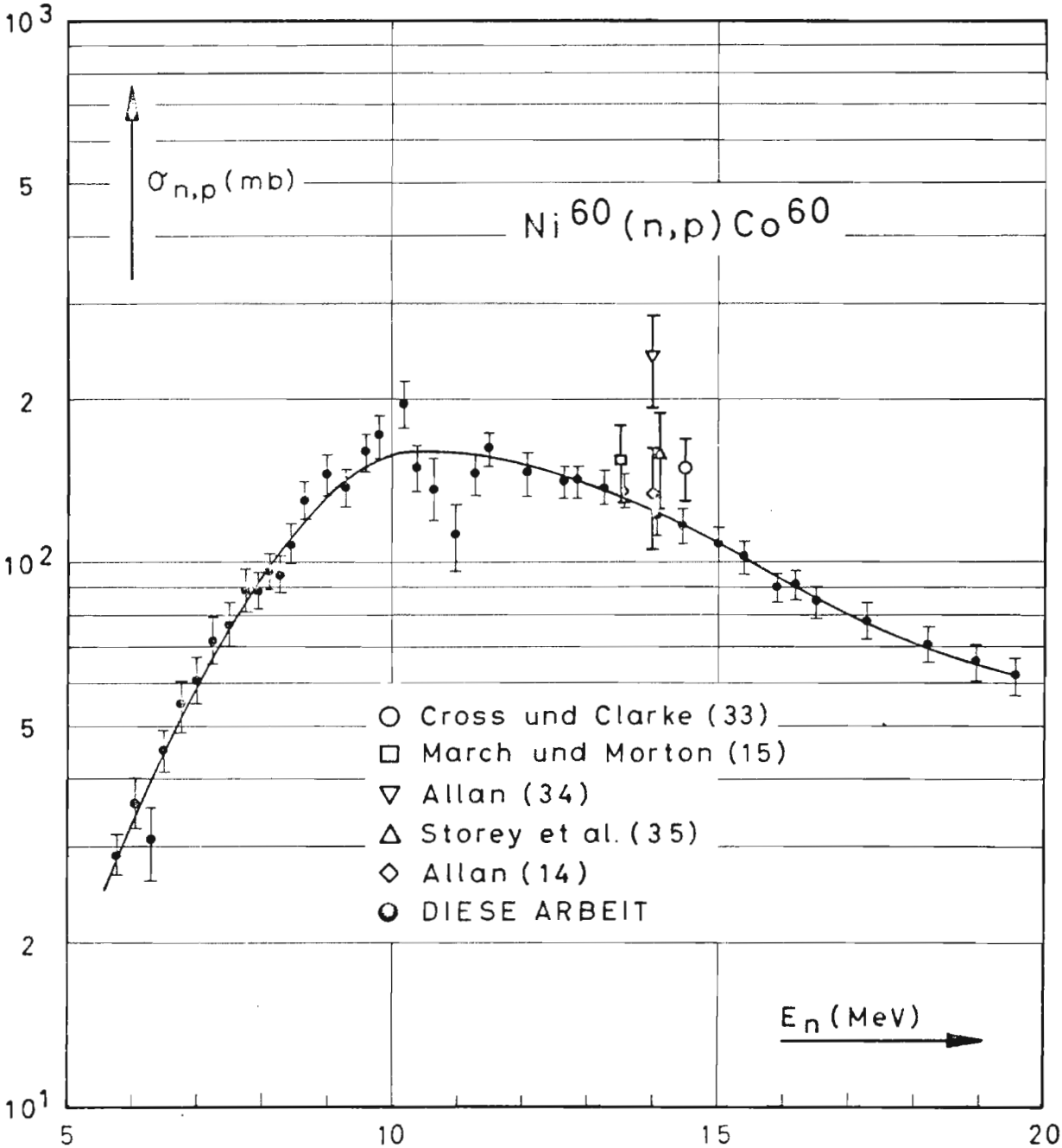
10^3
5
2
10^2
5
2
10^1
$\sigma_{n,p}$ (mb)
$Ni^{60}(n,p)Co^{60}$
Cross und Clarke (33)
March und Morton (15)
Allan (34)
Storey et al. (35)
Allan (14)
DIESE ARBEIT
E_n (MeV)
5
10
15
20

Fig. 1

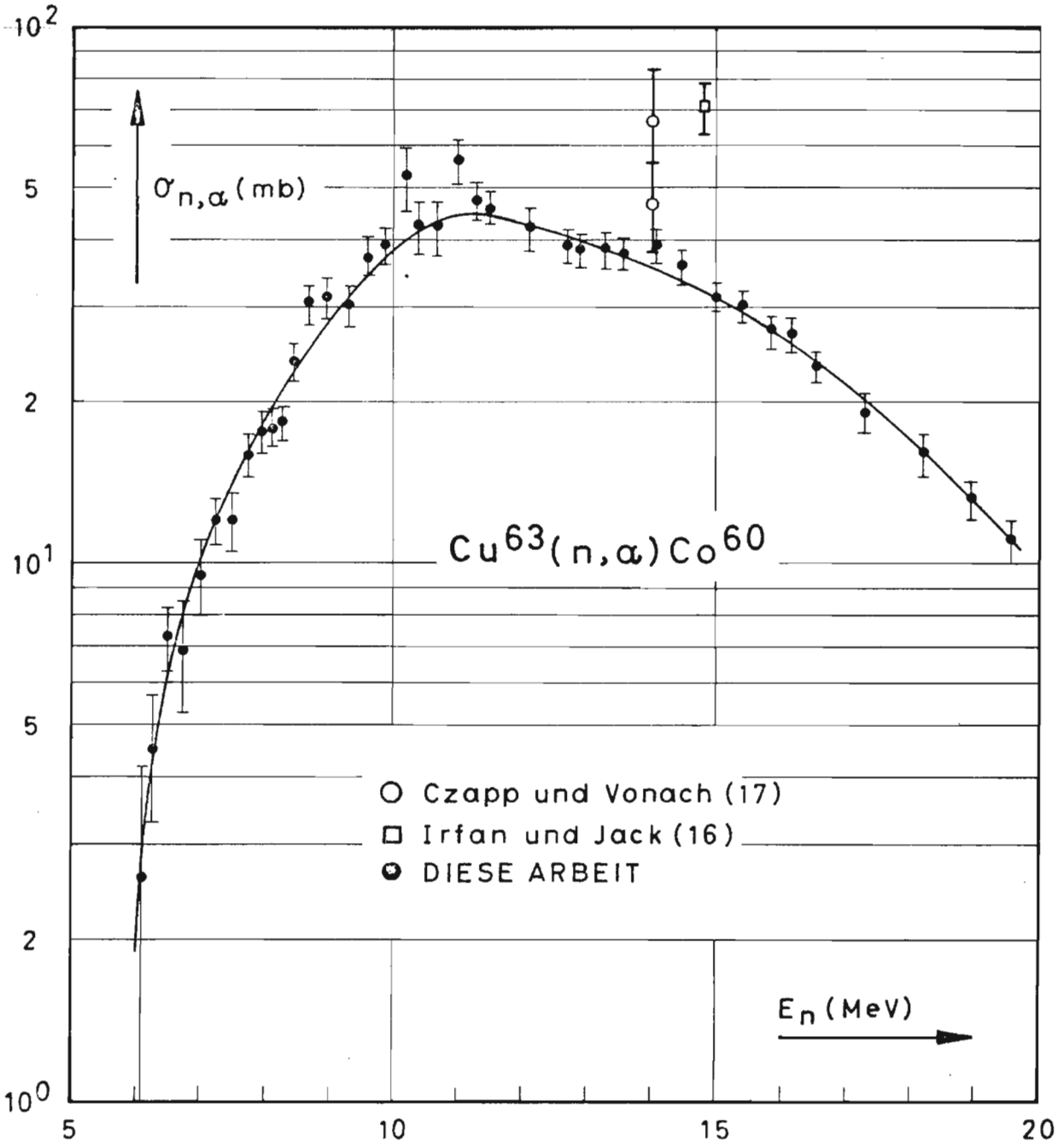
10^2
5
2
10^1
5
2
10^0
$\sigma_{n,\alpha}$ (mb)
$Cu^{63}(n,\alpha)Co^{60}$
Czapp und Vonach (17)
Irfan und Jack (16)
DIESE ARBEIT
E_n (MeV)
5
10
15
20

Fig. 2

A research was carried out for the spin cut-off factor σ in ^{60}Co using the method of Huizenga and Vandenbosch. For this purpose cross sections for the production of the isomeric state of ^{60}Co ($T_{1/2}$ = 10.35 min) were measured at 8.2 and 14.0 MeV for for the $^{60}Ni(n,p)$ reaction and at 8.2 MeV for $^{63}Cu(n,\alpha)$. Furthermore, cross sections for both the ground and isomeric state were determined at 1.8, 2.2, 6.2, and 14.0 MeV for the capture reaction $^{59}Co(n,\gamma)^{60}Co$. From these results together with those from Kantele and Gardner at 14.7 MeV for the $^{63}Cu(n,\alpha)^{60}Co^{m}$ reaction and from Keisch for the thermal capture ratio σ_m/σ_{tot}, a value of $\sigma = 4.3 \pm 0.3$ at E = 7.5 MeV was derived by means of the sophisticated γ-cascade model of Pönitz. This spin cut-off factor is in good agreement with a nuclear moment of inertia for a rigid sphere. A compound spin J = 4 was obtained for the 132 eV neutron resonance in ^{59}Co which is in agreement with the results of Jain et al. A paper is prepared for publication.

Cross sections for (n,3n)-reactions were determined with neutrons in the energy range 18.2 - 19.3 MeV for the odd-even nuclei ^{103}Rh, ^{107}Ag, ^{113}In, ^{127}J, ^{133}Cs, and ^{141}Pr. The statistical concept of the compound nucleus model was expanded to successive emission of three particles after compound nucleus formation. The experimental (n,3n)-cross section results are consistent with the prediction of this model. A paper on this subject is prepared for publication.

A 0.6 cm^3 Li-drifted Ge-crystal has been put into operation as a γ-spectrometer, the efficiency curve and counting geometry of which may be seen from fig.3.

1.1.2. Measurement of neutron fluxes

The work for development of a neutron proportional counter was continued. There are still discrepancies

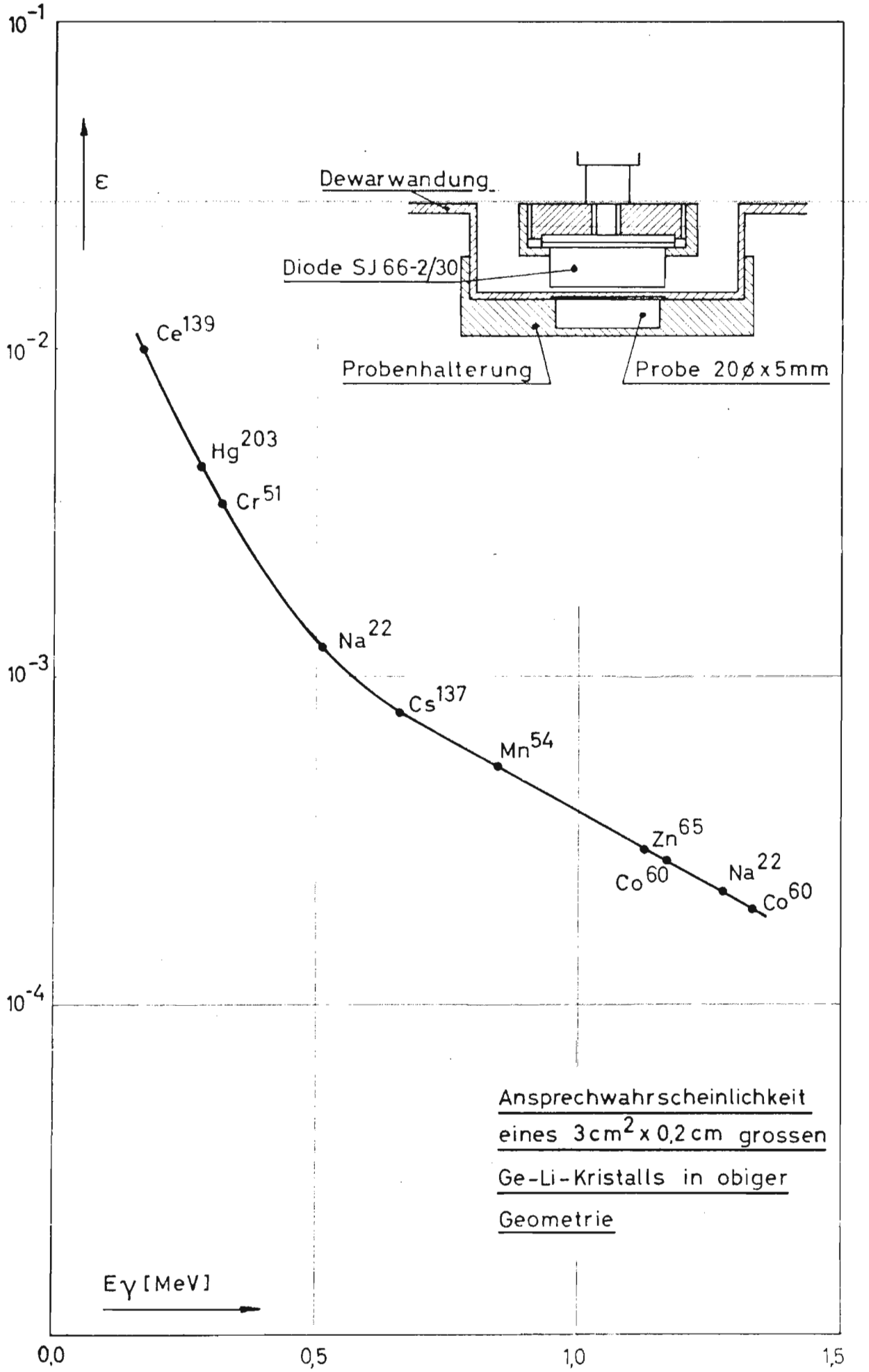
10^-1
10^-2
10^-3
10^-4
ε
Dewarwandung
Diode SJ 66-2/30
Probenhalterung
Probe 20ø x 5mm
Ce139
Hg203
Cr51
Na22
Cs137
Mn54
Zn65
Co60
Na22
Co60
Ansprechwahrscheinlichkeit
eines 3cm2 x 0,2 cm grossen
Ge-Li-Kristalls in obiger
Geometrie
Eγ [MeV]
0,0
0,5
1,0
1,5

in absolute neutron flux obtained with this proportional counter and the telescope counter at 1 MeV neutron energy. But remeasurements of some $^{7}Li(n,p)$ and $T(p,n)$ angular distributions resulted in agreement with the data of LA-2014 within the experimental uncertainties. This gives indication for a reliable relative response with neutron energy.

1.1.3. Computer programs and theoretical work

A program for Hauser-Feshbach calculations was successfully applied. Also the spin distribution program of Hafner et al. (ANL 6662) and the new γ-cascade program of Pönitz were used, although associated with some difficulties. Our statistical theory program was modified for the use of different level density formulas. A series of calculations for the excitation functions of the reactions $^{60}Ni(n,p)^{60}Co$ and $^{63}Cu(n,\alpha)^{60}Co$ showed evidence for the true level density function being somewhat between the Fermi gas formula $\exp 2(aU)^{1/2}$ and the constant nuclear temperature level density $\exp(U/T)$. The studies concerning the spin cut-off factor σ of ^{60}Co confirmed an energy dependence $\sigma \sim U^{1/4}$ and made evident that the neglection of this energy dependence is a serious source of error.

1.1.4. Publications

Liskien, H., A. Paulsen, Cross sections for the $^{63}Cu(n,\alpha)^{60}Co$, $^{60}Ni(n,p)^{60}Co$ and some other threshold reactions using neutrons from the $^{9}Be(\alpha,n)^{12}C$ reaction, Nukleonik 8, 315(1966).

Liskien,H., A. Paulsen, Compilation and measurement of differential cross sections for neutron induced threshold reactions, Proc. Conf. Radiation Measurement in Nuclear Power, Berkeley U.K., Sept. 1966, in press.

Paulsen, A., H. Liskien, Cross sections for some (n,p)-reactions near threshold, Proc. IAEA Conf. Nuclear Data, Paris, October 1966, paper CN-23/90, in press.

Liskien, H., A. Paulsen, Compilation of cross sections for some neutron induced threshold reactions, Supplement sheets, EUR 119.e, Vol. I and II.

1.2. Fast-neutron time-of-flight measurements

M. Coppola, H.H. Knitter

1.2.1. Scattering measurements on ^{7}Li

The measurement of elastic and inelastic neutron scattering angular distributions on ^{7}Li in the energy range from 1.1 to 2.3 MeV has been completed. The measured data and additional cross section values were prepared for the computer calculations of various important corrections (flux attenuation, multiple scattering, finite geometry). In fig. 4 an example of uncorrected elastic and inelastic angular distributions is shown.

1.2.2. Scattering measurements on ^{6}Li

Fourteen neutron elastic scattering angular distributions were measured in steps of 100 keV in the energy range between 1.0 and 2.3 MeV. Also in this case the experimental data and the additional neutron cross sections were prepared in the form needed for the already mentioned computer calculations. The evaluation of the final absolute differential and total elastic scattering cross sections is being made. Fig. 5 gives an example of an uncorrected elastic angular distribution.

1.2.3. Scattering measurements on Si

For natural silicon 8 elastic and inelastic neutron scattering angular distributions were measured in steps of 250 keV in the energy range between 4 and 5.75 MeV. The neutrons were produced via the $D(d,n)^{3}He$ reaction. A deuteron gas target was used, which yields much more neutrons compared with an occluded target of the same thickness. In fig. 6 an example of uncorrected elastic and inelastic angular distributions is shown.

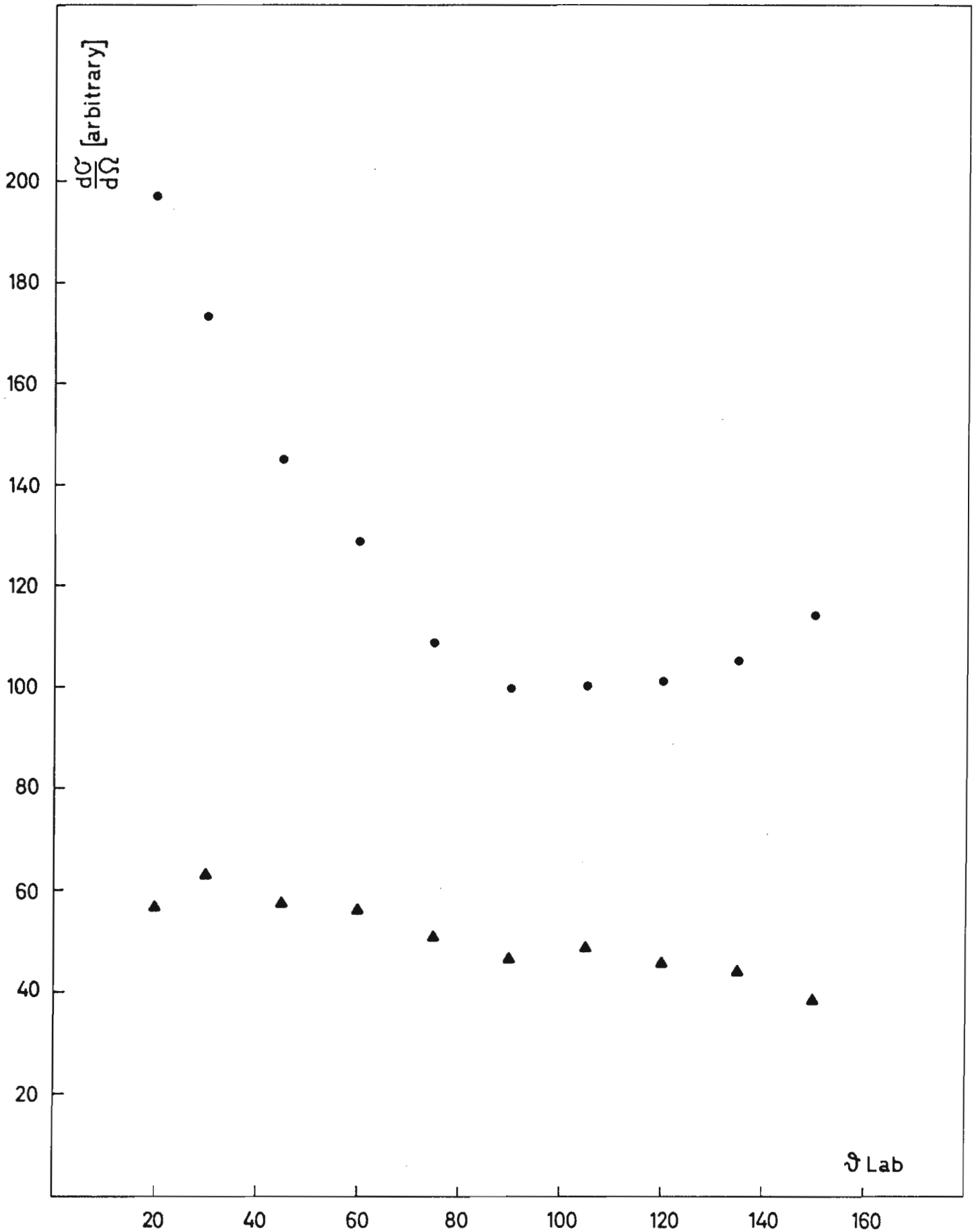

Fig.4 • $^{7}Li(n,n)^{7}Li$ neutron angular distribution at $E_n = 1.74$ MeV

▲ $^{7}Li(n,n')^{7}Li^{*}$ $Q = -0.48$ MeV neutron angular distribution at $E_n = 1.74$ MeV

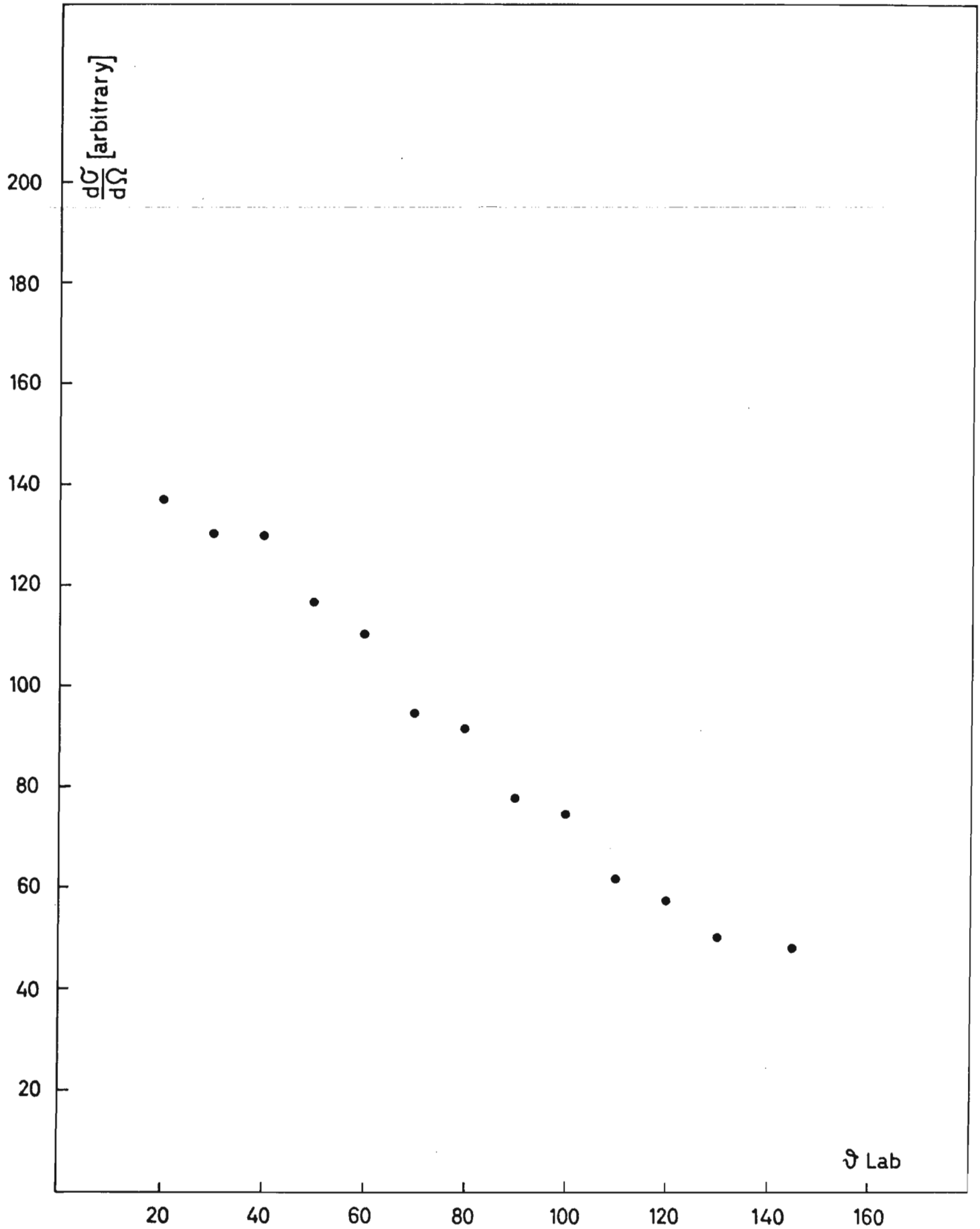

Fig. 5 $^{6}Li(n,n)^{6}Li$ neutron angular distribution at $E_n = 1.8$ MeV

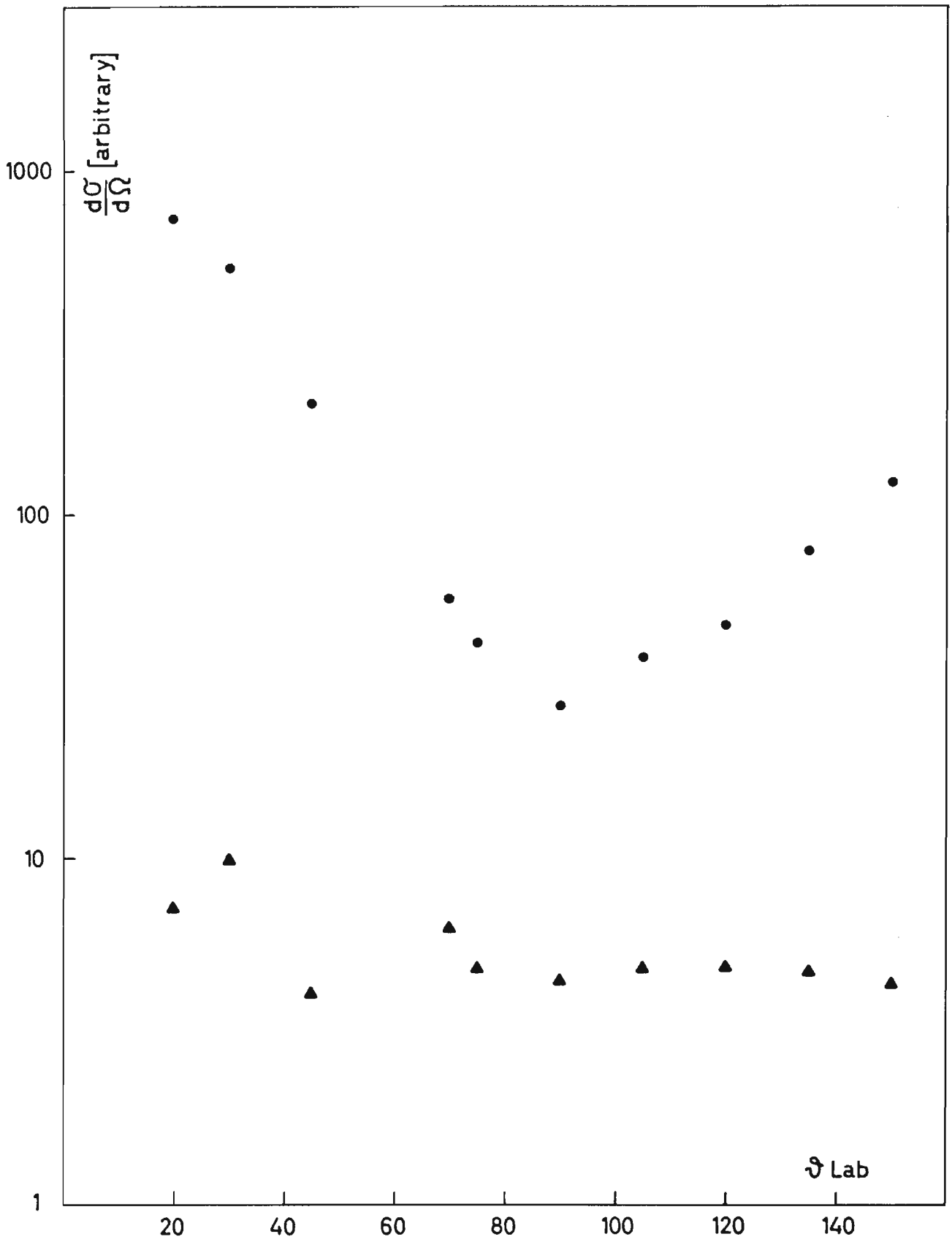

Fig. 6 • Si(n,n)Si neutron angular distribution at $E_n = 5.0$ MeV

▲ Si(n,n')Si* neutron angular distribution at $E_n = 5.0$ MeV

1.2.4. Angular distributions for the reactions $^{14}C(d,n)$ and $^{15}N(d,n)$

These reactions are used as neutron sources at the 3 MeV-Van de Graaff, giving neutrons between 8.5 and 11.5 MeV, for the determination of threshold reaction cross sections with the activation technique by Paulsen and Liskien. For this work it was necessary to know the relative angular distributions of the emitted neutrons. They were measured with the scattering time-of-flight spectrometer for the two reactions at 3 primary deuteron energies. In addition to the neutron angular distributions to the ground state groups it was possible to resolve in the time-of-flight spectra also 3 neutron groups which correspond to excited states in the residual nuclei. Due to energy resolution the evaluation of the corresponding angular distributions was, however, only possible in the case of $^{14}C(d,n)^{15}N^{*}$ at primary deuteron energies E_d = 1.35 MeV and 2.0 MeV, and in the case of $^{15}N(d,n)^{16}O^{*}$ at E_d = 1.0 MeV. All the angular distributions are evaluated and results are available.

1.2.5. Equipment

The construction of three counters using 56 AVP photomultiplier tubes is on the way. The simultaneous use of more than one high energy neutron detector will allow a more efficient utilisation of the accelerator, especially for angular distribution measurements.

Three more time-to-pulse-height converters of the kind already in use are going to be completed within the beginning of next year. In the case of simultaneous use of several neutron detectors the output of these converters will be addressed towards a multiple input unit of the existing 4096-channel analyser and will be stored in different sections of the magnetic memory. Such an input unit will allow up to four different signals to be independently processed.

In conjunction with the previously mentioned detectors, appropriate shieldings were made ready. The possibility of using various detector diameters as well as different collimating openings was foreseen. The outside shielding parts and the collimators were filled with a mixture of paraffin and lithium carbonate, while lead inserts were built for gamma-ray background attenuation.

Most of the operations needed for data recording and sample changing are now automatic, so that only occasional control from the operator is needed during the measurement runs.

A neutron detector with a neutron energy threshold of about 30 keV was realized. While a more accurate determination of the counter efficiency is in progress, the results of a preliminary test are already available and shown in fig. 7. Here the curve was obtained using the direct neutrons from the $T(p,n)^3He$ reaction at proton energy $E_p = 1.0$ MeV and at laboratory angles between 0 and 130 degrees. Results were corrected for the intensity variation of neutron yield with angle.

The feasibility of an accurate determination of the $^{10}B(n,\alpha)^7Li$ cross section at neutron energies around 100 keV is under study. For this purpose a simple preliminary experimental apparatus was designed.

1.2.6. Publications

Coppola, M., H.H. Knitter, Elastic scattering of neutrons from natural silicon, EUR 2798.e (1966).

Coppola, M., H.H. Knitter, A study of levels in the highly excited ^{29}Si-nucleus, submitted to Nucl.Phys. (1966).

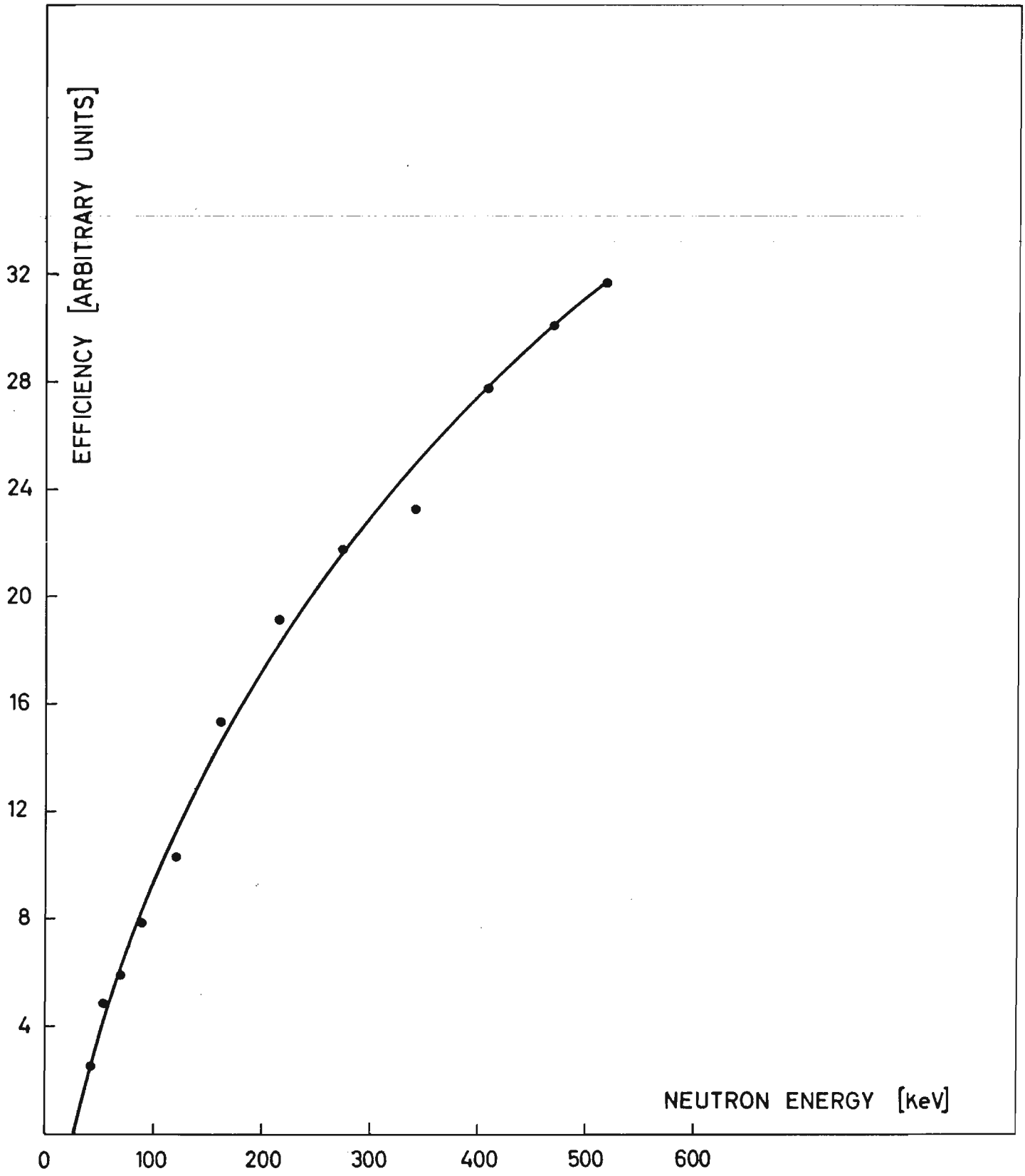

Fig.7 Efficiency curve of the low energy threshold neutron counter (preliminary results)

2. Linear accelerator

2.1. Total cross sections

K.H. Böckhoff, A. De Keyser, W. Kolar, H. Martin*

2.1.1. Total cross section of ^{240}Pu in the resonance region

The automation of the data acquisition system for total cross section measurements includes the different operations of the sample changers (sample "in" and "out", background sample "in" and "out") which are controlled by preset BF_3-monitor counts. It includes further the transfer of data accumulated in the different sample changer positions to magnetic tape and the print out of the information of various scalers (central BF_3-monitors, local BF_3-monitors, time, sum of analysed counts, identification numbers of the experimental runs).

Special care has been devoted to the reduction of the backgrpund counts of the ^{10}B-NaI-detector. By shielding the detector with a massive heterogeneous structure of heavy concrete, paraffin and Li_2CO_3 it was possible to reduce the constant component of the background by a factor of two.

The first series of measurements on ^{240}Pu during which 3 disks of plutonium (98% enriched in ^{240}Pu) of 3" diameter and a total weight of about 30 g were employed covered the neutron energy range from 20 eV to 800 eV. Besides this, a survey transmission measurement was made in the energy range from 800 eV to 5 keV as an orientation for later runs and to locate already the resonances.

In total 158 resonances have been detected between 20 eV and 5 keV, most of which were not known before. Between 20 eV and 750 eV, 35 neutron resonance widths Γ_n could be determined. The CBNM values for the neutron widths agree well - except for a few resonances -

* Now at Euratom Headquarters, Brussels

with the preliminary results of simultaneously performed Harwell measurements.

Measurements in the energy range from 800 eV to 6 KeV with 10 nsec burst and channel width have been started. The total quantity of ^{240}Pu used in this measurement is 73 g. In order to save time by covering the range between 800 eV and 6 keV in one run, the TMC 4096-channel analyzer has been transformed into a 20480-channel analyzer by a suitable combination of the functions of the analyzer core memory with that of a magnetic tape unit. Data accumulation was not yet finished for this experimental run at the end of the year. Table I summarizes the main characteristics of this experiment.

Table I: Characteristics of total cross section measurements on ^{240}Pu

Quantity	Neutron energy range		
	20 - 350 eV	300 - 800 eV	800 eV - 6 keV
Linac beam energy	50 MeV	50 MeV	50 MeV
Peak beam current	0.45 A	1.5 A	2.2 A
Burst repetition frequency	100/300 pps	400 pps	600 pps
Burst width	300 nsec	50 nsec	10 nsec
Channel width	320 nsec	40 nsec	10 nsec
Number of channels	4096	4096	20480
Sample changer at	50 m	50 m	50 m
Detector at	100 m	100 m	100 m
Moderator (polyethylene)	20x20x2.4 cm^3	dito	dito
Background samples			
a) always in the beam	Mn	Bi	-
b) in separate background run	^{238}U, Co, Mn	Bi, Mn	Bi, Co

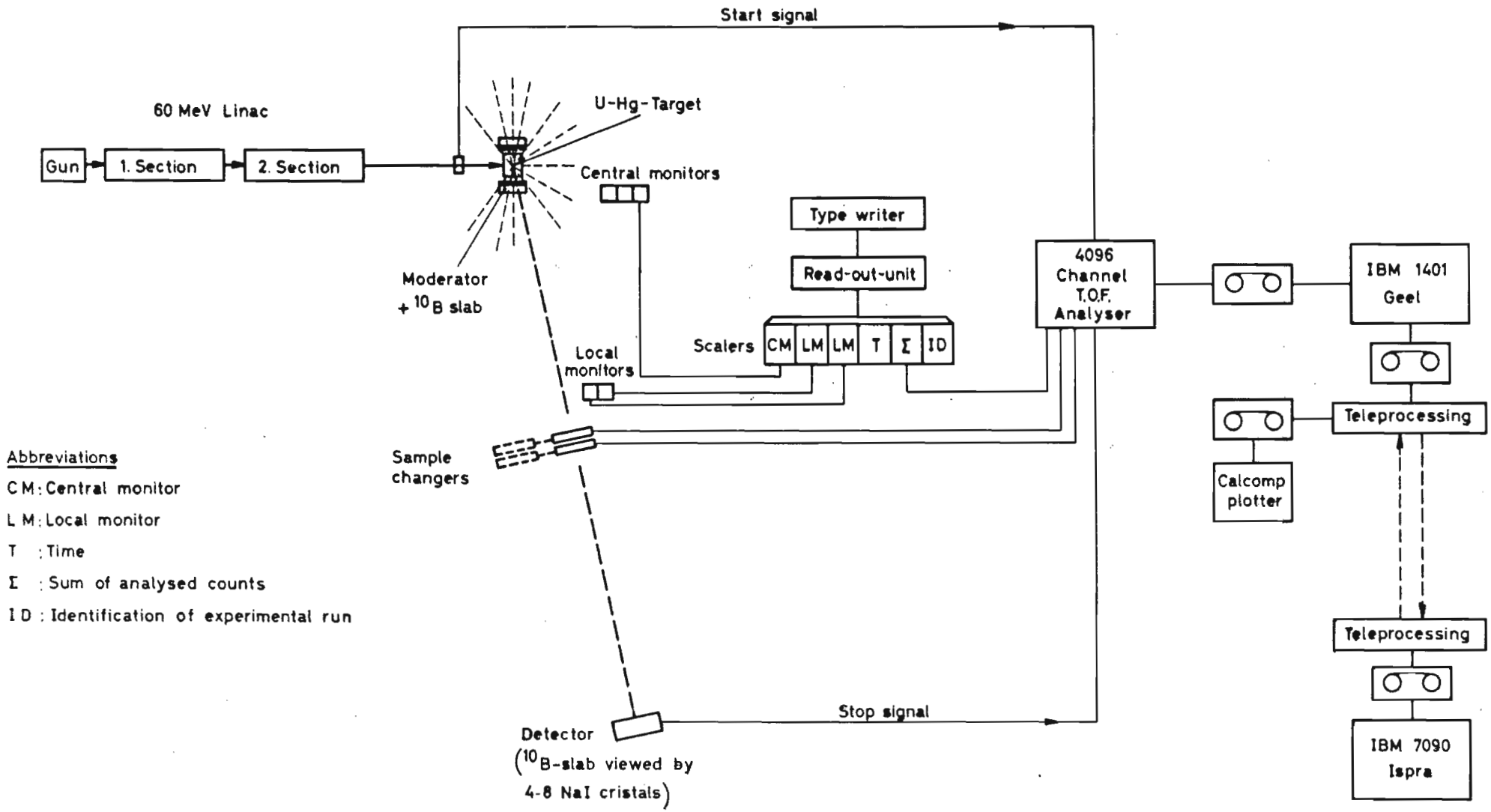

Fig. 8 Linac neutron time of flight spectrometer

—Total cross section experiment—

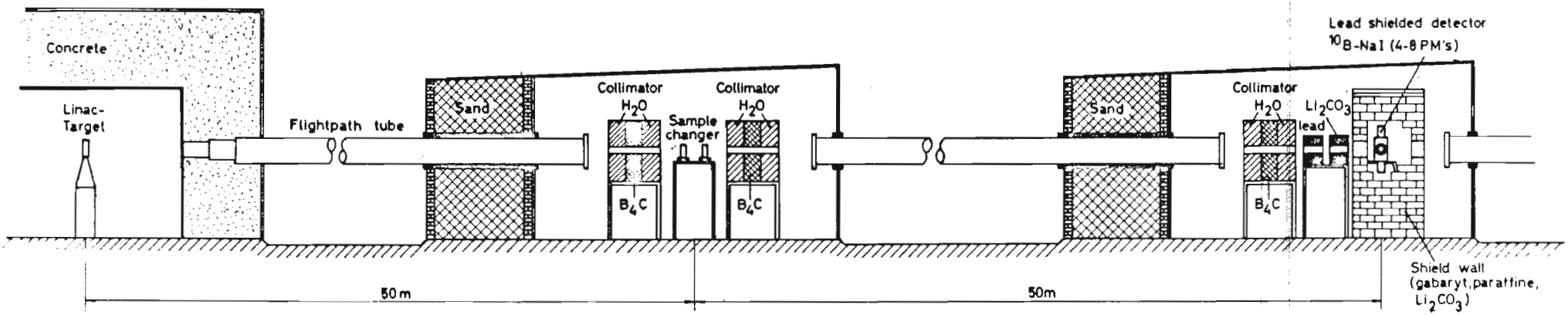

Fig. 9 Experimental set-up for total cross section measurements

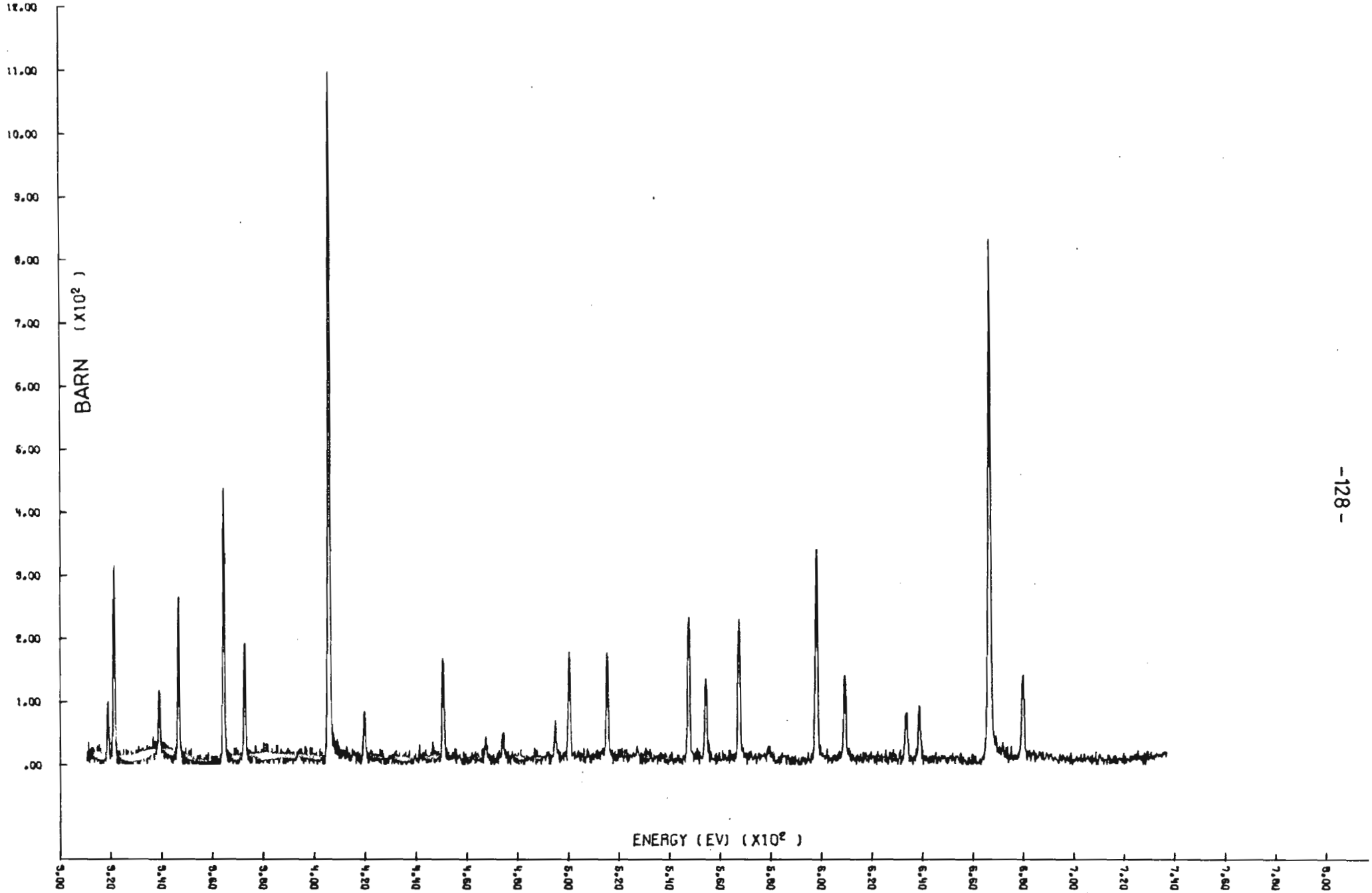

FIG. 10

TOTAL CROSS SECTION IN THE ENERGY RANGE FROM 300 TO 800 eV

Fig. 8 shows the general lay-out of the experiment. Fig. 9 shows the experimental set-up along the neutron flight path. Fig. 10 gives the structure of the total cross section in the energy range from 300 eV to 800 eV.

2.1.2. Total neutron cross sections in the high energy range

Preliminary equipment for high resolution transmission measurements in the energy range between 0.5 MeV and 10 MeV has been installed. The detector consisted of a large area (45 cm diameter) plastic scintillator viewed by one 60 AVP photomultiplier. It was placed at a distance of 400 m from the target. Preliminary tests, using a bare uranium target, showed paralysis effects due to the γ-flash. In order to minimize these effects a new version of the detector has been built which consists of three 60 AVP photomultipliers viewing the same scintillator with pulse coincidence condition. The new detector has been checked in the laboratory but not yet in a true experimental situation.

2.1.3. Publication

Böckhoff, K.H., A. De Keyser, W. Kolar, H. Martin, Measurement of the neutron total cross section of ^{240}Pu, Proc. IAEA Conf. Nuclear Data, Paris, Oct. 1966, paper no. CN-23/89, in press.

2.2. Fission data measurements

E. Migneco, J. Theobald, J. Winter

2.2.1. Fission detector development

The investigation of the properties of this detector which was described already in the last annual report has been completed with an efficiency mapping along the sensitive area and an absolute efficiency determination by means of a crystal monochromator at the Belgian BR2-reactor. A description of the detector has been published.

A wire-to-plate spark chamber for fission cross section measurements on highly α-active nuclides has been studied mainly with respect to its discrimination properties against α-backgrounds and detection efficiency for fission fragments. Variable parameters were: the filling gas, the humidity, the gas pressure, the distance wire-to-plate, the voltage, the wire diameter, the electrode material.

The stability of the detector and the reproducibility of the count rates could be improved, and the concept of a spark chamber for time-of-flight measurements is now ready.

A gaseous scintillation detector has been realized which allows coincident detection of the two fission fragments by viewing the two gas volumina at each side of a 4π fissile layer with two photomultipliers. The scintillation behaviour is now being studied by means of a ^{252}Cf source.

2.2.2. Fission cross section of ^{235}U between 4.7 and 300 eV

High resolution fission cross section measurements on ^{235}U have been simultaneously carried out by fission neutron and fragment detection along two neutron flight-paths which are symmetrically positioned with respect to the moderator axis. Also the multichannel analyzers serving both experiments were operated with identical channel settings. The detectors which were placed at the same distance (60 m) from the target were:

a) a multiplate ionisation chamber with 6 resp. 8 deposits of uranium-uranyl acetate of 26 cm diameter and a thickness of 1 mg/cm^2 ^{235}U,

b) a liquid scintillator fission neutron detector, already described in the last annual report.

The relative shapes of the spectra of primary neutrons were determined by two banks of BF_3 counters. For the background determination the black resonance method was used. The characteristics of these experiments are given in table II.

For one energy range of the experiment a special magnetic tape recording system was used which increases the analyzing capacity from 4096 to 65440.

The data are taken and their analysis is in progress.

Table II. Characteristics of the simultaneous fission experiments

Quantity	Neutron energy range		
	4.7 - 47 eV	30 - 300 eV	> 240 eV
Linac beam energy	50 MeV	dito	dito
Peak beam current	0.45 A	1.2 A	1.5 A
Burst repetition frequency	100 pps	150 pps	400 pps
Burst width	300 nsec	80 nsec	50 nsec
Channel width	160/320/640/1280 nsec ("accordion")	80 nsec	80/640 nsec ("accordion")
Number of channels	4096	16384	4096
Moderator (polyethylene)	20x20x2.8 cm	dito	dito
Background samples	Mo, Au	W,Mo,Bi,Mn,Co	Mo,Bi,Mn
Detectors at	60 m	dito	dito

2.2.3. Measurement of $\bar{\nu}$ and of the multiplicity of fission neutrons

For the measurement of the energy dependence of the individual and average number of neutrons per fission event a gadolinium loaded liquid scintillator is under construction together with a multiplate ionisation chamber which will be inserted into the scintillator tank. Following a fission event in the ionisation chamber,

the number of fission neutrons will be counted after the prompt radiation associated with fission has been gated out.

An electronic device which corrects the time-of-flight uncertainty for the different one-after-the-other placed ionisation chambers is ready. The detector tank is under construction.

2.2.4. Publication

Böckhoff, K.H., E. Migneco, J. Theobald, J. Wartena, A large area fission fragment detector with fast response, Nucl. Instr. Methods 45, 233 (1966).

2.3. Scattering cross sections

E. Migneco, J. Theobald

2.3.1. Bright line method

A preliminary scattering experiment has been performed, using the 18.8 eV level of W as a test resonance in order to study the background conditions for the bright line technique with a shielded Linac target. A vertical and excentric test flight tube (not looking at the target) has been installed through the target bunker roof. At its end a BF_3 counter bank served as neutron detector.

With an optimized shielding the background turned out to be still a factor 5 - 10 too high for scattering experiments on fissile isotopes under the chosen experimental conditions.

An improved bright line system with an excentric flight tube outside and tangential to the target bunker is under construction.

2.3.2. Improved classical method

A modification of the scintillator tank for the $\bar{\nu}$-measurement will be used as an anticoincidence shield for fission

and capture events. The tank is so constructed that it can be adapted to both experiments. The scattered neutrons will be detected by a ^{10}B-loaded liquid scintillator.

2.4. Neutron capture data

2.4.1. Capture cross sections

G. Carraro, H. Weigmann

A new detector for neutron capture cross section measurements which is essentially an improved version of the well known Moxon-Rae detector has been developed and tested.

Principally, the detector consists of a stack of 6 optically isolated sheets of plastic scintillator, each 3.5 cm thick, which are alternatively connected to two photomultipliers. By demanding coincidences between the two photo tubes one imposes essentially the same condition on the detection of a γ-quantum as is valid for the Moxon-Rae detector, namely that the associated electron travels from one plastic scintillator sheet into the neighbouring one. So, as for the Moxon-Rae detector, one expects a linear response function with γ-energy and, thereby, for a γ-cascade an efficiency independent of the decay scheme. In order to correct for wrong coincidences due to detection of different quanta of a γ-ray cascade in two scintillator sheets viewed by photomultipliers 1 and 2, respectively, a pair of detectors (A and B) is used with the sample placed in between, and also coincidences A1 B1 (and A2 B2) are counted and subtracted from the number of coincidences A1 A2 (and B1 B2).

The pair of detectors has been compared with a pair of normal Moxon-Rae detectors. The energy response functions were determined in both cases with calibrated γ-ray sources up to a total γ-ray energy of 4.12 MeV (^{24}Na). Above that energy capture γ-rays from several Ag- and Mo-resonances have been used employing a neutron beam of

the CBNM Linac. Assuming the Moxon-Rae detector to have a linear response function, the efficiency of the new detector has been obtained as a function of the energy of γ-ray cascades up to about 9 MeV. As may be seen from fig. 11, the efficiency of the new detector has a linear dependence on γ-ray energy above 1 MeV. The absolute efficiency at 8 MeV is about 10%, i.e. larger than that of a Moxon-Rae detector by a factor of 4.

The detector is being used to measure the capture cross section of natural Mo at a 30 m station of the CBNM Linac. An area analysis program will be used to obtain resonance parameters. As a preliminary evaluation, time-of-flight spectra observed for neutron energies above 1 keV have been artificially smeared out in order to obtain the mean capture cross section as a function of neutron energy. The relative shape of the neutron flux at the detector station has been measured with a ^{10}B-slab viewed by a NaI-crystal. An absolute calibration of the product detector efficiency times neutron flux constant has been obtained by observing neutron capture events in "black" resonances with known parameters. The resultant mean capture cross section of natural Mo is shown in fig. 12 together with the results of some previous measurements. The experimental characteristics are given in table III.

Besides measurements on Mo also preliminary measurements on ^{240}Pu have been carried out demonstrating the applicability of the detector also for this isotope.

Fig. 11: Efficiency times solid angle ($\varepsilon\Omega$) as a function of total γ-ray energy as obtained from calibrated γ-ray sources and from radiative neutron capture in different Ag- and Mo-resonances; the solid angle covered by the detector in these measurements was about 20%.

Table III: Characteristics of the capture cross section measurements

Quantity	Neutron energy range	
	3 eV - 200 eV	> 200 eV
Linac beam energy	50 MeV	50 MeV
Peak beam current	0.450 A	1.5 A
Burst repetition frequency	150 pps	400 pps
Burst width	80 ns	50 ns
Detector at	30.7 m	30.7 m
Moderator(polyethylene)	20x20x2.3 cm^3	20x20x2.3 cm^3
Overlap filter	$^{10}B_4C$	$^{10}B_4C$
Background measurement samples	Ag, Bi, Co, W	Bi, Co, Cu
Analyzer channel widths	80/160/320/640 ns	40 ns (above 200 eV) 160 ns (200-100 eV)

Fig. 12: Mean neutron capture cross section of natural Mo as a function of neutron energy; x these measurements (other symbols represent previous measurements); the full line gives the cross section as calculated by Dovbenko et al.; the broken line represents the presently recommended cross section of J.J. Schmidt.

2.4.2. Capture γ-ray spectra

H. Weigmann, J. Winter

A two-dimensional experiment (dimension I: neutron flight time, dimension II: γ-ray signal amplitude) with a Li-drifted Ge-detector is under preparation. A 30cm^3 Ge-crystal, an analogue-to-digital converter with 4096 channels and a stabilizing system have been ordered. A data storage system using one 20-track magnetic tape unit with a capacity of more than 1 million channels is under construction.

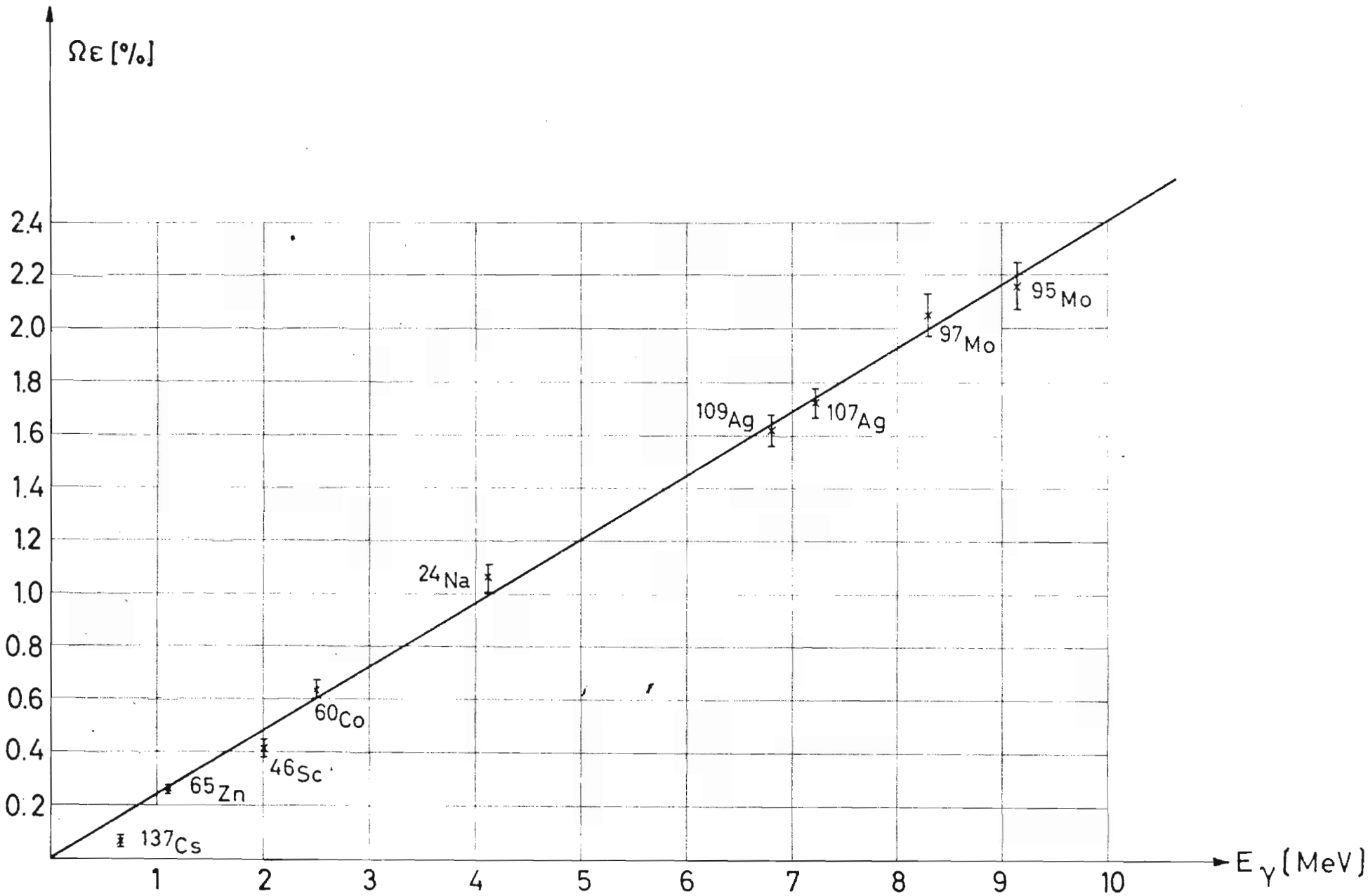
ΩE [%]
2.4
2.2
2.0
1.8
1.6
1.4
1.2
1.0
0.8
0.6
0.4
0.2
1
2
3
4
5
6
7
8
9
10
E γ (MeV)
137Cs
65Zn
46Sc
60Co
24Na
109Ag
107Ag
97Mo
95Mo

Fig.11

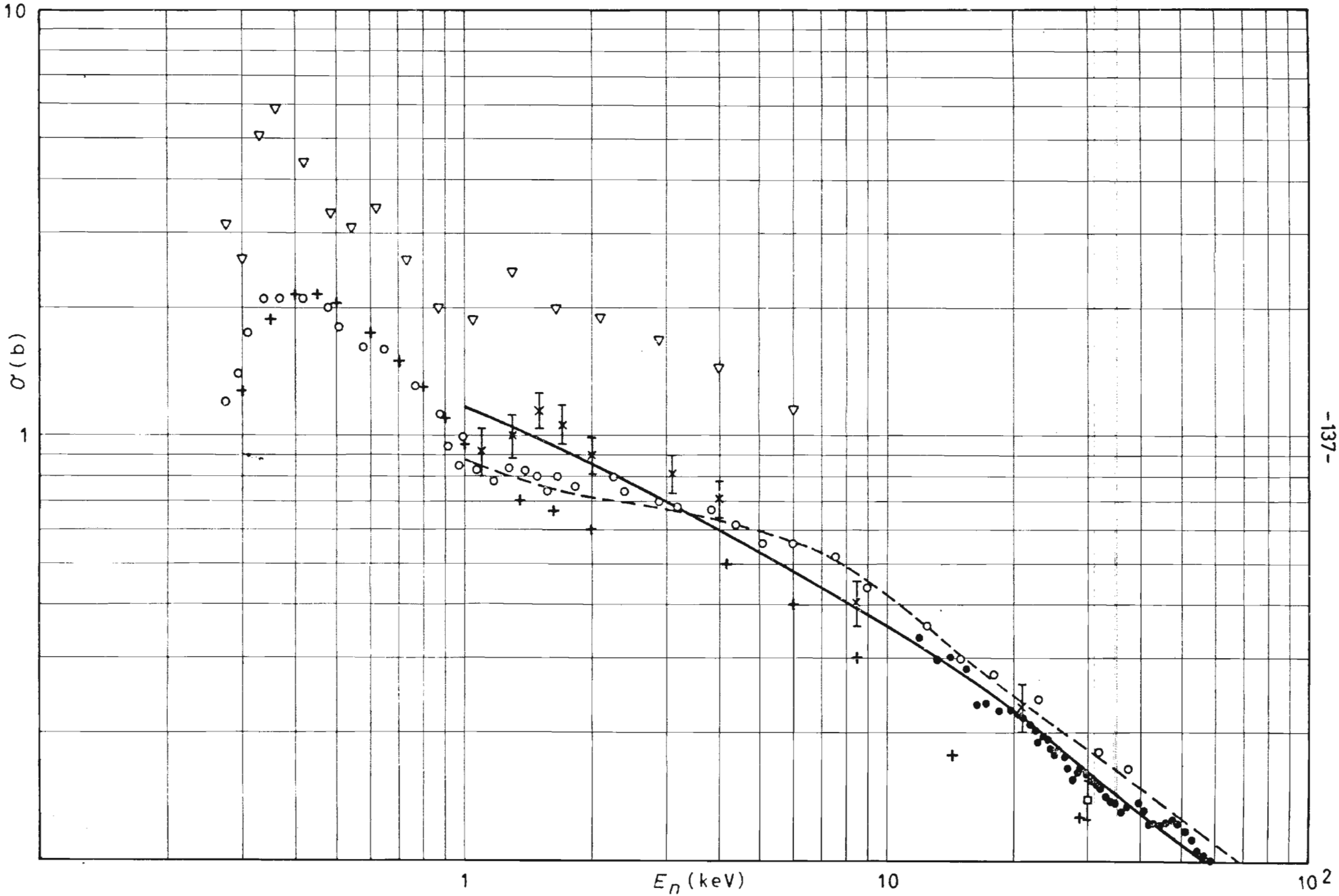

Fig.12

Low noise preamplifiers, a time pick-up system, main amplifiers and a command unit which permits the simultaneous operation of time and amplitude converters are under development.

2.4.3. Publications

Weigmann, H., G. Carraro, K.H. Böckhoff, A new detector for neutron capture cross section measurements, Nucl. Instr. Methods, in press (1967).

2.5. Spin determinations

2.5.1. Spin measurements of resonances of fissile nuclei

A.J. Deruytter, C. Wagemans*, C. Furetta.

Within the framework of a joint program with SCK-CEN (Mol), two solid-state detector sets were prepared for a careful study of the ratio of binary to ternary fission in a few resonances in ^{235}U. Detector sets and electronic equipment are tested and installed.

Also a computer program was further developed to analyze two-dimensional data from a back-to-back fission experiment in view of further applications.

2.5.2. Spin assignment of resonances

C. Coceva**, F. Corvi**, P. Giacobbe**, G. Carraro

The measurement of the spins of s-wave neutron resonances of some nuclei has been started as a joint program between CNEN and CBNM.

The method for spin assignment is essentially the same as that used for ^{105}Pd in an earlier work with the fast chopper of Ispra[1].

At the "Centro di Calcolo" of Bologna, the program for the simulation of neutron capture gamma ray cascade has

---

* Belgian Research fellow NFWO (Univ. Ghent)

**CNEN, Italy

been considerably improved: for different detection thresholds it calculates, besides the spectra $\langle\nu\rangle$, $\langle\nu(\nu-1)\rangle$, $\langle\nu(\nu-1)(\nu-2)\rangle$, $\langle\nu^4\rangle$, the distribution of the multiplicities $P(\nu)$ for $1 < \nu < 15$, and the population of isomeric states. With the output data of this program it is possible to calculate the ratio "singles" to "coincidences" of the two detectors, for different thresholds of the "singles", and the variance of the result.

This allows us to see principally:

a) if the ratios "single" to "coincidence" (for the two possible spin states of the compound nucleus) are different enough to be measured;

b) to choose the most convenient threshold for the "singles".

Collimators, shielding and two 6" x 6" NaI(Tl) detectors have been installed on a flight path length of 50 m.

Preliminary measurements were performed on Hf and Nb. The first results show indeed that for ^{177}Hf, ^{179}Hf and ^{93}Nb the spin dependence of the ratio "singles to coincidences" exists in a measurable amount. Spin assignments could in fact be made for the easiest cases of isolated resonances.

This experiment is, however, still in a preliminary stage and many refinements are in progress, both in the measurements and in the numerical analysis of the data.

2.5.3. Publication

[1] Coceva, C., F. Corvi, P. Giacobbe, M. Stefanon, Phys.Lett. 16 (1965) 159.

3. Thermal neutron data

A.J. Deruytter, P. Pelfer

In the framework of a joint program with the Euratom-CEN group GEX-BR2, high precision measurements of thermal neutron data are performed.

3.1. Branching ratio of the $^{10}B(n,\alpha)^{7}Li$-reaction

Pulse-height spectra of the products of the $^{10}B(n,\alpha)^{7}Li$- and $^{10}B(n,\alpha_{1\gamma})^{7}Li^{*}$-reactions were recorded with a surface-barrier detector. The thermal neutron beam was extracted from the Belgian BR 1-reactor. The resolution of the spectra was such that a precise determination was possible of the ratio of the reaction in ^{10}B leading to the ground state and first excited state. Only minor corrections to the experimental data were required to deduce the value of the branching ratio.

The data accumulation was extended until more than 10^{6} counts were registered in the ground state transition. Similar spectra were recorded with a Cd-sheet in the beam until 10^{4} events were registered in the ground state α-peak. After the epi-Cd correction was applied we obtained the following results for a thermal neutron beam

$$\frac{\sigma(n,\alpha_{o})}{\sigma(n,\alpha_{1\gamma})} = (6.733 \pm 0.007)\% \quad \text{and}$$

$$\frac{\sigma(n,\alpha_{o})}{\sigma(n,\alpha_{o})+\sigma(n,\alpha_{1\gamma})} = (6.308 \pm 0.006)\% \ .$$

3.2. Q-values for $^{10}B(n,\alpha)^{7}Li$ and $^{6}Li(n,\alpha)^{3}H$ reactions

Pulse height spectra for these reactions were recorded in a solid-state detector simultaneously with the α-spectra from a ^{239}Pu-^{241}Am-mixture serving as energy standard. Corrections for the zero-point of the analyzer and for energy loss in detector window and sources were applied. The energies of the main lines in the decay of ^{239}Pu and ^{241}Am were taken as (5155.0 $\pm$ 1.0)keV and (5487.5 $\pm$ 1.0)keV. The result obtained for the

ground state Q-value of the $^{10}B(n,\alpha_o)^7Li$ reaction is (2800.8 ± 7.6)keV, and the Q-value for $^6Li(n,\alpha)^3H$ is (4794 ± 12)keV. The errors indicated are two standard deviations because of the difficulty of adding absolute and statistical errors. These values have to be compared with the Q-values deduced from mass excesses (Lauritsen, Ajzenberg-Selove, Nucl.Phys. 78, 1, 1966): Q_o (^{10}B) = (2792 ± 2) keV; Q_o(^6Li) = (4785 ± 2) keV.

3.3. Intercomparison of standard boron and fission foils

A completely automatic apparatus was set up to compare standard foils of evaporated boron on gold-coated quartz backings in a reactor beam. Foils are successively brought in the same geometry with respect to a gold-silicon surface-barrier detector and neutron beam. The comparison can be made with the total intensity of the beam (monitored with a very stable fission foils - solid state detector monitor) or as a function of energy by the use of a slow chopper. In the latter case both time-of-flight and pulse-height spectra are automatically read out before switching to the next foil. In this way the total number of ^{10}B-atoms in two 1 mg foils can be compared with an accuracy of 0.1% within 24 hours.

In the same apparatus fission foils can be compared both by α- and by fission fragment counting.

3.4. Measurement of the thermal fission cross sections of ^{235}U and ^{239}Pu relative to the $^{10}B(n,\alpha)$-cross section

The equipment described above is being used for a high precision measurement of the thermal fission cross sections of ^{235}U and ^{239}Pu relative to the $^{10}B(n,\alpha)$-cross section. Possible small corrections, e.g. difference in scattering behaviour of α-particles and fission fragments, are studied. Preliminary results on ^{235}U are obtained.

3.5. Publication

Deruytter, A.J., P. Pelfer: Precise determination of the branching ratio and Q-value of the $^{10}B(n,\alpha)^{7}Li$-reaction and of the Q-value of the $^{6}Li(n,\alpha)^{3}H$-reaction, to be published in Nucl.Phys. (1967).

4. Data Handling

4.1. Equipment

A. De Keyser, H. Horstmann

In September 1966 the data handling equipment has been considerably improved by the installation of an IBM 1401 computer. This computer has been used for:

- Validity checks of the collected experimental data.
- Reduction of the experimental data in order to decrease the tele-processing time.
- Input/output operations for the IBM 7090 at Ispra to which the IBM 1401 is linked by off-line tele-processing.
- Calculations for data analysis.

Data acquisition from different experiments at the linear accelerator has been standardized. A multiplex unit for recording data of simultaneously operating multi-channel analyzers in the same format on magnetic tape has been completed. A new data acquisition system based on the on-line use of the IBM 1800 computer is being projected. Detailed studies of the front end for this computer have been started.

4.2. Computer programming and data analysis

M.G. Cao, H. Horstmann, H. Schmid

The following programming activities, analyses and calculations have been completed or are under way:

Processing of fission cross section data from linac experiments.

Calculations of kinematic parameters for two-body reactions $^{14}C(d,n)^{15}N$, $^{15}N(d,n)^{16}O$, $^{28}Si(n,n')$, $^{29}Si(n,n')$, $^{30}Si(n,n')$.

Calculations of energy, time and space dependent neutron capture in ^{10}B-slabs.

Differential cross section calculations for elastic neutron scattering on ^{28}Si.

Shape analysis for fission cross section data.

Area and shape analysis of total cross section data for ^{240}Pu.

Multiple scattering corrections for neutron scattering cross sections.

Calculations related to activation cross section measurements at the Van de Graaff.

Analysis of capture cross section data for Mo.

Processing of total cross section data.

Calcomp plotter programs for the IBM 1401.

IBM 1401 programs for processing of multi-channel analyzer data.

4.3. Development of electronic equipment for neutron data measurements and analysis

4.3.1. Nanosecond time coder

H. Verelst, H. Meyer

The second final version of a one-nanosecond digital time coder was realized and tested, also under very unfavorable conditions. After some minor mechanical perfections the equipment will be available for experiments.

The main characteristics are:

Analysis time interval range: adjustable between 256 ns and 3.14 ms in binary steps with a preset delay range from zero to 2.1 ms adjustable with an accuracy of 8 ns.

Channel width: from 1 ns to 1024 ns in binary steps.

Number of channels: 256 min. and 130000 max.

Accuracy and stability: better than 10^{-5}.

Minimum distance between counts during an analysis cycle: 290 ns.

Integral and differential nonlinearity are very small because of the system principle chosen (< 0.1%).
A fast buffer store (3 words, 20 bits) at the output will derandomize the statistically arriving data for further handling. A gate input is also provided to avoid a readout of analyzed background events.

Because of its wide range of features the coder can be used for experiments at Van de Graaff and Linac accelerators. A one-parameter multirange conditioner in preparation will allow a selection of eight independent analysis regions of different channel width.

4.3.2. Data storage systems

F. Colling, B. Idzerda, W. Stüber

A data storage system was completed and delivered for long range time-of-flight experiments at the Linac. Data words from coders with up to 16 bit word length and 4 bit general information can be stored on a 1" magnetic tape with great word density at data rates down to 0.3 words/sec. The stored information can be read out off-line for selective sorting and integration - also with reduced resolution - into a 12 bit address core memory in successive runs or into a computer later on.

The system contains a 10 word, 20 bit buffer store at the input and equipment for a stepwise propagation of tape at low data rates.

During long test periods of the system a redesign of the stepping mechanism, modifications of the buffer store and some other equipment inclusive units to be adapted to the system were performed.

After installation, some additional modifications were prepared for an automatic readout of data.

The second data storage system with extended features for handling of two-parameter data is now under construction. To find out the interesting analysis regions, sometimes time consuming search runs off-line during sorting might be necessary. An additional tape deck without the greater part of electronic instrumentation could be used as a slave to solve such problems. A second possibility to avoid long search runs would be the use of a storage display unit, off-line or on-line, having up to 10^6 storage places.

4.3.3. Publications

Colling, F.: Digital Comparators for handling of data from nuclear experiments, EUR 2799.e (1966).

Rieb, D., W. Stüber: An integrating storage display monitor with dark trace tube for nuclear two-parameter spectra, EUR 3117.e (1966).

Meyer, H.: Studies on the response speed of surface barrier detectors, when irradiated with different particles, I.E.E.E. Transact. Nucl. Sci. NS-13, 180 (1966).

5. Radionuclides

5.1. Standardization of sources and samples, development of counting methods

W. Bambynek, E. De Roost, A. Spernol, W. van der Eijk, R. Vaninbroukx

More than 100 special standard sources of more than 25 different nuclides have been prepared for research in and outside the CBNM. The activity of several of them (e.g. ^{239}Pu sources) has been determined to an accuracy of better than 0.1% (including 3 times the statistical error).

Approximately 50 sets of standard threshold detectors of very pure Ni, Ti, Fe, and Cu were distributed to different European centra and IAEA, for further limited distribution. After irradiation they will be measured at the CBNM and sent back to the participants together with sets of pure standards of ^{46}Sc, ^{54}Mn, ^{58}Co, and ^{60}Co. A test irradiation and measurement showed that the materials were properly chosen.

The preparation of about 10 different γ-standards, accurate to at least 0.5%, in the energy range of 5-500 keV has been started with investigations of the decay schemes of ^{203}Hg and ^{139}Ce. First sources of ^{203}Hg, ^{139}Ce, ^{51}Cr, ^{7}Be, and ^{181}W have been prepared, but the wanted accuracy was not yet reached. These standards will especially be used for the calibration of γ-spectrometers [1].

The investigations on the solid angle method have been further completed for X-rays [2], and extended by calculations of the error effects [3]. Higher accuracy was reached in counting α-radiation. For the latter an agreement of better than 0.1% was reached between plastic detector and surface barrier detector results,

while the statistical error was always kept below about 0.01%.

Investigations on the use of the Cerenkov radiation for counting β-active substances, which are insoluble in liquid scintillators, showed that the method is especially suitable for the measurement of extended sources of ^{32}P and ^{31}Si. These radionuclides result from neutron irradiation of the standard fast neutron detectors S and P. A comparison of different methods proved that accuracies of better than 1% can be obtained [4].

All our experimental results on gas counting of T, ^{14}C, ^{37}A, and ^{85}Kr of the last 7 years, especially all measured corrections, have been collected and published [5].

The determination of liquid drop weights has been investigated in every detail, using an electro balance and combining the extrapolation and pycnometer method. An accuracy of 2 μg on about 20 mg drops has been reached [6].

The measurements on foil absorption in 4π-counting have been finished and a final report has been published [7].

Several other counters, especially coincidence devices using fast detectors, have been constructed and are used mainly for decay scheme determinations.

5.2. Determination of nuclear constants

W. Bambynek, E. De Roost, H. Hansen, A. Spernol, W. van der Eijk, R. Vaninbroukx

The determination of the K-fluorescence yield ω_K of Cr (from ^{54}Mn) has been repeated under improved conditions.

Evaporated sources with negligible X-ray self absorption [8] have been used throughout. The $4\pi X$ pressure measurements have been done using chromium coated cover foils (thus reducing the X-ray absorption from previously about 11% to less than 0.5%). The X-medium-geometry measurements have also been improved considerably by the use of counters with very thin plastic windows. An overall accuracy of a few tenths of a percent will finally be reached for ω_K. The K-fluorescence yield of Cl (from ^{37}A) has been determined by gas counting with He/CH and Xe/CH gases to 0.0915 $\pm$ 3%. Calculations of some corrections are under way and will allow to improve the accuracy figure.

The final result of measurements on the γ-branching in the ^{85}Kr decay is 0.00435 $\pm$ 2% (max. error)[9].

K-conversion coefficients in the deacy of ^{139}Ce and ^{137}Cs have been measured by the e-X-coincidence method resp. to 0.0925 and 0.209 [10], using our electromagnetic β-spectrometer. Due to too slow electronics the accuracy was only several percent , which will be soon improved to a few tenths of a percent. Also the corresponding conversion ratios have been determined. In some preliminary experiments the total conversion coefficient in the decay of ^{203}Hg has been measured to 0.2255 using the efficiency extrapolation technique.

The branching ratios in the ^{65}Zn decay have finally been determined with about 0.1% accuracy to 50.65% for the γ-branch and 1.46% for the positron branch. As many as possible methods have been used including an e^+-γ_a-γ_a-coincidence method for the determination of the positron branch. This method is also applicable to other positron emitters.

Measurements were prepared for the extension to other nuclides of our previously used simple method for the measurement of thermal cross sections [11].

Many half life measurements on several isotopes have been performed. Together with the chemistry and mass spectrometry groups, the half life of ^{234}U has been determined to 2.44 10^5 y. This is a preliminary value from 3 measurements while many others have still to be evaluated. A final accuracy of 0.2% on the half life is expected. The half life of ^{204}Tl has been determined to 3.75 y using samples of $TlNO_3$ and metallic Tl as well. The measurements have to be continued for about 2 years in order to obtain an 0.1% accurate result.

By β-spectrometer measurements it has been shown that the branch of ^{95}Nb, indicated in Nuclear Data Sheets to be 1%, is in fact far below 0.1%.

5.3. Publications

[1] Vaninbroukx, R., G. Grosse, The use of a calibrated γ-spectrometer ....., Int.J.Appl.Rad.Isot. 17, 41, (1966).

[2] Bambynek, W., O. Lerch, A. Spernol, Eine auf 1% genau absolute Zählung von X-Strahlen geringer Energie, Nucl.Instr.Methods 39, 104 (1966).

[3] Bambynek, W., Precise solid angle counting, Proc. Symp. Standardization of Radionuclides, IAEA Vienna (1966).

[4] Vaninbroukx, R., Precision measurement of extended β-sources, Proc. Symp. Standardization of Radionuclides, IAEA, Vienna (1966).

[5] Spernol, A., The internal gas counter as a precise absolute counting device, Proc. Symp. Standardization of Radionuclides, IAEA, Vienna (1966).

[6] van der Eijk, W., H. Moret, The precise determination of drop weights, Proc. Symp. Standardization of Radionuclides, IAEA, Vienna (1966).

[7] van der Eijk, W., The correction for foil absorption in the 4π-counting..., Int.J.Appl.Rad.Isot. 17, 604 (1966).

[8] Bambynek, W., D. Reher, The self-absorption of X-rays and Augerelectrons in ^{54}Mn sources prepared by different methods, Int.J.Appl.Rad.Isot. 18 , 19 (1966).

[9] Denecke, B., E. De Roost, A. Spernol, R. Vaninbroukx, The gamma branching of ^{85}Kr, Nucl.Sci.Engng., in press (1967).

[10] Hansen, H., M. Delabaye, Precision coincidence counting of conversion electrons, Proc. Symp. Standardization of Radionuclides, IAEA, Vienna (1966).

[11] Vaninbroukx, R., The thermal neutron activation cross sections of ^{59}Co, Nucl.Sci.Engng. 24, 87 (1966).

6. Isotope Standards of Stable and Fissile Nuclides

6.1. Boron

P. De Bièvre, G.H. Debus

A calibration of the Boron Standard was based on eleven synthetic boron blends covering a $^{10}B/^{11}B$ ratio varying from 0.1 to 10. A constant instrumental bias factor of 0.9987 ± 0.0006 was obtained for all isotopic ratios.

The Boron Isotope Standard (100 kg boric acid) is now certified as:

$^{10}B/^{11}B$ atom ratio = 0.24726 ± 0.00032

corresponding to an isotopic composition of

19.824 ± 0.020 atom % ^{10}B

80.176 ± 0.020 atom % ^{11}B

and a relative atomic weight of (^{12}C = 12)

10.81178 ± 0.00020.

The uncertainties given include all statistical uncertainties of mass spectrometric measurement and isotopic blends as well as limits of known sources of systematic errors.

After the absolute calibration of the mass spectrometers, the isotopic composition of the boron samples, on which the 1962 CBNM measurements of the $^{10}B(n,\alpha)$ thermal neutron cross section have been performed, has also been remeasured (Table IV).

Table IV: Remeasurement of the ^{10}B thermal neutron absorption cross section

	atom % ^{10}B	$\sigma_{nA}(B)$ in barn	$\sigma_{nA}(^{10}B)$ in barn
Old results:			
natural B	19.81 ± 0.02	760.8 ± 1.9	3840 ± 11
enriched ^{10}B	96.515 ± 0.013	3703 ± 8.9	3837 ± 9
New results:			
natural B	19.838 ± 0.030	760.8 ± 1.9	3835 ± 11
enriched ^{10}B	96.525 ± 0.006	3703 ± 8.9	3836 ± 9

It should be stressed that the Standard boric acid cannot be used directly for the preparation of reliable thin layers of elemental boron. Certified solutions of Standard boric acid in light and heavy water can be obtained from CBNM. CBNM prepares also certified reference samples in the form of disks or plates covered with evaporated boron, of which the isotopic composition is checked against the Standard boron.

6.2. Lithium

P. De Bièvre, G.H. Debus

The chemical techniques needed for the preparation of high precision blends of ^{6}Li and ^{7}Li were developed. It is expected that by the end of 1967 a natural lithium and enriched ^{6}Li Standard will be available.

6.3. Deuterium

T. Babeliowsky, G.H. Debus

A calibration of the mass spectrometric measurements has been performed for heavy water. Heavy water of 99.8 mol % D_2O is now being measured with an accuracy of 0.003 mol % at the 95% confidence limit.

A study of the oxygen isotopes is made using CO_2 (method of equilibration) and O_2 (obtained by means of electrolysis) for mass spectrometric measurements. A correlation between density, H/D ratio and O-isotope content of heavy water is being examined.

6.4. Publications

Proc. EANDC Round Table on High Precision Mass Spectrometry and α-Counting, Brussels, 1965, EANDC 53 "S"(1966).

Debus, G.H., P. De Bièvre, Thermal neutron absorption cross section of boron. J.Nucl.Energy, A/B, in press. (1967).

7. Sample Preparation and Assaying

G.H. Debus, H.L. Eschbach, K.F. Lauer, H. Moret, G. Müschenborn, J. Van Audenhove, V. Verdingh

The year 1966 was characterized by a sharp rise of the number of applications received, especially for samples prepared by metallurgical techniques. Table V compares for 1964, 1965 and 1966 the number of samples delivered to different groups of applicants and table VI summarizes the techniques used for the preparation of these samples.

Some development of new sample types and new techniques has been achieved although most of the attention was focused upon fulfilling the direct needs:

mechanical shaping of α-materials,
electron beam welding,
ultra-high vacuum levitation evaporation,

fabrication of aluminium alloys,
shaping of Li-samples,
handling of ^{231}Pa,
forced electrospraying.

Table V: Repartition of orders according to institutions

Applicants	Number of orders			Number of samples		
	1964	1965	1966	1964	1965	1966
A. Inside the Community						
1. Euratom	38	66	97	1951	883	5746
2. National Laboratories	40	31	41	284	1167	1004
3. Universities	9	25	22	28	100	163
B. Outside the Community	1	7	4	5	356	307
Total	83	129	164	2268	2506	7220

Table VI: Repartition of orders according to preparation techniques

Techniques used for Preparation	Number of orders			Number of samples		
	1964	1965	1966	1964	1965	1966
Metallurgical techniques	37	72	109	1853	2251	6934
Chemical techniques	32	31	33	234	129	97
Vacuum evaporation	19	26	22	181	126	189
Total	88	129	164	2268	2506	7220

Publication

Van Audenhove, J., J. Joyeux, The preparation by levitation melting in argon of homogeneous aluminium alloys for neutron measurements, J.Nucl.Materials 19, 97 (1966).

XXI DEPARTEMENT DE RECHERCHE PHYSIQUE - SECTION DES MESURES NEUTRONIQUES FONDAMENTALES, CEA, Saclay, (France)

R. Joly.

1. Groupe des neutrons thermiques.

(H. Nifenecker)

Ces expériences ont été effectuées auprès de la pile EL.3 par A.Audias, P. Carlos, H. Nifenecker, R. Samama et C. Signarbieux.

1.1. Etudes du processus de capture radiative.

1.1.1. Mesure de corrélations angulaires.

On a étudié les corrélations angulaires (γ, γ) dans les réactions $V^{51}(n,\gamma)V^{52}$ et Ti^{48} (n,γ) Ti^{49}.

Les cibles utilisées étaient des échantillons métalliques naturels ou des oxydes. Les principes d'enregistrement et de dépouillement ont été décrits par ailleurs.(1) Le tableau I résume les résultats obtenus, nous avons admis que les transitions primaires de haute énergie sont des transitions dipolaires électriques.

Nos résultats ont été comparés aux prévisions théoriques de Vervier. L'accord est dans l'ensemble satisfaisant, en particulier le spin et la parité 3^+ du niveau fondamental du V^{52} sont confirmés.(2)

Les données obtenues dans la réaction Ti^{48} (n,γ) Ti^{49} sont en cours d'analyse. Dès à présent nous pouvons confirmer l'attribution des spins 3/2 et 1/2 aux niveaux de 1.38 MeV et 1.72 MeV respectivement, en accord avec des mesures antérieures. L'étude en coïncidence des cascades (γ, γ) doit permettre d'élucider certains aspects du schéma d'excitation du Ti^{49}.

1.1.2. Etude des rayonnements γ de capture à l'aide de détecteurs au germanium.

En collaboration avec l'équipe du Professeur Coche de Strasbourg et celle de M. Julien (SPNBE/Saclay), nous avons utilisé des diodes au germanium dopées au Lithium (diodes planaires de 10 cm^3) pour étudier le spectre γ de capture de haute énergie d'un certain nombre de noyaux, en particulier Cu^{63}+ n et Cu^{65} + n.(fig.1) D'autre part une mesure préliminaire des coïncidences entre rayons γ de capture dans la réaction Co^{59} + n a été effectuée. Cette dernière expérience a montré que les volumes des détecteurs au Ge-Li devaient encore être augmentés pour que des mesures en coïncidence puissent être effectuées dans des conditions satisfaisantes. Les difficultés proviennent

de la faible proportion d'interactions intéressantes (soit photoélectriques, soit avec création de paires mais sans émission de rayonnement de freinage) entre les photons et la diode. Ainsi dans les expériences de coïncidence entre un cristal INa et une diode environ une information sur mille informations enregistrées présente de l'intérêt. Il s'ensuit que les temps de mesure doivent être très longs.

1.1.3. Mesures sur les électrons de conversion.

A l'aide d'une jonction au Silicium-Lithium ayant une résolution de 4 KeV, nous avons étudié le spectre d'électron de conversion du Cadmium.(fig.2) Les taux de comptage nous ont paru fort encourageants. Nous envisageons d'utiliser des coïncidences rayons X-électrons afin de diminuer la composante due aux interactions γ avec la diode détectant les électrons.

1.2. Etudes sur la fission.

1.2.1. Etude du mode symétrique dans le cas de la fission thermique de l'U^{235}.

L'étude de la fission symétrique par des moyens physiques (mesures simultanées des deux énergies ou des deux vitesses des fragments) est rendue difficile par la présence d'évènements aberrants. Dans le but d'identifier ces évènements aberrants, nous avons utilisé une méthode qui consiste à enregistrer en plus des deux paramètres d'énergie cinétique, E_1 et E_2, un paramètre supplémentaire lié aux vitesses (différence des temps de vol) et à tester la cohérence de ces trois paramètres. Il a été possible ainsi de "décontaminer" totalement les données expérimentales et d'obtenir une valeur du rapport pic/creux de la distribution des masses en accord quantitatif avec la valeur de la radiochimie.

A partir de ces données nouvelles, nous avons calculé la variation de l'énergie cinétique totale moyenne en fonction de la masse des fragments : cette courbe présente un creux accentué à la symétrie - nous avons trouvé $21.2 \pm 0,8$ MeV comme différence entre la valeur maximum et la valeur à la symétrie (3) : cette valeur est inférieure d'environ 3 MeV aux valeurs publiées dans la littérature. (Tableau II).

1.2.2. Etude de la distribution corrélée angle-énergie des particules légères dans le cas de la fission ternaire de l'U^{235} induite par neutrons lents.

L'émission des particules α de long parcours se fait de préférence dans une direction presque perpendiculaire à celles des fragments. Cependant Soloveva (Dissertation Akad. Nank. USSR-1955) a observé, dans une expérience réalisée à l'aide d'émulsions nucléaires, la présence de particules ayant un très long parcours et émises de façon isotrope : elle avait conclu à l'existence d'une composante isotrope de grande énergie dans le spectre α de la fission ternaire.

Nous avons repris cette mesure au moyen de détecteurs à semi-conducteur, en mesurant simultanément les énergies d'un fragment et de la particule légère ainsi que l'angle des directions des 2 particules. Les premiers résultats semblent confirmer l'existence d'une composante isotrope. Nous allons entreprendre l'identification de la masse de ces particules par la méthode (E,dE/dx).

1.2.3. Mesure des rayons X émis au moment de la fission.

Nous avons repris nos mesures en améliorant des blindages de notre installation (utilisation de fluorure de lithium 6 fritté) en utilisant comme détecteur de rayons une diode au Si (Li) TMC donnant une résolution de 1 KeV et en utilisant un système amélioré de coïncidences entre le détecteur de rayon X et le détecteur de fission (convertisseur temps amplitude).

Nous avons ainsi pu obtenir le spectre des rayons X émis au moment de la fission de U^{235} (fig. 3). Ce spectre présente des structures fines très nettes. Nous entreprenons maintenant l'étude multiparamétrique du phénomène (Mesure des deux énergies des fragments et de l'énergie du rayonnement X).

2. Groupe des neutrons intermédiaires.

A. Michaudon.

Ce groupe utilise l'accélérateur linéaire de Saclay comme source de neutrons et comprend les physiciens suivants : MM. Bayer (stagiaire détaché à Saclay par le Centre d'Etudes Nucléaires de Prague, Tchécoslovaquie), J. Blons, B. Cauvin, H. Derrien, C. Eggermann, A. Fubini (détaché à Saclay par CNEN de Bologne, Italie), A. Lottin (détaché à Oak Ridge, USA, jusqu'à novembre 1966), A. Michaudon, D. Paya, P. Ribon, Melle Sanche, M. Silver (détaché à Saclay par Oak Ridge, USA, jusqu'à octobre 1966), J. Trochon.

En 1966, l'accélérateur a été utilisé pendant 20 semaines pour des mesures par temps de vol.

2.1. Implantation générale.

Durant l'été 1966, d'importants travaux ont été entrepris pour construire deux nouvelles bases de vol inclinées à 10° par rapport à la normale au ralentisseur (fig. 4) afin d'augmenter l'intensité du faisceau de neutrons relativement aux anciennes bases inclinées à 45° et surtout afin de réduire la perte de résolution due à l'inclinaison des bases.
Toutes les bases de vol sont équipées de bouchons d'eau et quatre d'entre elles sont fermées par du mylar pour éviter la présence de résonances parasites dans le spectre des neutrons incidents.

La chambre des cibles a été agrandie du côté des bases 7, 8 et 9, là où le massif de protection en béton était démontable. L'ascenseur de cible a été remplacé pour qu'à l'avenir, on puisse télécommander le changement de cible. L'installation complète de stockage et de télécommande des cibles sera probablement terminée courant 1967.

2.2. Acquisition et traitement des informations de temps de vol.

Les dispositifs et les programmes que nous utilisons sont décrits en détail dans une communication présentée au Congrès de Paris sur les Constantes Nucléaires (4). Nous rappelons brièvement la liste de l'appareillage dont nous disposons :
- 5 codeurs de temps de vol HC 25 (Intertechnique). Nombre maximum de canaux : 65.536. Largeur de canal minimum : 50 ns.
- 1 codeur de temps de vol HC 50 (Intertechnique). Nombre maximum de canaux : 65.536. Largeur de canal minimum : 10 ns.
- 2 unités d'enregistrement et de lecture à bande magnétique de 1 inch à 16 pistes.
- 1 unité d'enregistrement multiparamétrique et séquentiel à bande magnétique de 1 inch à 16 pistes.
- 1 calculateur CAE 510 ayant une mémoire rapide de 24.576 mots de 18 bits. Il est équipé de 2 unités de bande magnétique 7 pistes (une 3ème doit être installée prochainement), d'une unité de visualisation, d'une imprimante rapide, d'un lecteur et d'un perforateur de cartes, d'un traceur de courbes. Il peut être utilisé, soit en ligne, soit hors ligne.

2.2.1. Fonctionnement en ligne.

Le calculateur peut alors être couplé à plusieurs expériences comme il est schématisé sur la fig. 5 . Il peut recevoir les informations :

- soit directement d'une mémoire tampon pour une seule expérience 'exp.n°1). Le temps d'accès est alors de 30 µs et le temps de classement de chaque information dans les mémoires d'accumulation de 180 µs environ. Le taux de comptage moyen est donc limité à 6000 c/s. Sur les 24.576 mots de la mémoire, 16 384 au maximum sont affectés à des canaux de temps de vol et 8192 au programme.

- soit des blocs mémoires BM 96 à travers une unité de multiplexage. La durée de transfert des résultats vers le calculateur est de 1 seconde environ.

- soit d'échelles de comptage.

Dans le cas d'expériences automatisées, les différentes séquences s'enchaînent de la façon suivante :

a) Accumulation dans le calculateur (expérience n° 1 ; 16 384 canaux au plus) les blocs mémoires BM 96 (expériences n° 2, 3 et 4 ; 12 288 canaux au plus pour chacune d'elles) et les échelles.

b) Fin d'accumulation donnée par une horloge qui déclenche :

- l'arrêt de l'acquisition
- les modifications des conditions expérimentales (changement d'échantillons par exemple).
- le transfert sur la bande magnétique du calculateur du contenu de la mémoire rapide, des blocs mémoires et des échelles.

A ce moment-là, il est possible au conducteur du calculateur d'effectuer certaines opérations telles que la visualisation d'une expérience.

c) Reprise de l'accumulation lorsque tous les décodages et les modifications expérimentales sont terminées.

Afin d'accroître la souplesse de l'ensemble, il est possible d'interdire le décodage de toutes les expériences ou de certains blocs mémoires et, dans le cas de décodage de ces derniers, d'effacer ou non le contenu de leur mémoire à chaque séquence.

2.2.2. Fonctionnement hors ligne.

Il consiste essentiellement en :

- la lecture des bandes magnétiques 16 pistes
- le tracé de courbes par le traceur Calcomp

- les dépouillements préliminaires des résultats (addition de décodages partiels, correction de temps mort, soustraction de bruit de fond, lissage des spectres etc....)

Plusieurs de ces opérations pourront être effectuées pendant le fonctionnement en ligne du calculateur.

2.3. Mesures.

2.3.1. Sections efficaces totales.

Pu 239 - Nous avons repris quelques mesures avec les échantillons d'épaisseurs 14g/cm^2 et 1 g/cm^2. De plus, les mesures faites, en 1965 ont été débarrassées des résonances parasites dues au Pu 240 par transmission d'un échantillon de 1581,5 g de Pu O^2 à 10% de Pu 240, dans les mêmes conditions expérimentales que pour le Pu 239.

Np 237 - La mesure a été faite avec deux échantillons d'épaisseurs 0,0066 et 0,002 atomes par barn ayant respectivement les surfaces de 9,6 cm^2 et 14,5 cm^2. Pour chaque échantillon, la mesure a été partagée en 2 gammes, l'une à basse énergie (1 eV $< E <$ 20 eV) avec une base de vol de 16,7 mètres et une résolution de 22 ns/m. à 10 eV, l'autre à haute énergie (15 eV $< E <$ 35 keV) avec une base de vol de 53,7 mètres et une résolution de 2,8 ns/m. à 100 eV. La durée d'accumulation a été de 10 heures pour la 1ère mesure et de 100 heures pour la seconde.

Xénon - La section efficace totale, a été mesurée avec des échantillons gazeux (0,03 ; 0,23 et 0,556 g/cm^2) et solide (d'épaisseur 4,95 g/cm^2 de Xe F^2) de Xénon naturel. De même que pour le Np^{237} la mesure a été scindée en deux gammes, l'une à basse énergie (1 eV $< E <$ 20 eV) avec une base de vol de 17,7 mètres et une résolution de 23 ns/m. à 10 eV , l'autre à haute énergie (20 eV $< E <$ 900 eV) avec une base de vol de 53,7 mètres et une résolution de 1,2 ns/m. à 900 eV. De plus, en vue de l'attribution isotopique des résonances observées dans le Xénon naturel, une mesure de transmission a été entreprise avec un échantillon de Xénon faiblement enrichi en isotopes lourds (11,2 % de Xe ^{136} contre 8,9 % dans le Xénon naturel) d'épaisseur 0,013 g/cm^2 avec une base de vol de 17 mètres et une résolution de 12ns/m. à 100 eV.

Gadolinium - La mesure a été faite avec un échantillon de Gadolinium naturel et deux échantillons d'isotopes séparés, chacun contenant deux grammes d'oxyde, l'un des échantillons étant enrichi à 94,3% en Gd^{155}, l'autre à 93,7 %

en Gd^{157}. Ces isotopes, en provenance du laboratoire national d'Oak Ridge, nous ont été prêtés par l'U.S.A.E.C. Pour cette mesure, la longueur de vol était de 17 mètres et la résolution de 8,2 ns/m. à 100 eV. Nous présentons sur la fig. 6 une partie des résultats bruts pour le Gd^{155} et le Gd^{157} qui correspondent à une accumulation d'une dizaine d'heures pour chacun des isotopes.

Sodium - Cette mesure a été suggérée par les résultats obtenus par le Groupe de Cadarache qui montrent, en section efficace de capture, une résonance importante vers 35 keV. Pour la détecter en transmission, nous avons éliminé tout aluminium sur le parcours des neutrons : les bases de vol ont été fermées par des fenêtres minces en mylar et remplies d'hélium. La figure 7 représente les résultats obtenus après 14 heures d'accumulation sur une base de vol de longueur 103,7 m.,(largeur de canal du sélecteur 10 ns ; largeur de l'impulsion de l'accélérateur 15 ns). La résonance à 35 KeV est bien mise en évidence, ainsi qu'une autre résonance à 118 KeV. Depuis, ces résonances ont été également vues en section efficace de capture par le groupe de R.P.I.

2.3.2. Sections efficaces de fission.

La section efficace de fission du Np^{237} a été mesurée avec un scintillateur gazeux au Xénon à 12 cellules séparées optiquement, mais placées dans une même enceinte contenant au total 2 grammes de Np^{237} répartis sur deux plans parallèles distants de 8 cm. En vue de la normalisation de la section efficace de fission sur celle de l'U^{235}, l'une des douze cellules était équipée d'un dépôt contenant un mélange de Np^{237} (99,2 %) et d'U^{235} (0,8 %). L'expérience a été faite sur une base de vol de 12,4 m. inclinée de 18° par rapport à la normale au ralentisseur ; elle représente environ 350 heures d'accumulation. La mesure est perturbée d'une part, par les résonances parasites du Xénon (que nous avons pourtant conservé à cause de ses propriétés de gaz scintillant), d'autre part, par un bruit de fond important dû aux neutrons incidents mais dont l'origine n'est pas encore claire. Des essais sont en cours avec d'autres gaz scintillants.

Par ailleurs, une chambre d'ionisation compensée (pour réduire l'effet de l'éclair des rayons γ de la cible, et contenant 300 mg. de Np^{237} est en cours d'essais surtout en vue d'éliminer le bruit de fond important qui masque les petites résonances.

Nous avons reproduit sur la fig. 8 une partie des résultats relatifs à la

section efficace de fission et la section efficace totale du Np^{237}.
Un scintillateur gazeux à très basse température (77°K) à 12 cellules pouvant contenir jusqu'à 1 gramme de Pu^{239} est en cours de construction. Des essais préliminaires avec une seule cellule ont donné satisfaction.

2.3.3. Section efficace de diffusion.

Cette mesure est toujours destinée à la détermination du spin des résonances lorsque le spin du noyau cible est faible ($I \leq 3/2$).
Le détecteur est une couronne de 32 compteurs proportionnels à BF^3 à faible fluctuation de temps de réponse.
Des mesures ont été faites avec une base de vol de 14 mètres (inclinée à 45°) sur du Xénon naturel gazeux (épaisseurs : $2,68.10^{-4}$ at/barn et $6,69.10^{-4}$ at/barn), sur du gadolinium naturel et sur les isotopes séparés de Gadolinium utilisés pour les mesures de transmission. En vue de remplacer le détecteur actuel qui est insuffisant, des essais de laboratoire ont été menés avec une cellule de scintillateur liquide chargé au bore (de type étudié par H.E.Jackson à Argonne) couplée à un photomultiplicateur à grand gain et faible bruit (EMI 9514 SA ou 56 AVP 03). Avec une telle cellule, il a été possible d'utiliser une méthode de discrimination de forme qui rejette 999 ‰ des rayons γ tout en gardant 90 % des impulsions produites par des neutrons. Un grand détecteur composé de 8 cellules de ce type est en cours d'étude.

2.4. Analyse des résultats.

2.4.1. Pu^{239} - L'analyse des résonances a pu être poursuivie jusque vers 250 eV pour la fission et 400 eV pour la transmission. Les résultats de l'analyse ont été présentés à la Conférence de Paris d'Octobre 1966 (5), où la liste des paramètres des résonances jusqu'à 440 eV a été publiée. Nous nous bornerons à rappeler brièvement les principaux résultats :

- Espacement moyen apparent : $\langle D_{obs} \rangle = 2,39$ eV de 0 à 300 eV.
- Fonction densité : $S_o = (1,33 \pm 0,14).10^{-4}$ de 10 à 440 eV (on observe des oscillations de la valeur locale de S_o de part et d'autre de cette valeur moyenne).
- La distribution des largeurs neutroniques réduites est en accord avec une distribution de Porter et Thomas (8), surtout si l'on admet une perte de petits niveaux de 5 % environ (Fig. 9).
- La largeur totale de radiation fluctue peu de résonance en résonance. Sa valeur moyenne est de : $\langle \Gamma_\gamma \rangle = 41,6$ meV (pour 59 niveaux).

- La distribution des largeurs de fission est particulièrement intéressante (fig. 10). Elle est incomplète avec une seule famille. Pour rendre compte de la distribution expérimentale, il faut la comparer à un ensemble de deux familles ayant des largeurs moyennes très différentes: $\langle \Gamma_f \rangle = 42$ meV pour l'une et $\langle \Gamma_f \rangle = 1300$ meV pour l'autre. Ces deux familles peuvent correspondre aux deux voies de sortie 1^+ et 0^+ (5) (6).

- En faisant certaines hypothèses sur les paramètres Γ_f et Γ_γ , il est possible de connaître le spin d'une trentaine de résonances (fig.11) qui sont comparées soit à des mesures directes du spin, soit à des mesures indirectes comme la distribution en masse des produits de fission.

2.4.2. Np^{237} - Les paramètres de 143 résonances ont été obtenus (7).
Sur la fig.12 sont portées les distributions des espacements et des largeurs neutroniques réduites. On constate un manque de petits espacements et de petits niveaux, comparable à ce qui a été observé pour l'U^{235} et qui, dans le cas du Np^{237} a pu aussi être confirmé par une section simulée par une méthode de Monte Carlo.
La fig. 13 montre la distribution des largeurs de fission pour les résonances qui apparaissent dans la section efficace de fission. Nous étudions actuellement la façon de tenir compte des résonances manquées en fission. La valeur moyenne $\langle \Gamma_f \rangle = 0,37$ meV qui peut être grossièrement fausse, compte-tenu de ce dernier effet, est cependant en accord avec la formule de Wheeler en choisissant $\hbar\omega_f$ égal à 650 keV.
La fonction densité est égale à :

$S_o = (0,98 \pm 0,16).10^{-4}$ et l'espacement moyen des niveaux observé entre 0 et 4.0 eV est $\langle D_{obs.} \rangle = 0,67$ eV

2.4.3. Xénon - Les résultats préliminaires de l'analyse des mesures sur le Xénon ont été publiés à la Conférence de Paris d'Octobre 1966. -(9)

2.4.4. Gadolinium (9) - Le dépouillement est en cours. L'attribution isotopique pour le Gd^{155} et le Gd^{157} est terminée jusque vers 250 eV. La densité des niveaux du Gd^{155} est environ 2,5 fois plus élevée que pour le Gd^{157}. Le rapport exact ne pourra être donné qu'après l'évaluation des niveaux manqués, surtout pour le Gd^{155}. Ce rapport peut être expliqué en partie par la différence d'énergie de liaison de ces deux isotopes.

3. Groupe des neutrons rapides.

J.L. Leroy.

Ces expériences ont été effectuées auprès du Van de Graaff 5 MeV par D. Abramson, A.Arnaud, J.C. Bluet, E. Fort, J. Gentil, D.Hébert, J.L.Huet, C. Le Rigoleur, J.L. Leroy, Ph. Quentin, I. Szabo.

3.1. Commande de l'accélérateur et des expériences associées par un calculateur électronique.

Un calculateur CAE 90-10 sera installé prochainement auprès du Van de Graaff. Il aura pour rôle :

a) de faire le réglage de l'accélérateur et des différents paramètres de l'expérience (positions de compteurs, d'échantillons etc....).

b) de concentrer les données acquises et de les présenter sous une forme intelligible.

c) dans une étape ultérieure, de gérer le déroulement de l'expérience en fonction des résultats précédemment acquis. (par exemple déterminer la durée des comptages afin d'arriver à une erreur statistique déterminée).

A l'heure actuelle, la totalité du matériel assurant la liaison entre le calculateur et l'appareillage extérieur, a été réalisée; les programmes temps réel correspondants sont en cours de test.

3.2. Mesure absolue de flux de neutrons rapides par la méthode de la particule associée.

L'application de cette méthode à la réaction T (p, n) ^{3}He, qui était en cours de mise au point depuis deux ans, a été réalisée d'une façon satisfaisante. Elle a permis de faire une nouvelle mesure de la section efficace de la réaction ^{6}Li (n, α) T, pour des neutrons d'énergie comprise entre 150 KeV et 280 KeV. Ce travail a fait l'objet d'une communication à la Conférence de Paris d'Octobre 1966 (11).

3.3. Diffusion élastique des neutrons par ^{6}Li.

Il existe un certain nombre d'indications théoriques et expérimentales concernant l'existence de niveaux vers 9,6 MeV et 10 MeV d'excitation, dans ^{7}Li. Nous avons entrepris une mesure de la diffusion des neutrons par ^{6}Li, à un angle de 135° pour des énergies de neutrons allant de 2 MeV à 3,5 MeV, dans l'espoir de mettre en évidence ces niveaux.

L'expérience a été faite par la technique du temps de vol, en utilisant le Van de Graaff et son système de regroupement magnétique. La résolution du système

complet, (y compris les détecteurs de neutrons) est de 2,5 ns. La fréquence de répétition est de 3,5 MHz ou de 7 MHz, avec un courant moyen de 5 à 8 μA. Les résultats seront prochainement publiés.

3.4. Etablissement de codes de calcul.

La diffusion inélastique à partir de neutrons d'énergie élevée n'est pas traitée très correctement par la méthode de Hauser - Feshbach, il semble plus approprié d'utiliser la méthode de la D.W.B.A. Un code de calcul a été écrit en utilisant le formalisme de Satchler, et en adaptant la programmation aux particularités de l'ordinateur IBM 360-50 dont dispose le Centre de Cadarache. Les fonctions d'ondes optiques nécessaires au calcul des probabilités de transition ont été obtenues à partir d'un code de modèle optique.

Liste des publications.

1) R.SAMAMA, H. NIFENECKER, P. CARLOS, B. DELAITRE - Rapport C.E.A. R. 3034.
2) P. CARLOS, R. SAMAMA, A. AUDIAS, Nucl. Phys., à paraître.
3) C. SIGNARBIEUX, M. RIBRAG, Nucl. Phys., à paraître.
4) P. RIBON, B. CAUVIN, H. DERRIEN, A. MICHAUDON et M. SANCHE - Communication CN 23/71. Congrès sur les Constantes Nucléaires (Paris - Octobre 1966).
5) H. DERRIEN, J. BLONS, C. EGGERMANN, A. MICHAUDON, D. PAYA, Communication CN 23/70. Congrès sur les Constantes Nucléaires (Paris - Octobre 1966).
6) A. MICHAUDON. Exposé d'ensemble CN 23/123. Même congrès.
7) D. PAYA, H. DERRIEN, A. FUBINI, A. MICHAUDON, P. RIBON, Communication CN 23/69. Même congrès et article à paraître.
8) J. BLONS, H. DERRIEN, A. MICHAUDON, P. RIBON, G.de SAUSSURE, C.R. Académie des Sciences 262, 79 (1966).
9) P. RIBON, B. CAUVIN, H. DERRIEN, A. MICHAUDON, E. SILVER, J.TROCHON, Communication CN 23/72. Même congrès.
10) B. CAUVIN, P. RIBON, M. SANCHE, article à paraître (Onde Electrique).
11) E. FORT, J.L. LEROY, Communication CN 23/68. Même congrès.

TABLEAU I

ANISOTROPIE DES CASCADES DE DESEXCITATION DU V^{51}

Cascades	a_2 / a_o
7.150 - 0.125 Mev	$-0.06 < a_2 / a_o < 0.01$
6.87 - 0.295 Mev	$-0.03 < a_2 / a_o < 0.03$
6.87 - {0.419 Mev, 0.436 Mev}	$-0.07 < a_2 / a_o < 0$
6.51 - 0.645 Mev	$-0.17 < a_2 / a_o < -0.10$
6.51 - 0.793 Mev 6.46 - {0.824 Mev, 0.846 Mev}	$-0.07 < a_2 / a_o < 0.01$
5.9 - 1.4 Mev	$-0.11 < a_2 / a_o < 0.03$
5.75 - 1.55 Mev	$-0.12 < a_2 / a_o < 0.03$
5.52 - 1.78 Mev	$-0.15 < a_2 / a_o < 0$
5.22 - 1.96 Mev 5.15 - 2.15 Mev	$-0.15 < a_2 / a_o < 0$

TABLEAU II

ETUDE DE LA FISSION SYMETRIQUE

Auteurs	Méthodes	"Creux" d'énergie cinétique totale moyenne (MeV)		Taux d'évènements aberrants à la symétrie
		Valeurs mesurées	Valeurs corrigées	
Thomas (1965)	(E_1, E_2) détecteurs à jonction	31	26	50 %
Apalin (1965)	(E_1, E_2) chambre à grille	25	21	20 %
Aras (1965)	Radiochimie	24		
Schmitt (1966)	(E_1, E_2) détecteurs à jonction	24		
Présent travail	$(E_1, E_2, \Delta t)$ détecteurs à jonction	21,2 ± 0,8		< 4 %

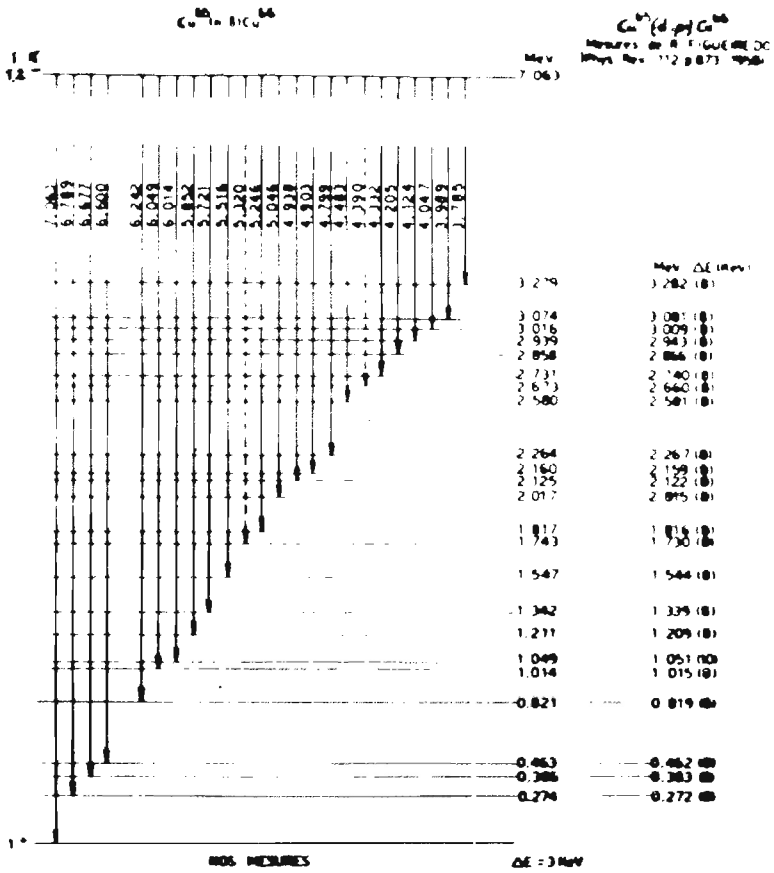
Cu(d,p)Cu
Mesures de R. Figueroa
Phys. Rev. 112, p.873 (1958)
MeV
7.063
3.279
3.074
3.016
2.939
2.858
2.731
2.653
2.580
2.264
2.160
2.125
2.017
1.817
1.743
1.547
1.342
1.211
1.049
1.014
0.821
0.463
0.386
0.274
MeV ΔE (MeV)
3.282 (8)
3.081 (8)
3.009 (8)
2.943 (8)
2.866 (8)
2.660 (8)
2.581 (8)
2.267 (8)
2.159 (8)
2.122 (8)
2.015 (8)
1.544 (8)
1.339 (8)
1.209 (8)
1.051 (10)
1.015 (8)
0.819
0.272
1+
NOS MESURES
ΔE = 3 MeV

Fig. 1

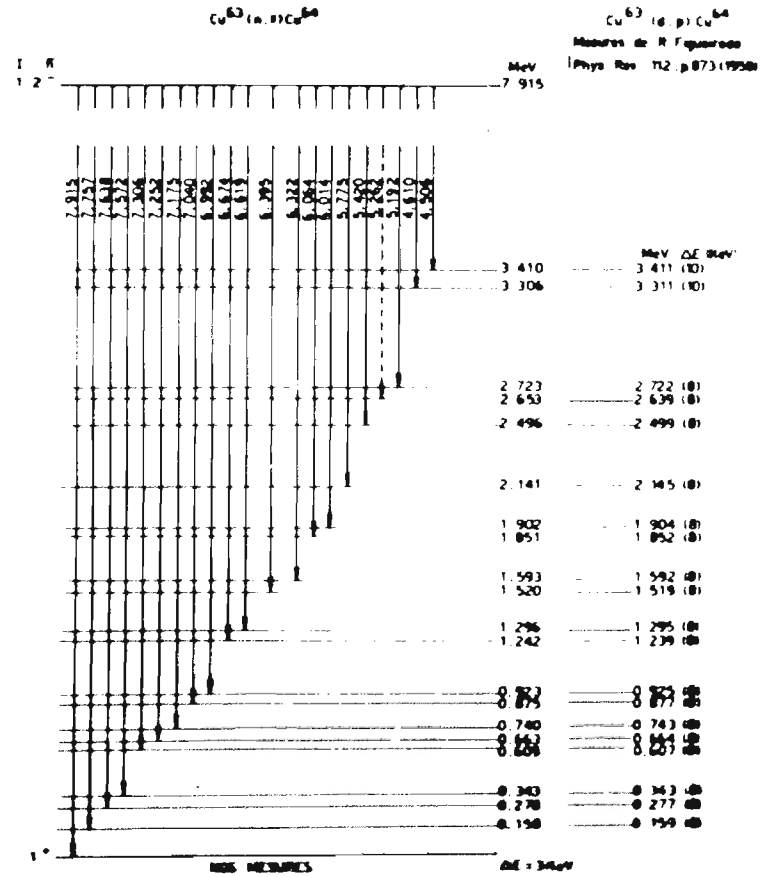
Cu(d,p)Cu
Mesures de R. Figueroa
Phys. Rev. 112, p.873 (1958)
MeV
7.915
3.410
3.306
2.723
2.653
2.496
2.141
1.902
1.851
1.593
1.520
1.296
1.242
0.740
0.278
MeV ΔE (MeV)
3.411 (10)
3.311 (10)
2.722 (8)
2.639 (8)
2.499 (8)
2.145 (8)
1.904 (8)
1.852 (8)
1.592 (8)
1.519 (8)
1.295 (8)
1.239
0.743
0.277
1+
NOS MESURES
ΔE = 3 MeV

ELECTRONS DE CONVERSION

DU Cd^{114}

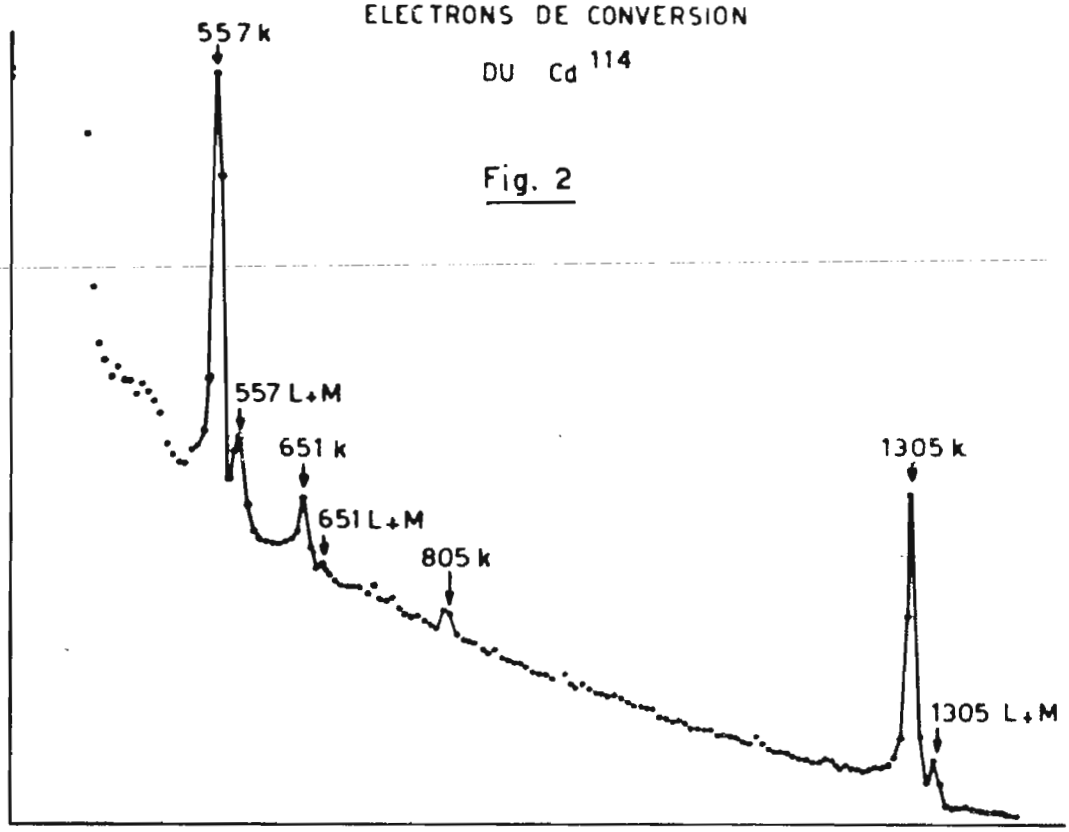

Fig. 2

SPECTRE DES RAYONS X

DES FRAGMENTS DE FISSION

DE L' U^{235}

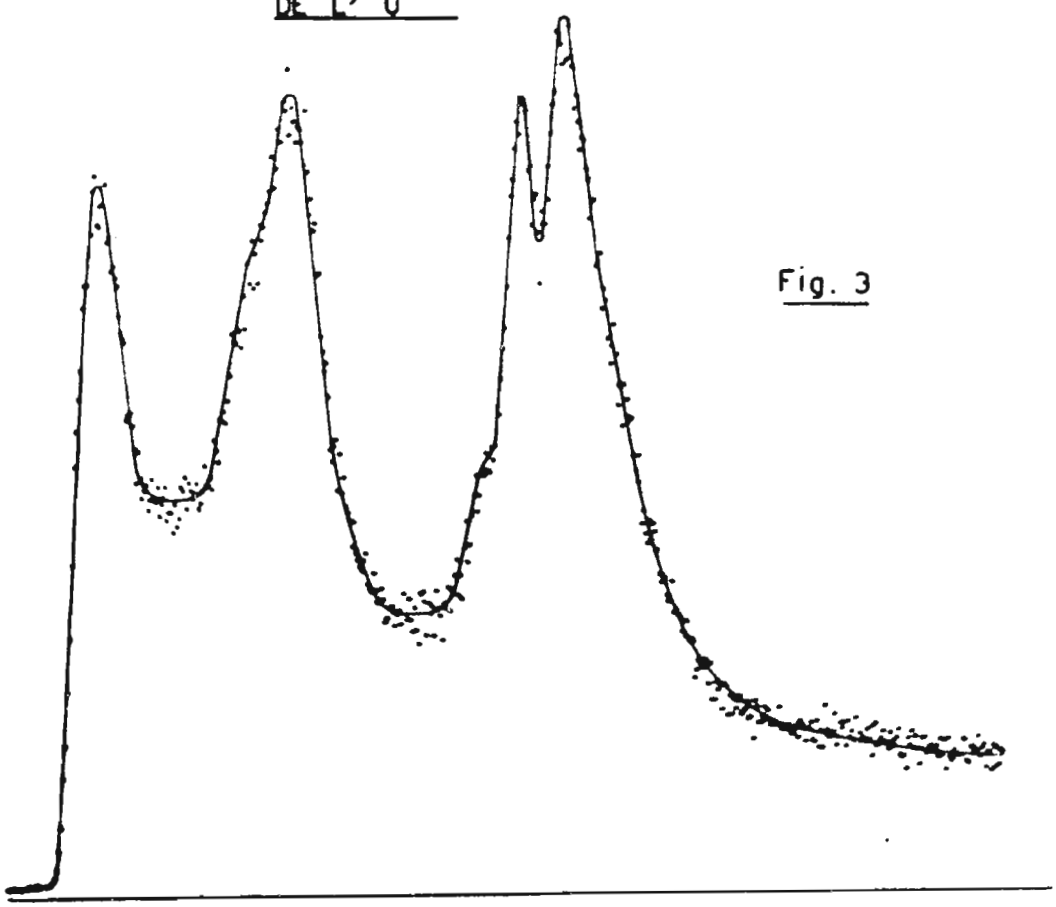

Fig. 3

ACCELERATEUR LINEAIRE 45 Mev

IMPLANTATION DES BASES DE TEMPS DE VOL

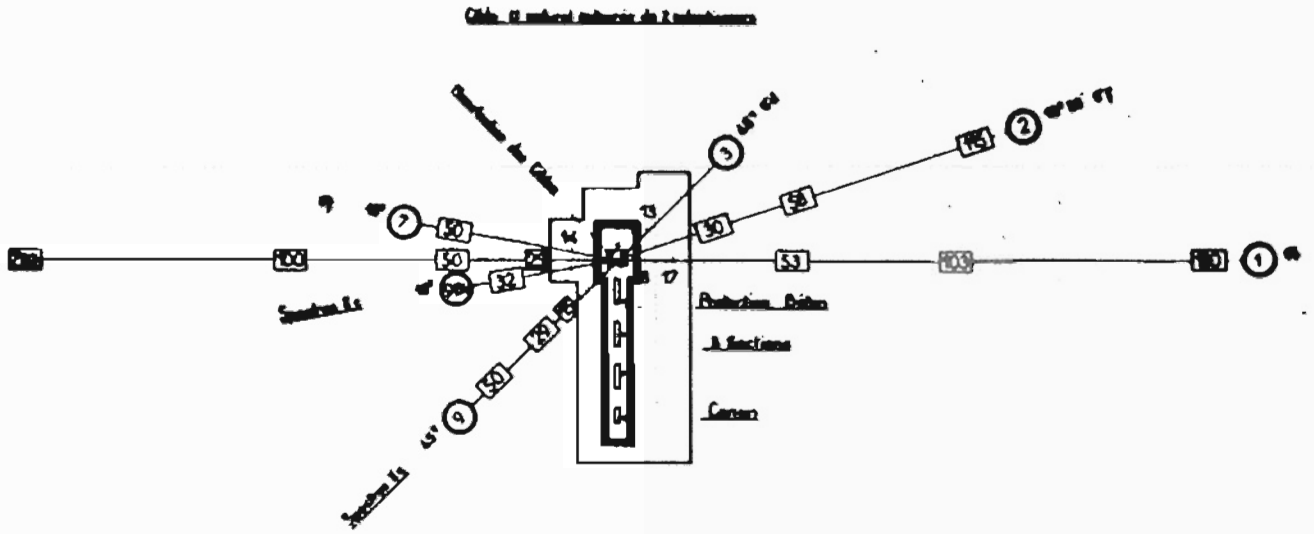

Bases 8 et 9bis : S.P.N.B.E.

Fig 4

CALCULATEUR C.A.E. EN LIGNE

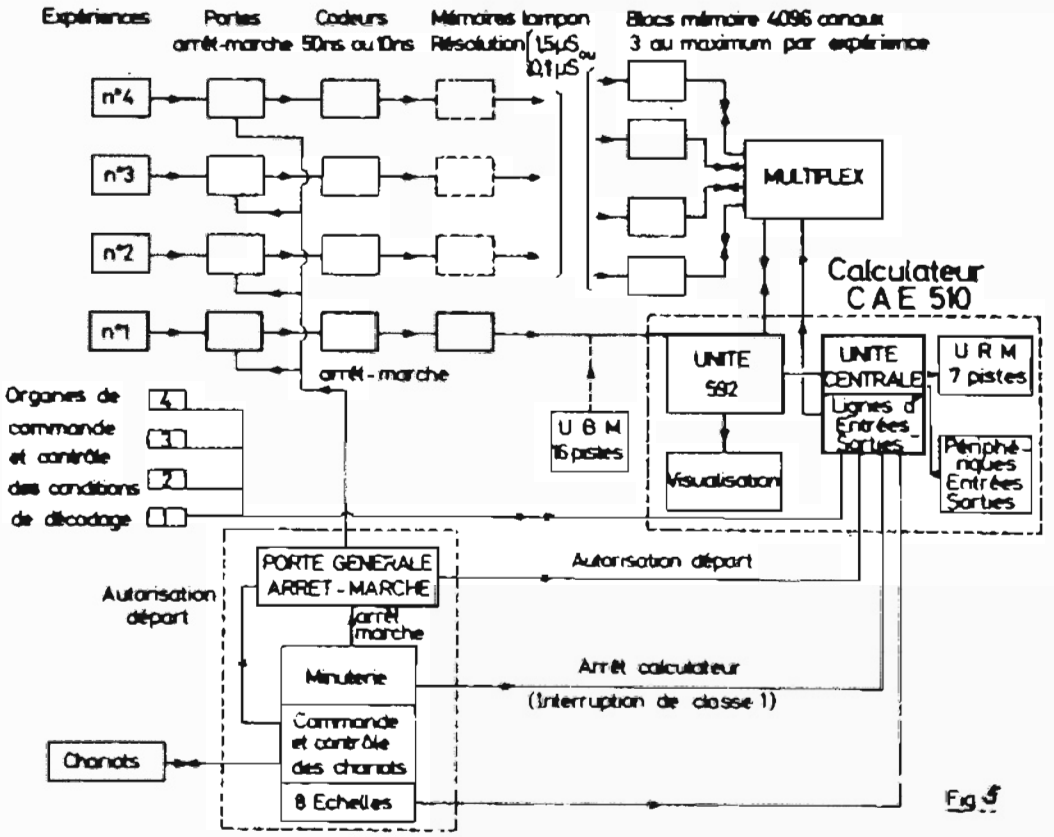

Fig 5

RESONANCES DU SODIUM

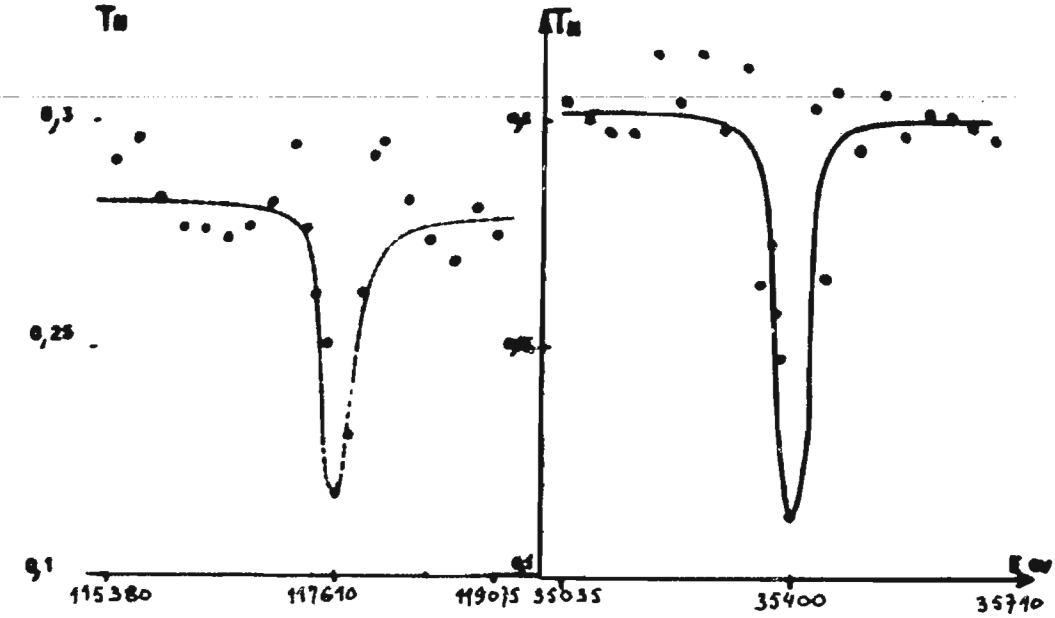

Fig. 7

TRANSMISSION DU GADOLINIUM

-1- Gd^{257} -2- Gd^{255}

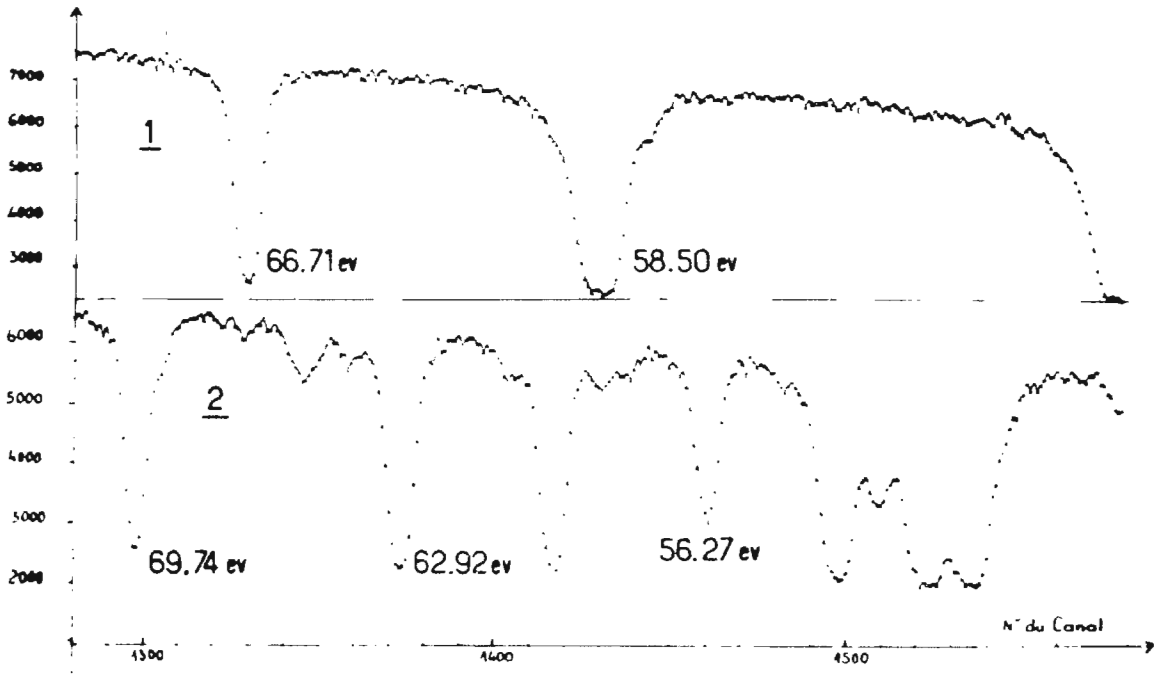

Fig. 6

SECTIONS EFFICACES TOTALE ET DE FISSION
DU Np^{237}

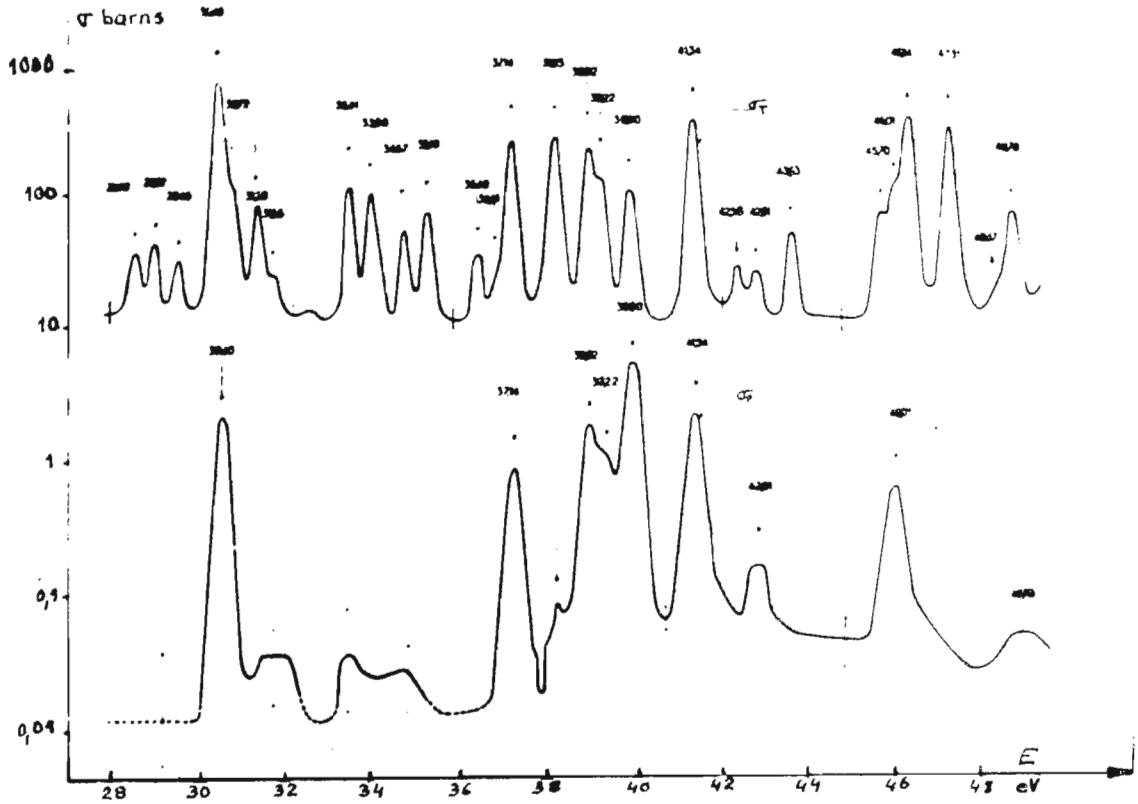

Fig. 8

DISTRIBUTION DES LARGEURS DE FISSION Γ_f
DES RESONANCES DU Pu^{239}

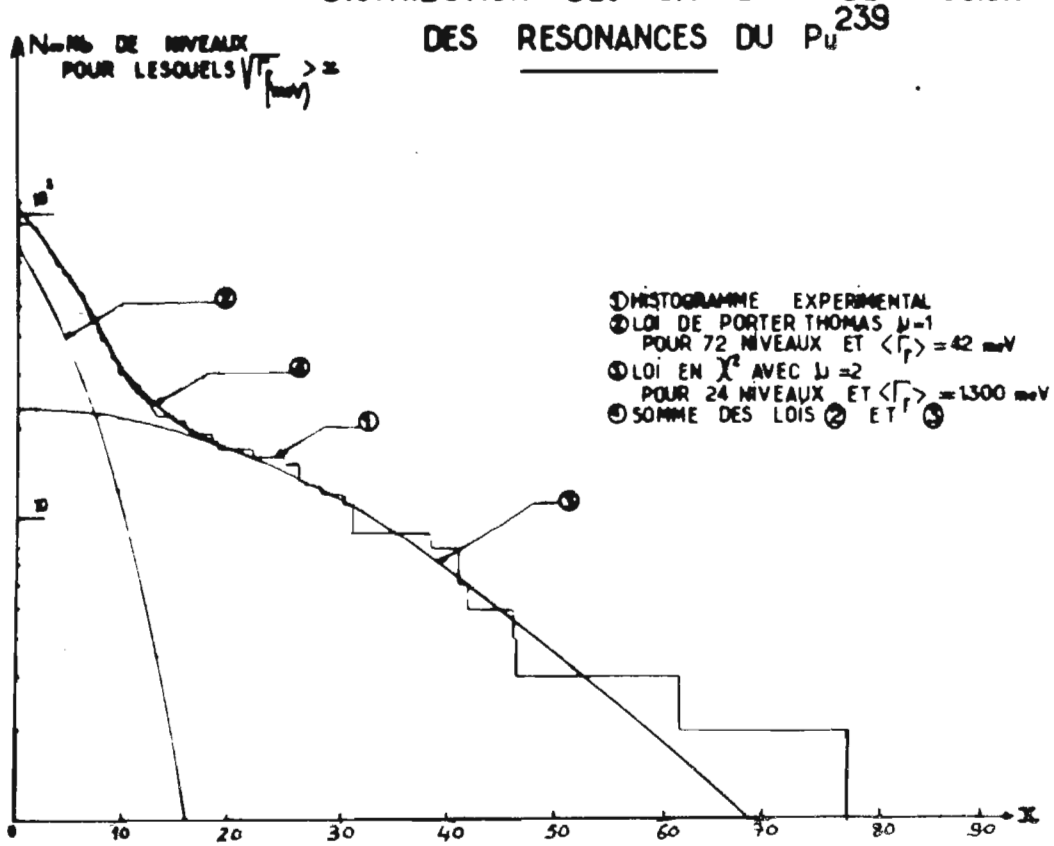

FIG. 10

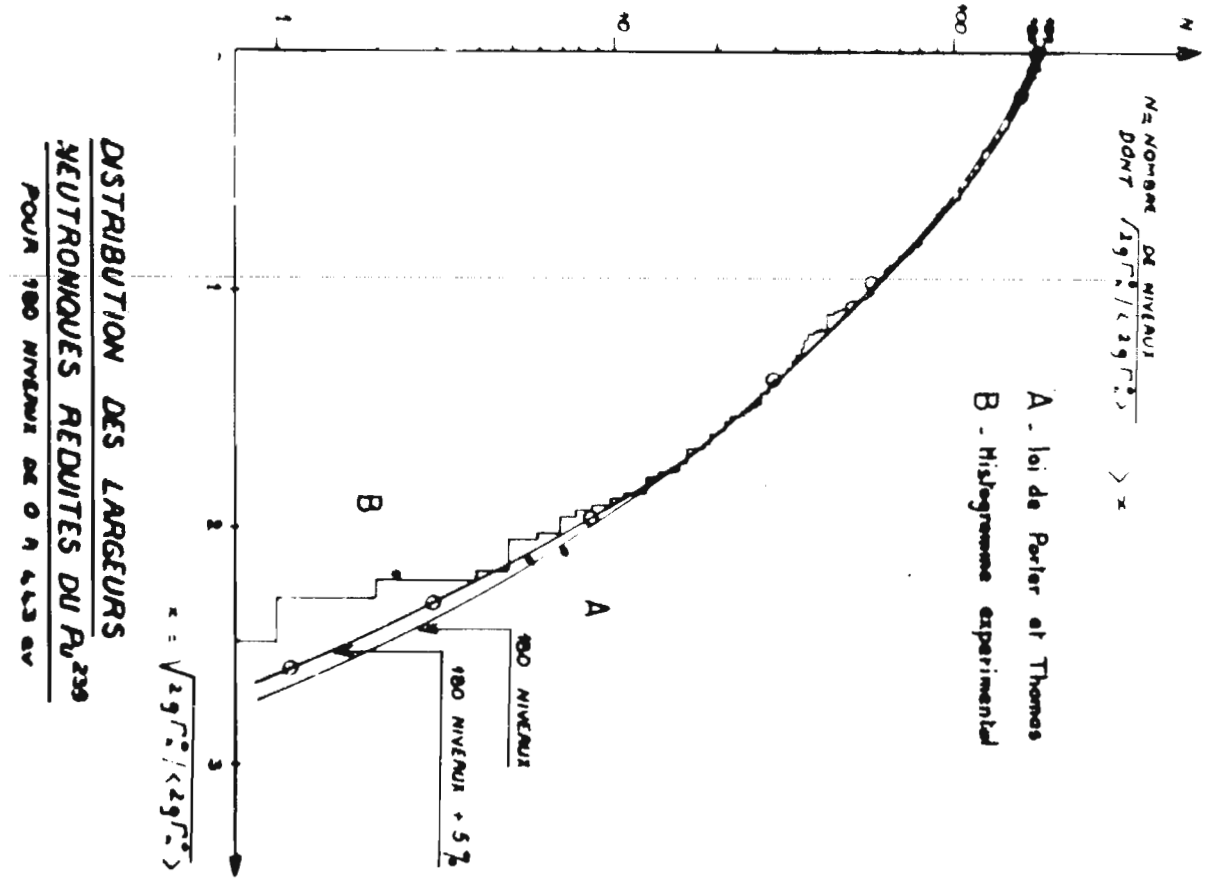

Fig 9

DISTRIBUTION DES LARGEURS DE FISSION DU Np^{237}

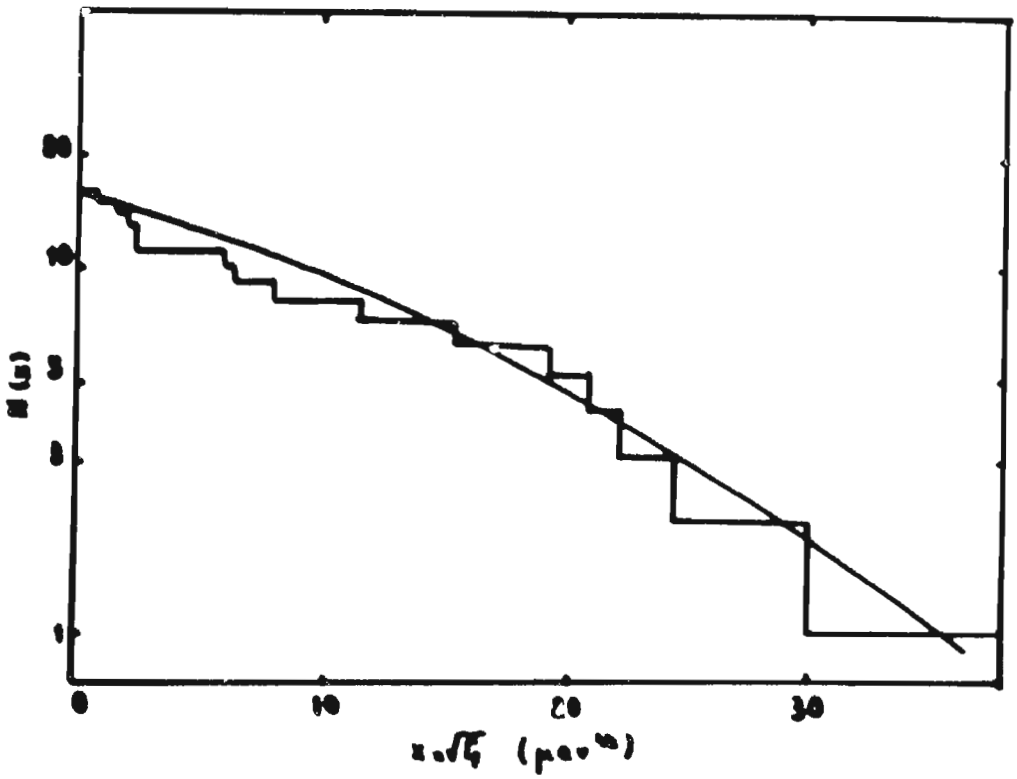

Fig 13

DETERMINATION DU SPIN DES RESONANCES DU Pu^{239}

ENERGIE (ev)	SPIN J ASHGAR	SPIN J DERRIEN	Γ_f (mev)	ENERGIE (ev)	SPIN J ASHGAR	SPIN J DERRIEN	Γ_f (mev)
90,75	1_g	1^e	17	196,7	0		59
95,36	0_g			199,4	0	1^e	90
96,49		0^d	1670	207,37	1	$(1)^f$	7
100,25		0^d	6000	211,1		0^d	800
103	1		13	216,5	0	$(0)^f$	10
105,3	0		6	220,2		1^f	4
106,67	(1)	1^f	26	223,2	0		~ 2
116,03	0		215	227,8		0^d	6000
118,83	0	1^e	43	231,40	1	1^e	4
126,2	0			234,3	0		14
131,75	0	0^d	3300	239,1	0	$(0)^f$	17
133,78	1		7	242,9	0	1^f	58
136,75	0		88	248,86	1	1^e	6
146,25	1	$(0)^f$	13	251,2	1	1^e	14
147,44		0^d	1000	262,5	0		
157,08	0	0^d	630	273,6	1		
164,54	1	1^e	8	276,9	0		
167,1	0	$(1)^f$	74	281	0		
171,08		0^d	1000	284,1	1		
177,22	1		5	299,7	1		
184,87		0^d	~500				

ENERGIE (ev)	SPIN J VOGT	FRASER	SAUTER	ASHGAR	COWAN	DERRIEN	Γ_f (mev)
-1,2	J_1^a						
0,3	J_2^a						0
7,82	J_1^a	1	1				47
10,93	J_1^a	1	1				143
11,5						0^d	~500
11,89		1	1				24
14,31			1^a				67
14,69		0	1	1			30
15,42			0^a		(1)	0^d	650
17,66		1	1	1	1		34
22,28		0	1	1	1		62
26,29				0	1		55
32,38			0^b		(0)		110
35,43			1^b				5
41,42 }		1^c	1^c	1^c	1^c		3
41,66 }							54
44,48		0	1	1	1		5
47,60			0	0	1		240
49,71					0	0^d	690
50,08				1	1		12
52,60			1	1	1		9
57,44					0	0^d	~500
58,84					0	0^d	~1100
59,22				0	1		133
60,94					0	0^d	~6000
65,71				1	1	$(1)^f$	74
66,57					0		
71,05				1			32
74,95			1	1	1	1^e	84
81,76					0	0^d	~2000
85,48				0			85

Fig 11

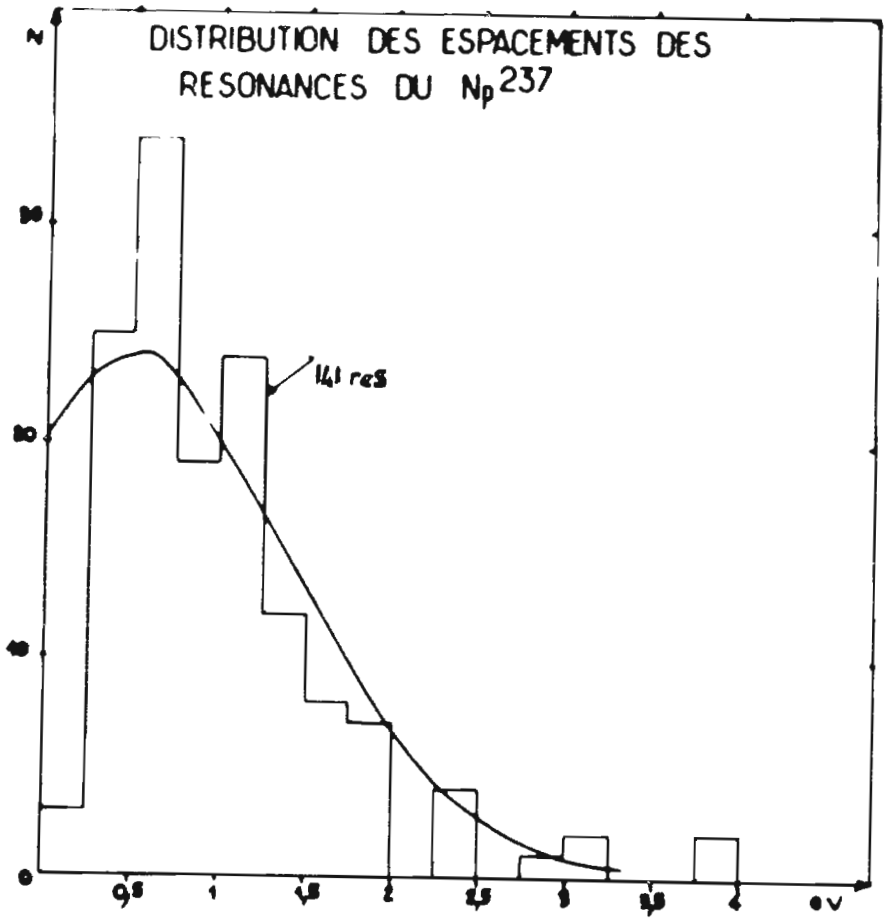
DISTRIBUTION DES ESPACEMENTS DES
RESONANCES DU Np237
N
141 res
0
0,5
1
1,5
2
2,5
3
3,5
4
eV

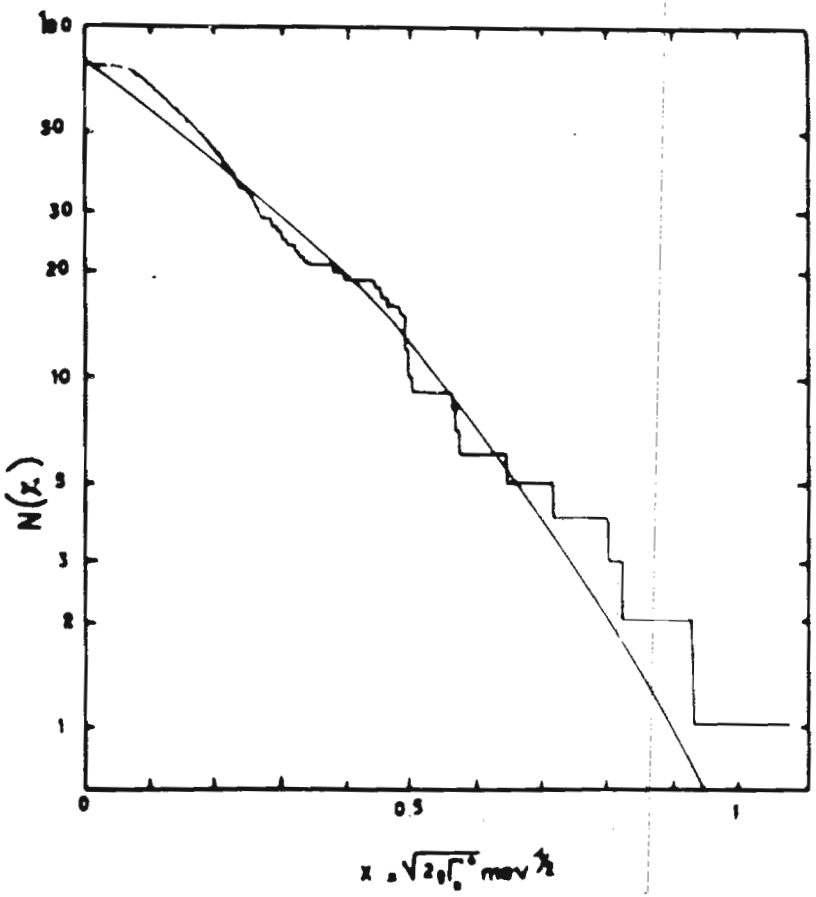
DISTRIBUTION DES LARGEURS NEUTRONIQUES
REDUITES DU Np237
N(x)
100
50
30
20
10
5
3
2
1
0
0.5
1

Fig 12

XXII DEPARTEMENT DE PHYSIQUE NUCLEAIRE - SERVICE DE PHYSIQUE NUCLEAIRE A BASSE ENERGIE, C.E.A., Saclay (France).

E. Cotton.

Le Groupe de neutronique a utilisé le faisceau pulsé de neutrons, produit par l'accélérateur linéaire de 45 MeV de Saclay pour des études des propriétés statistiques des niveaux nucléaires.

Pour les expériences de transmission, la mise en place d'une base de temps de vol de 200 m a permis d'obtenir une résolution deux fois meilleure dans la détection des neutrons.

Pour les expériences de capture radiative, l'utilisation de détecteurs au Ge-Li a permis de gagner un ordre de grandeur en résolution dans la détection des rayons γ.

1. Conditions expérimentales. Méthodes d'analyse.

Une résolution accrue nous a permis d'étudier un domaine d'énergie de plus en plus élevé ; l'énergie maximale possible dépend de l'espacement moyen des résonances. Pour les noyaux au-dessous de la masse 60, nous avons fait des mesures jusqu'à une énergie de 500 keV. Nous avons utilisé des bases de temps de vol de 53, 103 et 199 mètres. Les largeurs d'impulsions de l'accélérateur linéaire variaient de 20 à 100 nanosecondes suivant les expériences. Nous avons utilisé un codeur de temps de 65 536 canaux à largeur de canaux variable depuis 10 nanosecondes. Le nombre de canaux effectivement utilisés était généralement 8192.

Les mesures donnent une résolution électronique de 12 nanosecondes. En tenant compte de tous les facteurs, notre résolution minimale était de 0,17 nanoseconde par mètre (la meilleure résolution jamais atteinte dans ce type d'expériences). Cette résolution a été testée par analyse de forme d'une résonance dont l'aire était connue (la mesure de l'aire est indépendante de la résolution). La figure 1 donne un exemple d'une courbe de transmission obtenue avec la meilleure résolution.

Lorsque les largeurs des résonances de même spin sont très inférieures à leur espacement, on utilise la formule de Bethe. Quand cette condition n'est pas remplie, on utilise les formalismes rigoureux de Humblet et Rosenfeld ou de la matrice R qui conduisent d'ailleurs aux mêmes valeurs des largeurs

de diffusion dans la limite des erreurs expérimentales.

Des programmes (14)(15), tenant compte de l'effet Doppler et des effets de résolution, permettent la détermination des divers paramètres des résonances.

2. Fonction densité.

Les valeurs obtenues pour S_0 (neutrons "s") sont groupées dans les tableaux I et II. On voit que, pour les noyaux cibles I = 1/2, S_0 ne dépend pas de la valeur du spin du noyau composé (9)(10). Par contre, pour les noyaux cibles de spin I = 3/2, on trouve (3) (4) (5) (6) (7) :

$$S_0 \ (J = 2) = 2,2 \ S_0 \ (J = 1) \qquad J = I \pm \frac{1}{2}$$

Pour les noyaux étudiés, il a été vérifié que l'espacement moyen des niveaux obéit à une loi en $1/(2J + 1)$.

La figure 2 représente les variations de S_0 et du rayon effectif R' en fonction du nombre de masse A et leur comparaison avec différents modèles optiques ; celui de Chase, Wilets et Edmonds donne le meilleur accord.

Le cobalt a été étudié de 0 à 500 keV (2) (11) (12). La figure 3 représente, en fonction de l'énergie, la variation, d'une part de S_0 déterminée à partir des résonances individuelles, d'autre part de la section efficace moyenne correspondant à des intervalles d'énergie de 2 à 4 keV (l'espacement moyen des résonances dans le cobalt est de 1 keV, ce qui explique la dispersion des points). Les oscillations observées pourraient correspondre à des structures intermédiaires.

Le praséodyme étudié jusqu'à 6 keV fournit deux valeurs différentes de S_0 (tableau II) ; cette différence est due à un manque de niveaux J = 2 entre 1 keV et 3,5 keV, la probabilité d'une telle absence étant inférieure à 2 %.

Un exemple de détermination de S_1 par analyse de résonance individuelle est fourni par l'étude du niobium où 35 résonances l = 1 ont été mises en évidence au-dessous de 4 keV (12) (13).

3. Largeur radiative totale Γ_γ.

Pour un noyau donné, la valeur de Γ_γ est généralement constante et indépendante du spin pour les résonances "s". Le tableau III donne, par exemple, les valeurs de Γ_γ pour quelques résonances de ^{195}Pt de spin J = 0 et J = 1.

Γ_γ peut être différent si le schéma de désexcitation favorise, pour un état de spin, certaines transitions de haute énergie ; c'est, par exemple, le cas pour les isotopes ^{199}Hg et ^{201}Hg (13). On peut s'attendre à des valeurs de Γ_γ différentes pour les résonances "s" et "p", qui sont de parités opposées. Un tel résultat a été trouvé pour ^{93}Nb :

$$\langle \Gamma_\gamma (l = 0) \rangle = 150 \text{ meV} \quad \langle \Gamma_\gamma (l = 1) \rangle = 210 \text{ meV}$$

Les largeurs radiatives totales Γ_γ des noyaux cibles de A impair sont environ le double des valeurs Γ_γ des noyaux cibles de A pair. Ce résultat est général, à quelques exceptions près :

$$\langle \Gamma_\gamma (^{136}\text{Ba}) \rangle = 230 \text{ meV} \qquad \langle \Gamma_\gamma (^{135}\text{Ba}) \rangle = 110 \text{ meV}$$
$$\langle \Gamma_\gamma (^{198}\text{Pt}) \rangle = 150 \text{ meV} \qquad \langle \Gamma_\gamma (^{195}\text{Pt}) \rangle = 110 \text{ meV}$$

4. Distribution des espacements. Coefficients de corrélation.

On constate que le nombre de faibles espacements ($x \not\approx 0$) adapte la courbe théorique. La difficulté est de pouvoir distinguer deux résonances très proches. Il faut aussi disposer d'un échantillonnage statistique suffisant. Des résultats présentés par d'autres équipes révélaient un manque de faibles espacements qui, en fait, n'existe pas. Si plusieurs familles de noyaux sont mélangées, la distribution tend à devenir une distribution en e^{-x} (distribution au hasard). La valeur du coefficient de corrélation entre les espacements adjacents est trouvée égale à - 0,2, en accord avec la valeur théorique prévue. Cette valeur est très sensible au nombre de résonances omises et n'a de sens que si ce nombre de niveaux non détectés est très faible. Les valeurs du coefficient de corrélation entre espacements et largeurs de diffusion sont trouvées égales à zéro.

5. Largeurs radiatives partielles de ^{195}Pt.

Le noyau composé ^{195}Pt + n offre un nombre intéressant de résonances isolées de spin J = 1 et, en outre, un certain nombre de raies suffisamment intenses et isolées (19) (20).

Le développement récent des détecteurs au Ge-Li nous a conduits à reprendre une telle expérience à l'aide d'une cible naturelle de platine. Le détecteur avait un volume utile de 6 cm^3. La résolution de l'ensemble était de 15 keV à 7 MeV. La résolution en temps de vol était de 10 nanosecondes par mètre à 700 eV. Les données sont enregistrées à l'aide d'une chaîne bidimensionnelle.

Nous avons étudié 22 résonances et nous nous sommes limités aux trois transitions $1^- \rightarrow 0^+$, $1^- \rightarrow 2^+$ et $1^- \rightarrow 2^+$ aboutissant à l'état fondamental du noyau final ^{196}Pt et aux deux états excités situés à 356 et 689 keV. La figure 4 présente l'allure de quelques spectres typiques. Le tableau IV donne les intensités relatives I_i des trois rayonnements gamma. Ces données montrent que, aux erreurs statistiques près, les intensités I_i de chaque transition, moyennées sur l'ensemble des résonances, sont sensiblement constantes. Une estimation de leurs valeurs absolues est en assez bon accord avec le modèle à une particule de Weisskopf pour les transitions E1.

La distribution des largeurs expérimentales réduites $X_i = I_i / \langle I_i \rangle$ pour la population des 66 niveaux a été tracée sur la figure 5 ainsi que la loi en χ^2 à un et deux degrés de liberté.

Une simple comparaison montre que nos données sont compatibles avec $\nu = 1$ et non avec $\nu = 2$; on trouve $\nu = 1,31 \pm 0,22$ et $\nu = 3,71 \pm 1,00$ pour la somme des trois transitions. Une méthode de Monte-Carlo confirme définitivement ce résultat. Ainsi, les données de Saclay montrent que la distribution d'une largeur radiative partielle suit, comme la largeur de neutron, une loi en χ^2 à un degré de liberté.

Nous avons pu mettre en évidence 18 niveaux nouveaux du noyau ^{196}Pt entre 0 et 2300 keV. Certains spins ont pu être attribués. Le fait essentiel est que nous n'avons pu détecter le niveau situé à 1117 keV, dont la présence avait été signalée auparavant.

Le spectre de capture de la résonance à 96 eV de ^{198}Pt + n se trouve dominé par un rayon gamma très intense de 5456 keV. Une raie très faible, située à 47 keV de la précédente, ressort nettement. Nous avons trouvé quatre niveaux nouveaux de ^{199}Pt situés à 61, 114, 1126, 1512 keV au-dessus de l'état fondamental.

Références.

1 M. VASTEL, Thèse 3ème cycle, Paris, 1963.

2 J. MORGENSTERN et al., Nucl. Phys., 62, 529 (1965).

3 J. JULIEN et al., Nucl. Phys., 76 , 31 (1966).

4 J. JULIEN et al., Phys. Letters, 10 , 31 (1964).

5 J.JULIEN et al., Nucl. Phys., 66, 433 (1965).

6 P.CHEVILLON, Thèse 3ème cycle, Paris, 1966.

7 P. CHEVILLON , (à paraître).

8 J. JULIEN et al., Phys. Letters, 3 , 67 (1962).

9 S. de BARROS, Thèse d'Université, Paris, 1966.

10 S. de BARROS, (à paraître).

11 J. MORGENSTERN et al., Intern. Conf. Study Nucl. Structure with Neutrons, Anvers, 531, 1965.

12 G. LE POITTEVIN et al., Nucl. Phys., 70, 497 (1965).

13 G. LE POITTEVIN, Thèse 3ème cycle, Paris, 1965.

14 C.R. CORGE, Rapport CEA R 1998, 1961.

15 C.R. CORGE, Rapport CEA R 2780, 1965.

TABLEAU I

Noyau. Nombre de résonances détectées et nombre de résonances à valeur de spin attribuée	Valeur de la fonction densité eV-1/2 suivant la valeur du spin	Probabilité de trouver un rapport égal ou supérieur en supposant $S_o(I+1/2)=S_o(I-1/2)$
$^{69}Ga + n$ $\begin{cases} J = 2 \\ J = 1 \end{cases}$ 12 résonances dont 7 attribuées	$S_o = 1,8 \pm 0,9\ 10^{-4}$ $S_o < 0,4\ 10^{-4}$	
$^{75}As + n$ $\begin{cases} J = 2 \\ J = 1 \end{cases}$ 55 résonances dont 27 attribuées	$S_o = 2,5 \pm 0,6\ 10^{-4}$ $S_o = 1 \pm 0,3\ 10^{-4}$	~ 0,01
$^{79,81}Br + n$ $\begin{cases} J = 2 \\ J = 1 \end{cases}$ 80 résonances dont 25 attribuées	$S_{o_{J=2}}/S_{o_{J=1}} \sim 2$	~ 0,07 pour chaque isotope
$^{197}Au + n$ $\begin{cases} J = 2 \\ J = 1 \end{cases}$ 63 résonances dont 44 attribuées	$S_o = 2,46 \pm 0,53\ 10^{-4}$ $S_o = 1,17 \pm 0,3\ 10^{-4}$	~ 0,02
^{63}Cu $\begin{cases} J = 2 \\ J = 1 \end{cases}$ Pour les deux isotopes 34 résonances dont 23 attribuées	$S_o = 2,75$ $S_o = 1,6$	0,2
^{65}Cu $\begin{cases} J = 2 \\ J = 1 \end{cases}$	$S_o = 1,76\ 10^{-4}$ $S_o = 1,06\ 10^{-4}$	0,2
^{135}Ba $\begin{cases} J = 2 \\ J = 1 \end{cases}$	$S_o = 1,34\ 10^{-4}$ $S_o = 0,47\ 10^{-4}$	0,06
^{137}Ba $\begin{cases} J = 2 \\ J = 1 \end{cases}$ 3 résonances	$S_{o_{J=2}}/S_{o_{J=1}}$ 3	
$\frac{n_i}{n} \frac{S_o(J=2)}{S_o(J=1)}$ n = 254 résonances	2,24	0,002

$\sum$ est étendue à tous les noyaux ci-dessus ; n_i = nombre de résonances de chaque isotope ; $n = \sum n_i$.

$^{195}Pt + n$					
J = 1			J = 0		
E (eV)	Γ_γ (meV)	$\sum \Gamma_{\gamma i}$	E (eV)	Γ_γ (meV)	Γ^o_n
11,8	112 ± 7	332	67,1	130 ± 30	22
19,4	100 ± 8	122	119,25	70 ± 20	2,4
67,5	137 ± 20	306	154,7	152 ± 20	34,6
111,7	127 ± 15	182	204,8	100 ± 10	4,2
120,5	140 ± 15	286	261,7	64 ± 15	3,9
139,5	110 ± 13	462	309,6	64 ± 25	11
150,4	90 ± 15	53	453,2	82 ± 50	45
188,5	117 ± 10	262	515,2	72 ± 30	3
222,2	130 ± 13	511			
256,6	103 ± 15	94	706	105 ± 50	17
280	98 ± 25	245			
285,6	105 ± 15	283			
302,3	89 ± 20	314			
382,8	100 ± 20	65			
410,1	88 ± 10	90			
484,8	182 ± 32				
529,3	144 ± 26	717			
558,7	142 ± 31	369			
659,8	168 ± 25	99			
680	118 ± 25	21			

TABLEAU III

Energie résonance eV	Transition $1^- \to 0^+$ 7920 keV	Transition $1^- \to 2^+$ 7564 keV	Transition $1^- \to 2^+$ 7231 keV
11,8	3193 ± 66	102 ± 30	24 ± 34
19,4	704 ± 43	194 ± 33	318 ± 46
67,5	1690 ± 87	1317 ± 78	64 ± 49
111,7	710 ± 85	615 ± 91	480 ± 97
119,6	2077 ± 113	4 ± 50	689 ± 87
139,5	552 ± 75	227 ± 74	3537 ± 182
149,9	289 ± 54	59 ± 41	230 ± 60
188,5	756 ± 145	145 ± 107	1724 ± 215
222,2	1069 ± 120	2751 ± 179	62 ± 109
256,9	115 ± 53	42 ± 52	469 ± 106
280	469 ± 115	169 ± 114	1615 ± 234
285,6	2376 ± 178	9 ± 75	423 ± 114
302,3	15 ± 59	2821 ± 170	44 ± 81
382,8	41 ± 49	390 ± 83	187 ± 90
410,1	481 ± 88	181 ± 78	9 ± 86
529,3	717 ± 155	497 ± 154	4165 ± 322
548,8	3266 ± 266	1915 ± 252	633 ± 208
558,7	950 ± 147	1106 ± 161	1366 ± 188
590,4	3440 ± 336	992 ± 217	380 ± 213
632,6	535 ± 438	107 ± 430	535 ± 545
659,8	417 ± 150	246 ± 124	25 ± 123
680	187 ± 108	80 ± 107	27 ± 134

TABLEAU IV

Noyau	Spin	Domaine énergie	Nombre total de résonances détectées ou analysées et nombre de résonances de J connu			Valeur S_0 en 10^{-4} $eV^{-1/2}$	
^{77}Se	I = 1/2	0 - 2000 eV	11	8	J = 1	S_0 = 0,3	J = 1
				3	J = 0	S_0 = 2,2	J = 0
$^{107,109}Ag$	I = 1/2	0 - 760 eV	103	26	J = 1	S_0 = 0,65 ± 0,15	J = 1
				11	J = 0	S_0 = 0,55 ± 0,2	J = 0
^{169}Mo	I = 1/2	0 - 780 eV	95	49	J = 1	S_0 = 1,5 ± 0,2	J = 1
				16	J = 0	S_0 = 1,5 ± 0,4	J = 0
^{195}Pt	I = 1/2	0 - 800 eV	50	27	J = 1	S_0 = 1,8 ± 0,3	J = 1
				9	J = 0	S_0 = 1,7 ± 0,5	J = 0
^{141}Pr	I = 5/2	0 - 6000 eV	80	17	J = 2	S_0 = 1,4 ± 0,5	J = 2
				16	J = 3	S_0 = 2,3 ± 0,7	J = 3
^{55}Mn	I = 5/2	0 - 80000 eV	46	9	J = 2	S_0 = 4,2 ± 1	J = 2
				10	J = 3	S_0 = 3,8 ± 0,8	J = 3
^{59}Co	I = 7/2	0 - 80000 eV	69	15	J = 3	S_0 = 3,46 ± 1	J = 3
				18	J = 4	S_0 = 2,23 ± 0,5	J = 4
		0 - 40 keV				S_0(J=3 + J=4) = 3,9 ± 1	
		40 - 80 keV				S_0(J=3 + J=4) = 2,1 ± 0,6	
		80 - 120 keV				S_0(J=3 + J=4) = 3,6 ± 1,5	

TABLEAU II

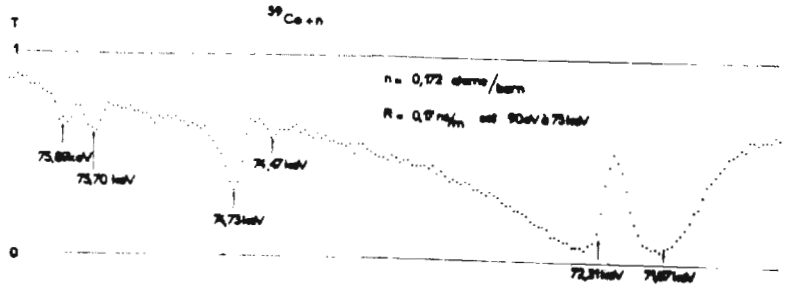

Fig 1

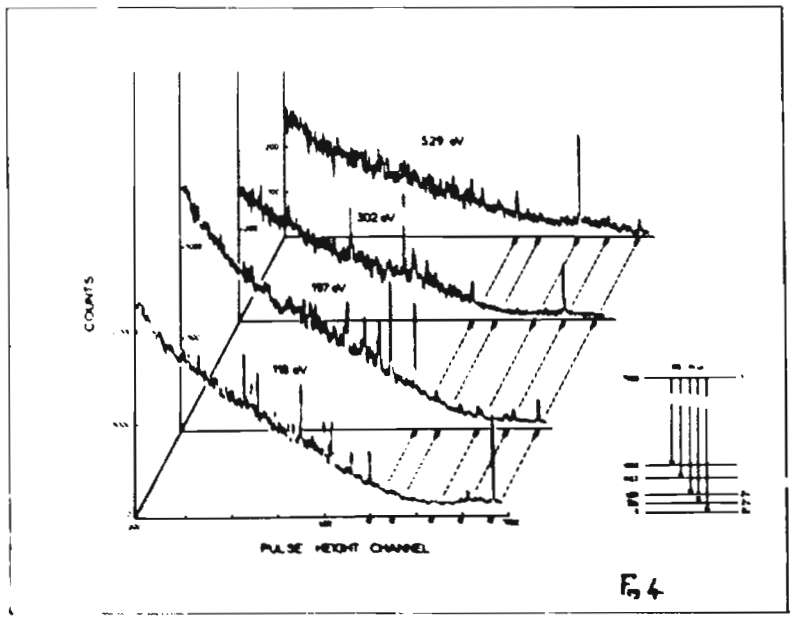

Fig 4

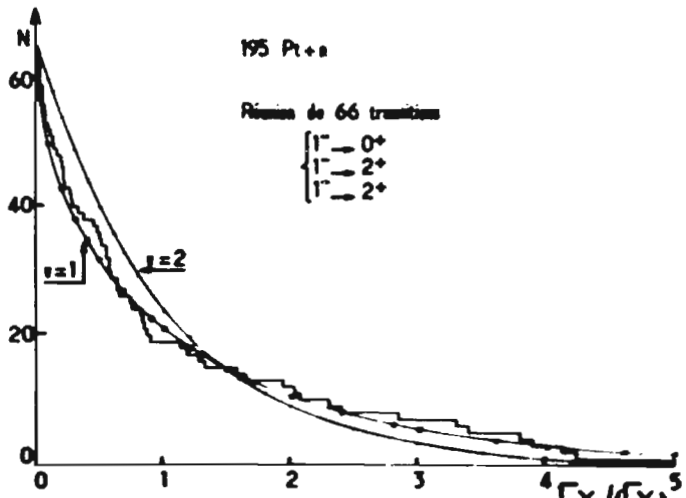

Fig 5

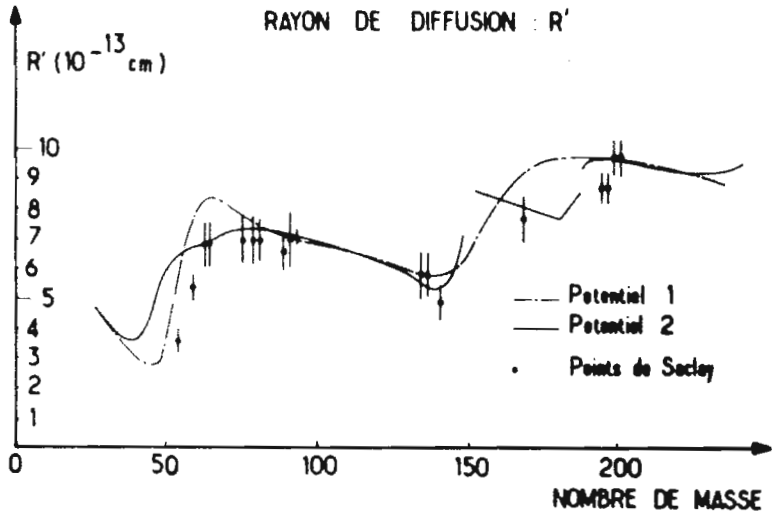

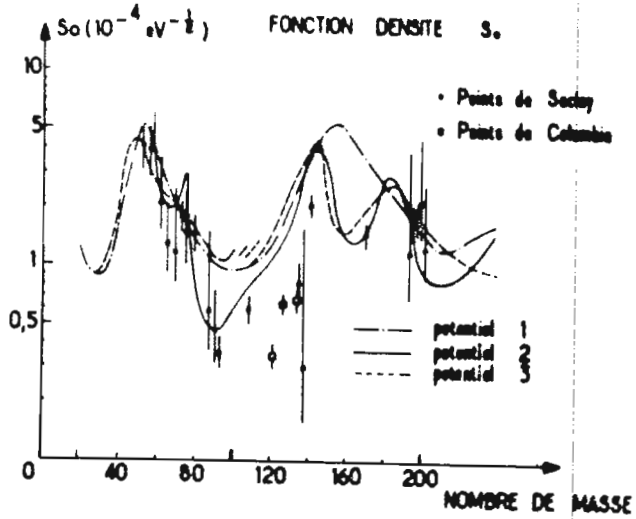

FIGURE 2

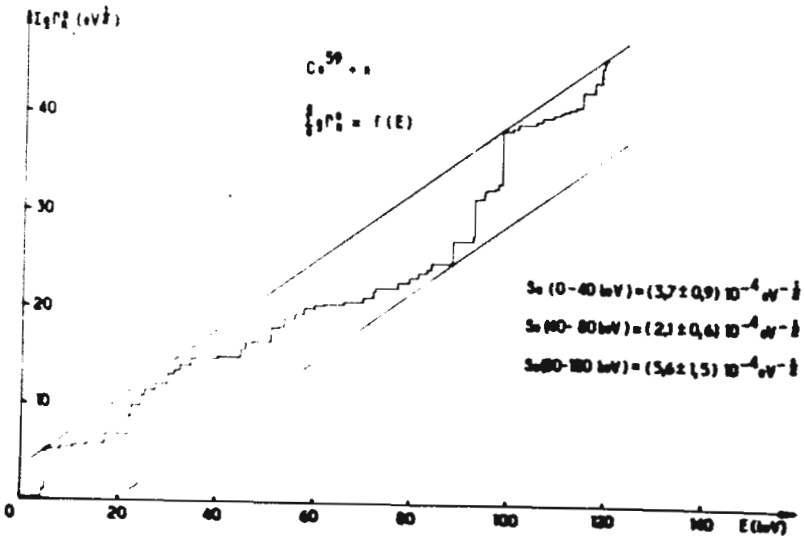

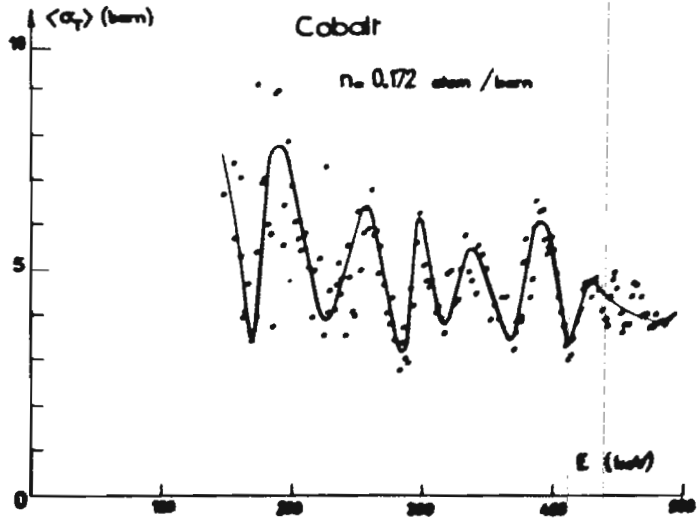

FIGURE 3

XXIII SERVICE DE PHYSIQUE EXPERIMENTALE DU COMMISSARIAT A L'ENERGIE ATOMIQUE (France).

J.Jacquesson, P. Leuba.

1. Appareillage.

1.1. Améliorations apportées à l'Accélérateur Tandem Van de Graaff 12 MeV. (A. Dandine).

1.1.1. Installation du High Transmission Kit (HTK) et des tubes à champ incliné.

Pour un courant négatif de 25 à 30 µA de protons (ou de deutérons) délivrés par une source Duoplasmatron à échange de charges, les performances de la machine sont passées de : 4 µA jusqu'à 10 MeV et 0,5 µA de 10 à 12 MeV à : 8 à 9 µA de 4 à 12 MeV.

Un résultat plus spectaculaire a été obtenu pour la montée en énergie : après un arrêt, l'énergie de 12 MeV peut être obtenue en moins de quinze minutes.

1.1.2. Amélioration de l'optique ionique après accélération.

Des essais sont en cours pour une amélioration des performances en courant analysé de l'accélérateur grâce à une redistribution des lentilles de focalisation le long du trajet du faisceau après accélération.

Après les fentes de sortie de l'analyseur réglé pour une précision de $\pm \frac{1}{1000}$ en énergie, les intensités de protons suivantes ont été obtenues sur une cage de Faraday :

Energie	1,5 MeV	3 MeV	6 MeV	9 MeV	12 MeV
Avant modification de l'optique I µA	4,5	7,8	8,2	7,5	8
Après modification de l'optique I µA	8,6	14,7	12	10,5	11,5

1.1.3. Installation du "Pulsing kit".

Cet appareillage permet de réaliser les performances suivantes :

- Intensité de la bouffée : entre 50 et 70 µA
- Longueur de la bouffée : 4 à 5 nanosecondes
- Fréquence de répétition : 2,5 Mc/s.

1.2. Système d'acquisition et de traitement CAE 510.(P.Fernier, J.Labbe, J.P. Laget).

Un ensemble d'exploitation utilisant un calculateur CAE 510 a été installé auprès de l'accélérateur Tandem 12 MeV. Son programme Moniteur est capable de gérer l'exécution de différents programmes d'exploitation sans interrompre l'acquisition en ligne.

Une console d'exploitation facilite l'appel des programmes et permet de suivre le déroulement des expériences, grâce à un écran de visualisation, des voyants et des indicateurs lumineux.

2. Réactions des deutérons sur les noyaux légers.(G.Bruno, J.Decharge, L. Faugere, A. Perrin, M.Y. Radenac, C. Thibault).

2.1. Etudes faites sur le Tandem Van de Graaff 12 MeV.

Pour compléter les mesures faites précédemment sur le carbone et l'oxygène (fonctions d'excitation), les distributions angulaires des diffusions $^{12}C(d,d)^{12}C$ et $^{16}O(d,d)^{16}O$ et des réactions $^{12}C(d,p)^{13}C$ ont été mesurées pour des énergies voisines de 5 et 6 MeV. Ces mesures en valeur relative, ont été faites pour des angles de 40 à 170° Lab.

2.2. Etudes faites sur le Van de Graaff 2 MeV.

2.2.1. Diffusion des deutérons sur le ^{6}Li.

On a tracé une fonction d'excitation de $^{6}Li\ (d,d)^{6}Li$ à 136° Lab. et les distributions angulaires de cette réaction pour des énergies comprises entre 1,5 et 1,9 MeV. Ces mesures sont données en valeur absolue par comparaison avec la réaction $^{6}Li\ (d,\alpha)\alpha$ dont la section efficace avait été obtenue en valeur absolue au cours d'une mesure antérieure. (1)

2.2.2. Réactions à trois corps.

L'étude de la réaction $^{7}Li\ (d,\ \alpha_1)^{5}He \hookrightarrow \alpha_2 + n$

aboutissant finalement à trois corps a été poursuivie. On a enregistré en biparamétrique, différents spectres correspondant à la corrélation α-α pour des énergies incidentes Ed = 0,7 et 1,5 MeV. L'un des détecteurs était fixé à 90° Labo, l'autre mobile. A chaque énergie on donnait plusieurs valeurs à l'orientation de celui-ci. Les distributions angulaires ont été aussi mesurées à Ed = 0,7 et 1,5 MeV pour les α_1 de la première séquence de la réaction $^{7}Li\ (d,\alpha_1)^{5}He$. Les résultats sont en cours d'exploitation.

Une interprétation basée sur la méthode indiquée par PHILLIPS et al.(calculs de densité d'état) et dans lesquels il est tenu compte de la distribution angulaire des α_2 issus de ^{5}He mesurée précédemment, (2) et de la distribution angulaire des α_1 de ^{7}Li (d,α_1)^{5}He donne des résultats qui, bien qu'encore partiels, semblent encourageants.

3. Courbe d'excitation de la réaction ^{63}Cu (n,p)^{63}Ni de 16,680 à 17,725 MeV. (G. Bardolle, J. Cabe, M. Laurat, M.Longueve).

La section efficace partielle de la réaction ^{63}Cu (n,p)^{63}Ni a été mesurée en valeur relative pour les protons émis dans un angle solide de 0,5 steradian centré sur $\theta = 0°$. Les neutrons étaient obtenus par la réaction T(d,n)^{4}He, les deutérons étant accélérés par un Van de Graaff 2 MeV. La résolution en énergie des neutrons était de 25 keV environ.
Les protons étaient détectés par un télescope formé d'un ensemble de détecteurs solides (dE/dx, E).

Le flux de neutrons était mesuré par deux moniteurs : un scintillateur organique couplé à un photomultiplicateur muni d'une discrimination neutron-gamma, et un télescope à protons de recul.

L'erreur sur la valeur relative de la section efficace est de 6 à 7 % suivant les points. La courbe obtenue, (fig.1) qui a été corrigée de la variation d'efficacité des détecteurs neutrons avec l'énergie ne présente aucune structure particulière.

4. Etude des réactions ^{10}B(d,α)2 ^{4}He et ^{9}Be (^{3}He, α)2 ^{4}He.(D.Didier, J.Ph. Laugier, G.Mouilhayrat, F.Perrault, P. Thouvenin).
L'étude de nombreux spectres de particules alpha en coïncidence a montré que le processus séquentiel, avec passage par un état de ^{8}Be est le plus probable.

Les spectres des particules alpha ont été calculés dans l'hypothèse d'une répartition statistique de l'énergie disponible entre les trois particules.

Nous avons montré que la contribution d'un tel processus ne peut excéder 15 %. Les cas étudiés sont les suivants :

^{10}B (d, α) 2 ^{4}He à 1,5 MeV et 9 MeV

^{9}Be (^{3}He, α) 2 He à 1,5 MeV

L'interaction de la première particule alpha émise avec le ^{8}Be excité à 11 MeV ($\tau \sim 10^{-23}$ s) se traduit par une diminution de la largeur apparente du niveau en question.

Les résultats obtenus montrent que le premier niveau excité de ^{8}Be se situe à 2,7 $\pm$ 0,05 MeV.

Cette valeur est le fruit de nombreux ajustements faits sur des spectres libres et des spectres en coïncidence.

5. Diffusion élastique des neutrons de 600 keV à 1 MeV par le Fer 56.
(G. Bardolle, J. Cabe, M.Laurat, M.Longueve).
Ce travail fait suite à des mesures de sections efficaces totales sur le Fer entre 400 keV et 1200 keV (3). La moyenne des points expérimentaux à l'aide de ΔE variant entre 20 keV et 300 keV fait apparaître un maximum qui se conserve pour des ΔE compris entre 60 keV et 150 keV (Figure 2). Ceci nous a conduits à étudier la diffusion élastique des neutrons dans cette gamme d'énergie. Le travail a été possible grâce à l'amabilité du Professeur DECONNINCK de l'Université de Louvain qui a bien voulu mettre à notre disposition le Van de Graaff 4 MeV pulsé. La méthode du temps de vol nous a permis de tracer deux courbes d'excitations à $\theta = 90°$ et $\theta = 55°$ valeurs qui annulent les polynômes de Legendre d'ordre 1 et 2 (Fig.3) ainsi que trois distributions angulaires aux énergies de 685 keV, 755 keV et 845 keV que nous avons comparées à un développement en série des polynômes de Legendre (Figure 4). Tous ces résultats ont été obtenus avec une dispersion en énergie de 70 keV de façon à supprimer les variations fines mises en évidence dans notre première mesure. Les résultats sont corrigés de l'absorption dans l'échantillon ainsi que des diffusions multiples par une méthode de MONTE-CARLO . Les erreurs expérimentales sont de l'ordre de 5 à 6 %.

6. Mesure de la diffusion élastique et inélastique des protons par le ^{7}Li entre 0,9 et 6 MeV. (G. Bardolle, J. Cabe, M. Laurat, M.Longueve).
Nous avons mesuré les sections efficaces différentielles de diffusion élastique et inélastique des protons de 0,9 MeV à 2 MeV (4) et poursuivi ces mesures jusqu'à 6 MeV, à l'aide d'un Van de Graaff Tandem 12 MeV. Nous espérons les mener à bien jusqu'à une énergie de 12 MeV. Le faisceau est collecté par une cage de Faraday pour la mesure du courant. Les protons sont détectés par des diodes RCA du type C.4.400.2 auxquelles sont associées

des chaînes de spectrométrie ORTEC. Les cibles sont constituées d'un dépôt métallique de 10 à 20 $\mu g/cm^2$ de Lithium 7 (enrichi à 99,3 %) sur support de carbone. Le poids est déterminé à l'aide de la méthode du quartz (5).

Les figures 5 et 6 présentent deux courbes d'excitation à 170° et 155° (système du laboratoire) qui comparent les sections efficaces différentielles de la diffusion élastique et inélastique. La figure 7 est une étude détaillée du "cusp" au voisinage du seuil de la réaction (p, n). Nous présentons enfin plusieurs distributions angulaires comprises entre E_p = 1,000 MeV et E_p = 4,2 MeV pour les deux diffusions (Figure 8). Les sections efficaces ont été obtenues en valeur absolue avec une erreur inférieure à 5 %.

7. Mesure de la diffusion inélastique des protons par le ^6Li de 4 MeV à 12 MeV. (G. Bardolle, J. Cabe, M. Laurat, M. Longueve).

Pour mesurer la section efficace différentielle de diffusion inélastique (excitation du niveau à 2,184 MeV) des protons par le ^6Li, les protons sont accélérés par un Van de Graaff Tandem 12 MeV. Le faisceau est collecté dans une cage de Faraday pour la mesure du courant. Les protons sont détectés par des diodes au Silicium RCA du type C.4.400.2, auxquelles sont associées des chaînes de spectrométrie ORTEC. Les cibles sont constituées d'un dépôt métallique de 10 à 20 $\mu g/cm^2$ de ^6Li enrichi à 99 % sur support de Carbone.

Nous présentons sur la Figure 9 deux courbes d'excitation à 135° et à 150° où nous comparons les sections efficaces de diffusion élastique et inélastique. La figure 10 représente quatre courbes d'excitations de la diffusion inélastique aux angles respectifs de 165°, 150°, 75° et 60 °. La figure 11 est relative aux distributions angulaires de la diffusion inélastique (Q = - 2,184 MeV) pour des énergies protons comprises entre 4,2 et 8,75 MeV.

8. Mesure de $\bar{\nu}$ pour l'Uranium 235 avec les neutrons incidents d'énergie comprise entre 7 et 14 MeV.(J. Frehaut, J. Gauriau, M.Labat, J.Perchereau, M. Soleilhac).

8.1. Dispositif expérimental.

8.1.1. Réactions productrices de neutrons.

Les neutrons incidents entre 7 et 13 MeV ont été produits par réaction D-D en bombardant, à l'aide d'un faisceau de deutons une cible gazeuse de 11 cm

de long chargée en deutérium à une pression variant entre 1 et 1,8 atmosphère suivant l'énergie étudiée.

Pour éliminer les réactions parasites (break-up) importantes dans ce domaine d'énergie, nous avons utilisé pour toutes les mesures un faisceau de deutons pulsé à un taux de répétition de 2,5 Mhz, donnant des bouffées de $5\ 10^{-9}$ seconde à mi hauteur. Nous avons conservé uniquement les fissions induites par les neutrons dont le temps de vol correspondait à l'énergie recherchée.

Le point à 14,4 MeV a été obtenu en utilisant les neutrons produits par réaction d-T sur une cible solide de tritium bombardée par des protons accélérés dans un petit accélérateur de 120 keV. Afin d'éliminer le plus possible de neutrons parasites (thermiques), nous avons utilisé la technique de la particule associée.

La cible de matériau fissile était placée à 0° par rapport au faisceau du Tandem, alors qu'elle était à 45° par rapport au faisceau du 120 keV.

La largeur du pic de temps de vol obtenu était comprise entre 5,5 et $6,5\ 10^{-9}$ seconde sur le Tandem et était de 2,5 nanosecondes sur le 120 keV.

Le nombre de fissions induites par des neutrons thermiques a été mesuré simultanément de deux façons différentes.

8.1.2. Mesure du nombre moyen de neutrons de fission.

Nous n'entrerons pas ici dans le détail de la technique du gros scintillateur liquide qui nous permet d'individualiser les neutrons de fission, détectés avec une efficacité légèrement supérieure à 80 %.

Signalons qu'afin de réduire le bruit de fond dû aux neutrons incidents diffusés par la chambre à fission et détectés par le scintillateur liquide, dès qu'une fission est détectée, on envoie le faisceau de l'accélérateur en dehors de la cible. Ce décentrage réalisé avec un déflecteur électrostatique dure 50 microsecondes, temps pendant lequel nous détectons les neutrons de fission.

Dans ces conditions nous réduisons d'un facteur compris entre 4 et 2 le bruit de fond détecté dans les 50 microsecondes qui suivent une fission (ce facteur diminue quand l'énergie des particules augmente).

Afin de mesurer l'efficacité du scintillateur liquide, entre chaque mesure effectuée de jour en fissions provoquées, nous avons, la nuit, mesuré l'efficacité du scintillateur liquide en utilisant les neutrons de fission spontanée du ^{252}Cf.

La chambre à fission renfermant 50 mg de ^{235}U à 93 % est du type CFU 7 à géométrie cylindrique.

8.2. Corrections.

Nous nous contenterons de citer ici les différentes corrections effectuées :

- Correction de bruit de fond :

Le taux moyen de bruit de fond varie suivant l'énergie entre 0,2 et 0,8 coup par 50 microsecondes. Il est dû essentiellement aux neutrons incidents diffusés par les matériaux qui constituent la chambre.

- Correction de temps mort :

Le temps mort fixe et minimum imposé par l'électronique était de $65\ 10^{-9}$ seconde dans ces mesures.

- Correction d'efficacité :

Les mesures de l'efficacité du scintillateur liquide pour les neutrons ont été faites en prenant $\bar{\nu} = 3,782$ pour le ^{252}Cf.

- Fissions parasites :

Nous avons supposé que toutes les fissions autres que celles dues aux neutrons d'énergie espérée étaient produites dans la fenêtre de coïncidence par des neutrons thermiques.

- Empilement de fissions :

Si deux fissions risquent de s'empiler en 50 microsecondes, nous rejetons la mesure correspondante.

- L'énergie des neutrons incidents :

L'énergie des neutrons incidents a été corrigée pour tenir compte du ralentissement provoqué sur le faisceau de particules chargées lors de la traversée de la cible.

Dans les résultats présentés ici nous n'avons pas tenu compte :

- Des impuretés contenues dans le matériau fissile (correction de l'ordre de 0,1 %)
- De l'anisotropie des neutrons de fission. (correction de l'ordre de 0,1 %)
- De la différence des spectres en énergie pour les neutrons du ^{252}Cf et pour ceux de la fission provoquée sur ^{235}U.

8.3. Résultats expérimentaux.

Pour chaque énergie de neutrons incidents nous avons enregistré au moins 10.000 fissions, obtenues avec une statistique moyenne de 10 évènements par minute.

Le tableau I rassemble les résultats expérimentaux obtenus.

La figure 12 représente la variation de $\bar{\nu}$ en fonction de l'énergie.

La figure 13 situe nos résultats parmi ceux publiés dans le domaine d'énergie étudiée.

L'application de la méthode des moindres carrés à nos résultats donne :

$$\bar{\nu}(E) = 0,139\ E + 2,421$$

8.4. Conclusion.

Ces résultats nous permettent de conclure que la variation de $\bar{\nu}$ en fonction de l'énergie des neutrons incidents serait linéaire à mieux que 1 % dans le domaine d'énergie 7 à 14,4 MeV.

Il faut noter toutefois que la valeur absolue de ces résultats peut être entachée d'une erreur systématique de l'ordre de $\pm$ 1 %, erreur due au doute qui plane actuellement sur la valeur de l'étalon adopté et pourtant le mieux connu le ^{252}Cf.

Durant le premier trimestre 1967 nous effectuerons des mesures sur l'^{235}U entre 3 et 7 MeV en utilisant la réaction p-T sur accélérateur Tandem 12 MeV et nous ferons les mêmes mesures en ^{239}Pu entre 3 et 14 MeV.

Publications.

(1) G.BRUNO, J. DECHARGE, A.PERRIN, G. SURGET et C.THIBAULT. J. de Phys. 27 , 517 1966.
(2) G.BRUNO, J.DECHARGE, A. PERRIN, G. SURGET. C.R.Acad. Sc.259, 3995 1964.
(3) J.CABE, M.LAURAT, P.YVON. EANDC (E) 57 U - Fév. 65.
(4) G. BARDOLLE, J.CABE, J.F.CHRETIEN,M. LAURAT. J. de Phys. 3 . 4 , C 1.96 1966.
(5) J. JOUANIGOT, G.BARDOLLE, J.CABE, J.F.CHRETIEN, M. LAURAT. Nucl. Inst.and Meth. (à paraître).

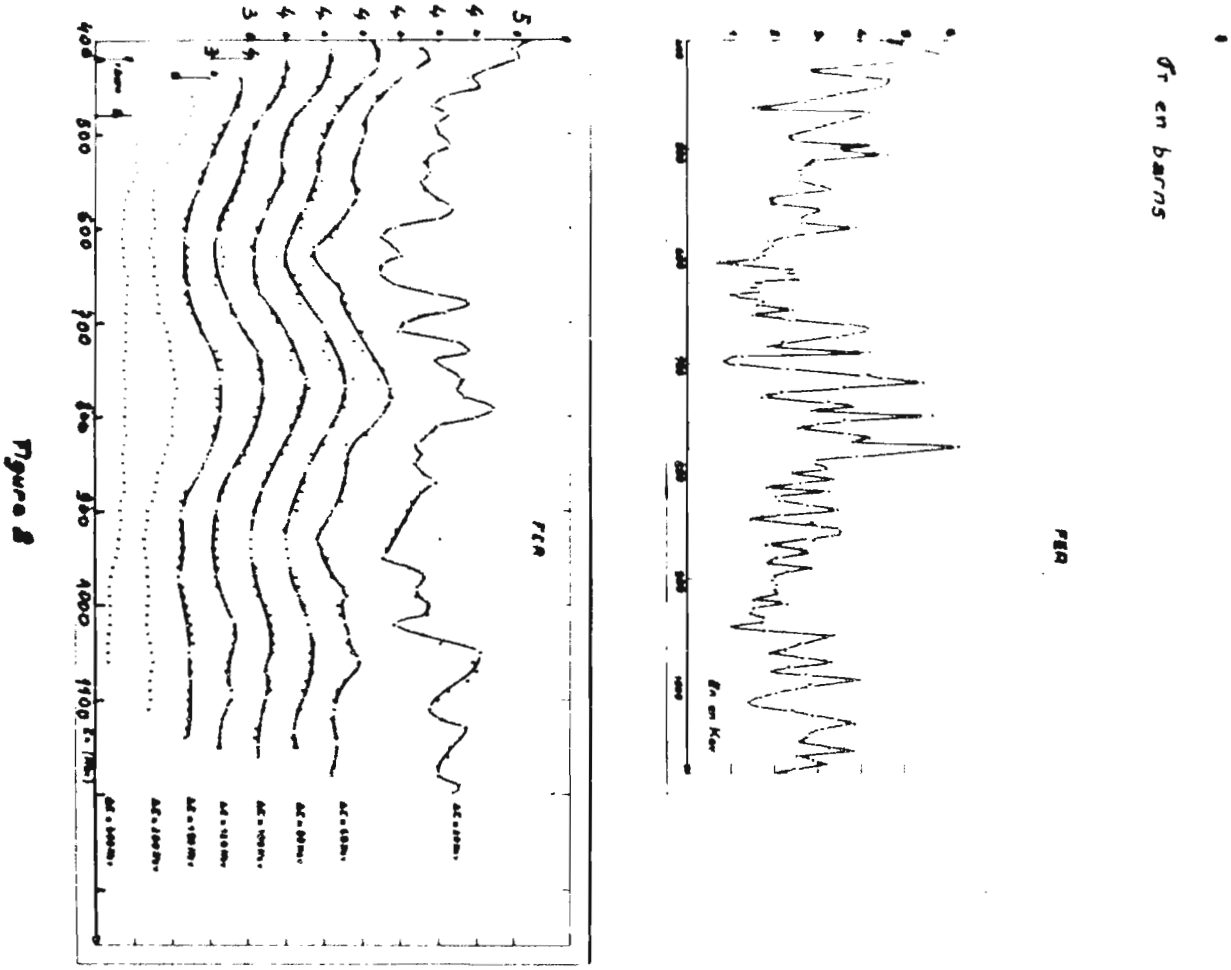

Figure 8

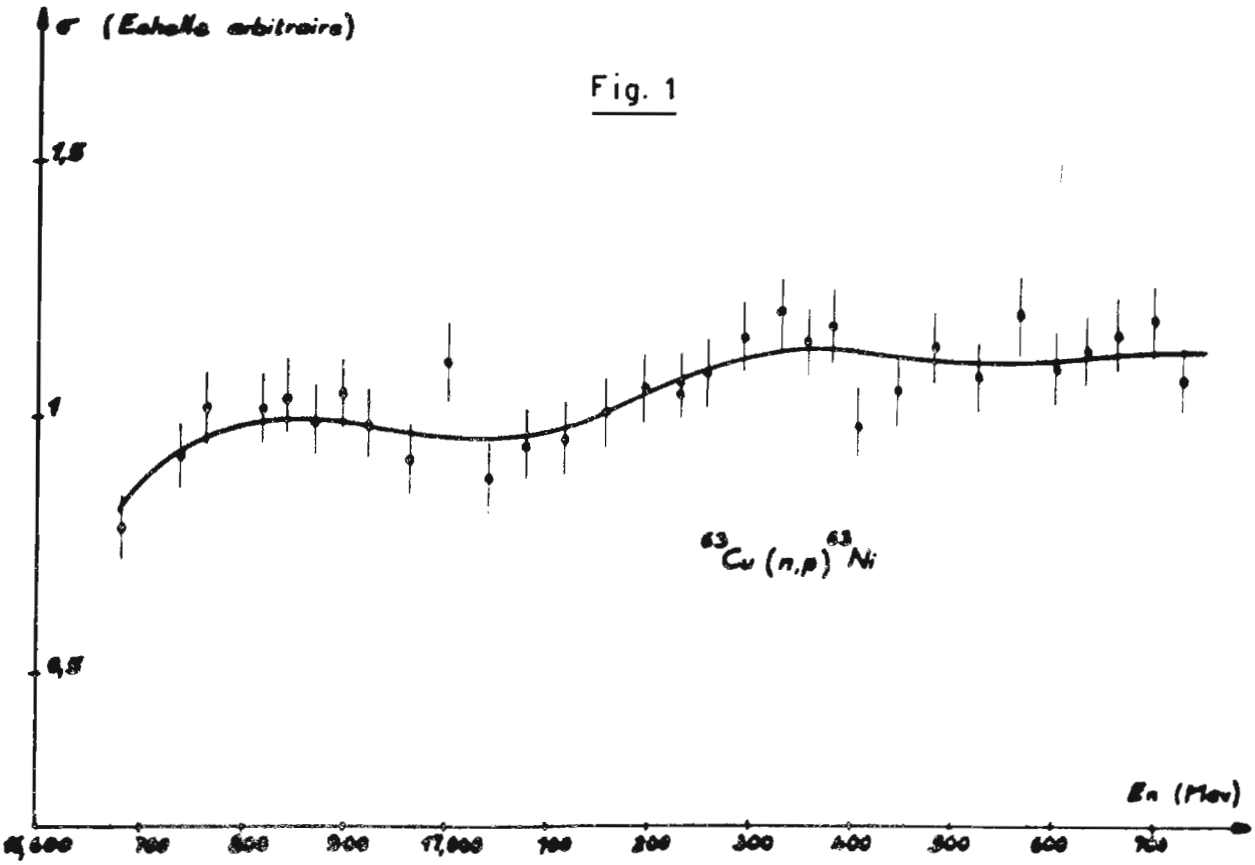

Fig. 1

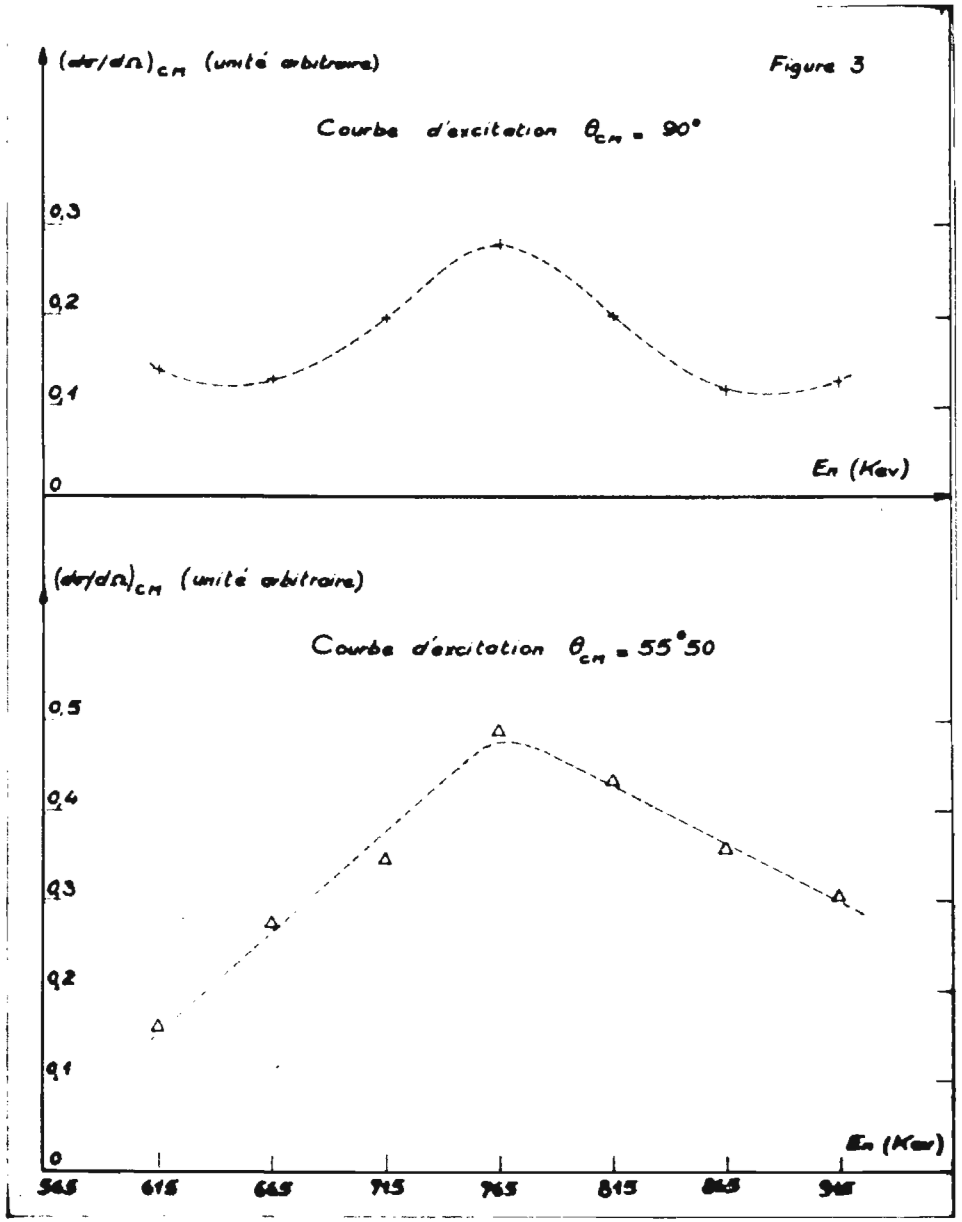

Figure 3

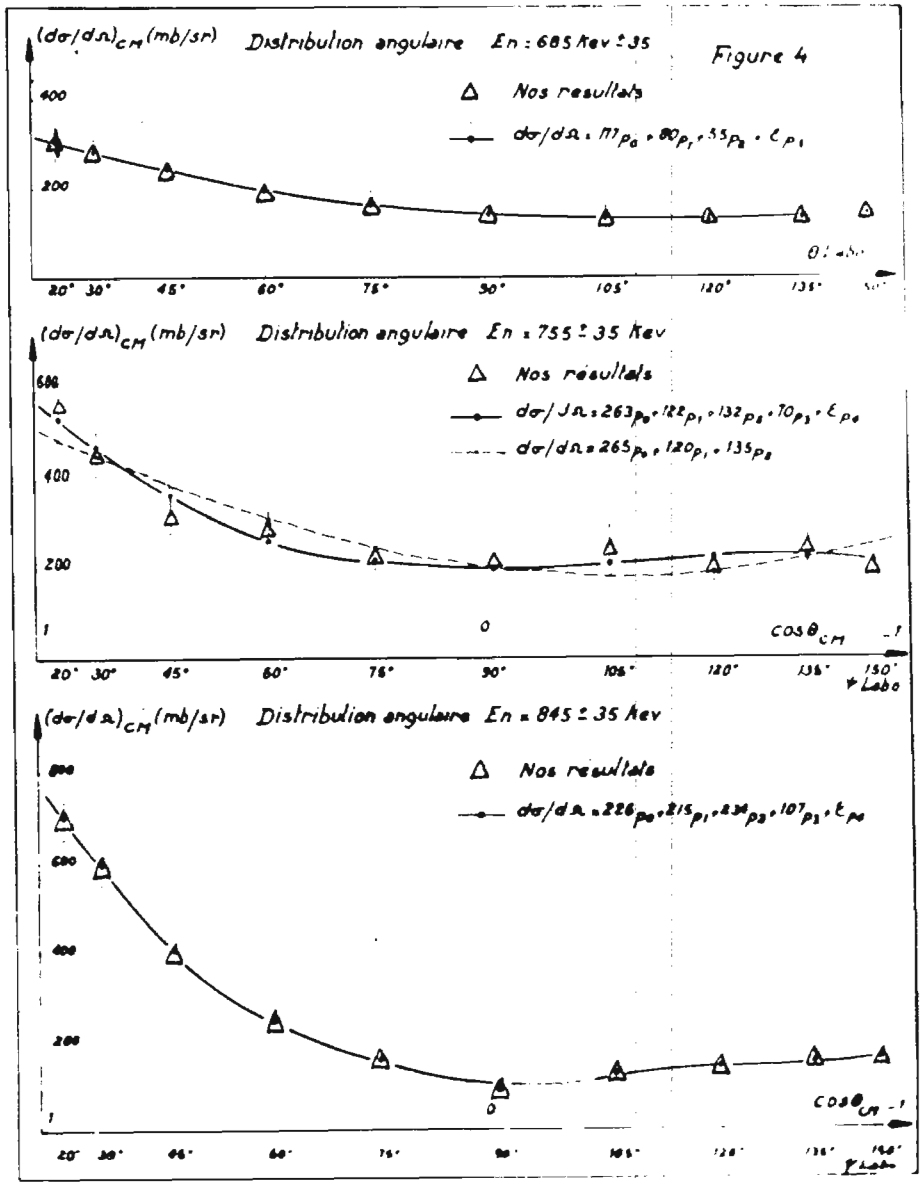

Figure 4

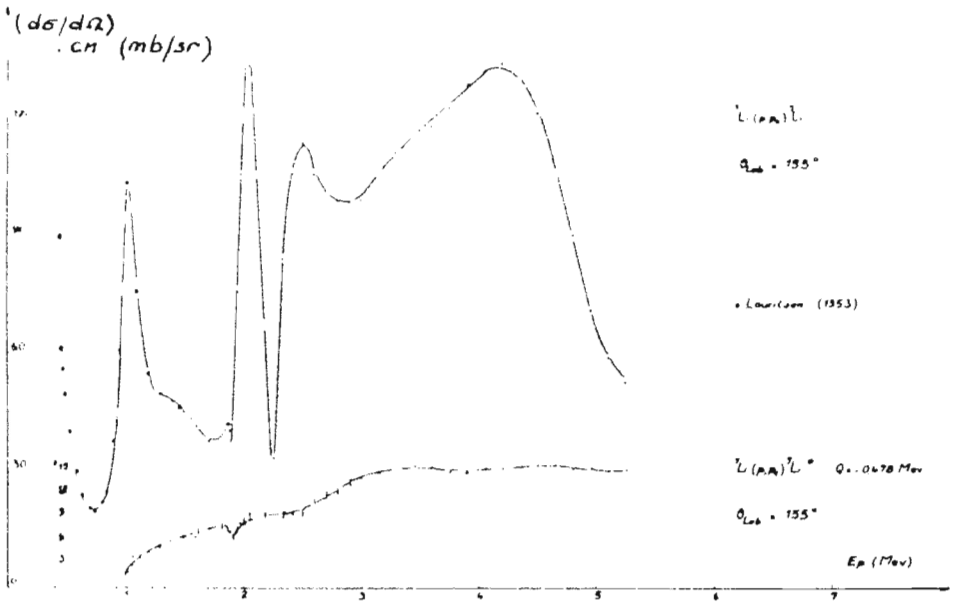

Fig 6

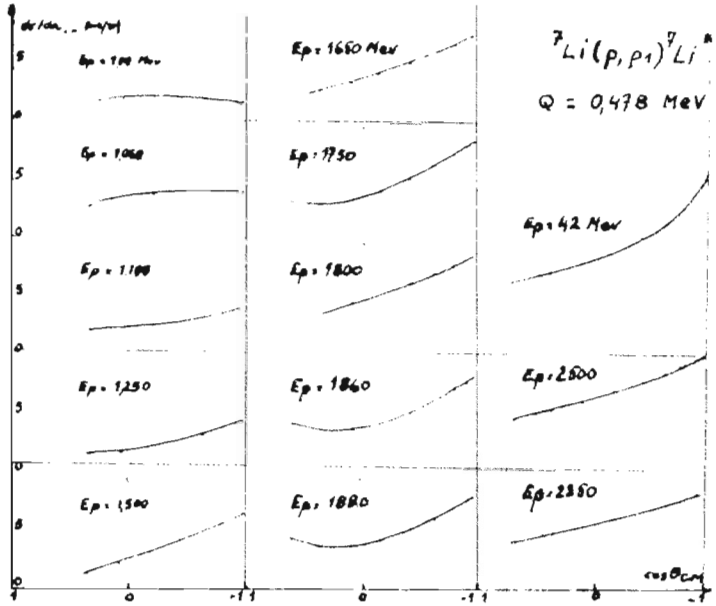

Fig 8

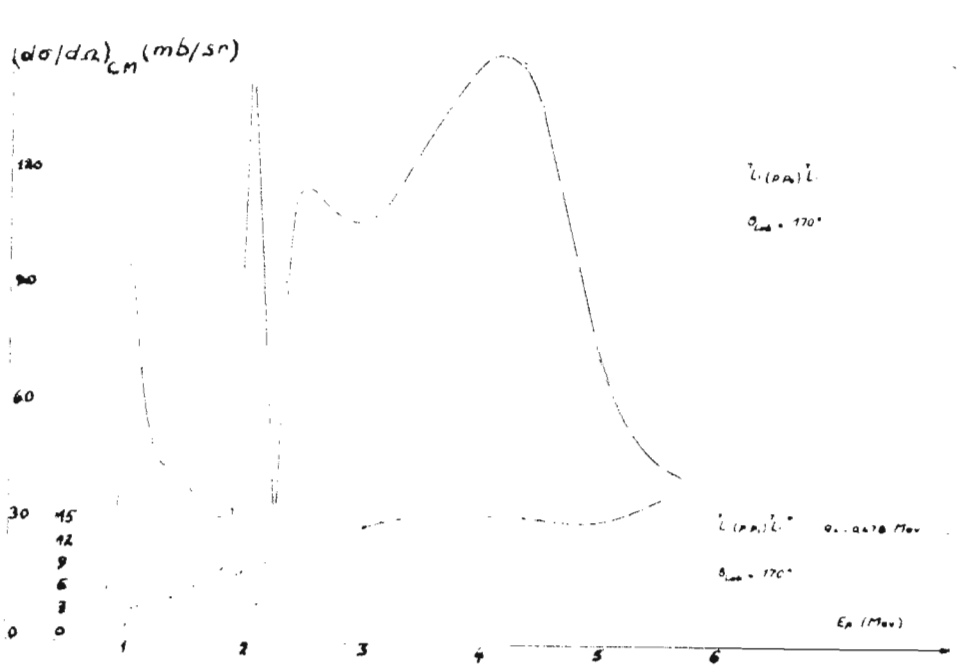

Fig 5

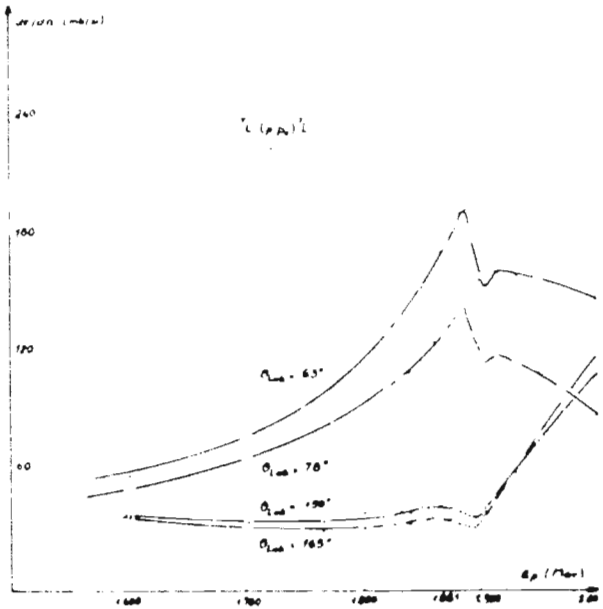

Fig 7

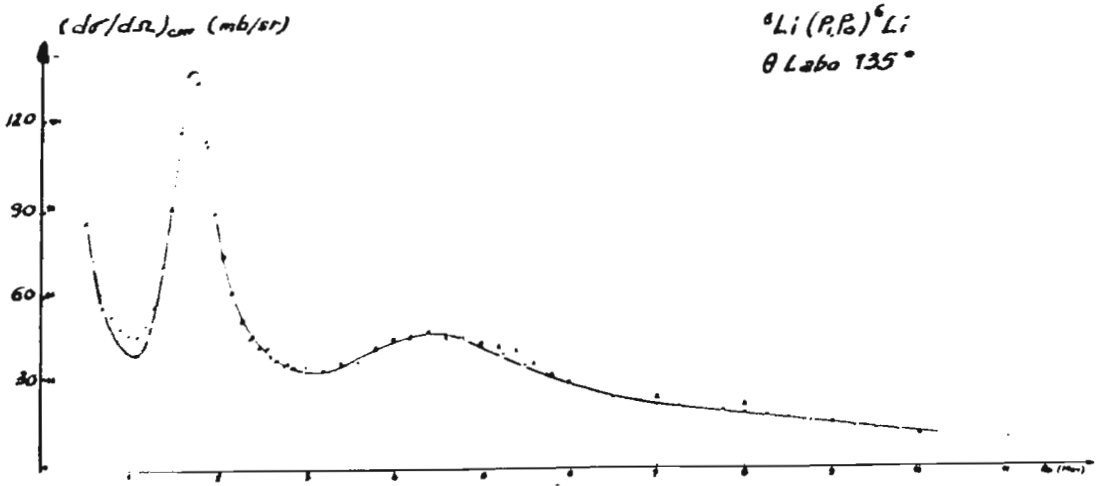

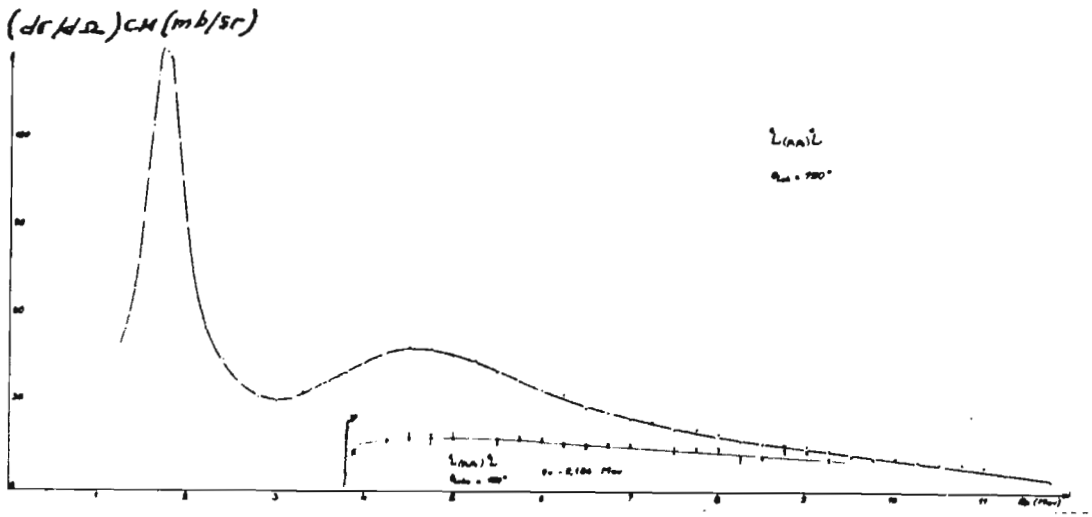

- Fig 9 -

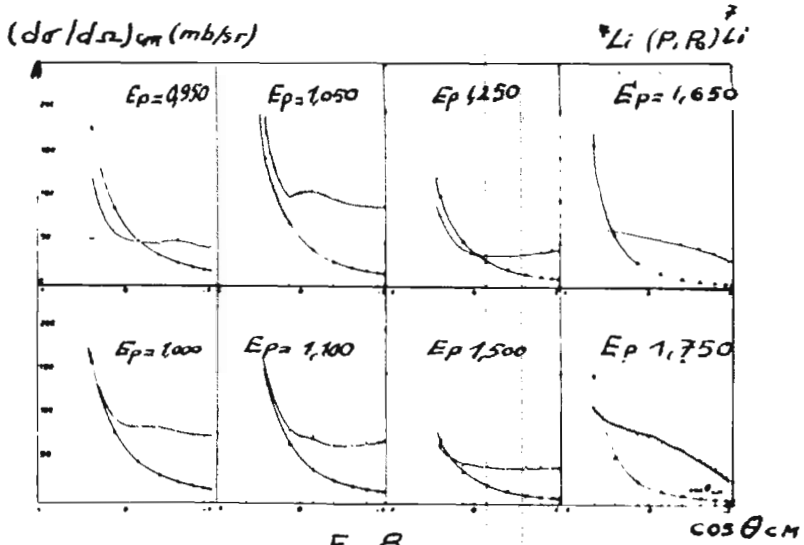

- Fig 8 -

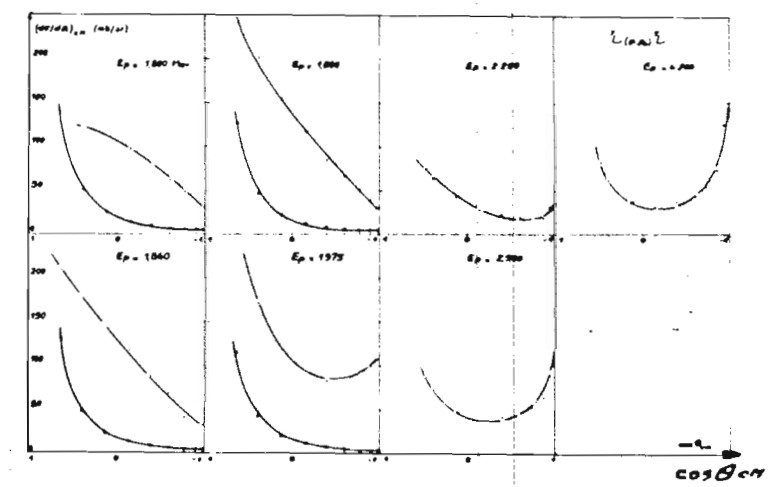

- Fig 8 -

Fig 10

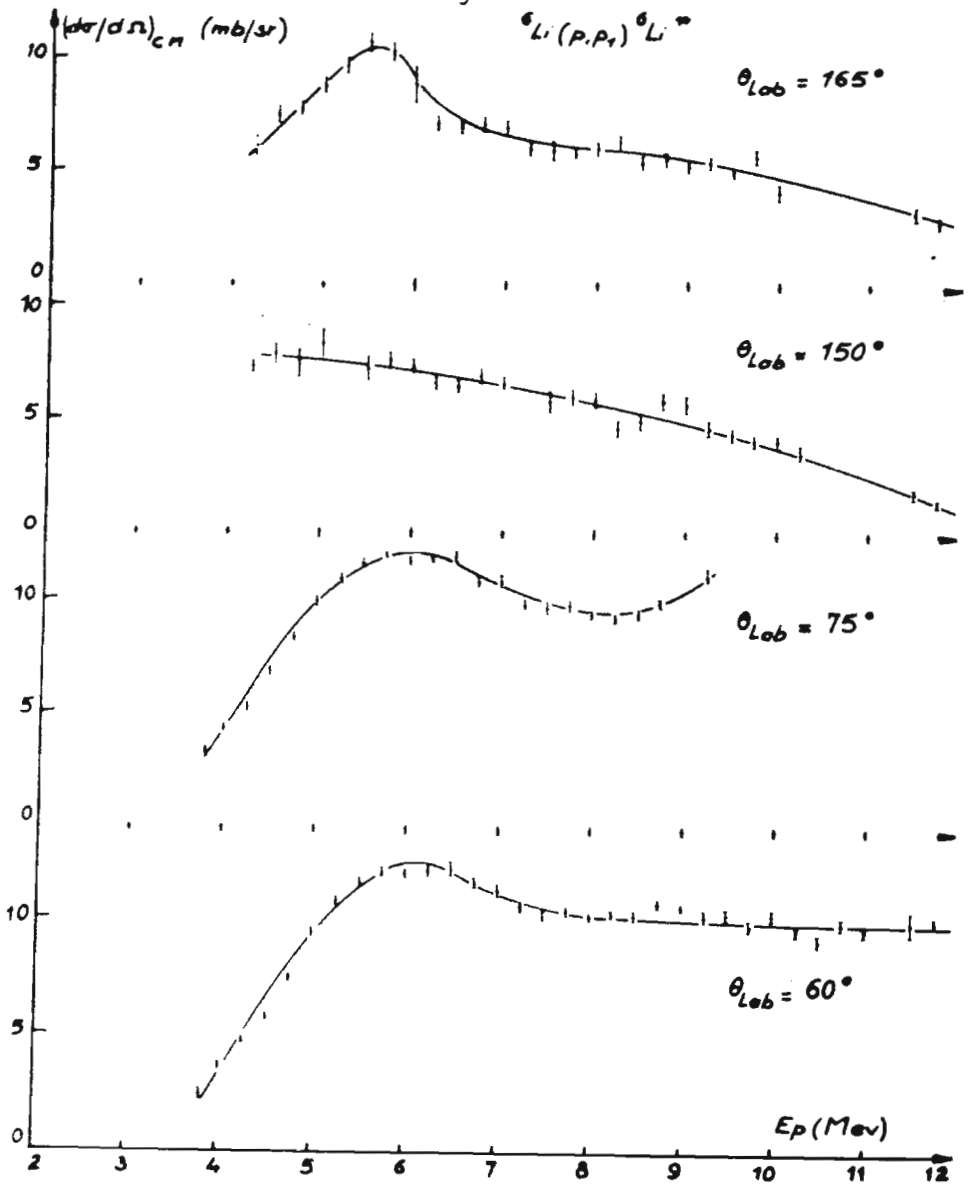
$(d\sigma/d\Omega)_{cm}$ (mb/sr)
$^6Li(p,p_1)^6Li^*$
$\theta_{Lab} = 165°$
$\theta_{Lab} = 150°$
$\theta_{Lab} = 75°$
$\theta_{Lab} = 60°$
E_p (Mev)

Fig 11

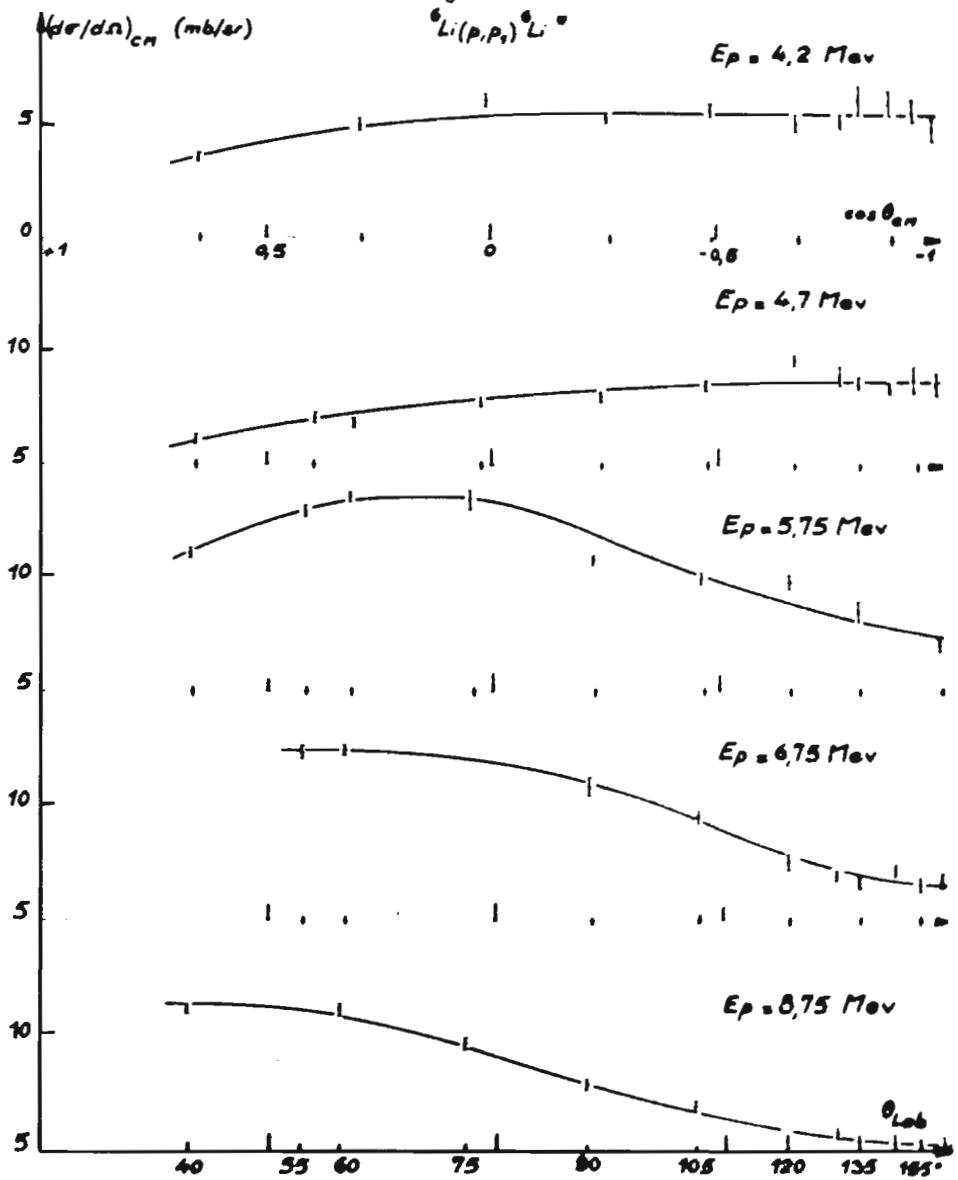
$(d\sigma/d\Omega)_{cm}$ (mb/sr)
$^6Li(p,p_1)^6Li^*$
$E_p = 4,2$ Mev
$E_p = 4,7$ Mev
$E_p = 5,75$ Mev
$E_p = 6,75$ Mev
$E_p = 8,75$ Mev
$\cos\theta_{cm}$
θ_{Lab}

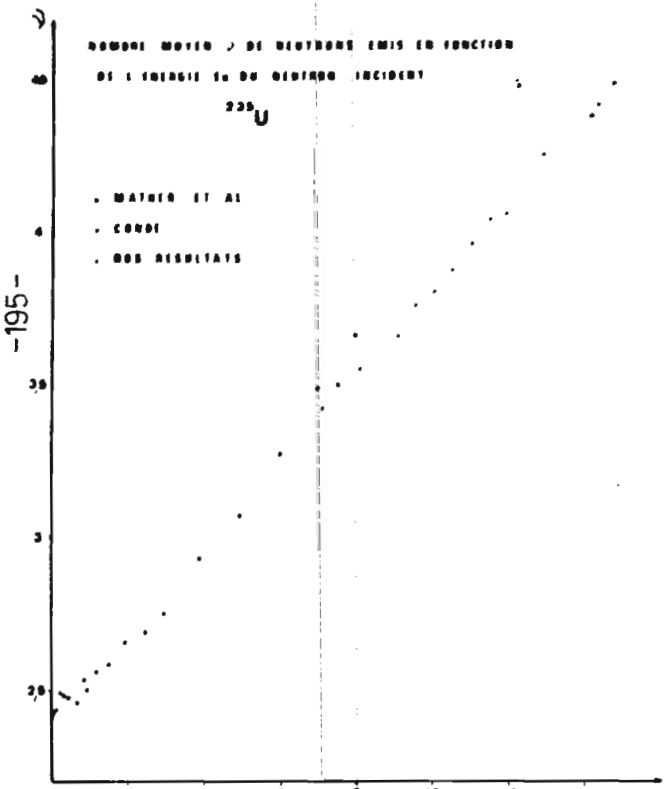

Figure 13

Réaction Productrice de neutrons	Energie Moyenne des neutrons MeV	Définition en Energie (1) keV	$\bar{\nu}$	$\Delta\bar{\nu}$
D-D	7, 08	183	3, 422	0, 008
D-D	8, 30	150	3, 541	0, 015
D-D	9, 08	130	3, 658	0, 009
D-D	9, 97	120	3, 731	0, 011
D-D	10, 25	120	3, 823	0, 009
D-D	10, 54	110	3, 874	0, 012
D-D	11, 03	90	3, 958	0, 012
D-D	11, 51	90	4, 040	0, 017
D-D	11, 98	85	4, 055	0, 014
D-D	12, 94	85	4, 254	0, 020
D-T	14, 40	150	4, 410	0, 011

(1) demi largeur totale du spectre de neutrons issus de la cible .

TABLEAU I

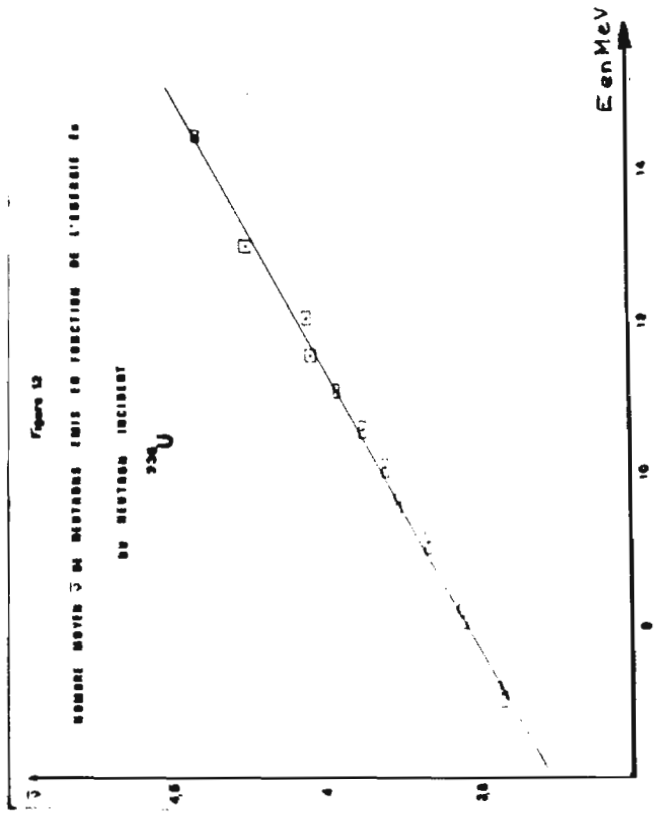

Figure 12

XXIV SERVICE DES EXPERIENCES NEUTRONIQUES (C.E.A. - Saclay - FRANCE)

D. Breton.

1. Mesures de sections efficaces effectives d'échantillons fissiles par la méthode d'oscillation.

Ce travail est effectué dans le cadre du contrat EURATOM "Recyclage du Plutonium" 002-64-9TRUF (RD).

1.1. Alliage Uranium-Plutonium

Les sections efficaces effectives et le des isotopes du Plutonium sont mesurés sur des échantillons d'alliage Uranium-Plutonium par la méthode d'oscillation dans une portion de réseau à eau lourde.

L'ensemble des résultats montre un très bon accord avec les valeurs calculées et confirment les sections efficaces tirées de la compilation de Wescott avec une précision voisine de 1 % pour les sections efficaces et de 0,2 % pour le du Pu 239.

1.2. Echantillons fissiles irradiés

Une série d'expériences a été effectuée en utilisant la même méthode sur des échantillons d'uranium enrichi à 1,6 % irradiés dans le réacteur à eau lourde EL 3 à des taux d'irradiation compris entre 300 et 7000 MWJ/T.

On étudie l'évolution des sections efficaces de capture et de fission du combustible à partir des analyses chimiques et isotopiques on peut en déduire la capture globale des produits de fission.

Le dépouillement et l'interprétation des résultats est en cours.

2. Mesures intégrales dans une portion de réseau de réacteur rapide

Cette expérience consiste à mesurer dans une portion de réseau de réacteur rapide (Assemblage I A de MASURKA) les taux de réaction des différents matériaux fissiles ou de structure entrant dans la composition du coeur d'un réacteur rapide.

Les mesures sont effectuées par la méthode d'oscillation au centre d'un assemblage de 30 cm de côté chargé d'uranium enrichi à 30 %, lui-même placé dans la cavité centrale du réacteur MINERVE. Une couverture en U naturel et acier assure la transition entre la zone nourricière et la zone rapide.

La configuration a été rendue critique à la fin de cette année et les expériences préliminaires ont été effectuées. Les études suivantes seront

entreprises :

- Mesure des indices de spectre avec détecteurs et chambres à fission et recoupement sur MASURKA avec des assemblages ayant la même composition.
- Mesure des effets en réactivité sur des échantillons fissiles (U 235, U 238, Pu 239 et Pu 240) de compositions variées et comparaisons avec MASURKA.
- Mesure sur des matériaux de structure (Oxyde - Fer - Acier - Sodium - etc...)
- Etude des effets d'hétérogénéité.
- Mesure des coefficients DOPPLER.

2.1. Etudes de Physique des réacteurs (M. SAGOT)

Les mesures effectuées en 1966 sont liées d'une part, à l'étude des combustibles reconstitués contenant du Pu, d'autre part, à l'étude des canaux de grande section dans des réseaux à pas important.

On a réalisé dans CESAR des mesures de k_∞ par cartes de flux, de structure fine dans la cellule et d'indices de spectres, en particulier avec des couples Pu/U, sur le combustible U naturel (Ø 29,2 mm au pas hexagonal de 225,16 mm) : à froid d'abord pour le réseau gavé et le réseau dégavé 1/3, à 100°C et 200°C pour le réseau gavé seul ensuite ; le coefficient différentiel de température du réseau gavé a été mesuré autour de 30°C, 110°C et 220°C.

Les mesures sur MARIUS ont porté sur un réseau de pas carré 316,8 mm chargé du barreau U naturel (Ø 50 mm) successivement au canal de Ø 90, 110, 140 et 170 mm : étude par cartes de flux du k_∞, de la structure fine complète et du coefficient de diffusion radial par la méthode de BENOIST. Deux substitutions des tubes de Ø 65 x 82 mm (T7) et 90 x 103 mm (T8) ont été réalisées au canal Ø 110 mm. Un programme de substitutions plus complet est prévu au canal Ø 170 mm début 1967.

Le facteur de conversion initial du combustible Ø 29,2 mm au pas carré de 224 mm, canal Ø 70 mm, a été mesuré dans MARIUS.

D'autres études ont été menées dans MARIUS :

- essais de gaines internes pour des gros tubes d'uranium,
- essais de noyaux en graphite à l'intérieur des tubes d'uranium.

2.2. Etude des réseaux contenant des combustibles reconstitués : substitutions

Trois jeux de combustibles reconstitués ont été étudiés dans CESAR par rapport à des combustibles en uranium d'enrichissement variable (0,69 % - naturel - 0,83 % - 0,86 %). Ces jeux ont les applications et constitutions suivantes :

1 P : U nat - 0,042 % Pu (en poids) à 6,2 % de Pu^{240}

2 P : U appauvri à 0,21% U_5 (en poids) - 0,29% Pu à 8,5% de Pu^{240}

3 P : U nat - 0,048 % Pu à 25 % de Pu^{240}.

Les mesures ont été effectuées par substitutions dans les réseaux Ø 29,2 U naturel et ont été assorties de structures fines et d'indices de spectre dans le modérateur et le combustible : à 20°C, en dégavé 1/3 et en gavé 3/3, substitution de l'ensemble des 6 jeux (3 jeux U_5 et 3 jeux U-Pu). A 100°C et 200°C, substitutions de l'ensemble des jeux, sauf le jeu) 0,86 % U_5 qui n'a pas été étudié à 100°C.

Le coefficient de température différentiel du jeu 2 P a été déterminé autour de 30°C, 100°C et 200°C par rapport à celui du réseau de référence.

2.3. Mesures de constantes neutroniques de combustibles reconstitués et irradiés

Ces mesures sont effectuées par la méthode d'oscillation. Janvier 1966 a vu se terminer une campagne d'oscillation menée à 20°C dans MARIUS au cours de laquelle ont été oscillés de nombreux échantillons U-Pu à teneur en Pu et compositions isotopiques du Pu variables et 18 cartouches de combustible Ø 28 mm irradiés dans G3 (irradiations comprises entre 500 et 4500 MWj/T).

La première campagne d'oscillation a débuté en décembre dans CESAR, à 20°C, elle portera uniquement sur des échantillons reconstitués et sera suivie de mesures à 200°C.

2.4. Etudes sur le graphite

Deux mesures de longueur de diffusion ont été réalisées par la méthode de l'expérience exponentielle en utilisant des coeurs de MARIUS comme source neutronique ; la première a porté sur le graphite de l'empilement MARIUS lui-même (nouvelle zone centrale) ; la seconde sur le graphite étudié en 1964/65 par la technique des neutrons pulsés. L'ensemble des résultats obtenus sur ce second graphite est cohérent.

La technique des neutrons pulsés a été utilisée jusqu'en octobre à la détermination de l'anisotropie aux neutrons thermiques d'un réseau, de pas carré 200 mm, de canaux vides dans du graphite. Les diamètres de canal étudiés sont 30, 50, 70, 90, 110 et 140 mm.

En fin d'année a commencé un programme d'étude de l'anisotropie, toujours en neutrons thermiques, des réseaux d'absorbants (fer) placés dans un canal d'air.